AD_____

Award Number: W81XWH-04-1-0844

TITLE: Prostate Cancer Progression and Serum Sibling (Small Integrin Binding N-Linked Glycoprotein) Levels

PRINCIPAL INVESTIGATOR: Neal S. Fedarko, Ph.D.

CONTRACTING ORGANIZATION: Johns Hopkins University
Baltimore, MD 21224

REPORT DATE: October 2008

TYPE OF REPORT: Final

PREPARED FOR: U.S. Army Medical Research and Materiel Command
Fort Detrick, Maryland 21702-5012

REPORT DOCUMENTATION PAGE

Form Approved
OMB No. 0704-0188

1. REPORT DATE	2. REPORT TYPE	3. DATES COVERED
1 Oct 2008	Final	15 Sep 2004 – 14 Sep 2008

4. TITLE AND SUBTITLE

Prostate Cancer Progression and Serum Sibling (Small Integrin Binding N-Linked Glycoprotein) Levels

5a. CONTRACT NUMBER

5b. GRANT NUMBER
W81XWH-04-1-0844

5c. PROGRAM ELEMENT NUMBER

6. AUTHOR(S)
Neal S. Fedarko, Ph.D.

E-Mail: ndarko@jhmi.edu

5d. PROJECT NUMBER

5e. TASK NUMBER

5f. WORK UNIT NUMBER

7. PERFORMING ORGANIZATION NAME(S) AND ADDRESS(ES)

Johns Hopkins University
Baltimore, MD 21224

8. PERFORMING ORGANIZATION REPORT NUMBER

9. SPONSORING / MONITORING AGENCY NAME(S) AND ADDRESS(ES)
U.S. Army Medical Research and Materiel Command
Fort Detrick, Maryland 21702-5012

10. SPONSOR/MONITOR'S ACRONYM(S)

11. SPONSOR/MONITOR'S REPORT NUMBER(S)

12. DISTRIBUTION / AVAILABILITY STATEMENT
Approved for Public Release; Distribution Unlimited

13. SUPPLEMENTARY NOTES

14. ABSTRACT
We have been studying a gene family termed SIBLINGs (for small integrin binding ligand N-linked glycoproteins) whose members include bone sialoprotein (BSP), osteopontin (OPN), dentin matrix protein-1 (DMP1), dentin sialophosphoprotein (DSPP) and matrix extracellular phosphoglycoprotein (MEPE). Our Specific Aims are to describe the distribution of serum-based measurements of SIBLINGs among (a) normal individuals, (b) individuals with benign prostatic disease, (c) individuals with clinically defined prostate cancer, and (d) longitudinal samples from individuals with prostate cancer before and after treatment; and to establish serum-based measurements which maximize sensitivity and specificity of SIBLINGs as markers for prostate cancer detection as well as for prostate cancer progression and response to treatment. Although the laboratory is still blinded to staging and progression data at this point in time, some significant observations can be made. The distribution of serum levels of BSP and DSPP suggest they have utility for prostate cancer detection. Whether used separately or as an adjunct to PSA screening, the preliminary data indicates that measurement of DSPP may have a significant effect on current prostate cancer management.

15. SUBJECT TERMS
Biomarkers, immunoassay, detection, receiver operating, characteristics (ROC), sensitivity, specificity, detection.

16. SECURITY CLASSIFICATION OF:			17. LIMITATION OF ABSTRACT	18. NUMBER OF PAGES	19a. NAME OF RESPONSIBLE PERSON
a. REPORT	b. ABSTRACT	c. THIS PAGE			USAMRMC
U	U	U	UU	154	19b. TELEPHONE NUMBER *(include area code)*

Table of Contents

Introduction

Prostate cancer is the leading cancer diagnosed among men in the United States. Detection is currently based on symptom presentation, physical examination including a digital rectal exam (DRE), measuring serum levels of prostate-specific antigen (PSA) and biopsy. The DRE can not detect certain tumors (that are nonpalpable or physically inaccessible) and PSA levels are elevated in certain non-cancerous conditions (acute prostatitis and benign prostatic hyperplasia). PSA measures have a high rate of false positive test results (the PSA is elevated but no cancer is present). False positives are associated with additional medical procedures, significant financial costs and mental stress. In addition both DRE and PSA can't detect early tumors and are sometimes uninformative in terms of predicting disease progression. Biopsies performed for confirmation of abnormal test results or to follow disease progression or response to treatment can have side-effects that impact profoundly upon the quality of life.

Our hypothesis is that serum levels of a gene family we have been studying are an informative marker for prostate cancer detection and progression. Members of this gene family, termed SIBLINGs for Small Integrin Binding LIgand N-linked Glycoproteins) are induced in different cancers [1] have been shown to bind and modulate matrix metalloproteinase (MMP) activity through both the activation of the latent proenzyme and reactivation of tissue inhibitor of matrix metalloproteinase (TIMP)-inhibited MMP [2]. MMPs have a well defined role in tumor angiogenesis, progression and metastasis [3]. The biological activity of SIBLINGs and MMPs is consistent with a role for SIBLINGs in early tumor progression. This biological plausibility suggests that the levels of these proteins in blood may be used as not only as adjuncts to conventional detection of prostate cancer, but also as serological markers for prostate cancer progression. A confounding facet of prostate cancer is the variable nature of progression (growth rate, metastasis, etc.) and the absence of non-invasive markers that consistently track with progression. The characterization of novel serum markers whose levels may correlate with disease progression will have a profound effect on current prostate cancer management. The work has the potential to benefit individuals with prostate cancer across the spectrum from early detection to disease progression monitoring and modulating therapy. This is a pre-clinical, translational study that will lay the groundwork for future large scale clinical trials.

Body

Overview:

At of the end of the fourth year of the grant (a no cost extension), all Tasks have been completed. The no cost extension had been requested to enable the completion of the SIBLING assays, accrual of longitudinal samples and unblinding of the study. During the development of the assays in creating the reagents (antibodies, recombinant proteins, adenoviral vectors, etc.) a number of novel observations were made on SIBLING biology that are summarized in the Results section, below the summaries of completed Tasks.

Statement of Work:

The tasks outlined in the original Statement of Work were to:

Task 1. To determine the utility of serum SIBLING (BSP, OPN, DMP1 and DSPP) levels in detecting cancer of the prostate (Months 1 - 8):

a. Using competitive ELISAs, measure the distribution of BSP, OPN, DMP1 and DSPP in 200 normal individuals free of prostate cancer.
b. Using competitive ELISAs, measure the distribution of BSP, OPN, DMP1 and DSPP in individuals with prostate cancer.
c. Using competitive ELISAs, measure the distribution of BSP, OPN, DMP1 and DSPP in 200 individuals with benign prostatic disease.
d. Determine sensitivity, specificity, positive and negative predictive values as well as receiver operating characteristic (ROC) curve analyses.

Task 2. To determine the utility of serum SIBLING (BSP, OPN, DMP1 and DSPP) levels in predicting prostate cancer progression (Months 9 – 22):

a. Using competitive ELISAs, measure BSP, OPN, DMP1 and DSPP in baseline samples from 200 prostate cancer patients with clinically characterized stage and progression state.
b. Using competitive ELISAs, measure BSP, OPN, DMP1 and DSPP in longitudinal samples collected yearly after initial diagnosis of prostate cancer in 200 patients.
c. Test for clinical association between serum SIBLING levels and tumor grade, stage and progression.

Task 3. To determine the utility of serum SIBLING (BSP, OPN, DMP1 and DSPP) levels in assessing response to treatment. (Months 23 - 36).

a. Using competitive ELISAs, measure BSP, OPN, DMP1 and DSPP in longitudinal samples from 200 prostate cancer patients undergoing treatment.

   Treatment: androgen-deprivation therapy (gonadotropin-releasing hormone peptide analogues) with a three year follow-up and serum samples drawn at baseline and every six months (1,400 samples total).

b. Test for statistical association between serum SIBLING levels and prostate cancer progression after treatment.

Results:

Task 1 Results. Determining the utility of serum SIBLING (BSP, OPN, DMP1 and DSPP) levels in detecting cancer of the prostate.

The major results of the SIBLING sera screen in prostate cancer were presented at a Gordon Research Conference on Small Integrin-Binding Proteins held August 8th, 2007 in Biddeford, ME. As well as at the Innovative Minds in Prostate Cancer Today (IMPaCT) meeting on September 8, 2007 in Atlanta, GA. The abstract describing the presentation at IMPaCT is included in the Appendix. A manuscript describing the distribution of SIBLINGs in normal and prostate cancer sera has been submitted and is also included in the Appendix.

In work that has been submitted for publication, the sensitivity and specificity of SIBLINGs in prostate cancer detection is described [10]. DSPP provided the best discriminatory power (Figure 1). When serum from subjects with benign prostatic hyperplasia (BPH) were also analyzed for SIBLINGs, the mean serum values for BSP and DSPP was significantly different from both normal and prostate cancer sera (Figure 2 and Table 1), though there was significant overlap between benign prostatic disease and prostate cancer values for BSP. Average OPN levels in BPH and prostate cancer were not significantly different. Again, DSPP provided the maximal sensitivity and specificity.

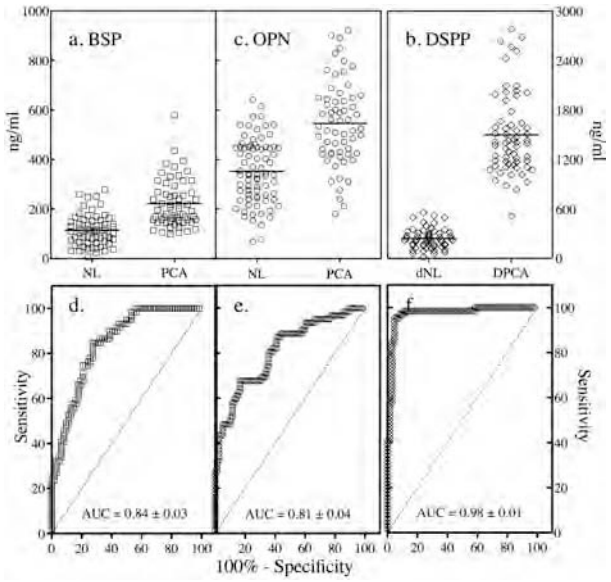

Figure 1. Serum levels of SIBLINGs in prostate cancer sera. Serum levels of (a) bone sialoprotein (BSP), (b) osteopontin (OPN) and (c) dentin sialophosphoprotein (DSPP) in samples from normal subjects (NL) and subjects diagnosed prostate cancer (PCA) were quantified using competitive ELISAs following sample extraction and clean-up. MEPE values were no different between normal and prostate cancer subjects, results not shown. Receiver Operator Characteristic plots were determined for (d) BSP, (e) DSPP and (f) OPN. Optimal cut-off values of 93, 358 and 500 for BSP, OPN and DSPP, respectively, were identified from the ROC analysis.

Table I. Average Serum SIBLING levels .

	NL	BPH	PCA	cut-off	Sensitivity	specificity
BSP (ng/ml)	114 ± 63	157 ± 42	222 ± 96	93 ng/ml	75%	40%
OPN (ng/ml)	353 ± 130	462 ± 179	546 ± 170	358 ng/ml	92%	30%
DSPP (ng/ml)	242 ± 122	358 ± 157	1500 ± 495	500 ng/ml	90%	100%

Figure 2. Serum SIBLING levels in subjects with benign prostatic disease. Serum levels of (a) bone sialoprotein (BSP), (b) osteopontin (OPN) and (c) dentin sialophosphoprotein (DSPP) in samples from normal subjects (NL), subjects with benign prostatic hyperplasia (BPH), and subjects diagnosed prostate cancer (PCA) and were quantified using competitive ELISAs following sample extraction and clean-up.

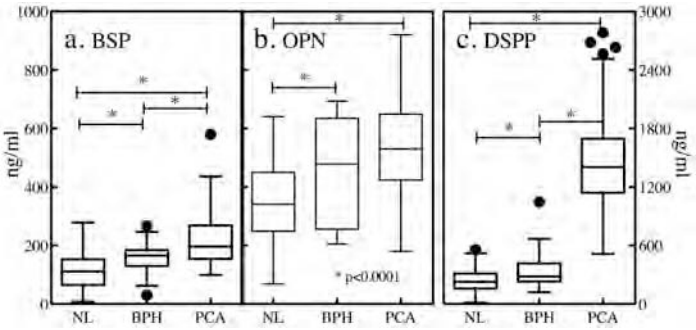

Task 2 Results. Determining the utility of serum SIBLING (BSP, OPN, DMP1 and DSPP) levels in predicting prostate cancer progression.

a. SIBLINGs and prostate cancer stage. The prostate cancer group, subjects whose serum was drawn at diagnosis and prior to any treatment, were clinically characterized by stage and were found to be distributed between stages II and IV. In order to assess early stage contribution of SIBLING levels,

additional prostate cancer sera were obtained from subjects with stage I disease (n = 18). The prostate cancer samples were segregated by stages (I, II, III and IV; where stage I cancer is localized and non-palpable by DRE, stage II cancer is localized within the prostate but palpable, stage III cancer has broken through the covering of the prostate but is still regional, and stage IV cancer has spread to other tissues. Only 18 subjects with stage 1 disease were identified for inclusion, while the rest of the prostate cancer samples were evenly distributed between stages II and IV. When the distribution of BSP, OPN and DSPP were profiled by stage using Tukey box plots, discrete patterns were observed (Figure 3). Both BSP and OPN only significantly increased in late stage disease, while DSPP was elevated from stage II onward.

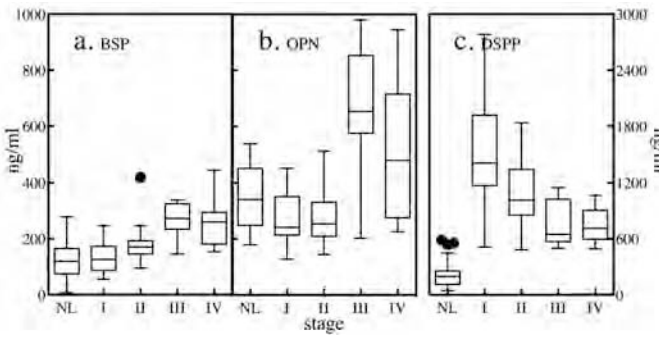

Figure 3. Serum SIBLINGs and prostate cancer stage. The distribution of SIBLING values between cancer stages was compared for (a) BSP, (b) OPN and (c) DSPP by box and whiskers plots. In Tukey plots, the box frame defines the lower and upper quartile, the whiskers depict 1.5 x the interquartile range, the line within the box marks the median value and the solid circles represent outliers.

b. SIBLINGs and disease progression.

The potential correlation of baseline SIBLING serum values with disease progression was investigated in subjects followed longitudinally for up to two years post diagnosis and treatment. Baseline SIBLING values were used to segregate study subjects by serum cut-off values. Progression was defined biochemically as an increase in at least two successive determinations of total serum PSA level (a significant increase taken as an increase of 0.5 ng/mL or more). The probability of remaining free of biochemical progression was estimated by Kaplan–Meier analysis (Figure 4).

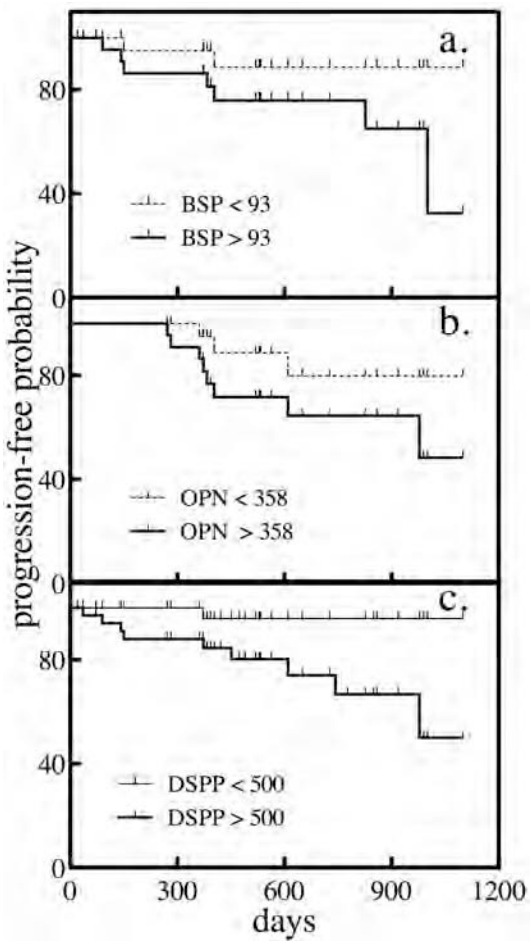

Figure 4. Baseline SIBLING values and disease progression. Biochemical progression-free rates in patients with clinically localized prostate cancer. Biochemical progression was defined as an increasing total serum prostate-specific antigen (PSA) level of 0.5 ng/mL or more.

Analysis of the biochemical progression of localized prostate cancer yielded one year survival rates of 95% for subjects whose baseline serum BSP was less than 93 ng/ml and 87% for subjects whose baseline BSP was greater than 93 ng/ml. For baseline OPN, survival rates were calculated to be 90% and 60 % for lees than and greater than the 358 ng/ml cut-off. For baseline DSPP, survival rates were calculated to be 100% and 88 % for lees than and greater than the 500 ng/ml cut-off, respectively. Two year survival rates for subjects with basekine SIBLING values above the fixed cut-off values ranged between 35 and 48 %. These results suggest that SIBLINGs can be employed for progression prediction.

Task 3 Results. Determining the utility of serum SIBLING (BSP, OPN, and DSPP) levels in assessing response to treatment.

Men with prostate cancer without metastatic disease, were grouped as having no treatment or treatment with gonadotropin-releasing hormone peptide analogues. A control group of age-matched men free of prostate cancer were recruited as controls. Serum samples were collected at baseline, 6 months and 12 months and BSP, OPN and DSPP were measured by competitive ELISA. The serum SIBLING levels of normal control males did not change at the different time points (Figure 5). In general, untreated prostate cancer patients demonstrated an increase in serum BSP, OPN and DSPP over baseline values. Adrogen depravation therapy (ADT) had no apparent effect on BSP levels, as both untreated and treated cancer patients exhibited significant increases in BSP levels. In contrast, ADT treatment was associated with a normalization of OPN serum values to that of control, untreated normal men. Serum DSPP levels were on average, reduced by ADT treatment to values below that of normal men. Because of the large subject to subject variation, a more definitive analysis of these SIBLINGs as either predictors or markers of response to treatment will require a larger sample size.

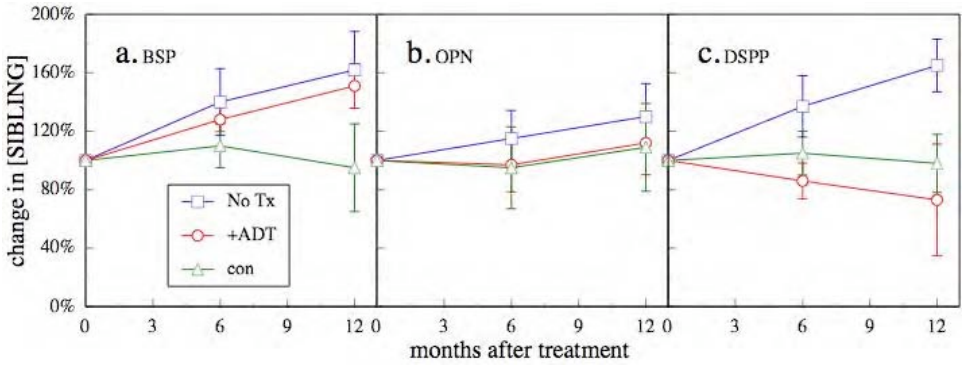

Figure 5. Percent change in serum SIBLINGs relative to baseline values. Normal men free of prostate cancer (n = 50), along with prostate cancer subjects without metastatic disease, receiving either no treatment (n = 50), or adrogen depravation therapy (n = 40) were followed for up to one year after initiation of treatment. Serum samples obtained every 6 months were analyzed by competitive ELISA for BSP, OPN and DSPP.

Implications from the completion of Tasks.

The data summarized above as well as that included in the attached manuscripts, indicate that SIBLINGs are promising markers for Prostate cancer. The SIBLING BSP appears to be a marker of disease progression, while OPN levels reflect immune or inflammatory components associated with prostate cancer. Of the SIBLINGs, DSPP has the highest sensitivity and specificity and by itself is a reasonable marker for prostate cancer detection. It is possible that DSPP measures, in combination with PSA measures may improve the specificity for prostate cancer detection, compared to PSA alone as a screen. Based on these results, the next logical steps are to move to larger scale clinical studies to assess SIBLINGs, and especially DSPP, as a marker for prostate cancer detection and progression.

Task-related Research:

An initial part of our research was to screen SIBLINGs for their pattern of expression in cancer [4]. The expression levels of five SIBLING gene family members – BSP, OPN, DMP1, MEPE, and DSPP as well as certain MMPs were determined using cancer profiling arrays containing normalized cDNA from both tumor and corresponding normal tissues from 241 individual patients representing 9 distinct cancer types. Significantly elevated expression levels were observed for BSP in cancer of the breast, colon, stomach, rectum, thyroid, prostate and kidney; OPN in cancer of the breast, uterus, colon, ovary, lung, rectum, prostate and thyroid; DMP1 in cancer of the breast, uterus, colon and lung; DSPP in breast, prostate and lung cancer. The degree of correlation between a SIBLING and its partner MMP was found to be significant within a given cancer type (e.g. BSP and MMP-2 in colon cancer, OPN and MMP-3 in ovarian cancer; DMP1 and MMP-9 in lung cancer). The expression levels of SIBLINGs were distinct within subtypes of cancer (e.g. breast ductal tumors compared to lobular tumors). In general, SIBLING expression increased with cancer stager [4].

We were also interested in SIBLING and MMP co-expression in normal epithelial tissues, the cells that upon transformation become the tumors studied above. All five SIBLINGs as well as MMP-2, -3 and -9 were found to be expressed in normal human salivary gland ducts [5]. In primates, all eight proteins were limited to the intercalated duct, striated duct, and to some degree the collecting ducts. Mature mouse salivary gland differed in two ways. First, all three of the MMPs and four of the five SIBLINGs were also expressed in the acini of mice. DSPP expression remained limited to the rodent ducts. Second, mature male mouse ducts under the strict control of androgens become almost exclusively granulated convoluted tubules and express none of the eight proteins. Salivary glands therefore show that a SIBLING and its MMP partner were always co-expressed and can be reasonably expected to form active complexes in the pericellular and extracellular spaces near these epithelial cells. These epithelial cells persist for many months or years and do not appear to be assisted by any other cell type in the maintenance of local matrix proteins. It is our hypothesis that the SIBLING/MMP partners are involved in the turnover of the pericellular and/or extracellular proteins of these metabolically active cells [5].

The SIBLING MEPE was unique in that its expression was not upregulated in any of the solid tumors that were investigated. MEPE was originally identified during a gene expression screen for oncogenic osteomalacia. The potential involvement of the SIBLING MEPE in linear nevus sebaceous syndrome (LNSS) was studied [6]. LNSS is a rare sporadic congenital phakomatosis that presents with epidermal hamartomas (tumor-like neoplastic anomalies) of unknown etiology. A recurrent phenotype of LNSS is bone loss similar to the hypophosphatemic vitamin D- resistant rickets associated with mesenchymal-derived neoplasms (tumor-induced osteomalacia). The serum levels and response to treatment of two phosphatonins (phosphate regulating hormones) fibroblast growth factor-23 (FGF-23) and MEPE was determined. A positive correlation between serum phosphorus and MEPE was found and the kinetics indicated that MEPE is downstream of FGF-23 [6].

Our previous work has shown that BSP can bind to matrix metalloproteinase-2 (MMP-2). Because of MMP activity in promoting tumor progression, potential therapeutic inhibitors were developed, but clinical trails have been disappointing. Using reagents developed during the course of the CDMRP-funded research, the effect of BSP on MMP-2 modulation by inhibitors was determined with purified components and in cell culture. Enzyme inhibition kinetic studies revealed that BSP increased the competitive inhibition constant (K_I) values between 15 and 47-fold for natural (TIMP2) and synthetic (ilomastat and oleoyl-N-hydroxylamide) inhibitors [7]. Two *in vitro* angiogenesis model

systems employing human umbilical vein endothelial cells (HUVECs) were used to follow BSP modulation of MMP-2 inhibition and tubule formation. Tubule formation by HUVECs co-cultured with dermal fibroblasts was reduced in the presence of inhibitors while the addition of BSP restored vessel formation. A second HUVEC cell culture system demonstrated that tubule formation by cells expressing BSP could be inhibited by an activity blocking antibody against MMP-2. BSP modulation of MMP-2 activity and inhibition may define its biological role in promoting tumor progression [7].

We had earlier observed that BSP can induce limited gelatinase activity in latent MMP-2 without removal of the propeptide and to restore enzymatic activity to MMP-2 previously inhibited by tissue inhibitor of matrix metalloproteinase-2 (TIMP2). Using reagents developed during this CDMRP-funded study, we identified structural domains in human BSP and MMP-2 that contribute to these interactions [8]. The 26 amino acid domain encoded by exon 4 of BSP is shown by a series of binding and activity assays to be involved in the displacement of MMP-2's propeptide from the active site and thereby inducing the protease activity. Binding assays in conjunction with enzyme activity assays demonstrate that both amino- and carboxy-terminal domains of BSP contribute to restoration of activity to TIMP2-inhibited MMP-2, while the MMP-2 hemopexin domain is not required for reactivation [8].

A manuscript describing the SIBLING gene family members, their association with cancer and potential utility as therapeutic targets was published in the March issue of the journal Nature Reviews Cancer [9]. In this review, we described the major characteristics of SIBLINGs including their proposed roles in normal tissue and the major activities they display during malignant progression. Finally, we discussed their potential as therapeutic targets and prognostic markers.

During a study of SIBLING expression in prostate cancer biopsies, an association was observed between macrophage infiltration and OPN staining. This lead to a study of serum levels of a marker of macrophage activation, neopterin, which was found to be correlated with OPN levels in prostate cancer but not in normal serum. Serum neopterin levels were found to be significantly elevated in prostate cancer and while the sensitivity of neopterin to detect prostate cancer would appear to be good (Figure 2), age and BMI were found to significantly modify neopterin values [11].

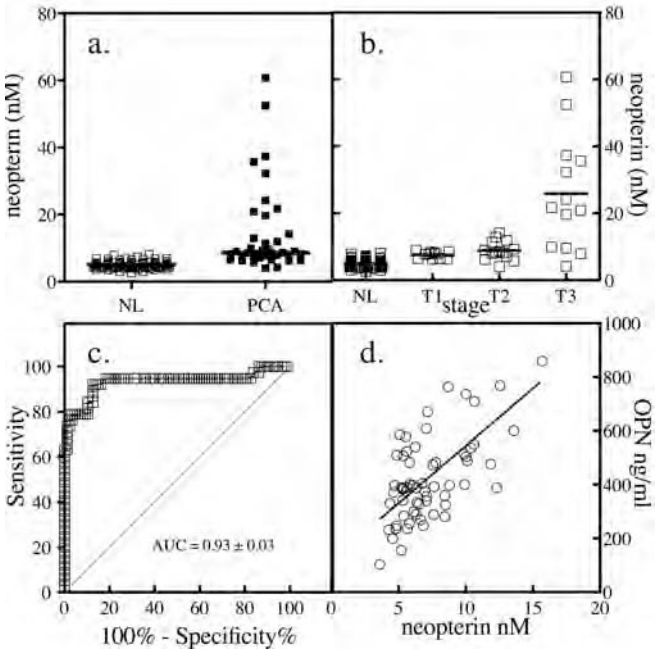

Figure 2. Immune activation in prostate cancer. Neopterin levels were measured by commercial ELISA in serum from a normal group and a group of subjects with prostate cancer (a). Samples were stratified by stage (b) and receiver operating characteristic curves were generated (c). Serum levels of neopterin and OPN were highly correlated, $r^2 = 0.4$, $p < 0.0001$ (d).

Similarly, the expression pattern of other SIBLINGs were found to be associated with apoptosis. DMP1 was positively associated while DSPP was negatively associated with apoptotic staining. This led

our research to testing three serum markers of apoptosis: soluble Fas (sFas), soluble Fas ligand (sFasL) and total cytochrome C (Cyt C). The marker sFasL is a pro-apoptosis factor, released Cyt C is a key intermediate and product of apoptosis, while sFas is anti-apoptosis factor. The distribution of these markers in a large well defined normal group as well as a group of recently diagnosed cancer patients was determined [12]. The study found that markers of apoptosis (sFasL and Cyt C) were decreased, while the anti-apoptosis marker sFas was elevated in prostate cancer (Figure 3.)

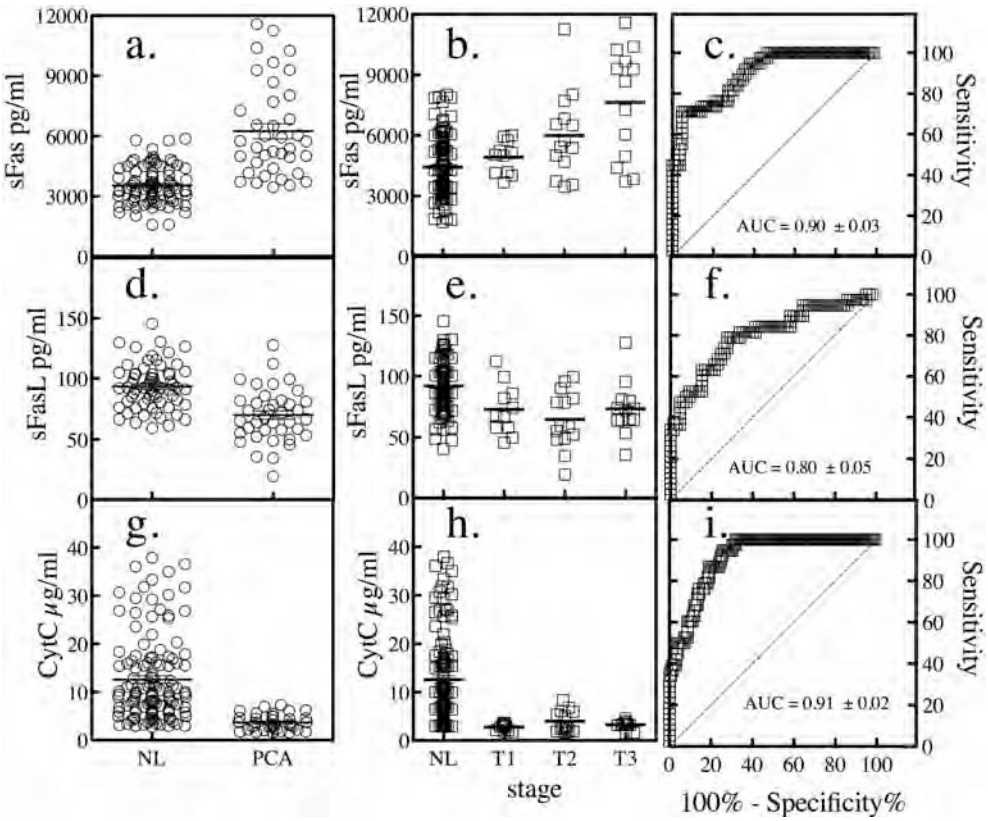

Figure 3. Global apoptosis is suppressed in prostate cancer. The anti-apoptosis marker sFas (a), pro-apoptosis marker sFasL (b) were measured by sandwich ELISA, while total Cyt C (c) was measured by a quantitative Western blot methodology. The markers were found to change with cancer stage (b, e, h) and exhibit reasonable sensitivity and specificity (c, f, i).

Chronic macrophage/immune activation (as reflected by elevated OPN and neopterin) and the shifting of the balance to block apoptosis (reduced sFasL and Cty C, elevated sFas) are likely to facilitate tumor development and progression. Macrophage activation modifies the extracellular environment, activating proteases, releasing and processing growth and angiogenic factors. Blocking apoptosis enables continued cancer cell survival.

Key Research Accomplishments

Assay Development:

Competitive ELISAs

completed for BSP, DSPP, MEPE and OPN.

Sandwich ELISAs

Completed for BSP, DMP1 and OPN

Assay stability

Reproducible results

Assay Application:

Competitive ELISAs of normal and prostate cancer sera completed for BSP, DSPP, MEPE and OPN
1,300 samples.

Results of note:

- SIBLINGs show a distinct staining pattern in prostate tumor biopsies.
- Of the SIBLINGs, DSPP exhibits the highest elevation in serum derived from subjects with prostate cancer.
- DSPP levels did not correlate with PSA values.
- DSPP exists as three distinct fragments in prostate cancer sera, while in normal serum the fragments are below the limit of detection.
- OPN levels reflect immune activation/macrophage infiltration in prostate cancer.
- BSP and DSPP are potentially informative markers for prostate cancer disease progression and response to treatment.

Reportable Outcomes

Publications

Fisher LW, Jain A, Tayback M, Fedarko NS. Small Integrin Binding Ligand N-Linked Glycoprotein (SIBLING) gene family expression in different cancers. Clin. Cancer Res. 2004; 10(24): 10:8501-8511.

Fisher LW, Karadag A, Ogbureke KUE, Fedarko NS. The SIBLING family of proteins; activators of MMPs. In: Proceedings of the 8th International Conference on the Chemistry and Biology of Mineralized Tissues. Sodek J, Landis WJ (eds). University of Toronto Press, (Toronto, Ontario, Canada) 2005. pp.170-173.

Hoffman WH, Jain A, Chen H, Fedarko NS. Matrix extracellular phosphoglycoprotein (MEPE) but not FGF-23, correlates with serum phosphorus prior to and during octreotide treatment and following excisional surgey in hypophosphatemic linear nevus sebaceous syndrome. Am J of Med Genet A, 2008; 146A(16):2164-8.

Jain A, Fisher LW, Fedarko NS. Bone sialoprotein alters MMP-2 affinity for natural and synthetic inhibitors. Biochemistry, 2008; 47(22): p. 5986-95.

Jain A, Karadag A, Fisher LW, Fedarko NS. Structural requirements for bone sialoprotein-binding and modulation of matrix metalloproteinase-2. Biochemistry, 2008; 47(38):10162-70.

Bellahcène A, Castronovo V, Ogbureke KUE, Fisher LW, Fedarko NS. Small Integrin-Binding LIgand N-linked Glycoproteins (SIBLINGs): Multifunctional proteins in cancer. Nature Cancer Reviews, 2008; 8:212-226.

Submitted Manuscripts:
Jain A, Fisher LW, Fedarko NS. Small Integrin Binding Proteins as Serum Markers for Prostate Cancer Detection. Clin Can Res. 2009 (included in Appendix)

Spencer ME, Jain A, Beamer BA, Leng SX, Matteini A, Punjabi NM, Walston JD, Fedarko NS. Associations of age, gender, BMI and disease stage with serum levels of the immune activation marker neopterin. J Geron Med Sci. 2008. (included in Appendix)

Invited Presentations

- "Emerging biomarkers." Advanced Studies in Translational Research on Aging (ASTRA) Pearl lecture series, National Institute on Aging, January 27th, 2005; Baltimore, MD.

- "What do bone proteins have to do with tumor progression?" The Sidney Kimmel Comprehensive Cancer Center At Johns Hopkins Longrifles Seminar Series, March 2nd, 2005; Baltimore MD.

- "MMP activation by SIBLINGs" Gordon Research Conference on Small Integrin-Binding Proteins, September 18th, 2005 Big Sky, MT.

- "The Small Integrin Binding Ligand N-linked Glycoprotein (SIBLING) family, protease activation and tumor progression. November 18th, 2005; University of Li∂ge, Belgium.

- "What do bone proteins have to do with cancer, inflammation and wound healing?" Johns Hopkins Bayview Medical Center Research Conference, February 16th, 2006; Baltimore MD.

- "A good death, cellularly." Clinical, Social, and Scientific Foundations of Geriatric Medicine, Division of Geriatric Medicine & Gerontology, Johns Hopkins University, June 20th, 2006; Baltimore, MD.

- "The role of bone proteins in tumor progression and metastasis." Johns Hopkins University Department of Orthopedics Grand Rounds, June 30th, 2006; Baltimore, MD.

- "Assessment of bone function by markers of bone turnover." Cancer-induced Bone Disease: Oncology RML Mid-Atlantic Training Session, July 27th, 2006; Baltimore, MD.

- "SIBLINGs as Serum Markers for Prostate Cancer." Gordon Research Conference on Small Integrin-Binding Proteins, August 8th, 2007 Biddeford, ME.

- "Small integrin binding proteins as serum markers for prostate cancer detection." Innovative Minds in Prostate Cancer Today (IMPaCT), Department of Defense Prostate Cancer Research Program. September 8, 2007; Atlanta, GA.

- "Biomarkers of aging and cancer." Clinical, Social, and Scientific Foundations of Geriatric Medicine, Division of Geriatric Medicine & Gerontology, Johns Hopkins University, October 2nd, 2008; Baltimore, MD.

Funding Received

- National Cancer Institute, NIH; R01 CA113865; "Small Integrin-Binding Proteins and Tumor Progression." The goal is to study the biological activity of SIBLINGs in regulated angiogenesis and metastasis in an MMP-dependent manner using both in vitro and in vivo animal model systems.

Conclusions

Significance

Prostate cancer is the leading cancer diagnosed among men in the United States. Detection is currently based on symptom presentation, physical examination including a digital rectal exam (DRE), measuring serum levels of prostate-specific antigen (PSA) and biopsy. The DRE can not detect certain tumors (that are nonpalpable or physically inaccessible) and PSA levels are elevated in certain non-cancerous conditions (acute prostatitis and benign prostatic hyperplasia). PSA measures have a high rate of false positive test results (the PSA is elevated but no cancer is present). False positives are associated with additional medical procedures, significant financial costs and mental stress. In addition both DRE and PSA can't detect early tumors and are sometimes uninformative in terms of predicting disease progression. Biopsies performed for confirmation of abnormal test results or to follow disease progression or response to treatment can have side-effects that impact profoundly upon the quality of life. Of the SIBLINGs, BSP and DSPP exhibit the highest discriminatory ability. The next step is to perform large population studies to confirm BSP and DSPP as markers of prostate cancer disease progression. If the utility of DSPP as an adjunct to PSA is replicated in a large population, it will have a significant effect on current prostate cancer management. The work has the potential to benefit individuals with prostate cancer across the spectrum from early detection to disease progression monitoring and modulating therapy. This was a pre-clinical, translational study that has set the groundwork for a large scale clinical trial.

Plans

The results so far indicate that a large scale clinical study of measuring DSPP serum levels is warranted. We also plan to pursue the identification of the prostate cancer-specific protease that cleaves DSPP and enables the appearance of the fragments in serum. Funding for a large population study is currently being pursued.

References

1. Fisher LW, Jain A, Tayback M, and Fedarko NS, *Small Integrin Binding LIgand N-linked Glycoprotein (SIBLING) gene family expression in different cancers.* Clin. Can. Res, 2004. **10**(24): p. 8501-8511.
2. Fedarko NS, Jain A, Karadag A, and Fisher LW, *Three small integrin binding ligand N-linked glycoproteins (SIBLINGs) bind and activate specific matrix metalloproteinases.* Faseb J, 2004. **18**(6): p. 734-6.
3. Freije JM, Balbin M, Pendas AM, Sanchez LM, Puente XS, and Lopez-Otin C, *Matrix metalloproteinases and tumor progression.* Adv Exp Med Biol, 2003. **532**: p. 91-107.

4. Fisher LW, Jain A, Tayback M, and Fedarko NS, *Small integrin binding ligand N-linked glycoprotein gene family expression in different cancers.* Clin Cancer Res, 2004. **10**(24): p. 8501-11.
5. Fisher LW, Karadag A, Ogbureke KUE, and Fedarko NS, *The SIBLING Family of Proteins; Activators of MMPs*, in *8th International Conference on the Chemistry and Biology of Mineralized Tissues*, J. Sodek and W.J. Landis, Editors. 2005, University of Toronto Press: Banff, Alberta, Canada. p. 70-173.
6. Hoffman WH, Jain A, Chen H, and Fedarko NS, *Matrix extracellular phosphoglycoprotein (MEPE) correlates with serum phosphorus prior to and during octreotide treatment and following excisional surgery in hypophosphatemic linear sebaceous nevus syndrome.* Am J Med Genet A, 2008. **146A**(16): p. 2164-8.
7. Jain A, Fisher LW, and Fedarko NS, *Bone sialoprotein binding to matrix metalloproteinase-2 alters enzyme inhibition kinetics.* Biochemistry, 2008. **47**(22): p. 5986-95.
8. Jain A, Karadag A, Fisher LW, and Fedarko NS, *Structural requirements for bone sialoprotein binding and modulation of matrix metalloproteinase-2.* Biochemistry, 2008. **47**(38): p. 10162-70.
9. Bellahcene A, Castronovo V, Ogbureke KU, Fisher LW, and Fedarko NS, *Small integrin-binding ligand N-linked glycoproteins (SIBLINGs): multifunctional proteins in cancer.* Nat Rev Cancer, 2008. **8**(3): p. 212-26.
10. Jain A, Fisher LW, and Fedarko NS, *Small Integrin Binding Proteins as Serum Markers for Prostate Cancer Detection.* Clini. Cancer Res., 2008. **Submitted**.
11. Spencer ME, Jain A, Beamer BA, Leng SX, Matteini A, Punjabi NM, Walston JD, and Fedarko NS, *Associations of age, gender, BMI and disease stage with serum levels of the immune activation marker neopterin.* J Gerontol A Biol Sci Med Sci, 2008. **Submitted**.
12. Kavathia N, Jain A, and Fedarko NS, *Serum markers of apoptosis (total cytochrome C, sFas, and sFasL) associate with gender age and cancer stage.* . J. Clin. Invest., 2008. **Submitted**.

Appendix

Fisher LW, Jain A, Tayback M, Fedarko NS. Small Integrin Binding Ligand N-Linked Glycoprotein (SIBLING) gene family expression in different cancers. Clin. Cancer Res. 2004; 10(24): 10:8501-8511..

Fisher LW, Karadag A, Ogbureke KUE, Fedarko NS. The SIBLING family of proteins; activators of MMPs. In: Proceedings of the 8th International Conference on the Chemistry and Biology of Mineralized Tissues. Sodek J, Landis WJ (eds). University of Toronto Press, (Toronto, Ontario, Canada) 2005. pp.170-173.

Hoffman WH, Jain A, Chen H, Fedarko NS. Matrix extracellular phosphoglycoprotein (MEPE) but not FGF-23, correlates with serum phosphorus prior to and during octreotide treatment and following excisional surgey in hypophosphatemic linear nevus sebaceous syndrome. Am J of Med Genet A, 2008; 146A(16):2164-8.

Jain A, Fisher LW, Fedarko NS. Bone sialoprotein alters MMP-2 affinity for natural and synthetic inhibitors. Biochemistry, 2008; 47(22): p. 5986-95.

Jain A, Karadag A, Fisher LW, Fedarko NS. Structural requirements for bone sialoprotein-binding and modulation of matrix metalloproteinase-2. Biochemistry, 2008; 47(38):10162-70.

Bellahcène A, Castronovo V, Ogbureke KUE, Fisher LW, Fedarko NS. Small Integrin-Binding LIgand N-linked Glycoproteins (SIBLINGs): Multifunctional proteins in cancer. Nature Cancer Reviews, 2008; 8:212-226.

“Small integrin binding proteins as serum markers for prostate cancer detection.” Innovative Minds in Prostate Cancer Today (IMPaCT), Department of Defense Prostate Cancer Research Program. September 8, 2007; Atlanta, GA. Abstract.

Jain A, Fisher LW, and Fedarko NS, Small Integrin Binding Proteins as Serum Markers for Prostate Cancer Detection. Clin. Cancer Res., 2009. **Submitted**.

Spencer ME, Jain A, Beamer BA, Leng SX, Matteini A, Punjabi NM, Walston JD, and Fedarko NS, *Associations of age, gender, BMI and disease stage with serum levels of the immune activation marker neopterin.* J Gerontol A Biol Sci Med Sci, 2008. **Submitted**.

Small Integrin Binding Ligand *N*-Linked Glycoprotein Gene Family Expression in Different Cancers

Larry W. Fisher,[1] Alka Jain,[2] Matt Tayback,[2] and Neal S. Fedarko[2]

[1]Craniofacial and Skeletal Diseases Branch, National Institute of Dental and Craniofacial Research, National Institutes of Health, Department of Health and Human Services, Bethesda, Maryland; and [2]Division of Geriatric Medicine, Department of Medicine, Johns Hopkins University, Baltimore, Maryland

ABSTRACT

Purpose: **Members of the small integrin binding ligand *N*-linked glycoprotein (SIBLING) gene family have the capacity to bind and modulate the activity of matrix metalloproteinases (MMPs). The expression levels of five SIBLING gene family members [bone sialoprotein (BSP), osteopontin (OPN), dentin matrix protein 1 (DMP1), matrix extracellular phosphoglycoprotein (MEPE), and dentin sialophosphoprotein (DSPP)] and certain MMPs were determined using a commercial cancer array.**

Experimental Design: **Cancer profiling arrays containing normalized cDNA from both tumor and corresponding normal tissues from 241 individual patients were used to screen for SIBLING and MMP expression in nine distinct cancer types.**

Results: **Significantly elevated expression levels were observed for BSP in cancer of the breast, colon, stomach, rectum, thyroid, and kidney; OPN in cancer of the breast, uterus, colon, ovary, lung, rectum, and thyroid; DMP1 in cancer of the breast, uterus, colon, and lung; and dentin sialophosphoprotein in breast and lung cancer. The degree of correlation between a SIBLING and its partner MMP was found to be significant within a given cancer type (*e.g.*, BSP and MMP-2 in colon cancer, OPN and MMP-3 in ovarian cancer; DMP1 and MMP-9 in lung cancer). The expression levels of SIBLINGs were distinct within subtypes of cancer (*e.g.*, breast ductal tumors compared with lobular tumors). In general, SIBLING expression increased with cancer stage for breast, colon, lung, and rectal cancer.**

Conclusions: **These results suggest SIBLINGs as potential markers of early disease progression in a number of different cancer types, some of which currently lack vigorous clinical markers.**

INTRODUCTION

The small integrin-binding ligand *N*-linked glycoprotein (SIBLING) gene family is clustered on human chromosome 4, and its members include bone sialoprotein (BSP), osteopontin (OPN), dentin matrix protein 1 (DMP1), matrix extracellular phosphoglycoprotein (MEPE), and dentin sialophosphoprotein (DSPP; ref. 1). SIBLINGs are normally thought to be restricted in expression to mineralizing tissue such as bones and teeth (1). Retrospective studies using pathological specimens have shown that OPN expression occurs in cancer of the breast, colon, stomach, ovary, lung, thyroid, kidney, prostate, and pancreas (2, 3). The expression of other SIBLING members in cancer has not been extensively studied. BSP expression was been reported in breast (4, 5), prostate (6), lung (7), and thyroid cancer (8). DMP1 has been shown to be strongly up-regulated in lung cancer (9). Elevated levels of MEPE mRNA expression by tumors from patients with hypophosphatemia and osteomalacia have been reported (10). The neoplastic expression pattern of DSPP has not been defined.

Matrix metalloproteinases (MMPs) are critical for development, wound healing, and the progression of cancer. We have recently shown that BSP, OPN, and DMP1 specifically bind to pro–MMP-2, pro–MMP-3, and pro–MMP-9, respectively, thereby activating the latent proteolytic activity (11). Furthermore, it was shown that active MMPs inhibited by either tissue inhibitors of MMPs or low molecular weight synthetic inhibitors were reactivated by their corresponding SIBLING. The current study was undertaken to determine the mRNA expression patterns of SIBLINGs in nine different types of cancer. An additional goal was to determine whether SIBLINGs exhibited expression levels that correlated with their MMP partners as well as various measures of tumor progression.

MATERIALS AND METHODS

Cancer Array Analysis. A cancer profiling array (product 7841-1; Clontech, Palo Alto, CA) containing normalized cDNA from tumor and corresponding normal tissues from 241 individual patients was used to screen for SIBLING and MMP expression (12). Several cancer profiling arrays were hybridized in ExpressHyb hybridization solution (Clontech) with ^{32}P-labeled cDNA probes as per the manufacturer's instructions. Briefly, 1 to 2 $\times$ 10^7 cpm of random-prime labeled cDNA was made single stranded by heating to 95°C for 5 minutes and allowed to hybridize with the prepared membrane overnight at 65°C. Membranes were washed in a series of high stringency washes as recommended by the manufacturer. The washed membranes were quantified by exposure to PhosphorImager screens for 1 to 24 hours, and the exposed screen was analyzed on a PhosphorImager (Amersham Biosciences, Piscataway, NJ)

Received 6/1/04; revised 9/10/04; accepted 9/17/04.
Grant support: Grants CA 87311 (N. Fedarko) and DAMD17-02-0684 (N. Fedarko).
The costs of publication of this article were defrayed in part by the payment of page charges. This article must therefore be hereby marked *advertisement* in accordance with 18 U.S.C. Section 1734 solely to indicate this fact.
Requests for reprints: Neal S. Fedarko, Room 5A-64 JHAAC, 5501 Hopkins Bayview Circle, Baltimore, MD 21224. Phone: 410-550-2632; Fax: 410-550-1007; E-mail: ndarko@jhmi.edu.

using the manufacturer's ImageQuant program. All polymerase chain reaction (PCR) products were subcloned into a shuttle plasmid, cloned, and sequenced, and the inserts were gel-purified before ^{32}P labeling by random priming. Unincorporated label was removed before hybridization.

SIBLING Probes. The labeled DNA used for probing was obtained as follows. Human BSP and OPN were cDNA inserts released from OP-10 and B6-5g plasmids, respectively (13, 14). Human DMP1 insert was the ~1.4-kb coding region of exon 6 (15) amplified from human genomic DNA subcloned into pBluescript at the *Eco*RI and *Bam*HI sites using oligonucleotides ATTATAGAATTCAAATGAAGACCCCAGTGACAG (forward) and TAATTAGGATCCAATAGCCGTCTTGGCAGTC (reverse). The MEPE probe was a 1.45-kb, exon 5, cDNA insert corresponding to the last exon of human MEPE, which constitutes 95% of the mature protein as defined by Rowe *et al.* (10). The exon was amplified by PCR from human genomic DNA using a 5′ oligonucleotide with a *Nde*I restriction site engineered in AGTACCCATATGAAAGACAATATTGGTTTTCACCAT and a 3′ oligonucleotide with a *Bam*HI site (CTGATGGGATCCCTAGTCACCATCGCTCTCAC). The PCRproduct was subcloned into pBluescript and sequenced, and the ~1.5-kb insert was released with *Nde*I plus *Bam*HI and labeled. The DSPP probe corresponding to the last exon was similarly amplified using a 5′ oligonucleotide with a *Hind*III restriction site engineered in CTGTTGGTACCGATATCGAAATCAAGGGTCCCAGCAG and a 3′ oligonucleotide with a *Kpn*I restriction site (GTGCAAAGCTTCTAATCATCACTGGTTGAGTGG), subcloned, and sequenced, and the released ~2.6-kb insert was labeled.

Matrix Metalloproteinase Probes. Specific probes of ~300 bp each for human MMP-2, MMP-3, and MMP-9 were made by PCR using human genomic DNA as template and the following oligonucleotides: MMP-2, ATTAGGATCCGGTCACAGCTACTTCTTCAAG (forward with *Bam*HI site added for subcloning) and ATATGGATCCGCCTGGGAGGAGTACAG (reverse with *Bam*HI site); MMP-3, ATATGGATCCAGCTGGCTTAATTGTTGAAAG (forward with *Bam*HI) and TAATGGATCCAACTGACAAATCGTCTTTATTA (reverse with *Bam*HI); and MMP-9, AATTGAATTCAGAGAAAGCCTATTTCTGCCAG (forward with *Eco*RI) and TAATGAATTCGGTTAGAGAATCCAAGTTTATTAG (reverse with *Eco*RI). In each case, the PCR products were subcloned into pBluescript and verified by sequencing, and the ~0.3-kb inserts were released and labeled. Membranes were used up to three times, each time removing the previous probe according to the manufacturer's instructions. The stripped membranes were reimaged by PhosphorImager to verify the removal of the previous probe.

Statistical Analysis. Clinical data linked to samples spotted on the cancer profiling array were accessed through the manufacturer's World Wide Web-based database.[3] Comparisons between normal and tumor tissue (derived from the same subject) were performed using a paired *t* test. The coordinated expression of SIBLINGs with MMP binding partners in tumors was tested by regression analysis. Significant differences in tumor subtype expression of SIBLINGs was tested by Student's *t* test. The association of SIBLING expression levels with tumor stage was investigated using a conservative statistical approach. The nonparametric Spearman rank order correlation was used to examine the correlation of tumor stage and SIBLING expression. The analysis was performed on untransformed data, and the adjusted Spearman correlation coefficient (r_S) is reported. All statistical calculations were carried out using StatView software (SAS Institute, Inc., Cary, NC).

RESULTS

SIBLINGs Are Elevated in Multiple Cancer Types. Because BSP and OPN protein expression have been found to be greatly increased in many separate, often immunohistochemistry-based studies of different neoplasms, the expression levels of five SIBLING gene family members were determined using a commercial cancer array. The array included normalized cDNA from tumor and corresponding normal tissues from 241 individual patients, as well as certain internal controls (Fig. 1). Because the sample sizes were too small for some tumor types on the array, the tissues reported for this study include only breast, uterus, colon, stomach, ovary, lung, kidney, rectum, and thyroid. In each array experiment, the patient's normal and tumor cDNA was separately hybridized with ^{32}P-labeled probes for BSP, OPN, DMP1, MEPE, and DSPP, and the array was digitized by PhosphorImager. Whereas BSP, DMP1, and DSPP exhibited minimal normal tissue expression, significant OPN expression by normal tissues was observed. In fact, the highest levels of expression of OPN were seen in normal kidney. Because MEPE expression was minimal in both normal and tumor tissue, its expression was not analyzed further (data not shown). The amount of hybridized probe was quantified, and the average expression values of BSP, OPN, DMP1, and DSPP in normal and tumor tissue were compared (Fig. 2). The expression levels of BSP were significantly elevated (from 2- to 6-fold) in cancer of the breast, colon, rectum, thyroid, and kidney. OPN expression was significantly elevated (2- to 4-fold) in cancer of the breast, uterus, colon, ovary, lung, rectum, and thyroid. DMP1 exhibited significant (1.7- to 3-fold) elevated expression in cancer of the breast, uterus, colon, and lung, whereas DSPP exhibited significant (2-fold) increase in cancer of the breast and lung. Elevated SIBLING family expression was greatest in breast cancer, in which expression of four different family members was increased. Colon, lung, and thyroid cancer had significantly elevated expression of three different SIBLING family members. Of the nine different types of tumors quantified, each one had a significantly high expression of at least one SIBLING.

Matrix Metalloproteinases Are Elevated in Multiple Cancer Types. We have recently shown that three members of the SIBLING family can specifically bind and modulate the activity of three different MMPs (11). The SIBLINGs BSP, OPN, and DMP1 were found to bind to and modulate the activity of MMP-2, MMP-3, and MMP-9, respectively. Corresponding MMP partners for DSPP and MEPE, if any, have yet to be identified. Because MMPs have been postulated to play major roles in tumor cell progression and metastasis (16), the expression levels of SIBLING-matched MMPs were screened in

[3] http://bioinfo.clonetech.com/dparray/array-list-action.do.

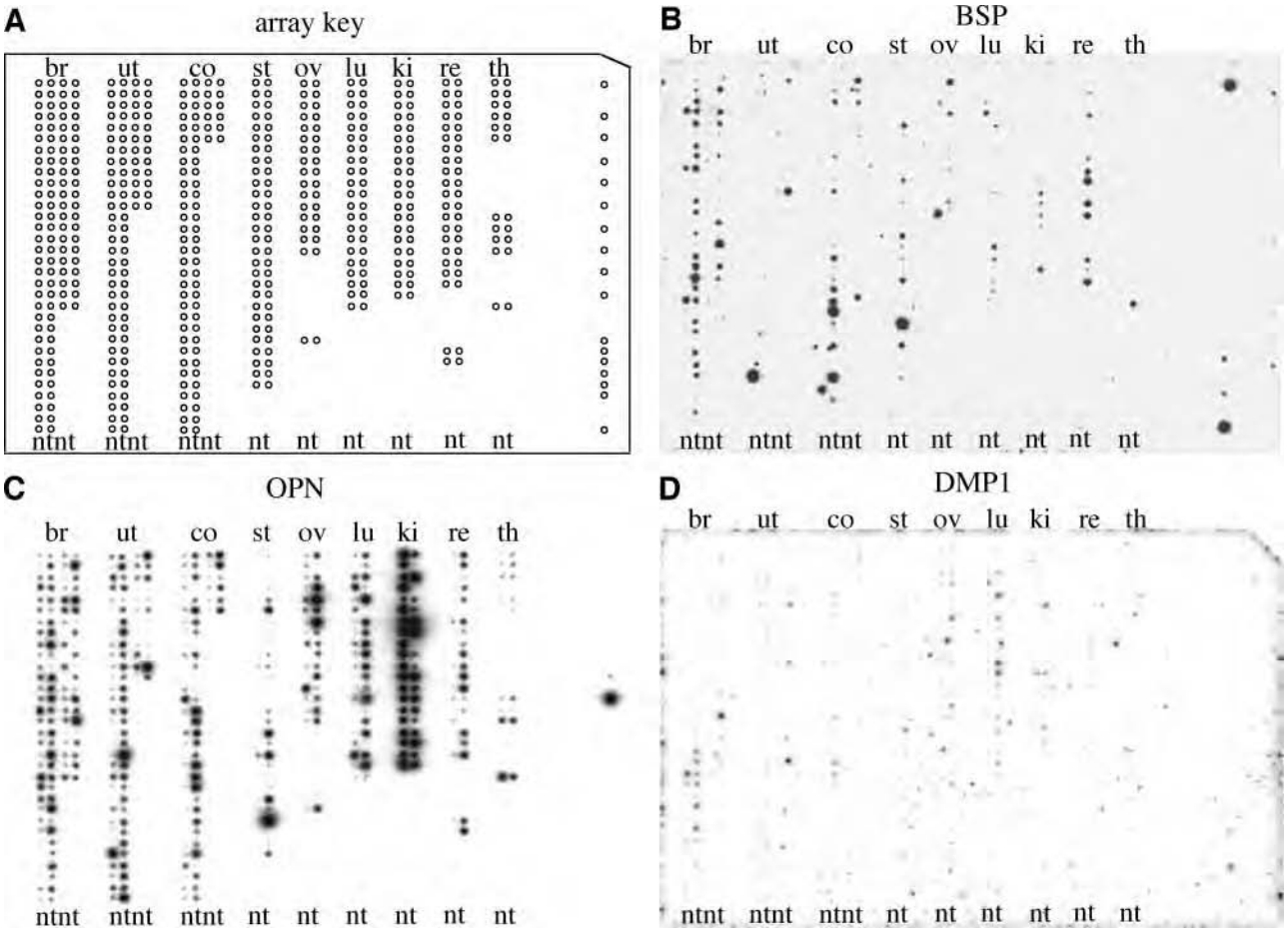

Fig. 1 SIBLING expression in different cancer types. A cancer profiling array was hybridized with cDNA probes for SIBLINGs. The arrays contained samples from 13 different types of cancer with paired normal and tumor tissue mRNA from individual subjects (*A*). The amount of hybridized probe for BSP (*B*), OPN (*C*), and DMP1 (*D*) was visualized by PhosphorImager. *br*, breast cancer; *ut*, uterine cancer; *co*, colon cancer; *st*, stomach cancer; *ov*, ovarian cancer; *lu*, lung cancer; *ki*, kidney cancer; *re*, rectal cancer; *th*, thyroid cancer; *n*, normal tissue; *t*, tumor tissue. Those hybridization spots that are not contiguous with the identified tumor types represent patient samples with tumor types too few in number to be statistically useful.

different cancer types. The cancer arrays were separately hybridized with probes for MMP-2, MMP-3, and MMP-9, and the expression values between normal tissue and the corresponding tumor sample for each patient were compared (Fig. 3). MMP-2 expression was significantly elevated in cancer of the colon, stomach, lung, and rectum. MMP-3 expression exhibited significant elevation in cancer of the breast, colon, stomach, and rectum. MMP-9 expression levels were significantly elevated in cancer of the breast, uterus, colon, stomach, ovary, lung, rectum, and kidney. The increases in expression ranged from 2- to 3-fold higher for MMP-2 and MMP-3, whereas expression levels were increased 2- to 7-fold for MMP-9.

Correlated Expression of SIBLINGs and Their Partner Matrix Metalloproteinases. Given the observed binding and activation specificity seen with SIBLINGs and their partner MMPs [BSP with MMP-2, OPN with MMP-3, and DMP1 with MMP-9 (11)], it was reasonable to postulate that SIBLINGs and their paired MMPs might exhibit correlated expression levels. When the levels of SIBLING and matched MMP expressed by individual tumors were analyzed by regression analysis, significant correlation was seen within different cancer types (Fig. 4). The expression of BSP and MMP-2 was significantly correlated in breast and colon cancer [$r^2 = 0.40$ ($P \leq 0.0001$) and $r^2 = 0.36$ ($P \leq 0.0001$), respectively]. OPN pairing with MMP-3 showed a significant correlation in stomach and ovarian cancer [$r^2 = 0.52$ ($P \leq 0.0001$) and $r^2 = 0.45$ ($P \leq 0.005$), respectively]. DMP1 and MMP-9 expression was significantly correlated in lung and kidney cancer [$r^2 = 0.60$ ($P \leq 0.001$) and $r^2 = 0.39$ ($P \leq 0.05$), respectively]. Mismatched pairs of BSP with MMP-3, OPN with MMP-2, or DMP1 with MMP-2, for example, showed no significant correlation (data not shown).

SIBLING Expression Is Distinct in Different Cancer Subtypes. Within cancers arising from a given tissue/organ, there are histopathologically defined subtypes that are often used in assessing disease course and treatment. There were sufficient numbers of breast cancer array samples to permit segregation by clinically defined subtypes of ductal *versus* lobular tumors. The results of microarray screening of SIBLING

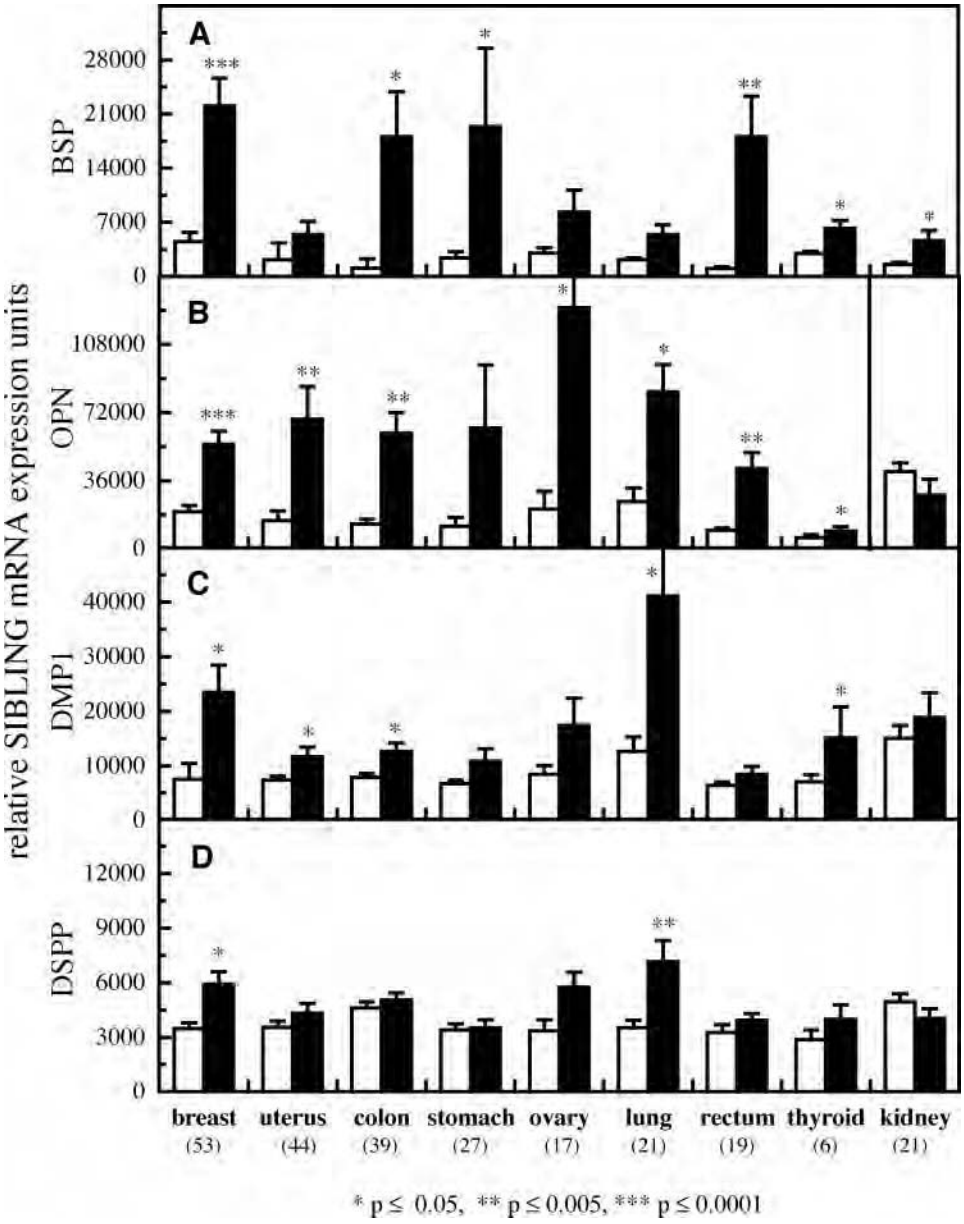

Fig. 2 SIBLING mRNAs are induced in multiple cancer types. Digitized exposures from Fig. 1 were quantified using ImageQuant software, and the mean values of relative expression of BSP (*A*), OPN (*B*), DMP1 (*C*), and DSPP (*D*) in normal tissue (□) and tumor tissue (■) were determined for each of nine different cancer types. *Asterisks* denote the statistical significance as determined by paired *t* tests. *, $P \leq 0.05$; **, $P \leq 0.005$; ***, $P \leq 0.0001$. *Error bars* represent the SE, and *numbers in parentheses* represent the number of subjects. OPN expression in both normal and tumor tissue from kidney is shown at one-tenth the actual mean values.

expression in breast cancer tissue were segregated by the pathological classification, and the average values of each group were compared (Fig. 5*A*). SIBLING mRNA levels were significantly higher in the ductal cancer groups, whereas the levels in the lobular group were intermediate between normal and ductal levels.

A similar analysis was carried out on uterine cancer samples, where there were sufficient numbers to permit segregation into clinically defined subtypes of adenocarcinoma, squamous cell, and benign tumors (Fig. 5*B*). OPN expression was significantly different between the two subtypes of malignant uterine tumors ($P \leq 0.005$) and between malignant and benign tumors ($P \leq 0.05$). The adenocarcinoma subtype expressed higher levels than the squamous cell subtype.

SIBLING Expression and Tumor Stage. Defined cancer stages represent how large the tumor is and how far it may have spread. The association of SIBLING expression levels with tumor progression was investigated by identifying tumor types with sufficient clinical detail to stratify into different tumor stages. Tumors from colon, rectal, and lung cancer were grouped by stage, and the distribution of SIBLINGs was compared (Fig. 6). In general, cancer stages mark tumors that were either localized and had a relatively small size (stage I), localized and larger in size (stage II), metastasized to lymph nodes (stage III), or metastasized to distant sites (stage IV). Colon cancer tumors exhibited mean values of BSP, OPN, DMP1, and DSPP that increased between stage I and stage III. Colon tumors with distant metastases exhibited SIBLING values with a sim-

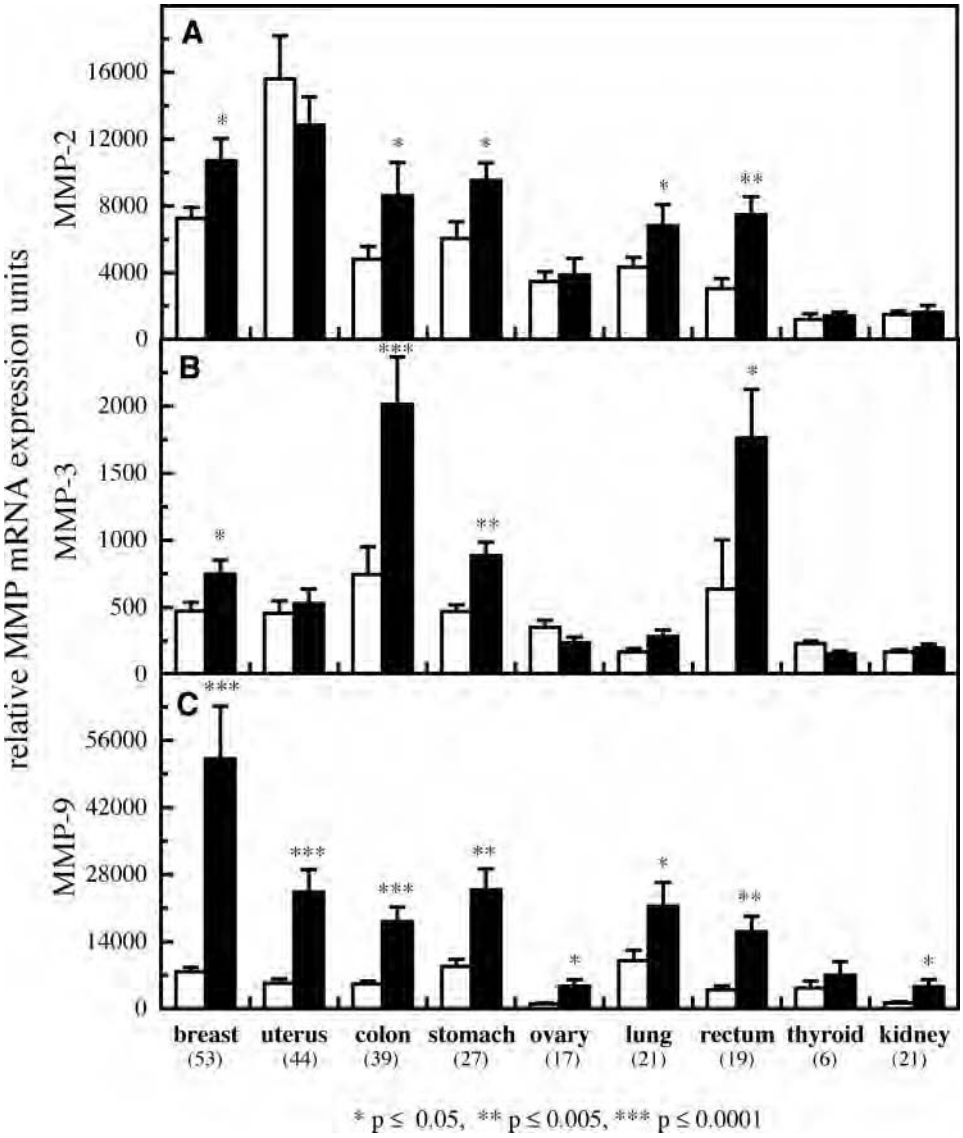

Fig. 3 MMP mRNAs are induced in multiple cancer types. Cancer profiling arrays were hybridized with cDNA probes for different MMPs, the amount of hybridized probe was quantified using ImageQuant software, and the mean values of expression of MMP-2 (*A*), MMP-3 (*B*), and MMP-9 (*C*) in normal tissue (□) and tumor tissue (■) were determined for each of nine different cancer types. *Asterisks* denote the statistical significance as determined by paired *t* tests. *, $P \leq 0.05$; **, $P \leq 0.005$; ***, $P \leq 0.0001$. *Error bars* represent the SE, and *numbers in parentheses* represent the number of subjects.

ilar or lower pattern of distribution than that of stage III tumors. Rectal cancer tumors showed increasing BSP, OPN, and DMP1 levels from stage I to stage IV, whereas DSPP values were unchanged across different stages. In lung cancer, BSP, OPN, and DSPP levels increased with increasing stage. When the association of SIBLING expression and tumor stage in colon cancer was analyzed by Spearman rank order correlation analysis, only BSP was significantly correlated (Table 1). In rectal tumors, BSP, OPN, and DMP1 levels correlated with stage, whereas for lung cancer, BSP, OPN, and DSPP levels correlated with stage.

Breast cancer tumors were stratified into tumor-node-metastasis (TNM) stages, which reflect tumor size (T), lymph node involvement (N), and metastatic state (M). Enough breast tumor samples were analyzed to enable the analysis of SIBLING expression and tumor progression. Tumors were grouped by TNM stage, and the stages were ordered in sequence of increasing progression. The sequence of tumors ranged from those with no nodal involvement or metastasis state (N_0M_0) that increased in size as well as N_1M_0 tumors that increased in size. For BSP, OPN, DMP1, and DSPP, significant differences were observed in the expression pattern as a function of tumor progression (Fig. 7; Table 1). Spearman rank order correlation analysis of SIBLING values and TNM stage yielded significant correlation for all four SIBLINGs.

DISCUSSION

Microarray technology has been typically used to screen the simultaneous expression of many genes using an array spotted with thousands of genes and measuring hybridization of target cDNA generated from a given tissue or cell type. In contrast, the cancer profiling array used in the current study was developed to enable the quantification of expression of a single

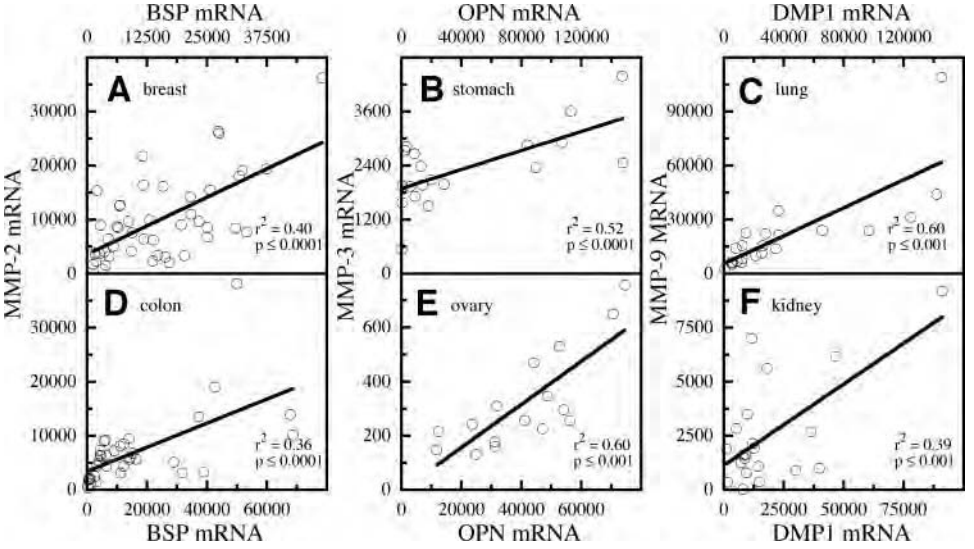

Fig. 4 Paired SIBLING and MMP expression is correlated in specific cancers. The expression levels of SIBLINGs and their respective binding partner MMPs were analyzed by regression analysis. BSP and MMP-2 levels in breast (*A*) and colon cancer (*D*), OPN and MMP-3 levels in stomach (*B*) and ovarian cancer (*E*), as well as DMP1 and MMP-9 levels in lung (*C*) and rectal cancer (*F*) were paired by subject and analyzed by regression analysis.

gene across multiple tissue types and tumor stages. The cancer profiling array contained multiple cDNA pairs from normal and tumor tissues including breast, uterus, colon, stomach, ovary, lung, kidney, rectum, thyroid, prostate, small intestine, pancreas, and cervix. Complementary DNA was generated by an efficient cDNA amplification technique that is based on the switching mechanism at the 5′ end of mRNA templates (17). This methodology has been shown to yield a high representation of mRNA transcripts, avoidance of biased amplification, linearity of signal, and recapitulation of the complexity of the original mRNA (12). Because the expression of individual housekeeping genes varies between normal and tumor tissue (18–20), the

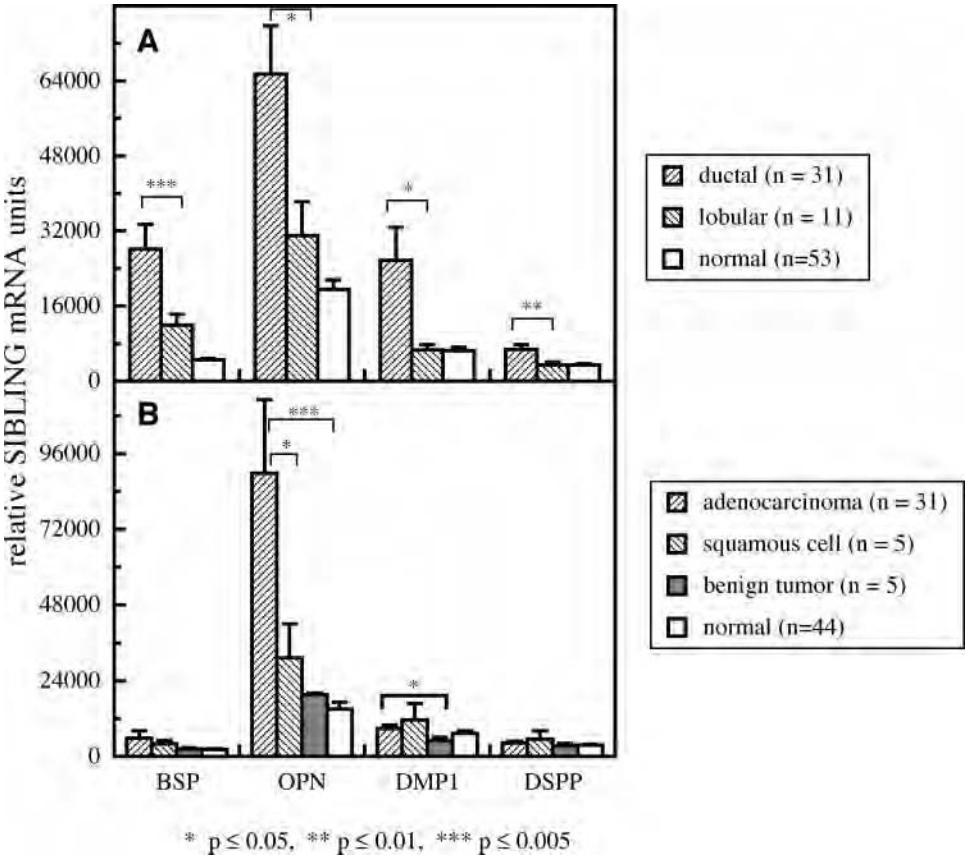

Fig. 5 SIBLING expression distinguishes cancer subtypes for breast and uterine tumors. The expression values of BSP, OPN, DMP1, and DSPP by breast cancer tumors were stratified by pathological classification (ductal *versus* lobular), and the average values were compared (*A*). Similarly, the expression of SIBLINGs by uterine tumors stratified into groups defined as adenocarcinoma, squamous cell, or benign tumor were averaged and compared (*B*). *Asterisks* denote the statistical significance as determined by *t* test. *, $P \leq 0.05$; **, $P \leq 0.01$; ***, $P \leq 0.005$. *Error bars* represent the SE.

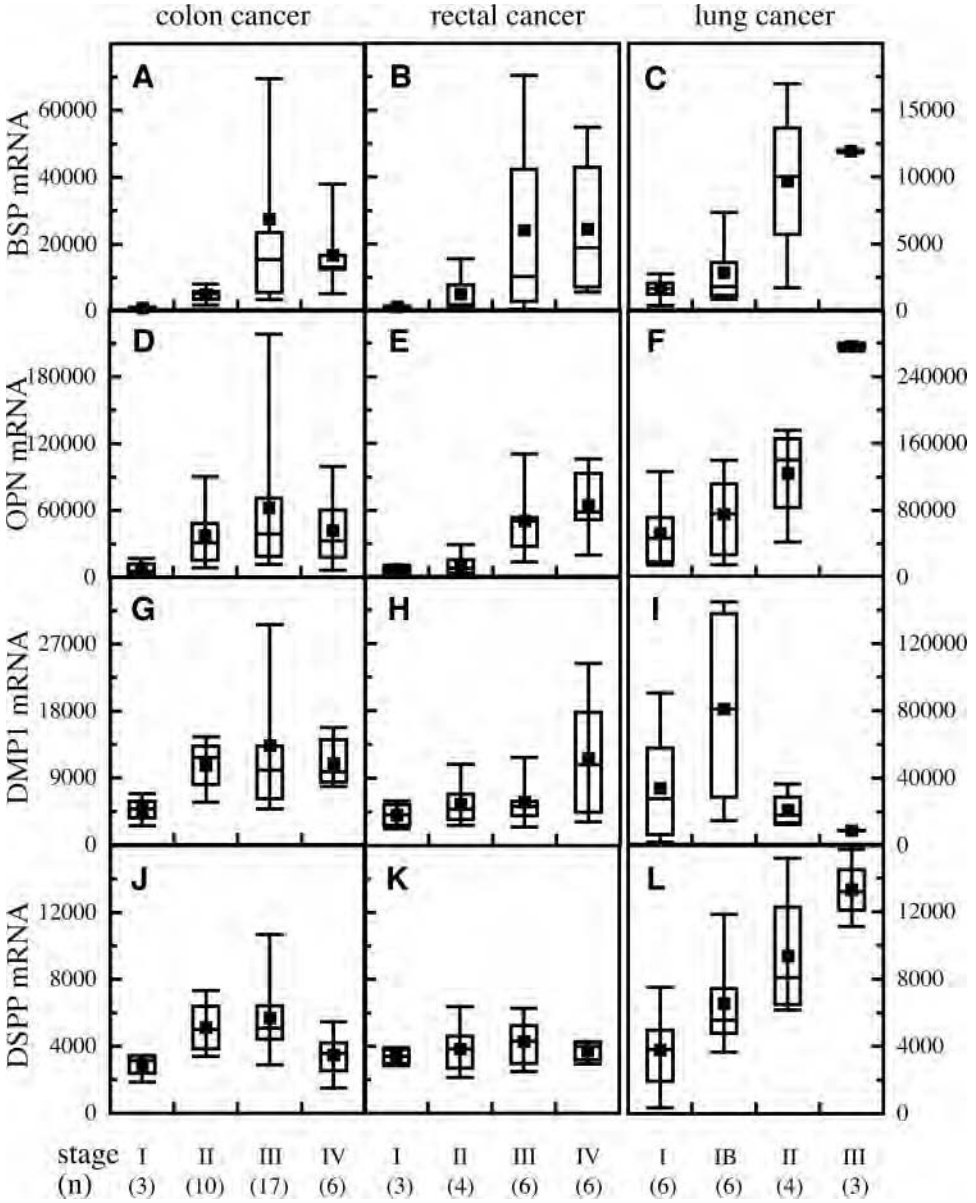

Fig. 6 Comparison of SIBLING mRNA levels with tumor stage in colon, rectal, and lung cancer. The expression values of BSP (*A*−*C*), OPN (*D*−*F*), DMP1 (*G*−*I*), and DSPP (*J*−*L*) by colon cancer tumors (*A*, *D*, *G*, and *J*), rectal cancer tumors (*B*, *E*, *H*, and *K*), and lung cancer tumors (*C*, *F*, *I*, and *L*) were stratified by pathological classification (stage), and the average values were compared. *Top line*, *bottom line*, and *line through the middle* correspond to 75th percentile, 25th percentile, and 50th percentile (median), respectively. *Error bar whiskers* represent the 10th and 90th percentile, whereas ■ indicates the arithmetic mean. Rectal and colon cancer stages were as follows: I, tumor invaded submucosa; II, tumor invaded through muscularis propia; III, invasive tumor with metastasis in one to three pericolic or perirectal lymph nodes; and IV, invasive tumor with metastasis in pericolic or perirectal lymph nodes and distant metastasis. Lung cancer stages were as follows: I, tumor $<$ 3 cm in greatest dimension; IB, tumor $>$ 3 cm in greatest dimension, involved main bronchus, associated with atelectasis or obstructive pneumonitis; II, metastasis to ipsilateral peribronchial and/or ipsolateral lymph nodes; and III, metastasis to ipsilateral mediastinal, and/or subcarinal lymph nodes. The number of subjects (*n*) for each group is shown at the *bottom*.

equal loading of cDNA onto the array membrane was carried out by normalizing to the average expression of three housekeeping genes: ubiquitin, β-actin, and M_r 23,000 highly basic protein (12, 21). The array has recently been used to profile a number of genes that exhibited either up- or down-regulation in cancer including gelsolin and glutathione peroxidase (12), netrin 1 (22), thiamin transporter THTR2 (23), PAGE 4 (24), and XAGE-1 (25). Strong correlation between tumor tissue expression by the current cDNA microarray and by *in situ* hybridization (24, 25) as well as reverse transcription-PCR and immunohistochemical staining (26, 27) has been observed.

The microarray design pairing normalized cDNA from an individual subject's tumor and normal tissue enabled differences in expression to be analyzed by paired *t* test, which provided a greater power to detect significant differences. Another method of evaluating the significance of biomarker elevation is to compare target tissue measures to a cut point of the mean of normal levels plus twice the SD (m + 2 SD). A value of $>m$ + 2 SD translates to a $<$5% probability that the elevation is due to chance (95% of normal values will lie within the m + 2 SD range). The overall significance of the microarray results was assessed by comparing concordance between these two methods of analysis, as well as comparison with the published results of other studies (Table 2). Elevated BSP expression was identified in two tissues (breast and thyroid), in agreement with previous studies. The current results for BSP did not replicate previous reports on elevated expression in cancer of the uterus or lung. Novel expression was identified in four different cancer types (colon, stomach, rectum, and kidney). Elevated OPN expression was observed in the current study in four different cancer types

Table 1 SIBLING expression and tumor staging

Spearman rank order correlation	BSP	OPN	DMP1	DSPP
Colon cancer*				
Spearman coefficient (r_S)	0.61	0.29	0.26	0.20
P	<0.001	>0.05	>0.05	>0.05
Rectal cancer*				
Spearman coefficient (r_S)	0.61	0.72	0.49	0.28
P	<0.005	<0.001	<0.05	>0.05
Lung cancer*				
Spearman coefficient (r_S)	0.70	0.70	−0.18	0.77
P	<0.001	<0.001	>0.05	<0.0005
Breast cancer†				
Spearman coefficient (r_S)	0.62	0.38	0.37	0.47
P	<0.0005	<0.05	<0.05	<0.005

* Spearman rank order correlation between mean SIBLING values and tumor stage. The Spearman coefficient value (r_S) is an adjusted value (corrected for ties). Tumor stages for colon, rectal, and lung cancer were defined as stated in the Fig. 5 legend.

† Correlation between mean SIBLING values and breast tumor progression. Spearman rank order correlation was performed on breast tumor SIBLING expression levels grouped by TNM stage and ordered across increasing progression ($T_1N_0M_0$, $T_2N_0M_0$, $T_3N_0M_0$, $T_1N_1M_0$, $T_2N_1M_0$, $T_3N_1M_0$). Breast tumor T stages were defined as stated in the Fig. 6 legend.

(breast, colon, ovary, and lung) in agreement with other published studies. For cancer of the stomach, thyroid, and kidney, the OPN expression levels and published literature were not in concordance. Novel expression of OPN in cancer of the uterus and rectum was identified. Elevated DMP1 expression was confirmed in lung cancer and newly identified in breast cancer. DMP1 levels in cancer of the uterus and colon, although significantly elevated by paired *t* test, did not satisfy the $>m + 2$

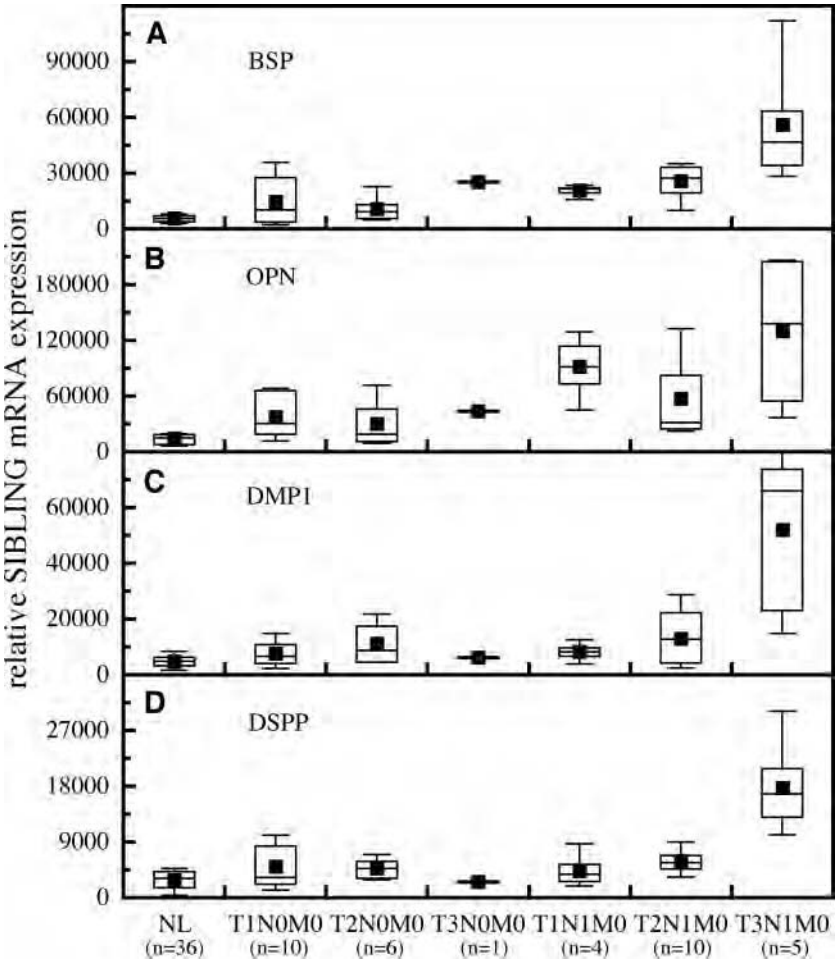

Fig. 7 Comparison of SIBLING mRNA levels and tumor stage in breast cancer. The expression values of BSP (*A*), OPN (*B*), DMP1 (*C*), and DSPP (*D*) by breast cancer tumors were stratified by increasing TNM stage, and the values were compared. *Top line*, *bottom line*, and *line through the middle* correspond to 75th percentile, 25th percentile, and 50th percentile (median), respectively. *Error bar whiskers* represent the 10th and 90th percentile, whereas ■ indicates the arithmetic mean. Breast cancer TNM staging was as follows: T_1, tumor ≤ 2 cm in greatest dimension; T_2, 2 cm < tumor < 5 cm; T_3, tumor > 5 cm; N_0, no regional lymph node metastasis; N_1, metastasis to movable ipsilateral axillary lymph node(s); N_2, metastasis to movable ipsilateral axillary lymph node(s) fixed to one another or to other structure; M_0, no distant metastasis; and M_1, distant metastasis. The number of subjects (*n*) for each group is shown at the *bottom*. The normal group consisted of the 36 normal breast tissue samples corresponding to the 36 paired tumor tissues with well-defined TNM stage.

Table 2 SIBLING expression in different cancer types

	Breast cancer	Uterine cancer	Colon cancer	Stomach cancer	Ovarian cancer	Lung cancer	Rectal cancer	Thyroid cancer	Kidney cancer
BSP									
t test*	Yes	No	Yes	Yes	No	No	Yes	Yes	Yes
$>m + 2$ SD†	Yes	No	Yes	Yes	Yes	Yes	Yes	Yes	Yes
Other studies (ref. no.)‡	4 and 28	29				7		8	
OPN									
t test*	Yes	Yes	Yes	No	Yes	Yes	Yes	Yes	No
$>m + 2$ SD†	Yes	Yes	Yes	Yes	Yes	Yes	Yes	No	No
Other studies (ref. no.)‡	30 and 31		32 and 33	34 and 35	36 and 37	38 and 39		40	2
DMP1									
t test*	Yes	Yes	Yes	No	No	Yes	No	No	No
$>m + 2$ SD†	Yes	No	No	No	No	Yes	No	No	No
Other studies (ref. no.)‡						9			
DSPP									
t test*	Yes	No	No	No	No	Yes	No	No	No
$>m + 2$ SD†	No	No	No	No	No	Yes	No	No	No
Other studies (ref. no.)‡									

* Significant elevation defined by a paired *t* test pairing individual subject's normal and tumor tissue expression levels.
† Significant elevation defined by a mean cancer tissue level of expression $>m + 2$SD.
‡ Published studies finding increased expression of SIBLINGs in a given tumor type.

SD criteria. DSPP expression was elevated significantly by both criteria in lung cancer, but only by paired *t* test in breast cancer. Cancers for which the two analysis methods were not in accordance are obvious targets for further, more extensive studies.

The observed increase in MMP-2 expression observed in tumor samples is consistent with previous studies of breast (41, 42), colon (43–47), stomach (48, 49), lung (50–53), rectal (43, 54), and kidney cancer (55–57). Whereas a strong association of increased MMP-3 has been found in breast cancer (41, 58–61), the increased expression levels observed in other tumor types are not as well supported by published literature. Altered MMP-3 levels have been observed in colon (62–64), stomach (65–67), and rectal (68) cancer, although in some cases, the increases were relatively small. In addition, studies have indicated that the MMP-3 source was not necessarily tumor cell but stromal cell or another infiltrating cell type, distinct from the tumor. The observed increases in MMP-9 expression are consistent with published studies of breast (41, 69), uterine (70, 71), colon (46, 53, 72), stomach (73–75), ovarian (76, 77), lung (50, 78), rectal (43, 79), and kidney cancer (56, 80).

A correlation of SIBLING message expression levels with MMP message levels of their partners (BSP with MMP-2, OPN with MMP-3, and DMP1 with MMP-9) was observed. That, in association with the recently described ability of these SIBLINGs to bind to and modulate the activity of specific MMPs, suggests that the same factors that activate SIBLING genes in tumor progression may be the same ones that can activate the corresponding MMP genes. It is also possible that the expression of one SIBLING member in a tumor may induce the production of its corresponding MMP partner, or *vice versa*. Interestingly, SIBLING production by tumors could facilitate angiogenesis because both BSP and OPN have been shown to possess angiogenesis activity *in vivo* (81, 82).

SIBLING expression was different between different subtypes of cancer. Whereas the historical basis for the distinction between the main two types of breast cancer (the belief that ductal carcinomas arose from ducts and lobular carcinomas from lobules) is subject to debate (both can arise from the terminal duct lobular unit), there is evidence that the two classes as used clinically refer to disease entities that differ in tumor size, shape, dissemination, and proliferation rates (83). The most common hallmark associated with the lobular classification is multifocality. Lobular tumors tend to be more slowly proliferating than ductal tumors. They also tend to frequently exhibit hormone receptor positivity and show distinct chromosomal changes (84, 85). The more rapidly progressing ductal tumors had an associated higher level of SIBLING expression. OPN was recently identified by microarray analysis as a discriminating marker between ductal and lobular cancer (86). In our current study, OPN, as well as BSP, DMP1, and DSPP were significantly different between lobular and ductal tumors. Similarly, the association of higher OPN expression with adenocarcinomas as opposed to squamous cell carcinomas in uterine cancer may be associated with different size, shape, and progression rates.

SIBLING expression correlated with tumor stages associated with changing size and lymph node involvement. These observations are consistent with SIBLING expression coupled with MMP activity modulation having an effect on early tumor progression. These results suggest SIBLINGs as potential markers of early disease progression in a number of different cancers. Future studies of SIBLING expression and serum levels will address the degree to which these tumor biomarkers can be correlated with disease progression.

REFERENCES

1. Fisher LW, Fedarko NS. Six genes expressed in bones and teeth encode the current members of the SIBLING family of proteins. Connect Tissue Res 2003;44(Suppl 1):33–40.

2. Brown LF, Papadopoulos-Sergiou A, Berse B, et al. Osteopontin expression and distribution in human carcinomas. Am J Pathol 1994; 145:610–23.

3. Coppola D, Szabo M, Boulware D, et al. Correlation of osteopontin protein expression and pathological stage across a wide variety of tumor histologies. Clin Cancer Res 2004;10:184–90.

4. Bellahcene A, Merville MP, Castronovo V. Expression of bone sialoprotein, a bone matrix protein, in human breast cancer. Cancer Res 1994;54:2823–6.

5. Waltregny D, Bellahcene A, de Leval X, et al. Increased expression of bone sialoprotein in bone metastases compared with visceral metastases in human breast and prostate cancers. J Bone Miner Res 2000;15: 834–43.

6. Waltregny D, Bellahcene A, Van Riet I, et al. Prognostic value of bone sialoprotein expression in clinically localized human prostate cancer. J Natl Cancer Inst (Bethesda) 1998;90:1000–8.

7. Bellahcene A, Maloujahmoum N, Fisher LW, et al. Expression of bone sialoprotein in human lung cancer. Calcif Tissue Int 1997;61: 183–8.

8. Bellahcene A, Albert V, Pollina L, et al. Ectopic expression of bone sialoprotein in human thyroid cancer. Thyroid 1998;8:637–41.

9. Chaplet M, De Leval L, Waltregny D, et al. Dentin matrix protein 1 is expressed in human lung cancer. J Bone Miner Res 2003;18:1506–12.

10. Rowe PS, de Zoysa PA, Dong R, et al. MEPE, a new gene expressed in bone marrow and tumors causing osteomalacia. Genomics 2000;67:54–68.

11. Fedarko NS, Jain A, Karadag A, Fisher LW. Three small integrin binding ligand N-linked glycoproteins (SIBLINGs) bind and activate specific matrix metalloproteinases. FASEB J 2004;18:734–6.

12. Zhumabayeva B, Diatchenko L, Chenchik A, Siebert PD. Use of SMART-generated cDNA for gene expression studies in multiple human tumors. Biotechniques 2001;30:158–63.

13. Fisher LW, McBride OW, Termine JD, Young MF. Human bone sialoprotein. Deduced protein sequence and chromosomal localization. J Biol Chem 1990;265:2347–51.

14. Oldberg A, Franzen A, Heinegard D. Cloning and sequence analysis of rat bone sialoprotein (osteopontin) cDNA reveals an Arg-Gly-Asp cell-binding sequence. Proc Natl Acad Sci USA 1986;83:8819–23.

15. Hirst KL, Simmons D, Feng J, et al. Elucidation of the sequence and the genomic organization of the human dentin matrix acidic phosphoprotein 1 (DMP1) gene: exclusion of the locus from a causative role in the pathogenesis of dentinogenesis imperfecta type II. Genomics 1997; 42:38–45.

16. Freije JM, Balbin M, Pendas AM, et al. Matrix metalloproteinases and tumor progression. Adv Exp Med Biol 2003;532:91–107.

17. Chenchik A, Zhu YY, Diatchenko L, Li R, Hill J, Siebert PD. Generation and use of high-quality cDNA from small amounts of total RNA by SMART PCR. In: Siebert P, Larrick J, editors. Gene Cloning and Analysis by RT-PCR. Natick, MA: Eaton Publishing; 1998. p. 305–19.

18. Blanquicett C, Johnson MR, Heslin M, Diasio RB. Housekeeping gene variability in normal and carcinomatous colorectal and liver tissues: applications in pharmacogenomic gene expression studies. Anal Biochem 2002;303:209–14.

19. Rondinelli RH, Epner DE, Tricoli JV. Increased glyceraldehyde-3-phosphate dehydrogenase gene expression in late pathological stage human prostate cancer. Prostate Cancer Prostatic Dis 1997;1:66–72.

20. Aerts JL, Gonzales MI, Topalian SL. Selection of appropriate control genes to assess expression of tumor antigens using real-time RT-PCR. Biotechniques 2004;36:84–6, 88, 90–1.

21. Zhumabayeva B, Chenchik A, Siebert PD, Herrler M. Disease profiling arrays: reverse format cDNA arrays complimentary to microarrays. Adv Biochem Eng Biotechnol 2004;86:191–213.

22. Thiebault K, Mazelin L, Pays L, et al. The netrin-1 receptors UNC5H are putative tumor suppressors controlling cell death commitment. Proc Natl Acad Sci USA 2003;100:4173–8.

23. Liu S, Huang H, Lu X, et al. Down-regulation of thiamine transporter THTR2 gene expression in breast cancer and its association with resistance to apoptosis. Mol Cancer Res 2003;1:665–73.

24. Iavarone C, Wolfgang C, Kumar V, et al. PAGE4 is a cytoplasmic protein that is expressed in normal prostate and in prostate cancers. Mol Cancer Ther 2002;1:329–35.

25. Egland KA, Kumar V, Duray P, Pastan I. Characterization of overlapping XAGE-1 transcripts encoding a cancer testis antigen expressed in lung, breast, and other types of cancers. Mol Cancer Ther 2002;1:441–50.

26. Sers C, Husmann K, Nazarenko I, et al. The class II tumour suppressor gene H-REV107-1 is a target of interferon-regulatory factor-1 and is involved in IFNgamma-induced cell death in human ovarian carcinoma cells. Oncogene 2002;21:2829–39.

27. Wiechen K, Diatchenko L, Agoulnik A, et al. Caveolin-1 is down-regulated in human ovarian carcinoma and acts as a candidate tumor suppressor gene. Am J Pathol 2001;159:1635–43.

28. Bellahcene A, Menard S, Bufalino R, Moreau L, Castronovo V. Expression of bone sialoprotein in primary human breast cancer is associated with poor survival. Int J Cancer 1996;69:350–3.

29. Detry C, Waltregny D, Quatresooz P, et al. Detection of bone sialoprotein in human (pre)neoplastic lesions of the uterine cervix. Calcif Tissue Int 2003;73:9–14.

30. Gillespie MT, Thomas RJ, Pu ZY, et al. Calcitonin receptors, bone sialoprotein and osteopontin are expressed in primary breast cancers. Int J Cancer 1997;73:812–5.

31. Tuck AB, O'Malley FP, Singhal H, et al. Osteopontin expression in a group of lymph node negative breast cancer patients. Int J Cancer 1998;79:502–8.

32. Yeatman TJ, Chambers AF. Osteopontin and colon cancer progression. Clin Exp Metastasis 2003;20:85–90.

33. Agrawal D, Chen T, Irby R, et al. Osteopontin identified as lead marker of colon cancer progression, using pooled sample expression profiling. J Natl Cancer Inst (Bethesda) 2002;94:513–21.

34. Maeng HY, Choi DK, Takeuchi M, et al. Appearance of osteonectin-expressing fibroblastic cells in early rat stomach carcinogenesis and stomach tumors induced with N-methyl-N′-nitro-N-nitrosoguanidine. Jpn J Cancer Res 2002;93:960–7.

35. Ue T, Yokozaki H, Kitadai Y, et al. Co-expression of osteopontin and CD44v9 in gastric cancer. Int J Cancer 1998;79:127–32.

36. Kim JH, Skates SJ, Uede T, et al. Osteopontin as a potential diagnostic biomarker for ovarian cancer. JAMA 2002;287:1671–9.

37. Tiniakos DG, Yu H, Liapis H. Osteopontin expression in ovarian carcinomas and tumors of low malignant potential (LMP). Hum Pathol 1998;29:1250–4.

38. Zhang J, Takahashi K, Takahashi F, et al. Differential osteopontin expression in lung cancer. Cancer Lett 2001;171:215–22.

39. Chambers AF, Wilson SM, Kerkvliet N, et al. Osteopontin expression in lung cancer. Lung Cancer 1996;15:311–23.

40. Tunio GM, Hirota S, Nomura S, Kitamura Y. Possible relation of osteopontin to development of psammoma bodies in human papillary thyroid cancer. Arch Pathol Lab Med 1998;122:1087–90.

41. Lebeau A, Nerlich AG, Sauer U, Lichtinghagen R, Lohrs U. Tissue distribution of major matrix metalloproteinases and their transcripts in human breast carcinomas. Anticancer Res 1999;19:4257–64.

42. Onisto M, Riccio MP, Scannapieco P, et al. Gelatinase A/TIMP-2 imbalance in lymph-node-positive breast carcinomas, as measured by RT-PCR. Int J Cancer 1995;63:621–6.

43. Liabakk NB, Talbot I, Smith RA, Wilkinson K, Balkwill F. Matrix metalloprotease 2 (MMP-2) and matrix metalloprotease 9 (MMP-9) type IV collagenases in colorectal cancer. Cancer Res 1996;56:190–6.

44. Ornstein DL, MacNab J, Cohn KH. Evidence for tumor-host cooperation in regulating MMP-2 expression in human colon cancer. Clin Exp Metastasis 1999;17:205–12.

45. Karakiulakis G, Papanikolaou C, Jankovic SM, et al. Increased type IV collagen-degrading activity in metastases originating from primary tumors of the human colon. Invasion Metastasis 1997;17:158–68.

46. Collins HM, Morris TM, Watson SA. Spectrum of matrix metalloproteinase expression in primary and metastatic colon cancer: relationship to the tissue inhibitors of metalloproteinases and membrane type-1-matrix metalloproteinase. Br J Cancer 2001;84:1664–70.

47. Papadopoulou S, Scorilas A, Arnogianaki N, et al. Expression of gelatinase-A (MMP-2) in human colon cancer and normal colon mucosa. Tumour Biol 2001;22:383–9.

48. Mori M, Mimori K, Shiraishi T, et al. Analysis of MT1-MMP and MMP2 expression in human gastric cancers. Int J Cancer 1997;74: 316–21.

49. Ohtani H, Nagai T, Nagura H. Similarities of in situ mRNA expression between gelatinase A (MMP-2) and type I procollagen in human gastrointestinal carcinoma: comparison with granulation tissue reaction. Jpn J Cancer Res 1995;86:833–9.

50. Nakagawa H, Yagihashi S. Expression of type IV collagen and its degrading enzymes in squamous cell carcinoma of lung. Jpn J Cancer Res 1994;85:934–8.

51. Yamamoto M, Mohanam S, Sawaya R, et al. Differential expression of membrane-type matrix metalloproteinase and its correlation with gelatinase A activation in human malignant brain tumors in vivo and in vitro. Cancer Res 1996;56:384–92.

52. Suzuki M, Iizasa T, Fujisawa T, et al. Expression of matrix metalloproteinases and tissue inhibitor of matrix metalloproteinases in non-small-cell lung cancer. Invasion Metastasis 1998;18:134–41.

53. Creighton C, Hanash S. Expression of matrix metalloproteinase 9 (MMP-9/gelatinase B) in adenocarcinomas strongly correlated with expression of immune response genes. In Silico Biol 2003;3:301–11.

54. Chan CC, Menges M, Orzechowski HD, et al. Increased matrix metalloproteinase 2 concentration and transcript expression in advanced colorectal carcinomas. Int J Colorectal Dis 2001;16:133–40.

55. Kitagawa Y, Kunimi K, Uchibayashi T, Sato H, Namiki M. Expression of messenger RNAs for membrane-type 1, 2, and 3 matrix metalloproteinases in human renal cell carcinomas. J Urol 1999;162: 905–9.

56. Hagemann T, Gunawan B, Schulz M, Fuzesi L, Binder C. mRNA expression of matrix metalloproteases and their inhibitors differs in subtypes of renal cell carcinomas. Eur J Cancer 2001;37:1839–46.

57. Slaton JW, Inoue K, Perrotte P, et al. Expression levels of genes that regulate metastasis and angiogenesis correlate with advanced pathological stage of renal cell carcinoma. Am J Pathol 2001;158:735–43.

58. Freije JM, Diez-Itza I, Balbin M, et al. Molecular cloning and expression of collagenase-3, a novel human matrix metalloproteinase produced by breast carcinomas. J Biol Chem 1994;269:16766–73.

59. Basset P, Bellocq JP, Anglard P, et al. Stromelysin-3 and other stromelysins in breast cancer: importance of epithelialstromal interactions during tumor progression. Cancer Treat Res 1996;83:353–67.

60. Iwata H, Kobayashi S, Iwase H, et al. Production of matrix metalloproteinases and tissue inhibitors of metalloproteinases in human breast carcinomas. Jpn J Cancer Res 1996;87:602–11.

61. Chenard MP, O'Siorain L, Shering S, et al. High levels of stromelysin-3 correlate with poor prognosis in patients with breast carcinoma. Int J Cancer 1996;69:448–51.

62. Baker EA, Bergin FG, Leaper DJ. Matrix metalloproteinases, their tissue inhibitors and colorectal cancer staging. Br J Surg 2000;87: 1215–21.

63. Gallegos NC, Smales C, Savage FJ, Hembry RM, Boulos PB. The distribution of matrix metalloproteinases and tissue inhibitor of metalloproteinases in colorectal cancer. Surg Oncol 1995;4:21–9.

64. Matrisian LM, Wright J, Newell K, Witty JP. Matrix-degrading metalloproteinases in tumor progression. Princess Takamatsu Symp 1994;24:152–61.

65. Murray GI, Duncan ME, Arbuckle E, Melvin WT, Fothergill JE. Matrix metalloproteinases and their inhibitors in gastric cancer. Gut 1998;43:791–7.

66. Nomura H, Fujimoto N, Seiki M, Mai M, Okada Y. Enhanced production of matrix metalloproteinases and activation of matrix metalloproteinase 2 (gelatinase A) in human gastric carcinomas. Int J Cancer 1996;69:9–16.

67. Saarialho-Kere UK, Vaalamo M, Puolakkainen P, et al. Enhanced expression of matrilysin, collagenase, and stromelysin-1 in gastrointestinal ulcers. Am J Pathol 1996;148:519–26.

68. Imai K, Yokohama Y, Nakanishi I, et al. Matrix metalloproteinase 7 (matrilysin) from human rectal carcinoma cells. Activation of the precursor, interaction with other matrix metalloproteinases and enzymic properties. J Biol Chem 1995;270:6691–7.

69. Pacheco MM, Mourao M, Mantovani EB, Nishimoto IN, Brentani MM. Expression of gelatinases A and B, stromelysin-3 and matrilysin genes in breast carcinomas: clinico-pathological correlations. Clin Exp Metastasis 1998;16:577–85.

70. Davidson B, Goldberg I, Liokumovich P, et al. Expression of metalloproteinases and their inhibitors in adenocarcinoma of the uterine cervix. Int J Gynecol Pathol 1998;17:295–301.

71. Davidson B, Goldberg I, Kopolovic J, et al. Expression of matrix metalloproteinase-9 in squamous cell carcinoma of the uterine cervix-clinicopathologic study using immunohistochemistry and mRNA in situ hybridization. Gynecol Oncol 1999;72:380–6.

72. Takeha S, Fujiyama Y, Bamba T, et al. Stromal expression of MMP-9 and urokinase receptor is inversely associated with liver metastasis and with infiltrating growth in human colorectal cancer: a novel approach from immune/inflammatory aspect. Jpn J Cancer Res 1997; 88:72–81.

73. Parsons SL, Watson SA, Collins HM, et al. Gelatinase (MMP-2 and -9) expression in gastrointestinal malignancy. Br J Cancer 1998;78: 1495–502.

74. Torii A, Kodera Y, Ito M, et al. Matrix metalloproteinase 9 in mucosally invasive gastric cancer. Gastric Cancer 1998;1:142–5.

75. Wang L, Zhang LH, Li YL, Liu Z. Expression of MMP-9 and MMP-9 mRNA in gastric carcinoma and its correlation with angiogenesis [in Chinese]. Zhonghua Yi Xue Za Zhi 2003;83:782–6.

76. Sakata K, Shigemasa K, Nagai N, Ohama K. Expression of matrix metalloproteinases (MMP-2, MMP-9, MT1-MMP) and their inhibitors (TIMP-1, TIMP-2) in common epithelial tumors of the ovary. Int J Oncol 2000;17:673–81.

77. Davidson B, Goldberg I, Gotlieb WH, et al. High levels of MMP-2, MMP-9, MT1-MMP and TIMP-2 mRNA correlate with poor survival in ovarian carcinoma. Clin Exp Metastasis 1999;17:799–808.

78. Kremer EA, Chen Y, Suzuki K, Nagase H, Gorski JP. Hydroxyapatite induces autolytic degradation and inactivation of matrix metalloproteinase-1 and -3. J Bone Miner Res 1998;13:1890–902.

79. Roeb E, Dietrich CG, Winograd R, et al. Activity and cellular origin of gelatinases in patients with colon and rectal carcinoma differential activity of matrix metalloproteinase-9. Cancer (Phila) 2001;92: 2680–91.

80. Inoue K, Kamada M, Slaton JW, et al. The prognostic value of angiogenesis and metastasis-related genes for progression of transitional cell carcinoma of the renal pelvis and ureter. Clin Cancer Res 2002;8: 1863–70.

81. Hirama M, Takahashi F, Takahashi K, et al. Osteopontin overproduced by tumor cells acts as a potent angiogenic factor contributing to tumor growth. Cancer Lett 2003;198:107–17.

82. Bellahcene A, Bonjean K, Fohr B, et al. Bone sialoprotein mediates human endothelial cell attachment and migration and promotes angiogenesis. Circ Res 2000;86:885–91.

83. Sainsbury JRC, Anderson TJ, Morgan DAL. Breast cancer. Br Med J 2000;321:745–50.

84. Coradini D, Pellizzaro C, Veneroni S, Ventura L, Daidone MG. Infiltrating ductal and lobular breast carcinomas are characterized by different interrelationships among markers related to angiogenesis and hormone dependence. Br J Cancer 2002;87:1105–11.

85. Gunther K, Merkelbach-Bruse S, Amo-Takyi BK, et al. Differences in genetic alterations between primary lobular and ductal breast cancers detected by comparative genomic hybridization. J Pathol 2001;193: 40–7.

86. Korkola JE, DeVries S, Fridlyand J, et al. Differentiation of lobular versus ductal breast carcinomas by expression microarray analysis. Cancer Res 2003;63:7167–75.

Proceedings of the 8th ICCBMT, pp.170-173, 2005

The SIBLING Family of Proteins: Activators of MMPs

Larry W. Fisher[1], Abdullah Karadag[1], Kalu Ogbureke[1], and Neal S. Fedarko[1,2]

[1]Craniofacial and Skeletal Diseases Branch, National Institute of Dental and Craniofacial Research, NIH, DHHS, Bethesda, MD, U.S.A.

[2]Division of Geriatrics, Department of Medicine, Johns Hopkins University, School of Medicine, Baltimore, MD, U.S.A.

The SIBLING family of proteins (BSP, DMP1, DSPP, MEPE and OPN) can modify hydroxyapatite initiation and growth *in vitro*. However, a variety of biochemical experiments proved that BSP, DMP1 and OPN can form stable complexes with MMP-2, MMP-9 and MMP-3, respectively. Furthermore, the complexes with proMMPs were active without removal of the propeptides and the propeptide-free MMP remained active in the presence of their inhibitors, TIMPs. Complement Factor H, with its higher affinity for the SIBLINGs, reversed both SIBLING-induced activations, suggesting that these activities may be limited to regions secreting the proteins. All five SIBLINGs as well as their three known MMP partners are co-expressed in cells of primate and rodent salivary glands, a mature, non-mineralizing tissue. These results suggest that the integrin-binding SIBLING family members may be playing important and perhaps related roles in the local activation of specific MMPs in both mineralizing and non-mineralizing tissues.

Keywords: SIBLING, MMP, BSP, OPN, DMP1, DSPP, MEPE

During the 1970s and 1980s, the acidic proteins entrapped within the mineralized matrices of bones and teeth were studied as possible hydroxyapatite nucleators and crystal growth modulators. Their biochemical properties permitted investigators to categorize the proteins into proteoglycans, phosphoglycoproteins, Gla-containing proteins, and other subgroups. The phosphoglycoproteins were so different in their primary protein sequences that it was difficult at that time to conclude that they were derived from a common primordial gene. Later, when the properties of the exon structures of bone sialoprotein (BSP), dentin matrix protein-1 (DMP1), dentin sialophosphoprotein (DSPP), osteopontin (OPN), and matrix extracellular phosphoglycoprotein (MEPE) genes were compared, we proposed that all five proteins were derived from a single ancient gene [1]. Some of the properties that were usually shared by the SIBLING (Small Integrin-Binding LIgand, N-linked Glycoprotein) family members were: a noncoding exon 1; a leader sequence plus the first two amino acids in exon 2; casein kinase II (CKII) phosphorylation consensus sequences in exons 3 and 5; a more proline-rich and often basic exon 4; and an integrin-binding tripeptide, RGD, within one of the last two much larger exons. Interestingly, exon 5, a short CKII domain, is often missing in natural splice variants of DMP1, OPN and MEPE. At the last meeting of the ICCBMT, the best data suggested that all five SIBLING genes were clustered within a 750,000 basepair region of human chromosome 4 [2]. A more refined analysis now shows them aligned with the same transcriptional orientation within a 372,000 bp region. Results for the mouse (chromosome 5) are similar.

Genetic analysis is interesting, but true families of proteins should also have related structures, binding partners, and functions. To date only two SIBLINGs (BSP and OPN) have had their structures solved and they were both found to be flexible (in solution) along their entire length within normal NMR timescales [1]. Flexibility is a common feature of proteins/domains that have many binding partners. All SIBLINGs are thought to bind to integrins via their RGD domain although rat DSPP (which lacks the RGD tripeptide) may use a unique, REDV fibronectin-like attachment domain. DMP1 and OPN have been shown to bind CD44 while BSP does not [3,4]. Complement Factor H binds with very high affinity to BSP, DMP1 and OPN in solution and can even mask the detection of SIBLINGs in serum [5]. BSP, DMP1 and OPN can bridge Factor H to cell surface integrins (all three) or CD44 (DMP1 and OPN) and protect the cell from the lytic pathway of complement [4,6]. Protection from complement may be important for the survival of a metastasizing cancer cell. DSPP and MEPE have not been purified in sufficient quantity to perform similar studies.

The newly-discovered ability of at least three members of the SIBLING family to bind and activate specific members of the MMP family of proteases was due to a fortuitous series of events. First, in 1996 Cheresh's group localized MMP-2 on the surface of invasive cells by direct interaction with $\alpha v\beta 3$ integrin [7]. Later we were making recombinant BSP, DMP1 and OPN in eukaryotic cells and gently purifying the proteins for structural analysis. We hypothesized that, since both the SIBLINGs family and MMP-2 bound to $\alpha v\beta 3$ integrin, it would be interesting to see if the SIBLINGs could displace the MMP-2 from the cell surface complex. Of course, in order to do this experiment, we had to be sure that none of the three purified SIBLINGs themselves were contaminated with MMP-2. To our surprise, small amounts of MMP-2 had co-purified with BSP while MMP-3 co-purified with OPN and MMP-9 co-purified with DMP1 under the non-denatur-

ing conditions. From there it was standard biochemistry using commercial sources of purified MMPs to show that purified SIBLINGs bound in a 1:1 stoichiometry with nM affinity to their partner MMPs but not to the other two MMPs. Upon binding of their partner MMPs, both the latent (proMMP) and active (MMP) forms underwent conformational changes that were easily detected using natural fluorescence of the MMP's tryptophan residues [8]. Furthermore, it was shown that when the SIBLING bound to its partner proMMP, the protease became active, apparently without removing the inhibitory propeptide (Figure 1A). This was a surprise because it is generally thought that the propeptide must be removed before the MMPs can be enzymatically active. It is reasonable to hypothesize that the conformational change induced in the MMPs by the bound SIBLING caused the propeptides to have lower affinities for their own binding domains, move out of the active sites, and allow substrates to be digested. Active MMPs that had been previously inhibited by addition of their corresponding purified tissue inhibitors of metalloproteinases (TIMPs) became re-activated upon binding of the appropriate SIBLING (Figure 1C). The TIMPs appear to have had their inhibitory binding sites within the MMPs altered by the SIBLING-induced conformational changes losing their ability to bind strongly and inhibit the MMPs [8]. To date, DSPP and MEPE have not been shown to have MMP partners with similar action.

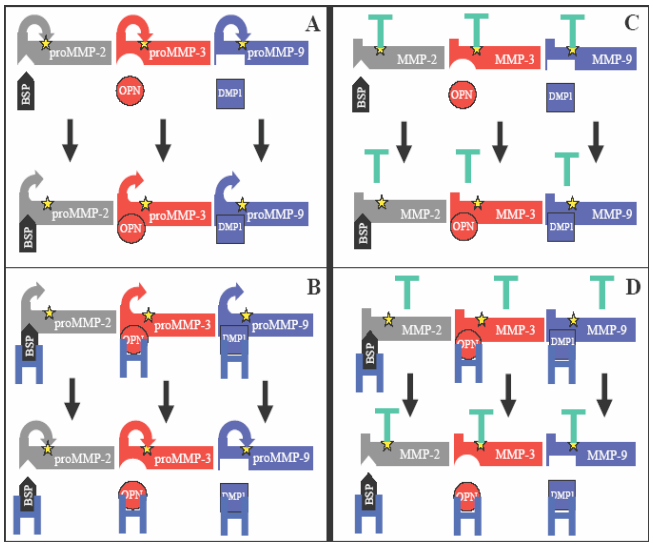

Figure 1. Latent MMPs with propeptide in active (star) site (A, top) upon binding partner SIBLING undergoes a conformational change exposing the active site to substrates (A, bottom). Factor H binds to the SIBLINGs (B, top), removing them and permitting the propeptide to reinsert into the active site (B, bottom). Propeptide-free MMPs inhibited by TIMPs (green T) (C, top) bind SIBLINGs, thereby inducing a conformational change. The TIMPs are released (C, bottom) activating the MMPs. Factor H removes the SIBLING from the complex allowing the TIMPs to bind and inhibit the MMPs (D).

Mechanisms for activating latent MMPs and/or interfering with the action of the TIMPs would not likely evolve unless there was also a mechanism for reversing these activation pathways. Fortunately, we knew from previous results mentioned above that complement Factor H has an approximately 100-fold higher affinity for BSP, DMP1 and OPN than the SIBLINGs have for their respective MMP partners. Factor H, which is present in the blood at about 1 mg/ml, apparently binds to the SIBLINGs on the latent (Figure 1B) and active (Figure 1D) MMPs and removes them from the protease complex [8]. The propeptides and TIMPs can then re-inhibit the protease activity. Therefore SIBLING-activation of MMPs will likely be local events, occurring within a short distance of their secretion.

At this point, all of the results discussed have been found using highly purified proteins in biochemical experiments. We next set out to determine if the SIBLING-MMP complexes could be shown to be important in experiments with living cells. Because many different types of cancers have been shown in paraffin sections to express high levels of various SIBLINGs, we used a number of cancer cell lines in a modified Boyden chamber assay to determine if any of the proteins could enhance invasion potential. BSP, but not DMP1 or OPN, could enhance the invasion potential of many cell lines derived from breast, prostate, lung, and thyroid cancers through a model basement membrane system, Matrigel [9,10]. The specificity of BSP suggested that MMP-2 may have been involved and, indeed, inhibitors of MMP-2 stopped the BSP-enhanced invasion. Because mutating the integrin-binding tripeptide, RGD, to the chemically similar but inactive KAE also stopped the enhanced invasion, we hypothesized that integrins were involved. Blocking the activity of αvβ3 integrin with an antibody stopped the BSP-enhanced invasion. Together these observations suggested that BSP bridges MMP-2 to αvβ3 integrin. In fact, beads with bound αvβ3 integrin were able to pull down much more MMP-2 if pre-treated with BSP compared to untreated beads or ones treated with BSP-KAE [9].

To be a biologically useful model of MMP activation, however, each SIBLING must also be shown to be co-expressed with its partner MMP by a cell *in vivo*. All SIBLINGs and the three MMPs are expressed in normal growing bones and/or teeth, but we were also interested in their co-expression in normal epithelial tissues, the cells that upon transformation become the tumors studied above. OPN had been known for many years to be expressed in normal salivary gland [11] and we first chose to look carefully at this tissue. Similar to the photomicrographs presented in a recent publication [12], Figure 2 shows that all five SIBLINGs as well as MMP-2, -3 and -9 are expressed in normal human salivary gland ducts. In primates, all eight proteins are limited to the intercalated duct, striated duct, and to some degree the collecting ducts. Mature mouse salivary gland differed in two ways. First, all three of the MMPs and four of the five SIBLINGs are also expressed in the acini of mice. DSPP

expression remains limited to the rodent ducts. Second, mature male mouse ducts under the strict control of androgens become almost exclusively granulated convoluted tubules (GCT) and express none of the eight proteins. Salivary glands therefore show that a SIBLING and its MMP partner are always co-expressed and can be reasonably expected to form active complexes in the pericellular and extracellular spaces near these epithelial cells. These epithelial cells persist for many months or years and do not appear to be assisted by any other cell type in the maintenance of local matrix proteins.

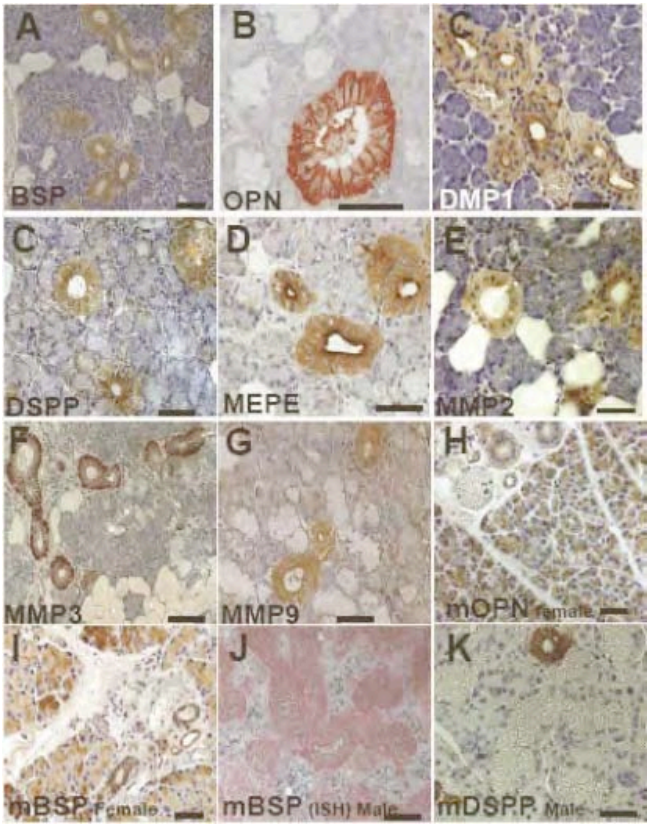

Figure 2. Immunolocalization (red/brown) of SIBLINGs and MMPs in the ducts of human salivary glands (A-G). Mouse salivary glands have staining also in the acini (OPN, H and BSP, I are shown). *In situ* hybridization of BSP (blue/purple) in mouse gland shows mRNA in acini but not granulated convoluted tubules (GCT) (J). DSPP immunostaining (red/brown) is only in non-GCT ducts (K), not in acini. Bar = 50 micrometers.

It is our hypothesis that the SIBLING/MMP partners are involved in the turnover of the pericellular and/or extracellular proteins of these metabolically active cells.

In summary, three SIBLINGs have been shown to bind and activate three different MMPs *in vitro* and the proteins are co-expressed *in vivo*, suggesting that these activities are likely to be biologically important.

REFERENCES

1. Fisher, L.W., Torchia, D.A., Fohr, B., Young, M.F., and Fedarko, N.S. (2001). Flexible structures of SIBLING proteins, bone sialoprotein, and osteopontin. *Biochem. Biophys. Res. Commun.* 280, 460-465.

2. Fisher, L.W., and Fedarko, N.S. (2003). Six genes expressed in bones and teeth encode the current members of the SIBLING family of proteins. *Proc. 7th ICCBMT. Connect. Tissue Res.* 44, 33-40.

3. Weber, G.F., Ashkar, S., Glimcher, M.J., and Cantor, H. (1996). Receptor-ligand interaction between CD44 and osteopontin (Eta-1). *Science* 271, 509-512.

4. Jain, A., Karadag, A., Fohr, B., Fisher, L.W., and Fedarko, N.S. (2002). Three SIBLINGs (small integrin-binding ligand, N-linked glycoproteins) enhance factor H's cofactor activity enabling MCP-like cellular evasion of complement-mediated attack. *J. Biol. Chem.* 277, 13700-13708.

5. Fedarko, N.S., Jain, A., Karadag, A., Van Eman, M.R., and Fisher, L.W. (2001). Elevated serum bone sialoprotein and osteopontin in colon, breast, prostate, and lung cancer. *Clin. Cancer Res.* 7, 4060-4066.

6. Fedarko, N.S., Fohr, B., Robey, P.G., Young, M.F., and Fisher, L.W. (2000). Factor H binding to bone sialoprotein and osteopontin enables tumor cell evasion of complement-mediated attack. *J. Biol. Chem.* 275, 16666-16672.

7. Brooks, P.C., Stromblad, S., Sanders, L.C., von Schalscha, T.L., Aimes, R.T., Stetler-Stevenson, W.G., Quigley, J.P., and Cheresh, D.A. (1996). Localization of matrix metalloproteinase MMP-2 to the surface of invasive cells by interaction with integrin alpha v beta 3. *Cell* 85, 683-693.

8. Fedarko, N.S., Jain, A., Karadag, A., and Fisher, L.W. (2004). Three small integrin binding ligand N-linked glycoproteins (SIBLINGs) bind and activate specific matrix metalloproteinases. *FASEB J.* 18, 734-736.

9. Karadag, A., Ogbureke, K.U., Fedarko, N.S., and Fisher, L.W. (2004). Bone sialoprotein, matrix metalloproteinase 2, and alpha(v)beta3 integrin in osteotropic cancer cell invasion. *J. Natl. Cancer Inst.* 96, 956-965.

10. Karadag, A., Fedarko, N.S., and Fisher, L.W. (2004). "The Formation of alpha-v beta-3 Integrin/Bone Sialoprotein/Matrix Metalloproteinase-2 Complex on the Cell Surface in Invasion by Breast Cancer Cells in vitro". In: *Proc. 8th ICCBMT*. W.J. Landis and J. Sodek (eds.), pp 170-173 (University of Toronto Press, Toronto).

11. Brown, L.F., Berse, B., Van de Water, L., Papadopoulos-Sergiou, A., Perruzzi, C.A., Manseau, E.J., Dvorak, H.F., and Senger, D.R. (1992). Expression and distribution of osteopontin in human tissues: widespread association with luminal epithelial surfaces. *Mol. Biol. Cell* 3, 1169-1180.

12. Ogbureke, K.U., and Fisher, L.W. (2004). Expression of SIBLINGs and their partner MMPs in salivary glands. *J. Dent. Res.* 83, 664-670.

Matrix extracellular phosphoglycoprotein (MEPE) correlates with serum phosphorus prior to and during octreotide treatment and following excisional surgery in hypophosphatemic linear sebaceous nevus syndrome

William H. Hoffman[1], **Alka Jain**[2], **Harold Chen**[3], and **Neal S. Fedarko**[2]

1 *Department of Pediatrics, Pediatric Endocrinology, Medical College of Georgia, Augusta, GA*

2 *Department of Medicine, Johns Hopkins University, Baltimore, MD*

3 *Department of Pediatrics, Louisiana State University Medical School, Shreveport, LA*

Keywords

oncogenic hypophosphatemic osteomalacia; phosphatonin; phakomatosis

To the Editor:

Hereditary and acquired forms of hypophosphatemia result in metabolic bone disease with significant degrees of disability in children, adolescents and adults. Linear sebaceous nevus syndrome (LSNS) is a rare sporadic congenital phakomatosis of unknown etiology with a variable phenotype that includes hypophosphatemia [Carey et al., 1986].

We have previously reported on a patient with LSNS and hypophosphatemia where the plasma phosphatonin, fibroblast growth factor-23 (FGF-23), was inversely related to the serum phosphorous prior to and after treatment with octreotide and excision surgery [Hoffman et al., 2005]. We now extend that observation by reporting on the positive correlation between serum phosphorus and matrix extracellular phosphoglycoprotein (MEPE), a downstream member of phosphate homeostasis and mineralization.

Briefly, the patient, a 7-year-old boy of Korean ancestry with LNSS (which followed Blaschko's lines and involved the left side of his face, trunk, upper and lower extremities and epidermal nevi of the limbus) began treatment for hypophosphatemic rickets with phosphate and calcitriol for vitamin D-resistant rickets. Octreotide (Sandostatin LAR) was added to the phosphate and calcitriol therapy when he was 16 years of age, due to increasing musculoskeletal symptoms and frequent stress fractures and persistent hypophosphatemia [Hoffman et al., 2005]. Further details of the treatment protocol are given in the legend for Figure 1. The competitive enzyme-linked immunosorbent (ELISA) assays for MEPE were performed as previously described [Jain et al., 2004]. The antibody employed in the competitive ELISA (LF-155, a kind gift of Dr. L.W. Fisher, N.I.D.C.R., N.I.H.) was raised against exon 4, the last coding exon of human MEPE, and was affinity-purified using recombinantly expressed protein. The assay entails an anion exchange column chromatography step to clean up the sample and

Corresponding Author: Neal S. Fedarko, Ph.D.,Johns Hopkins University, Department of Medicine, 5501 Hopkins Bayview Circle, Rm. 5A-64, Baltimore, MD 21224, Tel: 410-550-2632, Fax: 410-550-1007, Email: ndarko@jhmi.edu, ndarko@jhmi.edu.

Conflicts of interest: None

detects intact, full length MEPE. The bioactive acidic serine-aspartate-rich MEPE (ASARM) peptide was assayed by a competitive ELISA specific for ASARM-peptide epitopes [Bresler et al., 2004] in the laboratory of Dr. P Rowe. Associations between MEPE and phosphorus were analyzed by Pearson regression analysis.

FGF-23 decreased within 1 month following the first injection of depot octreotide, was suppressed during the 4 months of injections, and remained in the normal range over the following 6 months. After a further decrease following surgery, FGF-23 increased 2 months post surgery and remained stable for the next 2.5 years during phosphate and calcitriol therapy and in the absence of octreotide (Fig 1). This somewhat elevated level of FGF-23 was most likely due to incomplete excision of the tumor [Zimering et al., 2005]. It is of interest that tubular reabsorption of phosphate became normal 4 months after octreotide; serum phosphorus did not increase during octreotide, but began increasing immediately after octreotide, remained slightly below normal until after surgery, and remained normal throughout the remainder of follow up [Hoffman et al., 2005]. Thus phosphaturia continued after FGF-23 had returned to normal. The initial level of MEPE prior to octreotide was 464 ng/ml when serum phosphorus was 1.9 mg/dl. This MEPE value was significantly below aged-matched normal subjects whose mean values were 880 ± 160 ng/ml [Jain et al., 2004]. MEPE increased throughout the depot octreotide therapy, continued to increase and reached a maximal value of 760 ng/ml 2 months after incomplete excisional surgery for cosmetic reasons. MEPE was decreased 6 months after surgery and continued to gradually decline, reaching a pre octreotide level 2.5 years after surgery (Fig 1). MEPE and phosphorus had a significant positive correlation prior to and throughout treatment (Fig 2). During octreotide treatment intact MEPE was increasing, indicating that unlike FGF-23, MEPE was not suppressed by octreotide, suggesting a differential effect of octreotide on the phosphatonins and that MEPE had a phosphaturic effect. The latter seems unlikely since the MEPE values did not exceed the reported normal range [Jain et al., 2004].

However, it is of interest that serum ASARM, the biological active fragment of MEPE, exceeded the normal range of 3,250 ng/ml and paralleled the increase of MEPE, which could explain the phosphaturia [Bresler et al., 2004]. An alternative possibility is the presence of an additional phosphaturic peptide [White et al., 2006]. This possibility has recently been suggested by Elston et al., [2007] to explain persistent hypophosphatemia in a patient with oncogenic osteomalacia after a five- day course of octreotide had suppressed FGF-23. It is important to note that in the report of Elston et al., although the intact FGF-23 was suppressed, the C-fragment of FGF-23 increased for 16 days following surgery and then decreased over the following 5 months. Following octreotide treatment, our patient had significant improvement in the musculoskeletal symptoms, and no further stress fractures occurred. By the age of 20, the patient's T-Score of bone density had improved by −1.2 in the lumbar spine (from −3.2 to −2.1); by −1.0 in the femoral neck (from −4.4 to −3.4); and by −0.8 in the total hip (from −3.8 to −3.0). However, the values remained in the osteopenic (−1.0 to −2.5) and osteoportic (below −2.5) ranges.

The term "phosphatonin" was introduced in 1994 for the protein which has since come to be known as FGF-23 [Econs and Drezner, 1991]. MEPE, also known as osteoclast/osteocyte factor 45, is a glycoprotein which has more recently been identified as a putative phosphatonin [Rowe et al., 2000] based on its ability to inhibit phosphate-uptake and mineralization *in vivo* and *in vitro* [Rowe et al., 2004]. These phosphate-regulating hormones have rapidly gained recognition for their importance in influencing phosphate homeostasis and mineralization through a bone-kidney axis. MEPE and FGF-23 mediate the molecular mechanisms of the bone-kidney axis of phosphate metabolism by controlling the genes encoded for sodium phosphate cotransporters such as Npt2a [Rowe et al., 2004; Marsell et al., 2008], and by regulating vitamin D-1alpha-hydroxylase activity [Sommer et al., 2007; Barthel et al., 2007].

As with many peptide-hormones the biological functions of MEPE are linked to specific peptide fragments that differentially influence processing and handling of phosphate by the kidney [Martin et al., 2007]. Cleavage of MEPE releases acidic serine-aspartate-rich motif (ASARM peptide), the carboxy-terminal peptide that is responsible for MEPE activity *in vivo* [Rowe et al., 2005]. The positive correlation that we observed between MEPE and serum phosphorus prior to and following octreotide therapy is consistent with a cross-sectional study of normal subjects [Jain et al., 2004]. Also the hyperphosphatemia in a MEPE-TRG model correlates with up-regulation of Npt2a [Rowe et al., 2004] and contrasts with infusions of recombinant intact MEPE which result in increased fractional excretion of phosphate and hypophosphatemia in mice and rats [Dobbie et al., 2007].

We have no direct data to support that the positive correlation between MEPE and serum phosphorus is due to octreotide influencing the processing of MEPE. However MEPE, ASARM and serum phosphorus all increased with the initiation of octreotide treatment and decreased following excision of the LSN tumor. We posit the following sequence occurred in this case: first, octreotide resulted in a significant reduction in FGF-23 and a gradual increase in serum phosphorus; second, the dramatic decrease of FGF-23 resulted in an overcompensation of MEPE expression due to chronic and excessive suppression by FGF-23; (An additional explanation for the increase in MEPE could be that octreotide influences the processing of MEPE and possibly increases its expression.); and third, partial excision of the nevus resulted in a decrease and stabilization of MEPE, and after a brief decrease, FGF-23 stabilized followed by gradual stabilization of serum phosphorus, and urine phosphate excretion. Whether this stabilization is a long-term result of octreotide treatment [Eriksson and Oberg, 1999; Garcia de la Torre et al., 2002; Latuada et al., 2002] and/or the result of the natural course of the disease is uncertain. While the number of points studied for ASARM is limited, the correlation between MEPE and ASARM prior to and following surgery supports that octreotide directly or indirectly influenced the processing of MEPE. The two values at six months (12 months after octreotide therapy) and 24 months post partial excisional surgery suggest that MEPE and ASARM had different processing after an increased period off octreotide therapy.

It has been posited that phakomatoses are caused by dysregulation of cellular paracrine growth factors and the extracellular matrix [Kousseff, 1992]. The phosphatonins are an example of such growth factors. FGF-23, and to a somewhat lesser extent, MEPE, have been extensively studied in conditions of abnormal phosphate metabolism including the phakomatoses McCune-Albright syndrome [Yamamoto et al., 2005] and phakomatosis pigmentokeratotica [Saraswat et al., 2003; Bouthors et al., 2006]. The latter condition, along with LSNS [Hoffman et al., 2005; Heike et al., 2005], belongs to the group of epidermal nevus syndromes (ENS) which have a high prevalence of hypophosphatemic rickets [Vidaurri-de la Cruz et al., 2004]; and therefore, the phosphatonins likely have increased relevance in the abnormal phosphate metabolism. Whether the phosphatonin phenotypes are the same in the various forms of ENS remains to be determined.

This follow-up report is the first longitudinal measurement of both MEPE and FGF-23 and their response to medical and surgical treatment in tumor-induced hypophosphatemia, and illustrates the advances in the understanding of phosphate metabolism beyond that of parathyroid hormone and 1,25-dihydroxyvitamin D [Rowe, 2004]. The follow-up also indicates the need for continued close monitoring of urine phosphate excretion and serum phosphorus in patients who have FGF-23 (phosphatonin) tumor-induced hypophosphatemia, such as LSNS, to determine the short-and long-term benefit of octreotide when complete excision is not possible. Additional considerations are including FGF-23 and MEPE as part of the initial evaluation of hypophosphatemia and/or rare forms of chondrodysplasias [Zeger et al., 2007], as well as to direct and monitor treatment plans [Garabedian, 2007].

Acknowledgements

The authors are grateful to Dr. Peter Rowe for his critical review of the manuscript and performing ASARM assay. This research was supported in part by Department of Defense grants DAMD 17-02-0684 (N.S.F.) and NIH grant CA113865 (N.S.F.).

References

Barthel TK, Mathern DR, Whitfield GK, Haussler CA, Hopper HA 4th, Hsieh JC, Slater SA, Hsieh G, Kaczmarska M, Jurutka PW, Kolek OI, Ghishan FK, Haussler MR. 1-25-dihydroxyvitamin D3/VDR-mediated induction of FGF23 as well as transcriptional control of bone anabolic and catabolic genes that orchestrate the regulation of phosphate and calcium mineral metabolism. J Steroid Biochem Mol Biol 2007;103:381–388. [PubMed: 17293108]

Bouthors J, Vantyghem MC, Manouvrier-Hanu S, Soudan B, Proust E, Happle R, Piette F. Phacomatosis pigmentokeratotica associated with hypophosphataemic rickets, pheochromocytoma and multiple basal cell carcinomas. Br J Dermatology 2006;155:225–226.

Bresler D, Bruder J, Mohnike K, Fraser WD, Rowe PS. Serum MEPE-ASARM-peptides are elevated in X-linked rickets (HYP): Implications for phosphaturia and rickets. J Endocrinol 2004;183:R1–9. [PubMed: 15590969]

Carey DE, Drezner MK, Hamdan JA, Mange M, Ahmad MS, Mubarak S, Nyhan WL. Hypophosphatemic rickets/osteomalacia in linear sebaceous nevus syndrome: a variant of tumor-induced osteomalacia. J Pediatr 1986;109:994–1000. [PubMed: 3023599]

Dobbie H, Unwin RJ, Faria NJ, Shirley DG. Matrix extracellular phosphoglycoprotein causes phosphaturia in rats by inhibiting tubular phosphate reabsorption. Nephrol Dial Transplant. 2007 Nov 23; [PubMed: 18037620]Epub

Econs MJ, Drezner MK. Tumor-induced osteomalacia--unveiling a new hormone. N Engl J Med 1994;330:1679–1681. [PubMed: 8177274]

Elston MS, Stewart IJ, Clifton-Bligh R, Conaglen JV. A case of oncogenic osteomalacia with preoperative secondary hyperparathyroidism: description of the biochemical response of FGF23 to octreotide therapy and surgery. Bone 2007;40:263–241.

Eriksson B, Oberg K. Summing up 15 years of somatostatin analog therapy in neuroendocrine tumors: Future outlook. Ann Oncol 1999;10(Suppl 2):S31–S38. [PubMed: 10399030]

Garabedian M. Regulation of phosphate homeostasis in infants, children, and adolescents, and the role of phosphatonins in this process. Current Opinion in Pediatrics 2007;19:488–491. [PubMed: 17630616]

Garcia de la Torre N, Waas JAH, Turner HE. Antiangiogenic effects of somatostatin analogues. Clin Endocrinol 2002;57:425–441.

Heike CL, Cunningham ML, Steiner RD, Wenkert D, Hornung RL, Gruss JS, Gannon FH, McAlister WH, Mumm S, Whyte MP. Skeletal changes in epidermal nevus syndrome: does focal bone disease harbor clues concerning pathogenesis. Am J Med Genet Part A 2005;139A:67–77.

Hoffman WH, Jueppner HW, DeYoung BR, O'Dorisio MS, Given KS. Elevated fibroblast growth factor-23 in hypophosphatemic linear nevus sebaceous syndrome. Am J Med Genet Part A 2005;134A:233–236.

Imel EA, Hui SL, Econs MJ. FGF23 concentrations vary with disease status in autosomal dominant hypophosphatemia rickets. J Bone Miner Res 2007;22:520–526. [PubMed: 17227222]

Jain A, Fedarko NS, Collins MT, Gelman R, Ankrom MA, Tayback M, Fisher LW. Serum levels of matrix extracellular phosphoglycoprotein (MEPE) in normal humans correlate with serum phosphorus, parathyroid hormone and bone mineral density. J Clin Endocrinol Metab 2004;89:4158–4161. [PubMed: 15292364]

Kousseff BG. Hypothesis: Jadassohn nevus phakomatosis: a paracrinopathy with variable phenotype. Am J Med Genet 1992;43:651–661. [PubMed: 1621754]

Lattuada D, Casnici C, Venuto A, Marelli O. The apoptotic effect of somatostatin analogue SMS 201–992 on human lymphocytes. J Neuroimmunol 2002;133:211–216. [PubMed: 12446025]

Marsell R, Krajisnik T, Goransson H, Ohlsson C, Ljunggren O, Larsson TE, Jonsson KB. Gene expression analysis of kidneys from transgenic mice expressin fibroblast growth factor-23. Nephrol Dial Transplant 2008;23:827–833. [PubMed: 17911089]

Martin A, David V, Laurence JS, Schwarz PM, Lafer EM, Hedge AM, Rowe PS. Degradation of MEPE, DMP1 and release of SIBLING ASARM-peptides (minhibins). ASARM-peptide(s) are directly responsible for defective mineralization in HYP. Endocrinology. 2007 Dec 27; [PubMed: 18162525] Epub

Rowe PSN, de Zoysa PA, Dong R, Wang HR, White KE, Econs MJ, Oudet CL. MEPE, a new gene expressed in bone marrow and tumors causing osteomalacia. Genomics 2000;67:54–68. [PubMed: 10945470]

Rowe PSN. The wrickkened pathways of FGF23, MEPE and PHEX. Crit Rev Oral Biol Med 2004;15:264–281. [PubMed: 15470265]

Rowe PSN, Kumagai Y, Gutierrez G, Garrett IR, Blacher R, Rosen D, Cundy J, Navvab S, Chen D, Drezner MK, Quarles LD, Mundy GR. MEPE has the properties of an osteoblastic phosphatonin and minhibin. Bone 2004;34:303–319. [PubMed: 14962809]

Rowe PSN, Garrett IR, Schwarz PM, Carnes DL, Lafer EM, Mundy GR, Gutierrez GE. Surface plasmon resonance (SPR) confirms MEPE binds to PHEX via the MEPE-ASARM-motif: A model for impaired mineralization in X-linked rickets (HYP). Bone 2005;36:33–46. [PubMed: 15664000]

Saraswat A, Dogra S, Bansali A, Kumar B. Phakomatosis pigmentokeratotica associated with hypophosphatemic vitamin D-resistant rickets: improvement in phophate homeostasis after partial laser ablation. Br J Dermatol 2003;148:1074–1076. [PubMed: 12786855]

Sommer S, Berndt T, Craig T, Kumar R. The phosphatonins and the regulation of phosphate transport and vitamin D metabolism. J Steroid Biochem Mol Biol 2007;103:497–503. [PubMed: 17224271]

Vidaurri-de la Cruz H, Tamayo-Sanchez L, Duran-McKinster C, de la Luz Orozco-Covarrubias M, Ruiz-Maldonado R. Epidermal nevus syndromes: clinical findings in 35 patients. Pediatr Dermatol 2004;21:432–439. [PubMed: 15283784]

White KE, Larsson TE, Econs MJ. The roles of specific genes implicated as circulating factors involved in normal and disordered phosphate homeostasis: frizzled related protein-4, matrix extracellular phosphoglycoprotein, and fibroblast growth factor 23. Endocr Rev 2006;27:221–241. [PubMed: 16467171]

Yamamoto T, Imanishi Y, Kinoshita E, Nakagomi Y, Shimizu N, Miyauchi A, Satomura K, Koshiyama H, Inaba M, Nishizawa Y, Juppner H, Ozono K. The role of fibroblast growth factor 23 for hypophosphatemia and abnormal regulation of vitamin D metabolism in patients with McCune-Albright syndrome. Bone and Mineral Metabolism 2005;23:231–237.

Zimering MB, Caldarella FA, White KE, Econs MJ. Persistent tumor-induced osteomalacia confirmed by elevated postoperative levels of serum fibroblast growth factor-23 and 5-year follow-up of bone density changes. Endocr Pract 2005;11:108–114. [PubMed: 15901526]

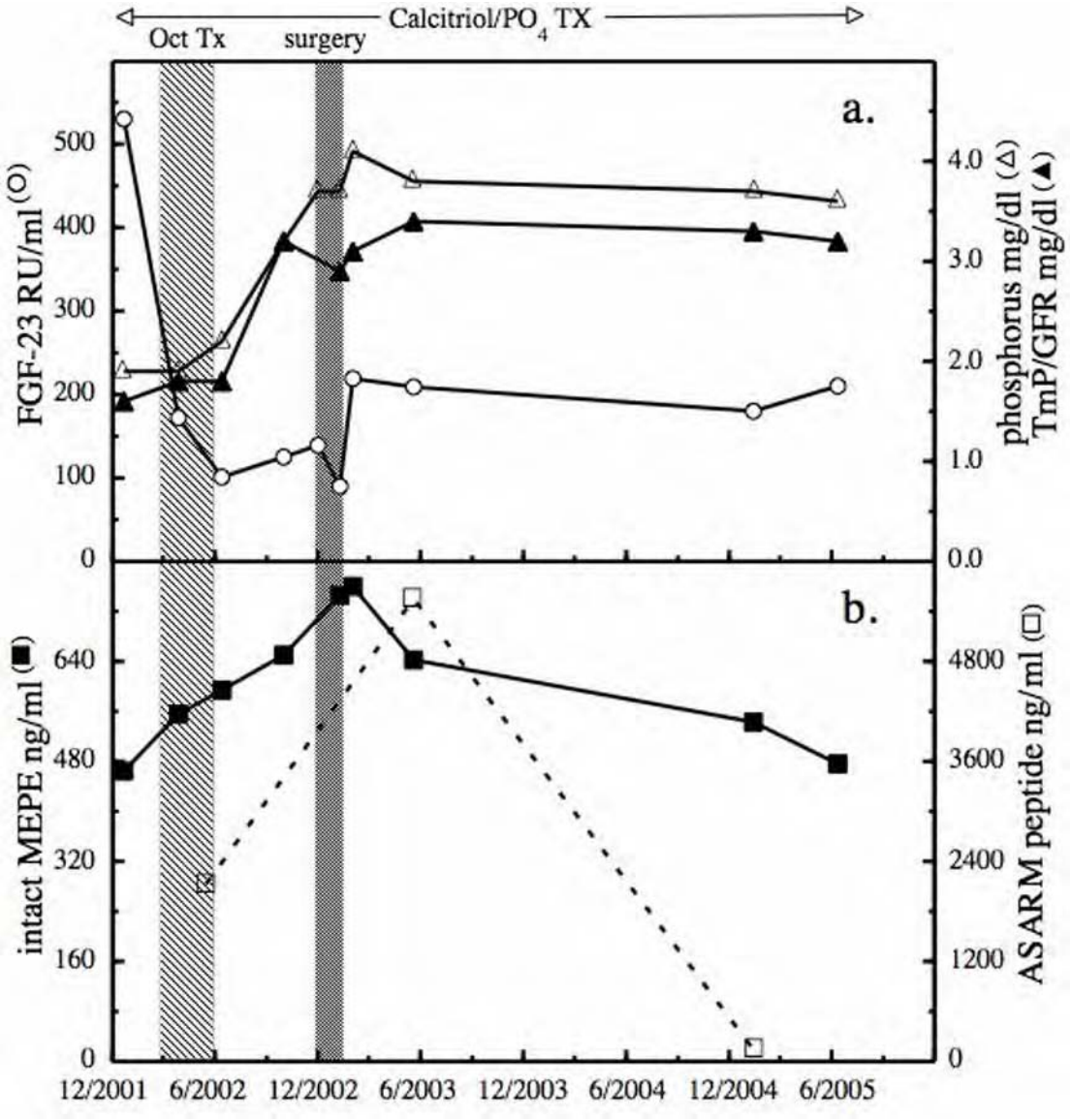

Figure 1.

Treatment effects on MEPE, FGF-23 and phosphorus. At 16 years of age, with a history of hypophosphatemia, musculoskeletal symptoms, recurrent insufficiency fractures and an elevated plasma level of FGF-23, octreotide therapy (Oct TX) was begun along with ongoing phosphate and calcitriol therapy. Initially octreotide acetate 50 mcg was administered subcutaneously daily for 3 days, followed by Sandostatin LAR depot 10 mg intramuscularly every 2 weeks for 4 months. Six months after completing the Sandostatin LAR, excision surgery was performed for cosmetic reasons. The levels of FGF-23 (open circle), serum phosphorus (open triangle), calculated TmP/GFR (solid triangle) (panel a) and total plasma MEPE (solid square) and ASARM peptide (open square) (panel b) were followed for up to 2.5 years after surgery.

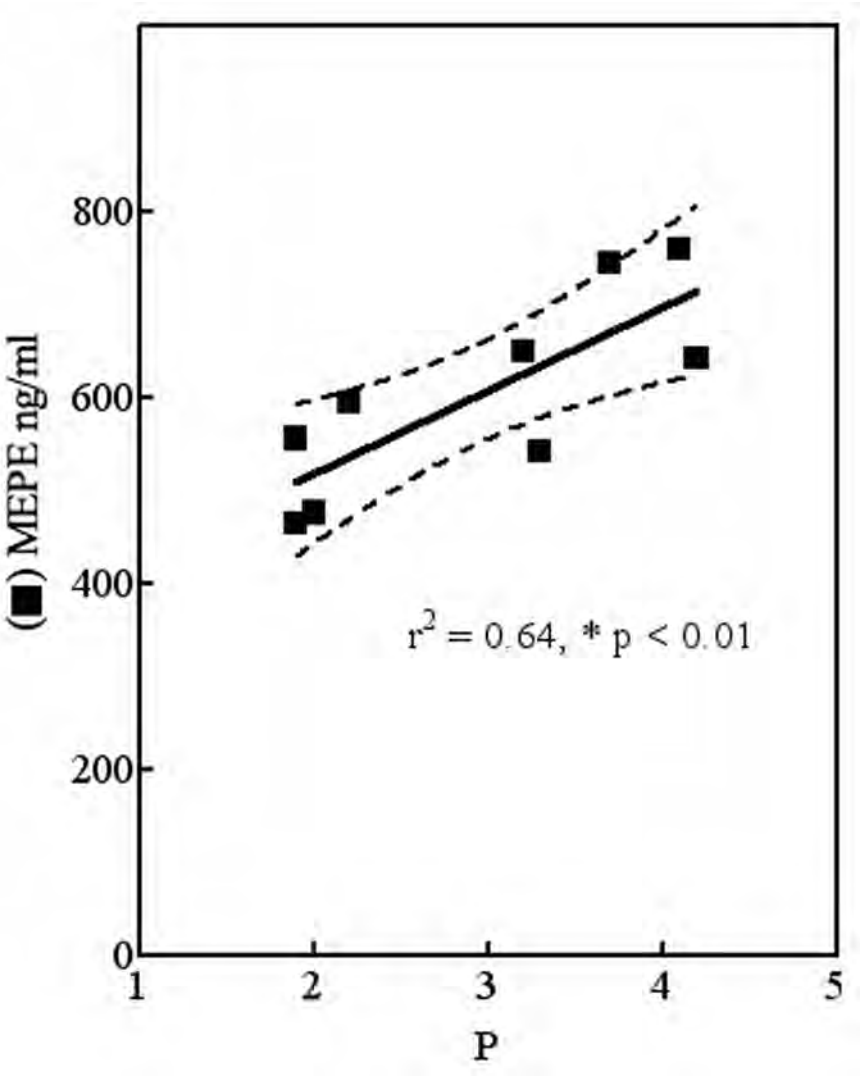

Figure 2.
MEPE, but not FGF-23, correlates with serum phosphorus. Determined values for serum phosphorus (P) and total MEPE across the 3 year follow-up were analyzed by regression analysis.

Published in final edited form as:
Biochemistry. 2008 June 3; 47(22): 5986–5995.

Bone sialoprotein binding to matrix metalloproteinase-2 alters enzyme inhibition kinetics†

Alka Jain‡, **Larry W. Fisher**§, and **Neal S. Fedarko**‡,*

‡ *Johns Hopkins University School of Medicine*

§ *National Institute for Dental and Craniofacial Research, National Institutes of Health*

Abstract

Bone sialoprotein (BSP) is a secreted glycophosphoprotein normally restricted in expression to skeletal tissue that is also induced by multiple neoplasms in vivo. Previous work has shown that BSP can bind to matrix metalloproteinase-2 (MMP-2). Because of MMP-2 activity in promoting tumor progression, potential therapeutic inhibitors were developed, but clinical trials have been disappointing. The effect of BSP on MMP-2 modulation by inhibitors was determined with purified components and in cell culture. Enzyme inhibition kinetics were studied using a low-molecular weight freely diffusable substrate and purified MMP-2, BSP, and natural (tissue inhibitor of matrix metalloproteinase-2) and synthetic (ilomastat and oleoyl-*N*-hydroxylamide) inhibitors. We determined parameters of enzyme kinetics by varying substrate concentrations at different fixed inhibitor concentrations added to MMP-2 alone, MMP-2 and BSP, or preformed MMP-2-BSP complexes and solving a general linear mixed inhibition rate equation with a global curve fitting program. Two in vitro angiogenesis model systems employing human umbilical vein endothelial cells (HUVECs) were used to follow BSP modulation of MMP-2 inhibition and tubule formation. The presence of BSP increased the competitive K_I values between 15- and 47-fold for natural and synthetic inhibitors. The extent of tubule formation by HUVECs cocultured with dermal fibroblasts was reduced in the presence of inhibitors, while the addition of BSP restored vessel formation. A second HUVEC culture system demonstrated that tubule formation by cells expressing BSP could be inhibited by an activity blocking antibody against MMP-2. BSP modulation of MMP-2 activity and inhibition may define its biological role in promoting tumor progression.

Keywords

Bone sialoprotein; matrix metalloproteinase; enzyme kinetics

The small integrin binding ligand N-linked glycoprotein (SIBLING)[1] gene family is clustered on human chromosome 4, and its members include bone sialoprotein (BSP), osteopontin, dentin matrix protein 1, matrix extracellular phosphoglycoprotein, and dentin sialophosphoprotein (1). BSP was once thought to be restricted in expression to mineralizing tissues such as bones and teeth (2) but has been shown to be induced in certain neoplasms

†This research was supported in part by Department of Defense grants DAMD 17-02-0684 (N.S.F.) and W81XWH-04-1-0844 (N.S.F.); NIH grant CA113865 (N.S.F.) and by the Intramural Research Program of the NIH, NIDCR (L.W.F.).

*Department of Medicine, Room 5A-64 JHAAC, 5501 Hopkins Bayview Circle, Johns Hopkins University, Baltimore, MD 21224. Phone: 410 550-2632; Fax: 410 550-1007, ndarko@jhmi.edu.

[1]The abbreviations used are: SIBLING, Small, Integrin-Binding LIgand, N-linked Glycoprotein; BSP, bone sialoprotein; MMP, matrix metalloproteinase; proMMP, pro-matrix metalloproteinase; HUVEC, human umbilical vein endothelial cell; CCK-8, (2-(2-methoxy-4-nitrophenyl)-5-(2,4-disulfophenyl-2*H*-tetrazolium monosodium salt); TIMP, tissue inhibitor of metalloproteinase; HRP, horseradish peroxidase; OA-Hy, oleoyl-N-hydroxylamide.

(3–11). SIBLINGs can be localized to the cell surface through binding of αVβ3 (as well as other integrins), and at least OPN and DMP1 can be bound by variants of CD44 (12–14), exhibit correlation between expression levels and tumor stage (15), and bind to and confer activity on specific latent matrix metalloproteinases (proMMPs) (16). Indeed, BSP has been shown to enhance the invasion potential of a number of human cancer cell lines in vitro by bridging MMP-2 to the cell surface of the cells through the αVβ3 integrin (14).

MMPs make up a family of structurally and functionally related endoproteinases that are involved in development and tissue repair as well as cancer angiogenesis and metastasis. We have recently shown that active MMPs inhibited by tissue inhibitors of metalloproteinases (TIMPs) can be reactivated by equimolar amounts of the appropriate SIBLING partner (16). The study presented here was undertaken to determine whether the mechanism of BSP action on MMP-2 activity involves the alteration of MMP affinity for TIMP2 and/or low-molecular weight inhibitors. The biological consequences of these interactions were tested using two in vitro model systems of angiogenesis.

MATERIALS AND METHODS

Reagents

ProMMP-2 and active human MMP-2 were obtained from Oncogene Research Products (Boston, MA) and Research Diagnostic Systems, Inc. (Minneapolis, MN). The inhibitors ilomastat {*N*-[(2*R*)-2-(hydroxamidocarbonylmethyl)- 4-methylpentanoyl]-L-tryptophan methylamide} and oleoyl-*N*-hydroxylamide, substrate Ac-PLG-(2-mercapto-4-methylpentanoyl)-LG-OC_2H_5, and 5,5'-dithiobis(2-nitrobenzoic acid) *(*DTNB) were obtained from Calbiochem (La Jolla, CA). Fluorescein-conjugated gelatin (fluorescein-gelatin) was obtained from Molecular Probes, Inc. (Eugene, OR). A cell counting kit containing the water-soluble tetrazolium salt CCK-8 [2-(2-methoxy-4-nitrophenyl)-5-(2,4-disulfophenyl- 2*H*-tetrazolium monosodium salt)] was purchased from Dojindo Molecular Technologies (Gaithersberg, MD). Human serum adsorbed goat anti-rabbit IgG conjugated to horseradish peroxidase (HRP) was obtained from Kirkegaard & Perry (Gaithersburg, MD). Recombinant human BSP and BSPKAE (where the RGD sequence has been changed to KAE) that included post-translational modifications were made using an adenovirus constructs and eukaryotic cells and purified (>95% purity as defined by acrylamide gel electrophoresis) as previously described (12). An activity blocking antibody against MMP-2 was obtained from Chemicon International (Temecula, CA).

Low-Molecular Weight Substrates

The activities of wildtype MMP-2 in the presence and absence of inhibitors (TIMP2, ilomastat, or oleoyl-*N*-hydroxylamide) and BSP were measured using a low-molecular weight thiopeptide substrate [Ac-PLG-(2-mercapto-4-methylpentanoyl)- LG-OC_2H_5]. Substrate was incubated in assay buffer [50 mM HEPES, 10 mM $CaCl_2$, 0.05% Brij 35, and 1 mM DTNB (pH 7.5)] with 10 nM MMP-2 and different concentrations of inhibitor, a 10 nM MMP-2-BSP preformed complex or an MMP-2-inhibitor-BSP complex added simultaneously. Data from the first 6 min were used to calculate velocity (picomoles per second) values. Substrate cleavage was monitored using a Perkin-Elmer Victor 2 multilabel plate reader, and absorbance was measured at 412 nM. Preformed MMP-2-BSP complexes were formed by incubation at 37 ° C for 30 min prior to addition to the reaction mixture. Global curve fitting of the family of substrate-velocity curves was performed using Prism 4 (GraphPad Software, Inc.) with V_{max}, K_m, K_{ic}, and K_{iu} set as shared parameters.

Coculture Angiogenesis Assay

Human umbilical vein endothelial cell (HUVEC) and human dermal fibroblast cocultures were grown in EGM-2 growth medium obtained from TCS Cell Works (Botolph Claydon, U.K.). The functional readout from this in vitro assay was tubule formation. Tubule formation was defined by the total number of tubules and number of branches. Test conditions were run in triplicate wells with eight conditions per 24-well plate. The cells were treated starting on day 6 of culture with multiple conditions, including 5 nM bFGF, 5 nM BSP, 5 nM BSPKAE, 5 nM TIMP2, 5 nM BSP and 5 nM TIMP2, 5 nM ilomastat, 5 nM ilomastat and 5 nM BSP, 33.6 nM oleoyl-*N*-hydroxylamide, 33.6 nM oleoyl-*N*-hydroxylamide and 5 nM BSP, or buffer alone. Medium was replaced every other day with fresh medium containing the positive control bFGF, BSP, BSP-KAE, and/or inhibitors. Cells were fixed in 70% ethanol on day 12, and tubule formation was quantified following immunostaining with a mouse anti-human PECAM-1 monoclonal antibody (TCS Cell Works), and secondary antibody with the substrate 5-bromo-4-chloro-3-indolyl phosphate/ nitro blue tetrazolium (BCIP/NBT, from Sigma). Images were visualized on a Nikon Diaphot inverted microscope and digitized with a Polaroid CCD digital camera and software. Two images per well were captured and digitized, and the number of tubules, the number of branch points (junctions) between tubules, and the total tubule length (in pixels) were determined using AngioSys version 1.0 (TCS Cell Works).

For MMP activity assays, a membrane-associated fraction was prepared from the HUVEC cocultures essentially as described by Ward et al. (17). Briefly, cells were scraped from culture wells in cold 5 mM Tris-HCl (pH 7.8) and homogenized, and crude membranes were prepared by centrifugation of the cell lysate at 10000*g* for 15 min at 4 °C. The supernatant was centrifuged at 105000*g* for 1 h at 4 °C; then, the supernatant was removed, and the membrane fraction was resuspended in 20 mM Tris-HCl (pH 7.8), 10 mM $CaCl_2$, and 0.05% Brij 35. A 20 μL aliquot of the membrane fraction pool was added to 12.5 μg/mL fluoresceinconjugated gelatin substrate conjugate in a 200 μL total volume of reaction buffer containing 50 mM Tris (pH 7.6), 150 mM NaCl, and 5 mM $CaCl_2$ as previously described (16). This substrate is highly substituted with fluorescein moieties so that the fluorescent signal is self-quenched until proteolytic cleavage liberates fragments and a robust fluorescent emission is measured. Fluorescence data were acquired with excitation at 485 nm and emission at 535 nm. Reactions were run in triplicate.

Collagen Sandwich Angiogenesis Assay

HUVECs were transfected with 10^4 pfu adenovirus/cell for 24 h in EGM-2 defined medium. The adenovirus contained the coding sequence for normal BSP (12) or was the null (empty) Ad5 virus. Cells were then released from the flasks by trypsin/ EDTA treatment, counted with a hemocytometer, and then seeded at a density of 10^4 cells/well onto wells that had been coated with type I collagen and allowed to gel. The collagen sandwich was made by mixing 8 volumes of a cold type acid-soluble 3 mg/mL type I collagen solution (pH 3.0) (Cellmatrix, Nitta, Osaka, Japan) with 1 volume of cold 10x concentrated MEM buffer without NaHCO3. The solution was carefully mixed, while on ice, an additional 1 volume of reconstitution buffer (2.2 g of $NaHCO_3$ in 100 mL of 0.05 N NaOH and 200 mM HEPES) was added and mixed. Wells of a 48-well plate were coated with 150 μL of the solution, and the plate was placed in a 37 °C incubator with 5% CO2 for 30 min to gel the solution. Cells were added to each well in a volume of 150 μL, and the plate was returned to the tissue culture incubator to enable cell attachment. After 2 h at 37 °C, the unattached cells in solution were aspirated from the wells, the wells were rinsed twice with serum-free medium, and a second 150 μL portion of the collagen solution was added to each well. After 30 min at 37 °C, endothelial cell basal medium (EBM-2, Cambrex Corp.) with or without 1.25 μg of an activity blocking anti-MMP-2 antibody was added to each well and HUVECs were grown in culture for up to an additional 48 h.

The cell number in the collagen gel culture system was followed by using the addition of CCK-8 to the medium at the start of the experiments following the manufacturer's protocol. CCK-8, which is less toxic then other tetrazolium salts such as MTT and can be used to monitor cell proliferation over days of continuous culture, is metabolized by cells to form a formazan dye whose absorbance value at 460 nm is directly proportional to the number of living cells. The fluorescein-conjugated gelatin substrate was used to follow MMP proteolytic activity in the collagen gels. A solution of 12.5 μg/mL fluorescein-substrate conjugate was added to the bottom collagen gel prior to polymerization. Fluorescence data were acquired with excitation at 485 nm and emission at 535 nm using a Victor 2 Multilabel plate analyzer. MMP enzyme activity was measured as the rate of change in fluorescence per minute, with the slope over the first 10 min determined. Zymography for MMP detection and Western blotting for profiling BSP protein expression were performed exactly as previously described (16).

RESULTS

TIMP Inhibition Kinetics

To determine the effect of BSP on active wild-type MMP-2 and TIMP2 reaction kinetics, a low-molecular weight substrate was employed to follow product evolution over time. MMP-2 incubated with increasing concentrations of TIMP2 exhibited the expected dose-dependent inhibition (Figure 1A). The level of inhibition by TIMP2 was significantly decreased either by the presence of a preformed MMP-2-BSP complex or by the simultaneous addition of BSP and TIMP2 to MMP-2 (Figure 1B,C). To investigate whether a decreased level of inhibition of MMP-2 by TIMP2 in the presence of BSP was associated with an altered affinity, we obtained substrate-velocity plots by varying substrate concentrations of each at different but fixed inhibitor concentrations. Reaction conditions included either TIMP2 and 10 nM MMP-2, TIMP2 and 10 nM preformed equimolar MMP-2-BSP complexes, or simultaneous mixes of TIMP2, 10 nM MMP-2, and 10 nM BSP (Figure 1D–F).

Because there are two distinct binding sites for TIMP2 on MMP-2, TIMP2 does not act purely as a competitive inhibitor (18). The common types of inhibition (competitive, uncompetitive, and noncompetitive) are all special cases of linear mixed inhibition (19). The generalized linear mixed inhibition equation $V = V_{max}[S]/[K_m(1 + [I]/K_{ic}) + [S](1 + [I]/K_{iu})]$ was employed to determine the reaction rate, where V_{max} is the limiting rate, K_m is the Michaelis constant, K_{ic} is the competitive inhibition constant, and K_{iu} is the uncompetitive inhibition constant. For competitive inhibition, $[I]/K_{iu}$ is negligible, while for uncompetitive inhibition, $[I]/K_{ic}$ is negligible. In pure noncompetitive inhibition, the inhibition constants are equal.

Global curve fitting of the family of substrate-velocity curves revealed a significant increase in K_{ic} and K_{iu} values for the MMP-2-BSP complex as well as the simultaneously added MMP-2 and BSP (Table 1). The inhibitor TIMP2 had K_{ic} and K_{iu} values for the MMP-2-BSP preformed complex increased 36- and 6-fold, respectively. The K_{ic} and K_{iu} values were increased 15- and 6-fold, respectively when all components were added simultaneously. These values indicate a relatively poor affinity of the inhibitor for MMP-2 in the presence of BSP. The fitted values for K_m and V_{max} were not significantly different with or without TIMP2 or BSP. The order of magnitude change in the apparent inhibitor affinity for MMP-2 in the presence of BSP indicates that SIBLING modulation of MMPs may be physiologically significant.

Low-Molecular Weight Inhibitor Kinetics

The MMP inhibitors ilomastat and oleoyl-*N*-hydroxylamide were utilized to test whether low-molecular weight drug inhibition of MMP-2 activity could be modulated by BSP. Ilomastat at a concentration of 1 nM inhibited the initial velocity of MMP-2 activity to 39% of control activity, while the same concentration of inhibitor reduced the activity of the MMP-2 with BSP

to only 70% of the control, suggesting that the inhibitor is much less effective against MMP-2 in the conformation resulting from the binding of BSP (Figure 2A). Similar to the studies with TIMP2, substrate-velocity plots of the enzyme activity of MMP-2 in the presence of different concentrations of ilomastat reacted with increasing substrate concentrations in the presence or absence of BSP were made. BSP reduced the level of inhibition by ilomastat whether it was added as a preformed complex with MMP-2 (Figure 2C) or added simultaneously to MMP-2 with the inhibitor (Figure 2D). Because ilomastat is a competitive inhibitor, kinetic parameters in the presence and absence of BSP can be determined by fitting the substrate-velocity curves to the equation for competitive inhibition $v = V_{max}[S]/K_m(1 + [I]/K_{ic}) + [S]$, where V_{max} is the limiting rate, K_m is the Michaelis constant, K_{ic} is the competitive inhibition constant, [S] is the substrate concentration, and [I] is the ilomastat concentration. The results indicated a significant increase (>30-fold) in the K_{ic} value of ilomastat for MMP-2 when BSP was included in the reaction mixture (Table 1). Thus, ilomastat exhibited a reduced affinity for MMP-2 in the presence of BSP.

The same substrate and reaction conditions were utilized to follow MMP-2 reaction velocities in the presence of the low-molecular weight inhibitor oleoyl-*N*-hydroxylamide. The addition of 10 μM oleoyl-*N*-hydroxylamide inhibited the activity of MMP-2 by 80%, while the inclusion of 10 nM BSP restored activity by ~50% (Figure 3A). Titration with increasing amounts of BSP revealed a dose response to the increase in enzymatic activity, with the highest dose, 100 nM BSP, restoring the activity of the inhibited enzyme to 75%. Substrate-velocity plots were made for reaction conditions of MMP-2 incubated with oleoyl-*N*-hydroxylamide alone, an MMP-2-BSP preformed complex incubated with oleoyl-*N*-hydroxylamide, and simultaneously added MMP-2, BSP, and oleoyl-*N*-hydroxylamide (Figure 3B–D). Global curve fitting of the family of substrate-velocity curves revealed a significant increase the value of K_{ic} for oleoyl-*N*-hydroxylamide in the presence of BSP (Table 1). The inhibitor oleoyl-*N*-hydroxylamide had its K_{ic} value for the MMP-2-BSP preformed complex increased 25-fold, while the K_{ic} value was increased 18-fold when all components were added simultaneously.

BSP Restores Activity to Inhibited MMPs in Vitro

The ability of BSP to restore enzymatic activity to MMP-2 inhibited by TIMP2, ilomastat, or oleoyl-*N*-hydroxylamide in a purified component assay led to a screen of the effects of BSP on MMP inhibitors in an in vitro model system with a biological readout (tubule formation). The model system used human umbilical vein endothelial cells (HUVECs) cocultured with normal adult human diploid dermal fibroblasts grown in a defined endothelial cell basal medium supplemented with EGM-2. Over the course of almost 2 weeks of culture, the endothelial cells form threadlike tubule structures and expressed endothelial cell-specific components that can be stained immunohostochemically with antibodies against PECAM-1 (Figure 4). BSP (5 nM) alone stimulated tubule formation by HUVECs above that of control. Treatment of the coculture system with a variant of BSP whose RGD sequence had been mutated to KAE (BSPKAE, which can not bind the $\alpha_v\beta_3$ integrin and is unable to be localized to the cell surface) caused a reduction in the level of tubule formation. Incubation separately with 5 nM TIMP2, 5 nM ilomastat, or 33.6 nM oleoyl-*N*-hydroxylamide inhibited tubule formation below control levels. The inclusion of BSP with MMP-specific inhibitors increased immunostained tubule structures.

Quantification of tubule formation using AngioSys version 1.0 revealed that incubation of the cells with 5 nM bFGF or 5 nM BSP alone resulted in a similar increase in tubule and junction/branching numbers (289 ± 55 tubules and 110 ± 21 branches for bFGF vs 335 ± 18 tubules and 145 ± 13 branches for BSP). Treatment with BSPKAE inhibited tubule formation by 50% and branching by 70%, relative to control (Figure 5A,B). The MMP inhibitors decreased the level of tubule formation and branching between 25 and 90%. The addition of BSP to TIMP2-,

ilomastat-, or oleoyl-*N*-hydroxylamide- treated cells significantly increased the number of tubules approximately 3-fold and the number of branch points approximately 5-fold compared to levels with inhibitor alone. The restoration of tubule formation by the addition of BSP to oleoyl-*N*-hydroxylamide-treated cells, although significant compared to conditions with inhibitor alone, was much weaker than that for control and other BSP treatment conditions. The effect of BSP on MMP activity in the in vitro coculture angiogenesis system was also studied using a large macromolecular substrate, fluorescein-gelatin, to measure MMP enzyme activity of plasma membrane preparations. When the gelatinase activity of membrane-associated MMPs was assayed in cohort wells treated under the same conditions, the pattern paralleled that of the number of tubules and branches (Figure 5C). Incubation of the cells with 5 nM bFGF alone resulted in an average membraneassociated enzyme activity of 225 ± 11 fluorescein-gelatin/ min, while 5 nM BSP was associated with 445 ± 67 fluorescein-gelatin/ min. The BSPKAE variant had a membrane-associated gelatinase activity of 78 ± 19 fluoresceingelatin/ min. MMP activity as a percentage of control values was 40% with TIMP2, 50% with ilomastat, and 10% with oleoyl-*N*-hydroxylamide. The addition of BSP to the culture medium significantly restored enzyme activity in the presence of each inhibitor ($p \leq 0.01$).

The coculture system requires multiple days of cell growth prior to tubule formation and as such was not ideal for demonstrating a direct linkage among BSP, MMP-2, and tubule formation. A second model system of angiogenesis was employed that required a much shorter time frame (14–24 h) and could be easily manipulated to incorporate MMP-specific blocking antibodies. HUVECs grown in EBM-2 medium were transfected with adenovirus for BSP, or null Ad5 virus as a negative control, and then transferred into collagen sandwiches. At 14, 24, and 48 h, cells in the collagen sandwich were visualized using a Nikon Daiphot microscope. Collagen gels containing null virus-transfected cells exhibited an isolated spherical pattern at 14 and 24 h, and by 48 h, few cells had elongated and associated to form tubules (Figure 6). In contrast, wells containing BSPtransfected cells showed cell elongation, association, and tubule formation by 14 h. The inclusion of a monoclonal antibody that specifically blocks the activity of MMP-2 with cells transfected with the BSP adenovirus in the collagen sandwich system visibly reduced the level of cell elongation and association at all time points.

Tubule formation was again quantified as the number of tubules and branches using AngioSys version 1.0. The small number of tubules in the null-transfected cells increased over the time course; however, the numbers remained relatively small (Figure 7). In the BSP adenovirus-transfected cells, the number of tubules increased between 6- and 14-fold over the 14, 24, and 48 h time points when compared to those of the null virus-transfected cells. The addition of the anti- MMP-2 antibody reduced the number of tubules 74–84%. Similarly, the number of branches remained low of the three time points in the null transfected cell, increased between 6- and 8-fold in the BSP adenovirus-transfected cells, and decreased 62–83% by the inclusion of the MMP-2 antibody. Because it is possible that the expression of BSP changed the proliferation of the cells which in turn altered tubule formation and branching, the number of cells in each well was profiled using the CCK-8 tetrazolium salt. The relative absorbance did increase to a small degree across the time points. The largest increase was observed in the BSP adenovirus cells which had a 13% increase in absorbance, while the inclusion of the MMP-2 antibody with the BSP adenovirus-transfected cells exhibited a 4% increase between 14 and 48 h. There were, however, no significant differences in cell number between any of the conditions and time points; thus, it is unlikely that effects of BSP on cell proliferation account for an increased level of tubule formation. We have observed that cells grown for more than 72 h in the collagen gel system do show differences in cell survival and cell number (data not shown). However, in the current assay, significant tubule formation occurred well before any changes in cell number.

The activity of MMPs in the gel culture system was monitored using the fluorescein-gelatin substrate. Cells transfected with the BSP adenovirus had between 3- and 5-fold higher enzyme activity then cells transfected with null virus, while the inclusion of the monoclonal antibody against MMP-2 reduced enzyme activity between 54 and 71% across the different time points. In the collagen gel system, membrane-associated MMP-2 activity was necessary for BSP-dependent tubule formation. The endothelial cells were used to test whether attachment of BSP to the cell membrane was required for tubule formation. HUVECs were transfected with null Ad5 virus, BSP, or BSPKAE adenovirus and grown in collagen gels for 24 h, and tubule formation was monitored by microscopy (Figure 8). Expression of BSP with an intact RGD sequence led to abundant tubule formation, while transfection with BSPKAE reduced the level of tubule formation below control levels. HUVECs transfected with null Ad5 virus or the BSPKAE virus had no detectable BSP in a membrane-associated pool (Figure 8D). The levels of active MMP-2 in the membrane-associated pool were elevated in the BSP-transfected cells and reduced in the BSPKAE-transfected cells. These observations are consistent BSP-dependent tubule formation requiring BSP and MMP-2 localization to the cell surface.

DISCUSSION

BSP is a member of the SIBLING gene family (2). It is extended and flexible in solution, and such a lack of ordered structure is shared by a number proteins that have multiple binding partners (1). BSP can bind the $\alpha_V\beta_3$ integrin via its RGD sequence (20,21) and to complement Factor H (12). BSP can also bind to and modulate the activity of MMP-2 (16). Binding of BSP to MMP-2 was associated with conformational changes as indicated by fluorescence quenching during BSP binding titration (indicating a change in the microenvironment of the MMP's tryptophans), and by increased susceptibility of a BSP-proMMP-2 complex to plasmin cleavage. BSP binding to pro-MMP-2 was associated with increased proteolytic activity, and BSP binding to TIMP2-inhibited MMP-2 restored activity (16). Taken together, the data suggest that conformational changes in MMP-2 induced by BSP binding may include changes in the shape of the active site and inhibitor binding domains. A trimolecular complex of BSP, $\alpha_V\beta_3$, and MMP-2 can be demonstrated by immunoprecipitation, flow cytometry, and in situ hybridization in cancer cells grown in vitro (14). BSP message was induced in multiple cancers and its expression correlated with paired MMP-2 expression as well as tumor stage (15).

MMP-2, a gelatinase that can degrade components of the extracellular matrix at physiological pH, is regulated in vivo by the naturally occurring TIMPs and RECK (22,23). TIMP2 binding to MMP-2 involves distinct domains on both the inhibitor and the enzyme (24–26). The binding and kinetics of MMP-2 and TIMP2 are more complex than simple competitive inhibition. In our analyses, we have used a mixed linear model of mixed inhibition (19) and observed inhibition constants at or below the nanomolar range. K_i values in the subnanomolar range for TIMP2 and MMP-2 using the same substrate have been reported in the literature (27–29), though a more recent analysis has yielded 3-4-fold higher estimates (30). The different reported values are most likely due to differences in sources and concentrations of substrate, enzyme, and inhibitor.

BSP was found to significantly reduce the affinity of low-molecular weight synthetic inhibitors (ilomastat and oleoyl- *N*-hydroxylamide) for MMP-2. Ilomastat as a hydroxamate class inhibitor blocks the activity of multiple MMPs and has been used to disrupt angiogenesis and metastasis (31–33). Ilomastat blocked TNFα processing (34), experimental autoimmune encephalitis (35), angiogenesis, and metastasis (31–33). The magnitude of the change in the apparent affinity of the inhibitor for MMP-2 in the presence of BSP indicates that SIBLING modulation of MMP inhibition by lowmolecular weight drugs can be physiologically significant.

Finally, cell culture model systems were used to test whether BSP modulation of MMP-2 occurs in vitro. The first model system utilized human umbilical vein endothelial cells (HUVECs) cocultured with normal adult human diploid dermal fibroblasts. The endothelial cells form small islands among the fibroblasts, proliferate, and migrate through the coculture matrix to form threadlike tubule structures. These cordlike structures join up to form a network of anastomosing tubules (36). The observed effects of BSP (stimulating basal tubule formation and restoring formation to TIMP2-, ilomastat-, or oleoyl-*N*-hydroxylamide-inhibited cultures) were consistent with BSP modulating MMP-2 activity. BSPKAE, which lacks the ability to bind to cell surface receptors, did not stimulate tubule formation. Profiling MMP-2 activity in the in vitro coculture system (by fluorescent substrate assays) demonstrated changes with BSP or BSPKAE treatment consistent with a requirement for BSP cell surface localization for BSP-dependent activity. The HUVEC culture in the collagen gel system similarly exhibited an increased level of tubule formation when cells expressed BSP. The inclusion of an activity-blocking antibody to MMP-2 significantly reduced the level of BSP-dependent tubule formation. Transfection with BSPKAE also led to a decreased level of tubule formation which was associated with reduced levels of active MMP-2 at the cell surface. In both culture systems, MMP enzyme activity correlated with the extent of tubule formation and presence of BSP. Thus, BSP promotion of HUVEC tubule formation most likely acts through BSP cell surface localization and the modulation of MMP-2 activity. It has been reported that BSP promotes angiogenesis in the chick chorioallantoic membrane system (37). These results indicate that BSP has biochemical and biological plausibility to be playing active roles in tumor progression in vivo. BSP is induced by multiple neoplasms in vivo, and its modulation of inhibitor affinity for MMP-2 might contribute to the relative lack of efficacy seen in the recent clinical trials of MMP inhibitors in numerous cancers (38). This suggests that the screening of new inhibitors of MMPs for potential therapeutic use should be done in the presence of BSP.

Acknowledgements

TIMP2 was a generous gift of Dr. H. Birkedal-Hansen (National Institute of Dental and Craniofacial Research, National Institutes of Health).

References

1. Fisher LW, Torchia DA, Fohr B, Young MF, Fedarko NS. The solution structures of two SIBLING proteins, bone sialoprotein and osteopontin, by NMR. Biochem Biophys Res Commun 2001;280:460–465. [PubMed: 11162539]
2. Fisher LW, Fedarko NS. Six genes expressed in bones and teeth encode the current members of the SIBLING family of proteins. Connect Tissue Res 2003;44:33–40. [PubMed: 12952171]
3. Bellahcene A, Menard S, Bufalino R, Moreau L, Castronovo V. Expression of bone sialoprotein in primary human breast cancer is associated with poor survival. Int J Cancer 1996;69:350–353. [PubMed: 8797881]
4. Ibrahim T, Leong I, Sanchez-Sweatman O, Khokha R, Sodek J, Tenenbaum HC, Ganss B, Cheifetz S. Expression of bone sialoprotein and osteopontin in breast cancer bone metastases. Clin Exp Metastasis 2000;18:253–260. [PubMed: 11315099]
5. Fedarko NS, Jain A, Karadag A, Van Eman MR, Fisher LW. Elevated serum bone sialoprotein and osteopontin in colon, breast, prostate, and lung cancer. Clin Cancer Res 2001;7:4060– 4066. [PubMed: 11751502]
6. Woitge HW, Pecherstorfer M, Horn E, Keck AV, Diel IJ, Bayer P, Ludwig H, Ziegler R, Seibel MJ. Serum bone sialoprotein as a marker of tumour burden and neoplastic bone involvement and as a prognostic factor in multiple myeloma. Br J Cancer 2001;84:344–351. [PubMed: 11161399]
7. Carlinfante G, Vassilioul D, Svensson O, Wendel M, Heinegard D, Andersson G. Differential expression of osteopontin and bone sialoprotein in bone metastasis of breast and prostate carcinoma. Clin Exp Metastasis 2003;20:437–444. [PubMed: 14524533]

8. Detry C, Waltregny D, Quatresooz P, Chaplet M, Kedzia W, Castronovo V, Delvenne P, Bellahcene A. Detection of bone sialoprotein in human (pre)neoplastic lesions of the uterine cervix. Calcif Tissue Int 2003;73:9–14. [PubMed: 14506948]
9. Fisher LW, Jain A, Tayback M, Fedarko NS. Small integrin binding ligand N-linked glycoprotein gene family expression in different cancers. Clin Cancer Res 2004;10:8501–8511. [PubMed: 15623631]
10. Papotti M, Kalebic T, Volante M, Chiusa L, Bacillo E, Cappia S, Lausi P, Novello S, Borasio P, Scagliotti GV. Bone sialoprotein is predictive of bone metastases in resectable non-small-cell lung cancer: A retrospective case-control study. J Clin Oncol 2006;24:4818–4824. [PubMed: 17050866]
11. Ogbureke KU, Nikitakis NG, Warburton G, Ord RA, Sauk JJ, Waller JL, Fisher LW. Up-regulation of SIBLING proteins and correlation with cognate MMP expression in oral cancer. Oral Oncol 2007;43:920–932. [PubMed: 17306612]
12. Fedarko NS, Fohr B, Gehron Robey P, Young MF, Fisher LW. Factor H binding to bone sialoprotein and osteopontin enables molecular cloaking of tumor cells from complement-mediated attack. J Biol Chem 2000;275:16666–16672. [PubMed: 10747989]
13. Jain A, Karadag A, Fohr B, Fisher LW, Fedarko NS. Three SIBLINGs (small integrin-binding ligand, N-linked glycoproteins) enhance factor H's cofactor activity enabling MCPlike cellular evasion of complement-mediated attack. J Biol Chem 2002;277:13700–13708. [PubMed: 11825898]
14. Karadag A, Ogbureke KU, Fedarko NS, Fisher LW. Bone sialoprotein, matrix metalloproteinase 2, and Rv 3 integrin in osteotropic cancer cell invasion. J Natl Cancer Inst 2004;96:956–965. [PubMed: 15199115]
15. Fisher LW, Jain A, Tayback M, Fedarko NS. Small Integrin Binding LIgand N-linked Glycoprotein (SIBLING) gene family expression in different cancers. Clin Cancer Res 2004;10:8501–8511. [PubMed: 15623631]
16. Fedarko NS, Jain A, Karadag A, Fisher LW. Three small integrin binding ligand N-linked glycoproteins (SIBLINGs) bind and activate specific matrix metalloproteinases. FASEB J 2004;18:734–736. [PubMed: 14766790]
17. Ward RV, Atkinson SJ, Slocombe PM, Docherty AJP, Reynolds JJ, Murphy G. Tissue inhibitor of metalloprotienases-2 inhibits the activation of 72 kDa progelatinase by fibroblast membranes. Biochim Biophys Acta 1991;1079:242–246. [PubMed: 1911847]
18. Kleiner DE Jr, Unsworth EJ, Krutzsch HC, Stetler- Stevenson WG. Higher-order complex formation between the 72-kilodalton type IV collagenase and tissue inhibitor of metalloproteinases-2. Biochemistry 1992;31:1665–1672. [PubMed: 1310615]
19. Cortes A, Cascante M, Cardenas ML, Cornish-Bowden A. Relationships between inhibition constants, inhibitor concentrations for 50% inhibition and types of inhibition: New ways of analysing data. Biochem J 2001;357:263–268. [PubMed: 11415458]
20. Oldberg A, Franzen A, Heinegard D. Cloning and sequence analysis of rat bone sialoprotein (osteopontin) cDNA reveals an Arg-Gly-Asp cell-binding sequence. Proc Natl Acad Sci USA 1986;83:8819–8823. [PubMed: 3024151]
21. Fisher LW, McBride OW, Termine JD, Young MF. Human bone sialoprotein. Deduced protein sequence and chromosomal localization. J Biol Chem 1990;265:2347–2351. [PubMed: 2404984]
22. Giannelli G, Antonaci S. Gelatinases and their inhibitors in tumor metastasis: From biological research to medical applications. Histol Histopathol 2002;17:339–345. [PubMed: 11813883]
23. Oh J, Takahashi R, Kondo S, Mizoguchi A, Adachi E, Sasahara RM, Nishimura S, Imamura Y, Kitayama H, Alexander DB, Ide C, Horan TP, Arakawa T, Yoshida H, Nishikawa S, Itoh Y, Seiki M, Itohara S, Takahashi C, Noda M. The membrane-anchored MMP inhibitor RECK is a key regulator of extracellular matrix integrity and angiogenesis. Cell 2001;107:789–800. [PubMed: 11747814]
24. Willenbrock F, Crabbe T, Slocombe PM, Sutton CW, Docherty AJ, Cockett MI, O'Shea M, Brocklehurst K, Phillips IR, Murphy G. The activity of the tissue inhibitors of metalloproteinases is regulated by C-terminal domain interactions: A kinetic analysis of the inhibition of gelatinase A. Biochemistry 1993;32:4330–4337. [PubMed: 8476862]
25. Nguyen Q, Willenbrock F, Cockett MI, O'Shea M, Docherty AJ, Murphy G. Different domain interactions are involved in the binding of tissue inhibitors of metalloproteinases to stromelysin-1 and gelatinase A. Biochemistry 1994;33:2089–2095. [PubMed: 8117665]

26. Hutton M, Willenbrock F, Brocklehurst K, Murphy G. Kinetic analysis of the mechanism of interaction of fulllength TIMP-2 and gelatinase A: Evidence for the existence of a low-affinity intermediate. Biochemistry 1998;37:10094–10098. [PubMed: 9665714]
27. O'Shea M, Willenbrock F, Williamson RA, Cockett MI, Freedman RB, Reynolds JJ, Docherty AJ, Murphy G. Site-directed mutations that alter the inhibitory activity of the tissue inhibitor of metalloproteinases-1: Importance of the N-terminal region between cysteine 3 and cysteine 13. Biochemistry 1992;31:10146–10152. [PubMed: 1420137]
28. Murphy G, Docherty AJ. The matrix metalloproteinases and their inhibitors. Am J Respir Cell Mol Biol 1992;7:120– 125. [PubMed: 1497900]
29. O'Connell JP, Willenbrock F, Docherty AJ, Eaton D, Murphy G. Analysis of the role of the COOH-terminal domain in the activation, proteolytic activity, and tissue inhibitor of metalloproteinase interactions of gelatinase B. J Biol Chem 1994;269:14967–14973. [PubMed: 8195131]
30. Olson MW, Gervasi DC, Mobashery S, Fridman R. Kinetic analysis of the binding of human matrix metalloproteinase- 2 and -9 to tissue inhibitor of metalloproteinase (TIMP)-1 and TIMP-2. J Biol Chem 1997;272:29975–29983. [PubMed: 9368077]
31. Boghaert ER, Chan SK, Zimmer C, Grobelny D, Galardy RE, Vanaman TC, Zimmer SG. Inhibition of collagenolytic activity relates to quantitative reduction of invasion in vitro in a c-Ha-ras transfected glial cell line. J Neurooncol 1994;21:141–150. [PubMed: 7861190]
32. Galardy RE, Grobelny D, Foellmer HG, Fernandez LA. Inhibition of angiogenesis by the matrix metalloprotease inhibitor N-[2R-2- (hydroxamidocarbonymethyl)-4-methylpentanoyl)]-L-tryptophan methylamide. Cancer Res 1994;54:4715–4718. [PubMed: 7520359]
33. Winding B, NicAmhlaoibh R, Misander H, Hoegh-Andersen P, Andersen TL, Holst-Hansen C, Heegaard AM, Foged NT, Brunner N, Delaisse JM. Synthetic matrix metalloproteinase inhibitors inhibit growth of established breast cancer osteolytic lesions and prolong survival in mice. Clin Cancer Res 2002;8:1932–1939. [PubMed: 12060638]
34. Solorzano CC, Ksontini R, Pruitt JH, Auffenberg T, Tannahill C, Galardy RE, Schultz GP, MacKay SL, Copeland EM III, Moldawer LL. A matrix metalloproteinase inhibitor prevents processing of tumor necrosis factor α (TNF α) and abrogates endotoxin-induced lethality. Shock 1997;7:427–431. [PubMed: 9185243]
35. Gijbels K, Galardy RE, Steinman L. Reversal of experimental autoimmune encephalomyelitis with a hydroxamate inhibitor of matrix metalloproteases. J Clin InVest 1994;94:2177–2182. [PubMed: 7989572]
36. Bishop ET, Bell GT, Bloor S, Broom IJ, Hendry NF, Wheatley DN. An in vitro model of angiogenesis: Basic features. Angiogenesis 1999;3:335–344. [PubMed: 14517413]
37. Bellahcene A, Bonjean K, Fohr B, Fedarko NS, Robey FA, Young MF, Fisher LW, Castronovo V. Bone sialoprotein mediates human endothelial cell attachment and migration and promotes angiogenesis. Circ Res 2000;86:885–891. [PubMed: 10785511]
38. Mandal M, Mandal A, Das S, Chakraborti T, Sajal C. Clinical implications of matrix metalloproteinases. Mol Cell Biochem 2003;252:305–329. [PubMed: 14577606]

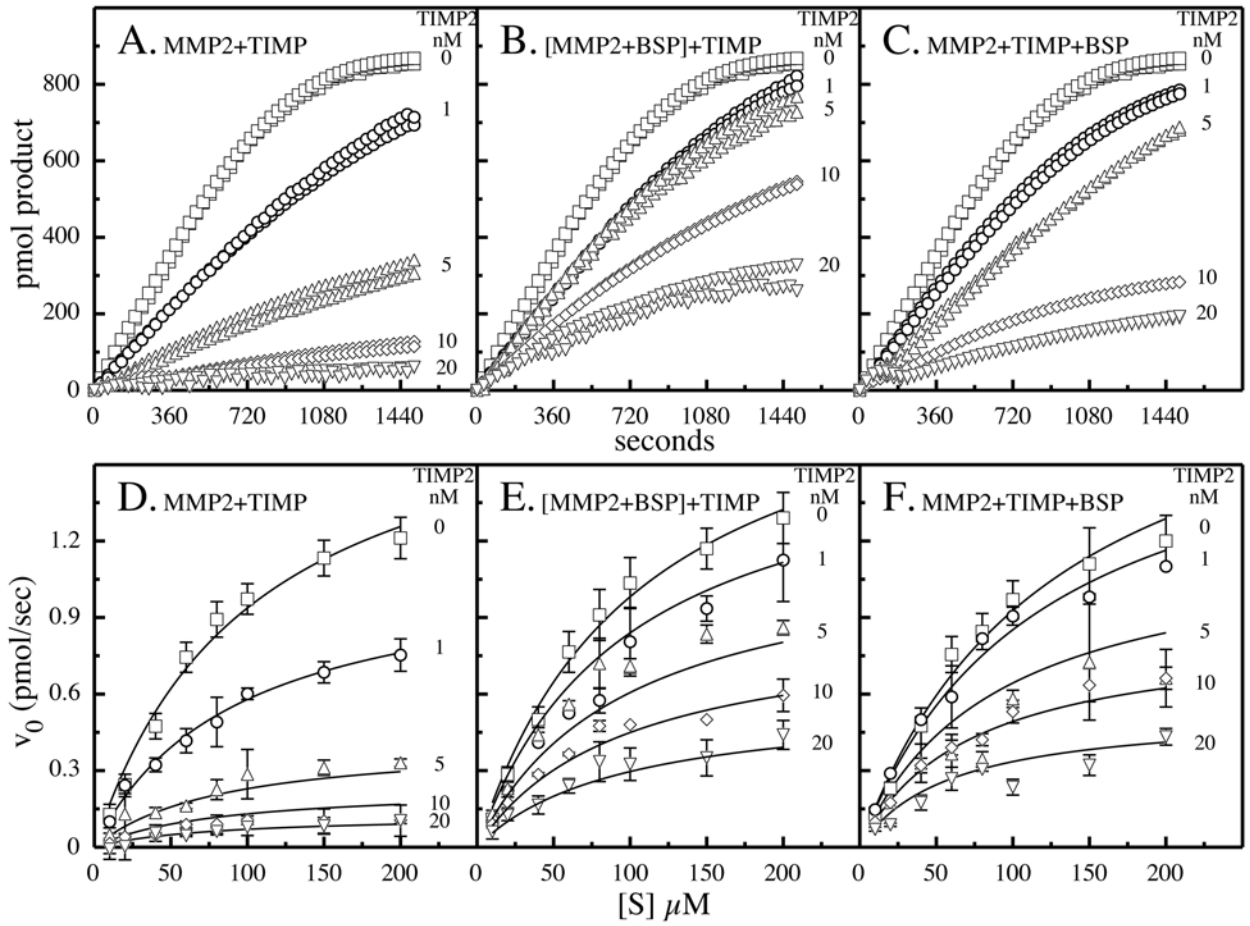

FIGURE 1.

Effects of BSP on TIMP2 inhibition of MMP-2. The substrate Ac-PLG-(2-mercapto-4-methylpentanoyl)-LG-OC_2H_5 was incubated in assay buffer at a final concentration of 100 μM with (A) 10 nM MMP-2 and different concentrations of TIMP2, (B) 10 nM MMP- 2-BSP preformed complex incubated with increasing concentrations of TIMP2, or (C) simultaneously added 10 nM MMP-2 and BSP and different concentrations of TIMP2. TIMP2 concentrations were 0 (□), 1 (○), 5 (△), 10 (◇), and 20 (▽). The concentrations MMP-2 and BSP were 10 nM. Reaction rates were profiled by increasing the substrate concentration from 10 to 200 μM. Data from the first 6 min of each reaction condition were used to calculate V_0 (picomoles per second) values. Substrate-velocity plots of MMP-2 incubated with different concentrations of TIMP2 (D), of MMP-2-BSP complexes incubated with varying concentrations of TIMP2 (E), or of MMP-2 incubated simultaneously with TIMP2 and BSP (F) were determined. MMP-2-BSP preformed complexes were formed by incubation at 37 °C for 30 min prior to addition to the reaction mixture. Six separate experiments were combined for each condition, and values represent the mean ± the standard deviation.

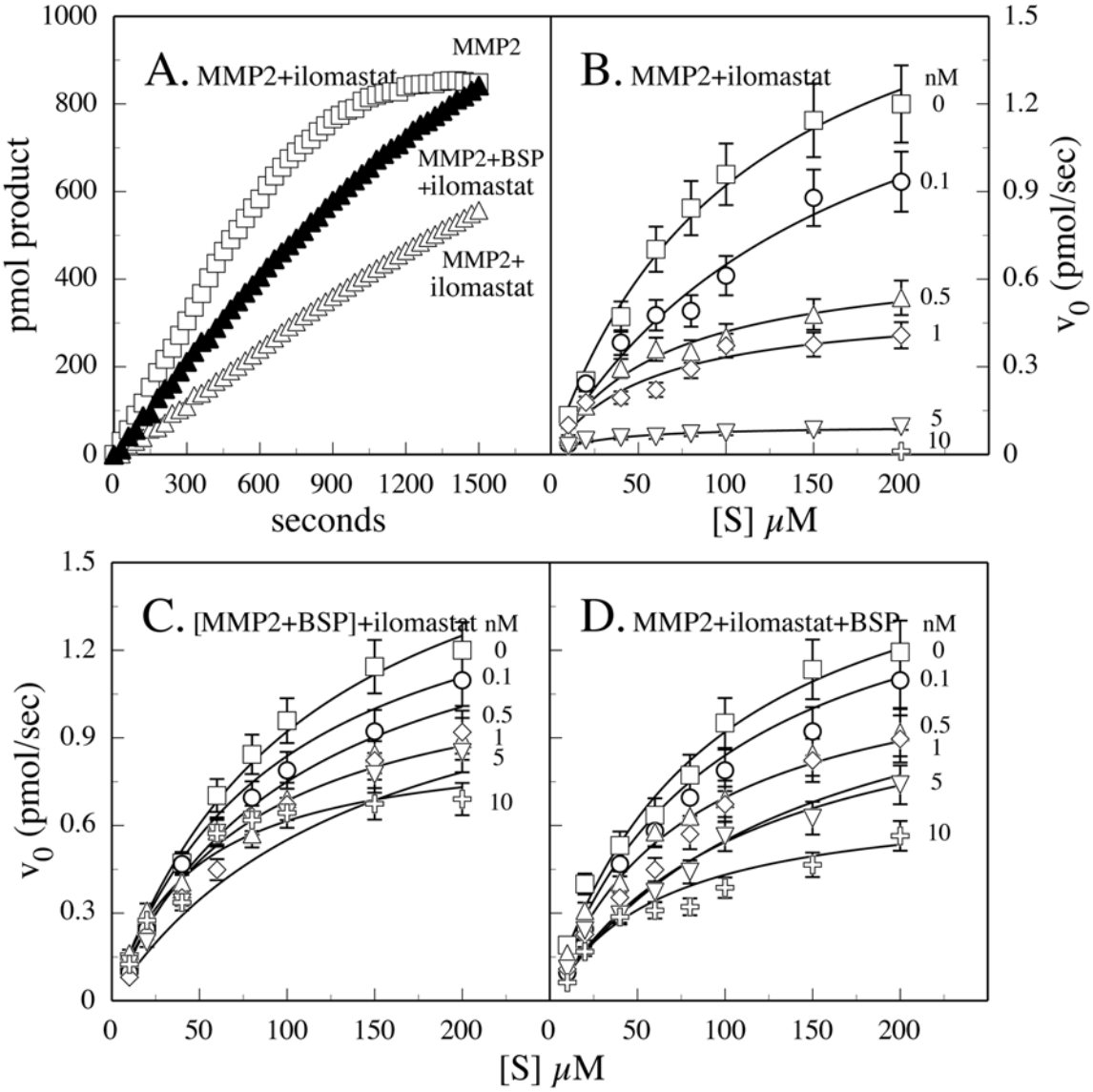

FIGURE 2.

Effects of BSP on ilomastat inhibition of MMP-2. Peptide substrate (100 μM) was incubated with 10 nM MMP-2 (□), 10 nM MMP-2 and 1 nM ilomastat (▵), or 10 nM MMP-2, 10 nM BSP, and 1 nM ilomastat (▲) and the evolution of product followed by absorbance at 405 nm (A). We generated substrate-velocity plots by increasing the substrate concentration at different fixed inhibitor concentrations with the slope over the first 6 min being used to calculate V_0 values (B–D). Active MMP-2 was incubated with ilomastat whose concentration varied: 0 (□), 0.1 (○), 0.5 (▵), 1 (◇), 5 (▽), and 10 nM (+). Inhibitor and substrate titrations were carried out by adding the inhibitor to (B) MMP-2, (C) an MMP-2-BSP preformed complex, or (D) simultaneously added 10 nM MMP-2 and BSP.

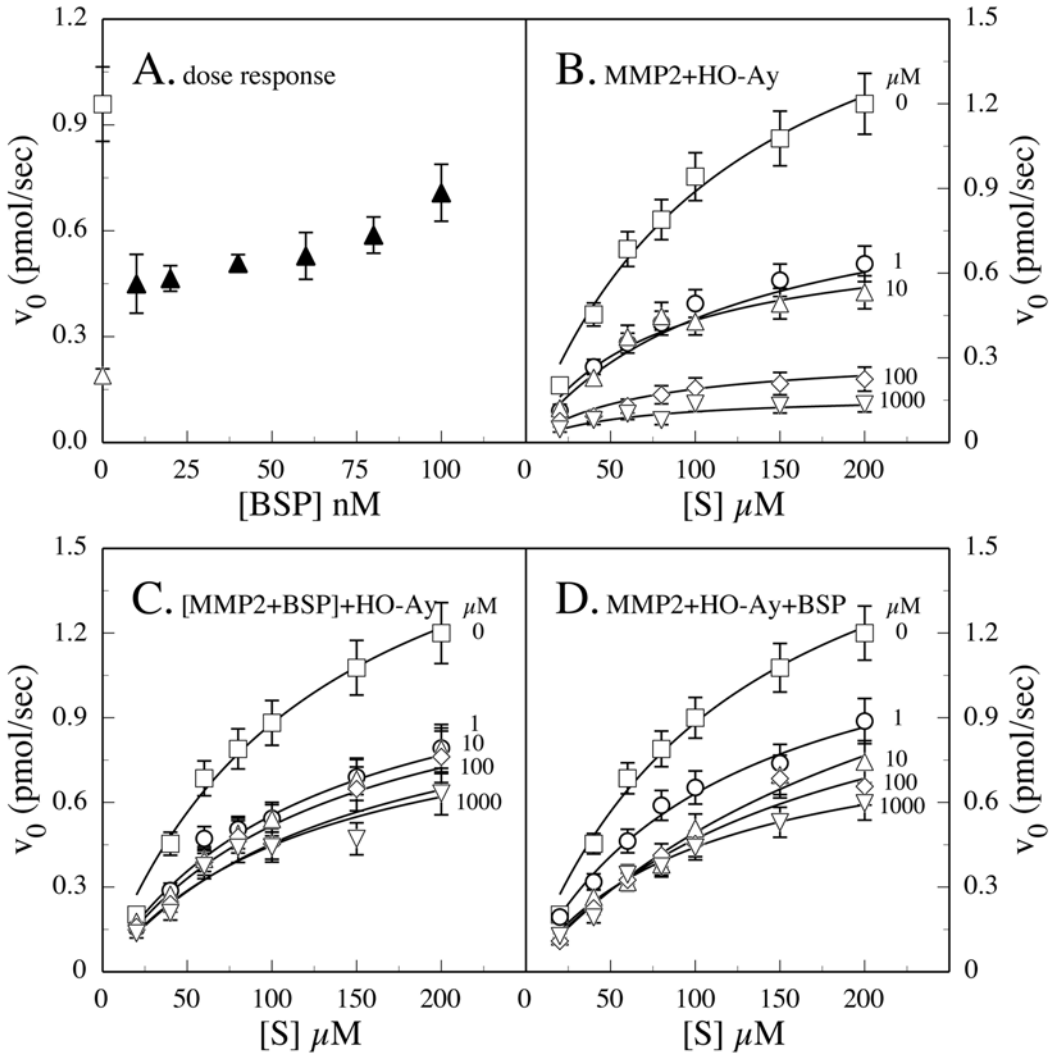

FIGURE 3.

Effects of BSP on oleoyl-*N*-hydroxylamide (HO-Ay) inhibition of MMP-2. Peptide substrate (100 μM) was incubated with 10 nM MMP-2 (□), 10 nM MMP-2 and 1 nM HO-Ay (▵), or 10 nM MMP-2, 1 nM HO-Ay, and varying concentrations of BSP (▲), and the evolution of product followed by absorbance at 405 nm over the first 6 min of the reaction was used to profile a dose response of BSP restoration of activity (A). Substrate-velocity plots were generated by increasing substrate concentrations at different fixed inhibitor concentrations with the slope over the first 6 min being used to calculate V_0 values (B–D). Active MMP-2 was incubated with HO-Ay, whose concentration varied: 0 (□), 1 (○), 10 (▵), 100 (◊), and 1000 μM (▽). Inhibitor and substrate titrations were made by adding the inhibitor to (B) MMP-2, (C) an MMP-2-BSP preformed complex, or (D) simultaneously added 10 nM MMP-2 and BSP.

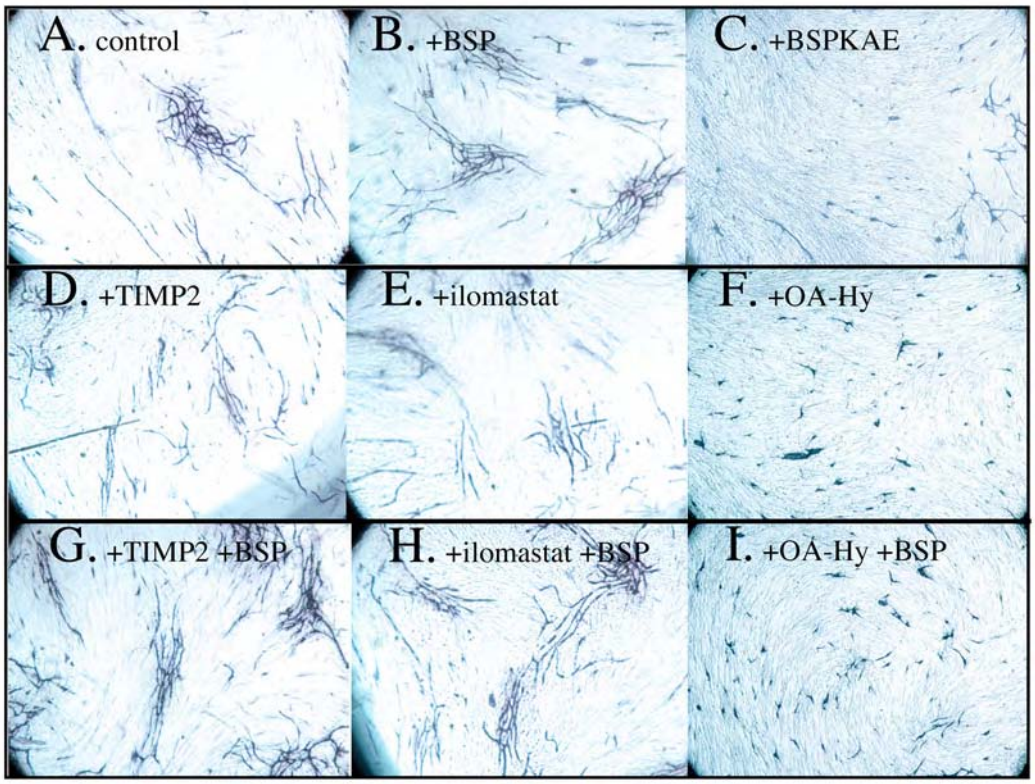

FIGURE 4.

BSP stimulates angiogenesis and overcomes MMP-2 inhibitors in vitro. HUVECs cocultured with fibroblasts were treated starting on day 6 of culture with (A) vehicle alone, (B) 5 nM BSP, (C) 5 nM BSPKAE, (D) 5 nM TIMP2, (E) 5 nM ilomastat, (F) 33.6 nM oleoyl-*N*-hydroxylamide (HO-Ay), (G) 5 nM BSP and 5 nM TIMP2, (H) 5 nM BSP and 5 nM ilomastat, or (I) 5 nM BSP and 33.6 nM oleoyl-*N*-hydroxylamide. The cells were fixed on day 12 and probed with a PECAM1 antibody (blue) to visualize tubule formation. Note that BSP stimulated tubule formation and in equimolar amounts reversed the inhibitory

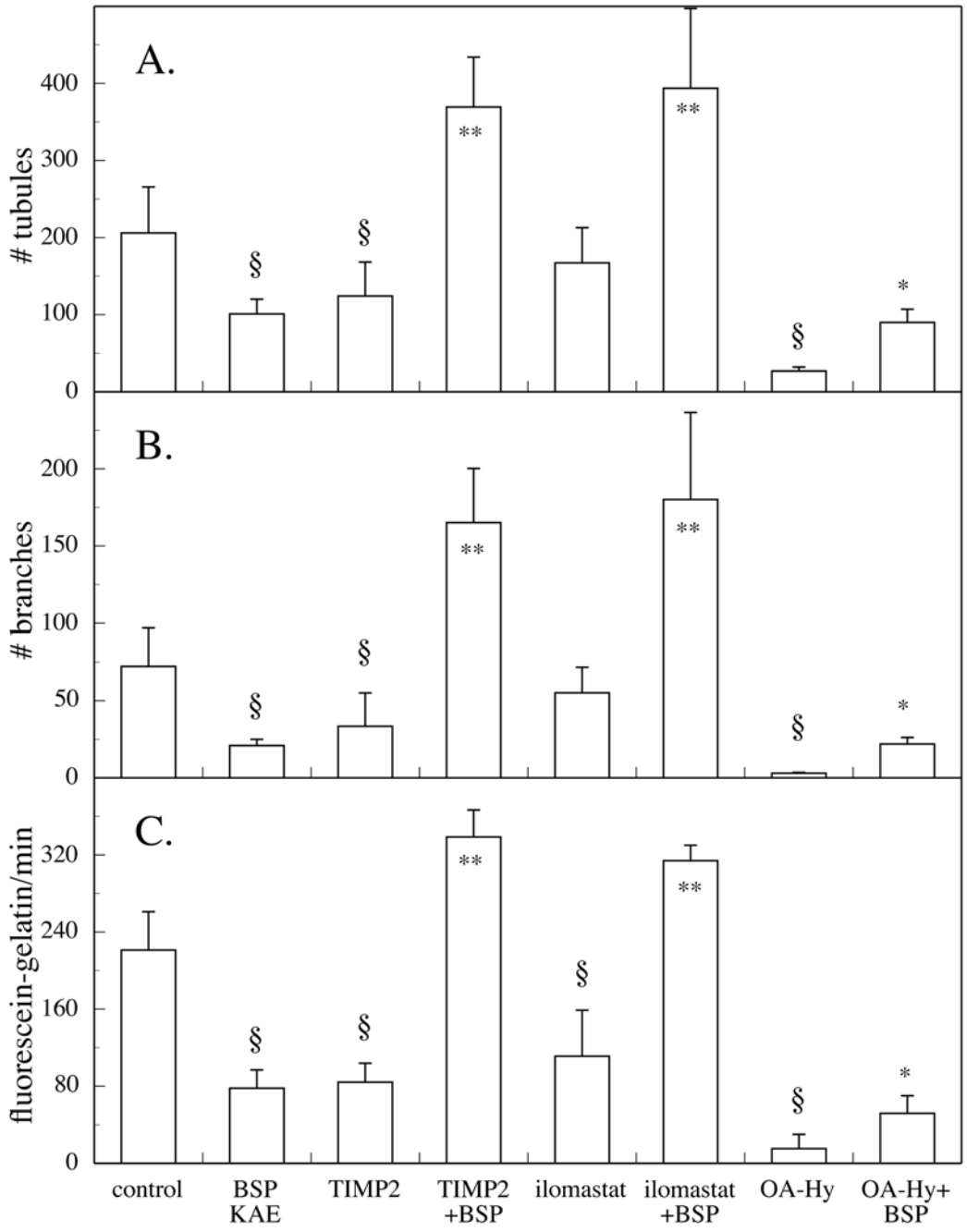

FIGURE 5.

Quantification of the effects of recombinant BSP on tubule formation and in overcoming the effects of MMP-2 inhibitors. Two distinct fields from each triplicate well of the experimental conditions described were digitized as .tif files and analyzed using AngioSys version 1.0 (TCS Cell Works). The image analysis package determined the number of tubules (A) and the number of branch points or junctions (B) between tubules. In addition, a cell surface-associated pool from day 10 cohort cultures was assayed for MMP activity by the large fluorescein-gelatin substrate assay (C). The § symbol represents an ANOVA p value of ≤ 0.05 for comparing control values vs with inhibitor. Asterisks represent t test p values with of ≤ 0.05 (one asterisk) and ≤ 0.01 (two asterisks) for comparing each inhibitor with or without BSP.

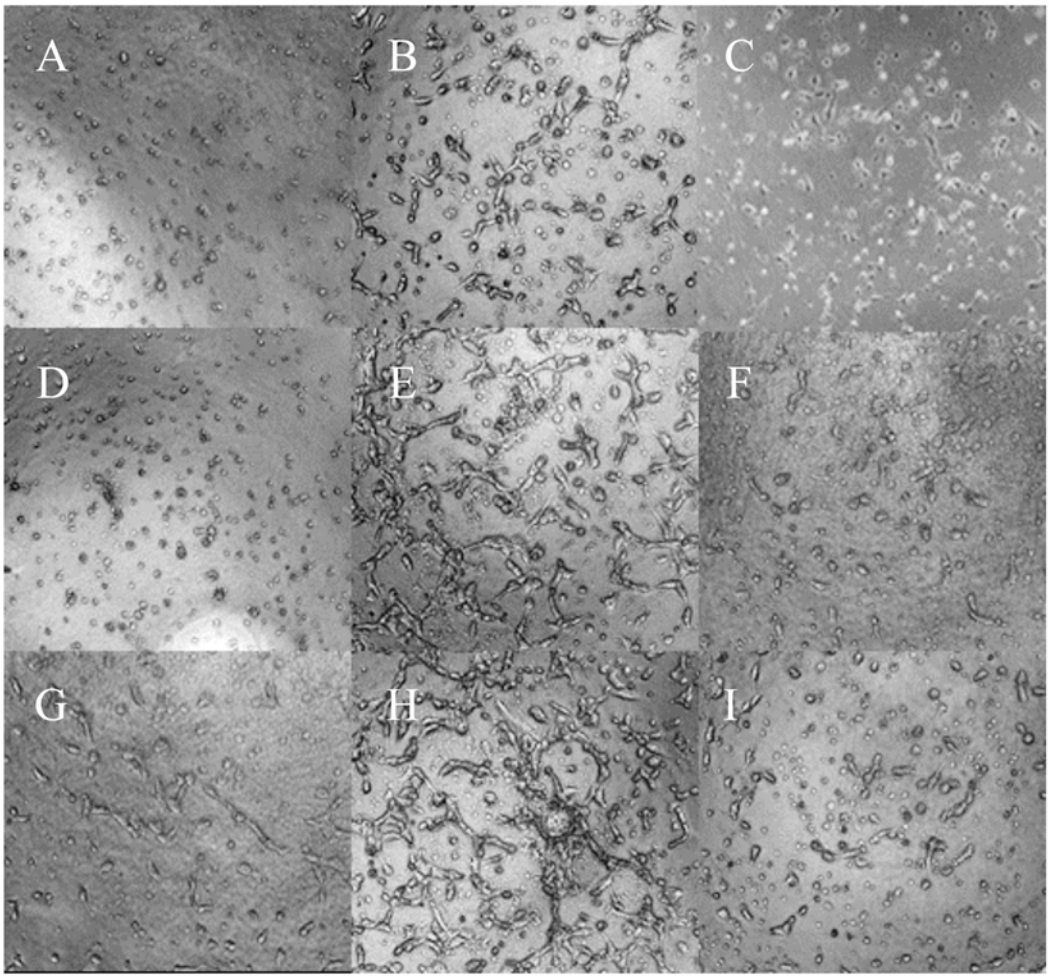

FIGURE 6.

BSP stimulation of HUVEC tubule formation is MMP-2-dependent. HUVECs that were transfected with an adenovirus encoding BSP or with null adenovirus were transferred onto type I collagen gels, and a second layer of collagen was layered on top of the adherent cells forming a collagen sandwich. A set of BSP adenovirus-transfected cells were also treated with an activity blocking antibody to MMP- 2. Null virus-transfected cells (A, D, and G), BSP virus-transfected cells (B, E, and H), and BSP adenovirus-transfected cells treated with 1.25 μg/mL MMP-2 antibody (C, F, and I) were visualized at 14 (A–C), 24 (D–F), and 48 h (G–I) on a Nikon Diaphot inverted microscope and digitized with a Polaroid CCD digital camera.

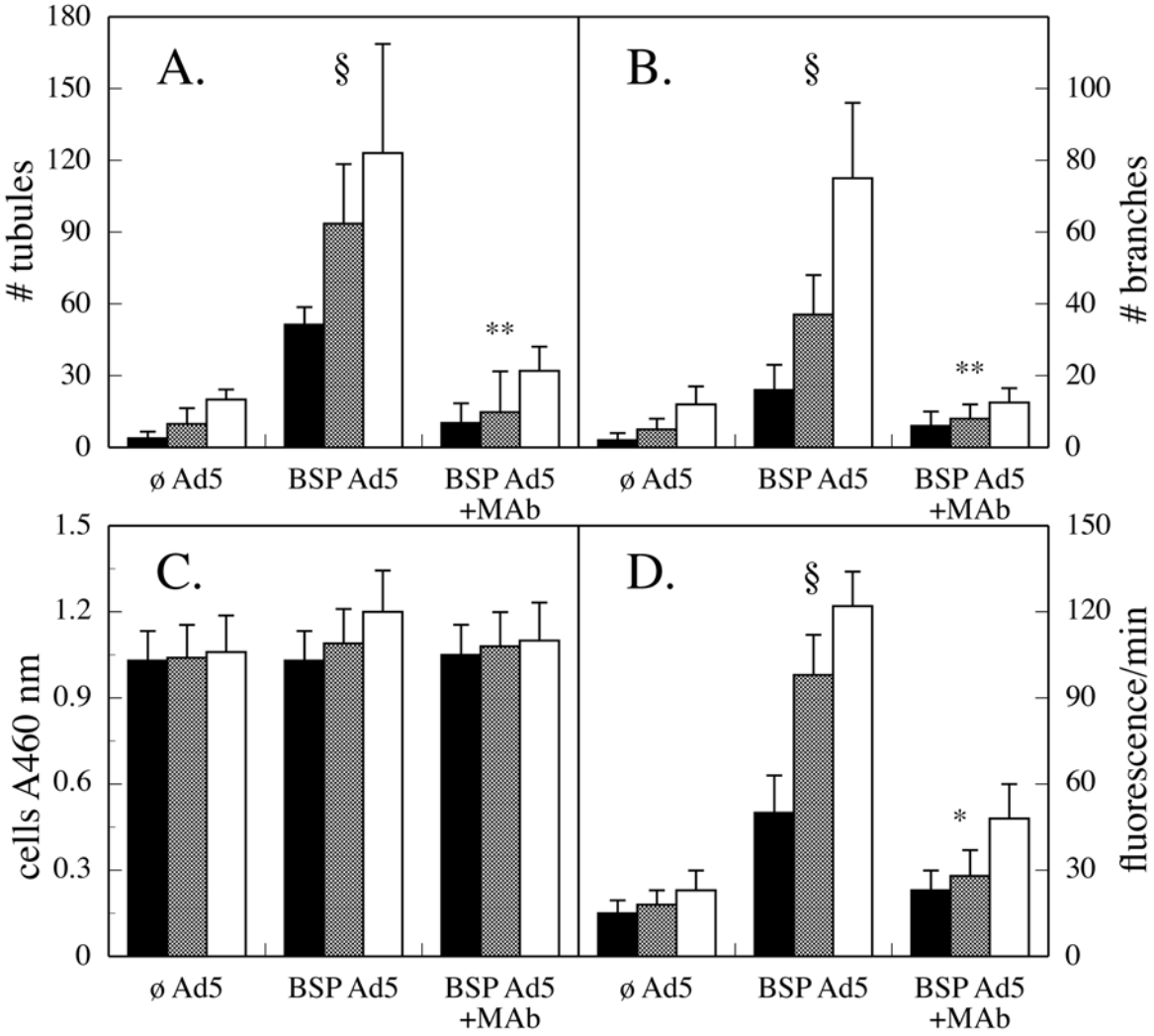

FIGURE 7.

Quantification of the effects of BSP expression on tubule formation. As in Figure 5, two distinct fields from each triplicate well of the null virus-transfected cells (øAd5), BSP adenovirus-transfected cells (BSP Ad5), and BSP adenovirus-transfected cells treated with MMP-2 antibody (BSP Ad5 + mAb) were digitized as .tif files and analyzed using AngioSys version 1.0. The number of tubules (A) and the number of branch points or junctions between tubules (B) were calculated. In addition, cell number was followed by absorbance using a water soluble MTT dye, CCK-8 (C), and MMP activity (D) was assayed by following fluorescein emission in wells where the large fluorescein-gelatin substrate had been incorporated into the collagen gel (C). The time points analyzed were 14 h (black bars), 24 h (gray bars), and 48 h (white bars). The § symbol represents a paired *t* test *p* value of ≤0.001 for comparing null virus- to BSP virus-transfected cells across the different time points. Asterisks represent *t* test *p* values of ≤0.01 (one asterisk) and ≤0.001 (two asterisks) for comparing BSP virus-transfected cells with or without MMP-2 antibody across the different time points.

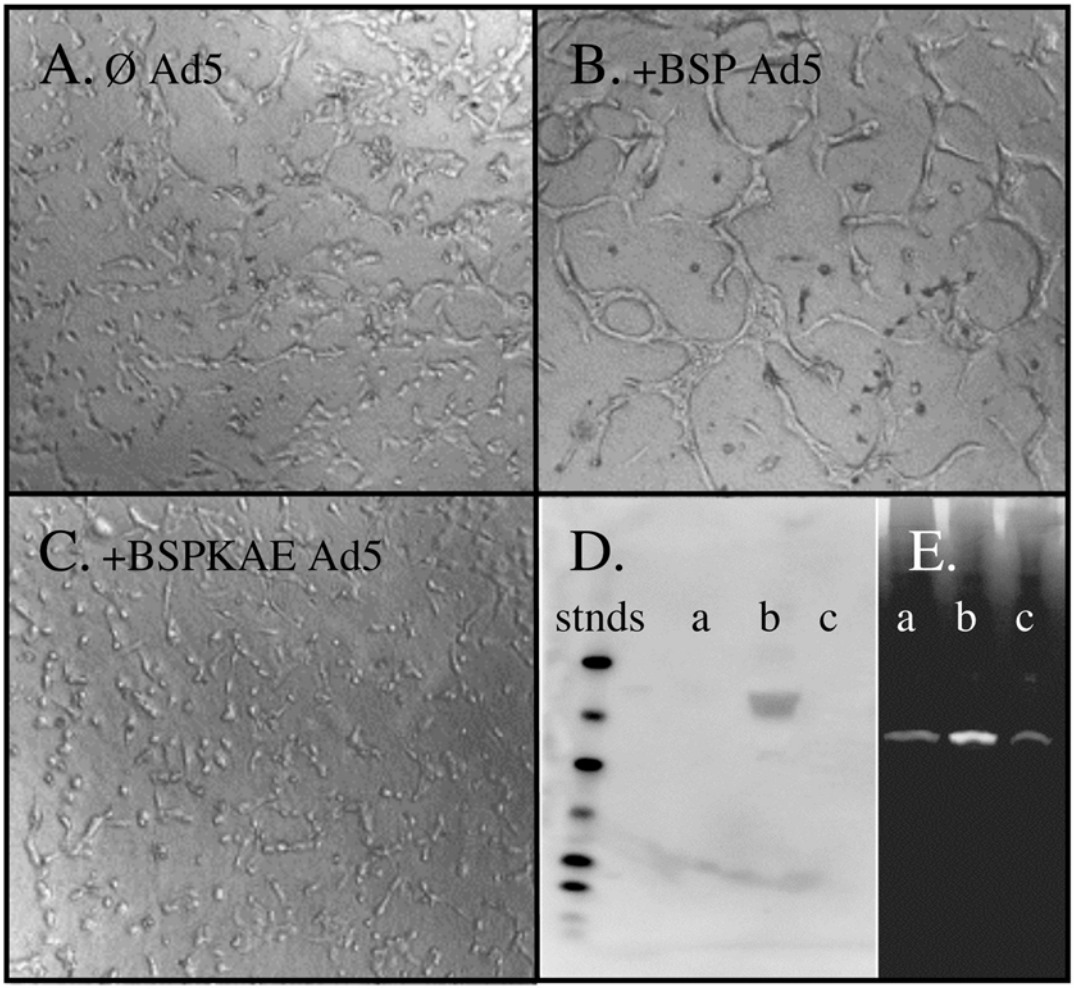

FIGURE 8.

BSP increases the level of active MMP-2 cell surface localization during tubulogenesis. HUVECs that were transfected with an adenovirus encoding BSP or BSPKAE or with null adenovirus were transferred into type I collagen gels. Null virus-transfected (A), BSP-transfected (B), and BSPKAE-transfected (C) cells were visualized at 24 h with a Nikon Diaphot inverted microscope and digitized with a Polaroid CCD digital camera. Plasma membrane-associated pools were generated from the different conditions and analyzed for BSP protein levels by Western blot (D) and for active MMP-2 levels by zymography (E).

Table 1

Bone sialoprotein effects on matrix metalloproteinase-2 kinetic parameters.

	K_m [a]	V_{max}	K_{ic} [b]	K_{iu} [b]
MMP2 [c]	103 ± 14	1.9 ± 0.1		
MMP2 + BSP	90 ± 10	2.1 ± 0.2		
MMP2+ TIMP2	103 ± 9	1.9 ± 0.8	0.67 ± 0.06	1.4 ± 0.2
[MMP2+BSP] + TIMP2	127 ± 18	2.1 ± 0.2	24 ± 12	9 ± 4
MMP2 + TIMP2 + BSP	98 ± 14	1.8 ± 0.1	10 ± 2	8 ± 2
MMP2+ ilomastat	106 ± 23	1.8 ± 0.5	0.3 ± 0.1	-
[MMP2+BSP]+ ilomastat	85 ± 14	1.5 ± 0.1	14 ± 4	-
MMP2 + ilomastat + BSP	88 ± 10	1.6 ± 0.2	9.8 ± 0.3	-
MMP2 + OA-Hy	97 ± 14	1.9 ± 0.3	5.9 ± 0.4	-
[MMP2+BSP]+ OA-Hy	127 ± 22	2.1 ± 0.4	150 ± 47	-
MMP2 + OA-Hy +BSP	135 ± 25	2.2 ± 0.5	106 ± 48	-

[a] For the substrate Ac-PLG-[2-mercapto-4-methyl-pentanoyl]-LG-OC_2H_5, K_m values are μM.

[b] K_{ic} and K_{iu} values were determined by fitting the generalized linear mixed inhibition equation. K_{ic} values for TIMP2 and ilomastat are nM, while OA-Hy is μM.

[c] Abbreviations: MMP2, matrix metalloproteinase-2; BSP, bone sialoprotein; TIMP2, tissue inhibitor of matrix metalloproteinase-2; OA-Hy, oleoyl-N-hydroxylamide.

Published in final edited form as:
Biochemistry. 2008 September 23; 47(38): 10162–10170. doi:10.1021/bi801068p.

Structural Requirements For Bone Sialoprotein Binding And Modulation Of Matrix Metalloproteinase-2

Alka Jain[‡], **Abdullah Karadag**[§,¶], **Larry W. Fisher**[§], and **Neal S. Fedarko**[‡,*]
Johns Hopkins University School of Medicine, National Institute for Dental and Craniofacial Research, National Institutes of Health, Department of Medicine, Room 5A-64 JHAAC, 5501 Hopkins Bayview Circle, Johns Hopkins University, Baltimore, MD 21224. Phone: 410 550-2632; Fax: 410 550-1007

Abstract

Bone sialoprotein (BSP) has been shown to induce limited gelatinase activity in latent matrix metalloproteinase-2 (MMP-2) without removal of the propeptide and to restore enzymatic activity to MMP-2 previously inhibited by tissue inhibitor of matrix metalloproteinase-2 (TIMP2). The current study identifies structural domains in human BSP and MMP-2 that contribute to these interactions. The 26 amino acid domain encoded by exon 4 of BSP is shown by a series of binding and activity assays to be involved in the displacement of MMP-2′s propeptide from the active site and thereby inducing the protease activity. Binding assays in conjunction with enzyme activity assays demonstrate that both amino- and carboxy-terminal domains of BSP contribute to restoration of activity to TIMP2-inhibited MMP-2, while the MMP-2 hemopexin domain is not required for reactivation.

A family of secreted proteins, termed SIBLINGs[1] (for *s*mall *i*ntegrin-*b*inding *li*gand, *N*-linked *g*lycoproteins), share many exon-related motifs including the integrin-binding tripeptide, Arg-Gly-Asp (RGD), as well as several conserved phosphorylation and glycosylation sites (1,2). Family members include bone sialoprotein (BSP), osteopontin (OPN), dentin matrix protein 1 (DMP1), matrix extracellular phosphoglycoprotein (MEPE), and dentin sialophosphoprotein (DSPP) (1). All of the genes are in a tandem cluster on human chromosome 4 and were first observed to be expressed in bones and teeth but have since been reported to all be expressed in active ductal epithelial cells (3). SIBLINGs are also induced in certain neoplasms (4–7). SIBLINGs can propagate biological signals by acting as integrin ligands initiating integrin signaling intracellularly and by binding and sequestering other proteins to the cell surface altering extracellular interactions (4). For example, BSP is a cell surface-associated protein through its binding of αvβ3 integrin (8,9). BSP can bind complement factor H and tether it to the cell surface where factor H prevents alternate complement-mediated cell lysis (8,10). In addition, BSP binds to and modulates the activity of matrix metalloproteinase- 2 (MMP-2) (11).

Author email Address: ndarko@jhmi.edu.
[‡]Johns Hopkins University School of Medicine.
[§]National Institute for Dental and Craniofacial Research, National Institutes of Health.
[¶]Current address: University of Sheffield Medical School, Sheffield, UK.

[†]This research was supported in part by National Institutes of Health (NIH) grant CA113865 (N.S.F.) and by the Division of Intramural Research, National Institute of Dental and Craniofacial Research Intramural Research Program, National Institutes of Health, Department of Health and Human Services, (L.W.F.).

[1]The abbreviations used are: SIBLING, Small, Integrin-Binding LIgand, N-linked Glycoprotein; RGD, arginine-lysine-aspartate; BSP, bone sialoprotein; OPN, osteopontin; DMP1, dentin matrix protein-1; MMP, matrix metalloproteinase; TIMP, tissue inhibitor of metalloproteinase; mMMP2, mutant hemopexin-free matrix metalloproteinase; DTNB, 5,5′-dithio-bis-2-nitrobenzoic acid; HRP, horseradish peroxidase; BSPΔx4, bone sialoprotein with exon 4 deleted.

MMP-2 is a member of a family of structurally and functionally related endoproteinases involved in development and tissue repair as well as cancer angiogenesis and metastasis. We have shown that latent proMMP-2 can be at least partially activated through the binding of BSP (11). More recently, we have shown that BSP binding to MMP-2 significantly reduced the affinity of both small molecular weight synthetic inhibitors (ilomastat and oleoyl-*N*-hydroxylamide) and the large molecular weight tissue inhibitor of metalloproteinase-2 (TIMP2) (12). The current study was undertaken to determine sequences in both BSP and MMP-2 involved in the binding and modulation of MMP activity.

MATERIALS AND METHODS

Reagents

ProMMP-2 and active human MMP-2 were obtained from Oncogene Research Products (Boston, MA) and Research Diagnostic Systems, Inc. (Minneapolis, MN). Recombinant human MMP-2 lacking the hemopexin domain was purchased from Biomol Research Laboratories, Inc. (Plymouth Meeting, PA). Small molecular weight MMP-2 substrate Ac-PLG-[2-mercapto-4-methylpentanoyl]-LG-OC_2H_5 and 5,5′-dithiobis(2-nitrobenzoic acid) (DTNB) were obtained from Calbiochem (La Jolla, CA). TIMP2 was a generous gift of Dr. H. Birkedal-Hansen, NIDCR, NIH. Human serum-adsorbed goat anti-rabbit IgG conjugated to horseradish peroxidase (HRP) was obtained from Kirkegaard and Perry (Gaithersburg, MD). Recombinant human BSP that included posttranslational modifications was made using an adenovirus construct and eukaryotic cells and purified (>95% purity as defined by acrylamide gel electrophoresis) as previously described (13). The synthesized and purified polypeptide VFKYRPRYYLYKHAYFYPHLKRFPVQ, corresponding to exon 4 of BSP, was obtained from the Center for Biologics Evaluation and Research, Food and Drug Administration.

Recombinant BSP-SIBLING Chimera/Mutants in Replication- Deficient AdenoVirus Constructs

BSP chimera were made by separately amplifying the cDNA encoding the amino terminus (exons 2–5) of human BSP, human OPN, or bovine DMP1 and selectively combining them to PCR products containing the remaining coding sequences for each SIBLING (Figure 1). The 5′ PCR products' sense strand oligos also incorporated an Asp718 restriction site 5′ to the Kozak/start Met sequences. The antisense strand oligos for the 5′ PCR constructs at the end of exon 5 included blunt end-producing restriction sites (*Bsr*BI for BSP and OPN and *P*V*u*II for DMP1). The sense strand oligos for the carboxyterminal- encoding 3′ PCR products all incorporated blunt end-producing restriction sites (*Sca*I for BSP and OPN and *Fsp*I for DMP1) for ligation to the 5′ PCR products, and all contained *Bam*HI restriction sites 3′ to their stop codons. All PCR reactions were done with high fidelity enzyme (Turbo Pfu; Stratagene). All base changes required to introduce the blunt cutter sites always maintained the same amino acid (e.g., Leu -> Leu). The two PCR fragments for each SIBLING were first treated with alkaline phosphatase (to make the ends unable to ligate), purified, and then digested with their respective blunt-cutting restriction enzymes to create new, ligation-competent blunt ends. The 5′ PCR product of BSP was ligated with the 3′ PCR product of OPN (denoted BSP/OPN) or DMP1 (BSP/DMP1). Similarly, the 3′ PCR product of BSP was ligated to the 5′ end of OPN (OPN/BSP) or DMP1 (DMP1/BSP). The ligation product was subjected to PCR using the appropriate 5′-most (containing the Asp718 site) and 3′-most (containing the *Bam*HI site) oligo for each chimera. Bands of the correct size were gel purified, digested with Asp718 and *Bam*HI, ligated into Asp718/*Bam*HI-digested vector (within the multipurpose cloning site between the CMV promoter and the SV40 polyA/message stabilization 3′ flanking mRNA domain of the pACCMV.pLpA adenovirus shuttle plasmid), and transformed into competent *E. coli* cells. Successful plasmids were sequenced and used in a standard recombination protocol to make adenovirus particles in HEK293 cells. Chimeric proteins were purified from

the serum-free media of the adenovirus-infected human marrow stromal fibroblast using standard ion-exchange chromatography procedures previously described for individual SIBLING proteins (10).

The BSP construct lacking exon 4 (BSPΔx4) was made using the Stratagene in situ mutagenesis kit and complementary oligonucleotides whose 5′ end encoded bases from the end of exon 3 and whose 3′ end encoded the beginning bases of exon 5 as per the manufacturer's instructions. Limited PCR amplification of the BSP insert in pBluescript was performed, and the original template plasmids were destroyed by *Dpn*I. After transformation, single *Escherichia coli* colonies on ampicillin plates were selected and grown in LB-amp media, the plasmid was purified, and the loss of exon 4 sequences in the SIBLING sequence was verified by DNA sequencing. The modified SIBLING insert was shuttled into the adenovirus plasmid, and the virus was prepared, with the protein made and purified as previously described (10).

Fluorescent Binding Studies

Intrinsic tryptophan fluorescence binding studies of wild-type and as well as the noted chimeric BSP constructs with both proMMP-2 and active MMP-2, and hemopexin-deleted MMP-2 mutant, were carried out as previously described (11). BSP contains no tryptophan groups while the chimeric BSP constructs (BSP/OPN, BSP/DMP1, OPN/BSP, and DMP1/BSP) have 1 tryptophan, MMP-2 contains 15 tryptophan residues, and hemopexin-deleted MMP-s contains 8 tryptophan residues. Briefly, the relative change in fluorescence in the area under the emission curve (300 to 500 at 295 nm excitation) was used to determine fractional acceptor saturation (f_a) as a function of nanomolar BSP added by calculating $f_a = (y - y_f)/(y_b - y_f)$, where y_f and y_b are the area under the curve of the fluorescent emission profile of free and fully bound MMP-2.

Solid-Phase Binding Assays

The binding of BSP to immobilized proMMP-2, active MMP-2, or hemopexin-deleted MMP-2 was measured by an indirect sandwich assay. Plates were coated with the different forms of MMP-2 by adding 0.1 mL of 3.5 nM recombinant purified MMP-2 in 50 mM $NaHCO_3$, pH 9.0, to each well of a Greiner High- Binding 96-well microtiter plate and incubated overnight at 4 °C. The plates were blocked with 5% (w/v) nonfat dry milk in Tris-buffered saline (TBS) containing 50 mM Tris, pH 7.4, and 150 mM NaCl for 60 min and then rinsed three times with TBS containing 0.05% Tween 20. BSP was added in nanomolar equivalents in TBS-Tween and incubated for 120 min at room temperature. After a second round of three washes, bound ligand was quantified by the addition of a 1:50000 dilution of specific rabbit anti-BSP antibody, LF100 (14), followed by a 60 min incubation. After three washes, secondary antibody (1:2000 goat anti-rabbit HRP-conjugated antibody) was added and incubated for a further 60 min. Color was developed using 3,3,5,5-tetramethylbenzidene substrate, and the absorbance at 405 nm was measured. Nonspecific binding was measured by determining the ligand binding to wells coated with 1% bovine serum albumin during the overnight coating step, and these values were subtracted from the corresponding values for MMP-coated wells.

High Molecular Weight Substrate Studies

Fluorescein-conjugated gelatin (Molecular Probes, Inc., Eugene, OR) substrate was used to follow gelatinase activity as previously described (11). This substrate is highly substituted with fluorescein moieties such that the fluorescent signal is self-quenched until proteolytic cleavage liberates fragments and a robust fluorescent emission is measured. For studies of proMMP-2 activation, 5 μg/mL large fluorescein-conjugated substrate was incubated with 10 nM proMMP-2 ± 10 nM BSP (or BSP chimera). For inhibition studies, typical reaction mixtures consisted of the 10 μg/mL fluorescein-substrate conjugate with 1.4 nM mutant hemopexin-free MMP-2 reacted with either 10 nM TIMP2, 10 nM TIMP2 + 10 nM BSP (or BSP chimera), or

buffer alone (50 mM Tris, pH 7.6, 150 mM NaCl, 5 mM $CaCl_2$). Relative velocity plots were determined by titrating the substrate concentration from 0.025 to 15 μg/mL and determining the change in fluorescence over the first hour of reaction. Inhibitor titrations were carried out by titrating TIMP2 concentration from 1.6 to 1600 nM. Fluorescent data were acquired on a Perkin-Elmer Victor 2 multilabel plate reader with excitation at 485 nm and emission at 535 nm. Reactions were run in duplicate in fluornunc microtiter plates.

Low Molecular Weight Substrate Studies

The activities of mutant hemopexin-free MMP-2 in the presence and absence of inhibitor (TIMP2) and BSP were measured using a small molecular weight thiopeptide substrate (Ac-PLG- [2-mercapto-4-methylpentanoyl]-LG-OC_2H_5). Substrate was incubated in assay buffer (50 mM HEPES, 10 mM $CaCl_2$, 0.05% Brij-35, 1 mM DTNB, pH 7.5) with 10 nM mutant MMP-2 + different concentrations of inhibitor or MMP2 + inhibitor + BSP added simultaneously. Data from the first 6 min were used to calculate initial velocity (pmol/s) values. Substrate cleavage was monitored using a Perkin-Elmer Victor 2 multilabel plate reader, and absorbance was measured at 412 nm.

RESULTS

Cysteine Switch Activation

MMPs are normally activated through disruption of a propeptide cysteine interaction with Zn^{2+} within the catalytic site. When recombinant human (latent) proMMP-2 alone is incubated with a large fluorescein-conjugated substrate, little enzyme activity is seen over a 4 h period, presumably because the propeptide is occupying the active site (Figure 2A). When recombinant human BSP was added to proMMP-2 and then incubated with substrate, significantly increased enzyme activity was observed, while the incubation of BSP alone with substrate led to no increase in fluorescence. Varying the substrate concentration and determining the relative velocity of the enzyme reaction in the absence and presence of BSP revealed that BSP conferred enzymatic activity to proMMP-2 over a large range of substrate concentrations (Figure 2B). If binding of latent MMP-2 leads to catalytic activity, then the binding should be associated with the breaking of the propeptide-associated zinc-cysteine bond. A cysteine trap assay, where free cysteine residues react with DTNB to stoichiometrically yield 2-nitro-5-thiobenzoic acid as a measure of free cysteine residues (15), was performed. BSP does not contain any cysteine. ProMMP-2 alone exhibited basal reactive cysteines. When BSP was added to proMMP-2, however, the amount of accessible cysteine increased (Figure 1C). This was consistent with zinc-binding cysteine residues becoming fully exposed and quantitatively labeled. MMP-2 has 14 cysteine residues in the mature active protein that are believed to be disulfide bonded, while the remaining 3 cysteines are present in the propeptide domain.

BSP's MMP-2 Binding and Activation Sequences

In order to determine the sequences in BSP that are involved in binding and modulating proMMP-2 activity, chimeras were made by swapping amino-terminal and carboxy-terminal domains between BSP and either OPN or DMP1. When binding was investigated by intrinsic fluorescence binding studies between proMMP-2 and wild-type BSP, the BSP binding was saturable with a K_d in the nanomolar range (Figure 3A,B, Table 1), while the chimera including only the first four coding exons of BSP (BSP/OPN and BSP/DMP1) exhibited two log order weaker but still saturable binding curves (Figure 3C,D). In contrast, OPN/BSP and DMP1/BSP chimera showed no saturable binding (inset, Figure 3C). Thus, important proMMP2-binding sequences lie within the first five small exons of BSP. Exon 2 contains the leader sequence and the first two amino acids of the mature protein. Exons 3 and 5 are short exons containing casein kinase II-type phosphorylation motifs as their major conserved sequences. Exon 4 is a well-conserved 26 amino acid exon that contains 6 tyrosines, 3 lysines, 3 arginines, and 2

histidines but no acidic residues. Unlike the tyrosines found flanking the RGD motif, the tyrosine groups in exon 4 are not thought to be sulfated due to the presence of these positively charged amino acids (16). When a BSP construct lacking exon 4 (BSPΔx4) was measured for binding activity, it did show saturable binding, though the K_d was a log order weaker than that of wild-type BSP (Figure 3E,F).

The activation of proMMP-2 by the same chimeric constructs was studied using the large molecular weight fluorescein-gelatin assay. Wild-type BSP added to proMMP- 2 resulted in the expected significant increase in enzymatic activity (Figure 4A). The BSP/OPN and BSP/DMP1 chimera, however, also conferred enzymatic activity to the latent MMP-2 (Figure 4B). In contrast, the OPN/BSP and DMP1/BSP chimera had, at best, minimal effects on enzymatic activity compared to the background autoactivation occurring for proMMP-2 alone (Figure 4C). These data suggest that sequences in the first four coding exons are involved in BSP conferring activity to latent MMP-2. In contrast, the BSPΔx4 protein added to proMMP-2 caused little change in basal activity (Figure 4D).

To further investigate the role of exon 4 in proMMP-2 activation, the 26 amino acid sequence coded for by exon 4 was synthesized and purified. The action of exon 4 peptide on proMMP-2 activation by wild-type BSP was studied using the large molecular weight gelatin-substrate assay. In the absence of any exon 4 peptide, full-length BSP conferred activity of proMMP-2, as exhibited by the linear increase in the fluorescent signal (Figure 5A). Titrating the levels of exon 4 peptide into reaction mixtures containing wild-type BSP and proMMP-2 led to a decrease in the evolution of the fluorescent signal. The rate of reaction was calculated by determining the change in fluorescence over the first 60 min (Figure 5B). Exon 4 peptide at 17 nM (with BSP and proMMP-2 at 10 nM each) decreased the reaction rate by 10%. Increasing the concentration of exon 4 peptide up to 1.7 μM decreased the reaction rate by 68%. The observation that the activity of proMMP-2 + wild-type BSP was reduced by the addition of exon 4 peptide to the enzyme reaction mixture suggests that this conserved exon likely plays a role in the activation process.

BSP Binding to MMP-2 Does Not Require the Hemopexin Domain

MMP-2 possesses a hemopexin-like domain believed to be involved in the binding of many natural substrates (17). Whether BSP interactions with MMP-2 require the hemopexin domain was investigated by studying the binding characteristic of BSP to recombinant human MMP-2 that lacks the hemopexin domain. When the intrinsic tryptophan fluorescence of the mutant MMP-2 (mMMP-2) was followed during titration with BSP, quenching of the signal similar to that previously reported for the intact MMP-2 was observed (Figure 6A). BSP binding was saturable, and its affinity for the mMMP-2 was actually slightly higher than that for intact MMP-2 (Figure 6B,C and Table 1). The accuracy of the determinations of the molarities of the three MMP proteins from the information originally supplied by the manufacturer may contribute to the apparent minor differences in calculated binding constants.

An alternative method to confirm BSP and mMMP-2 binding was also employed. Solid-phase binding assays confirmed that binding of BSP to MMP variants was saturable (Figure 6D) and K_d values were determined (Table 1). The K_d values for the two binding systems (solution versus solid phase) were both found to be in the nanomolar range. The minor difference in values may reflect differences in solid-phase binding conformation, orientation, or better accessibility of BSP-MMP contact points in the solution phase.

BSP Modulation of MMP-2 Activity Does Not Require the Hemopexin Domain

The effect of BSP on the activity of the hemopexin-free mMMP-2 was investigated using the gelatin-fluorescein large molecular weight substrate assay. The change in substrate

fluorescence caused by mMMP-2 alone compared to a complex of equimolar mMMP-2 + BSP was not significantly different (Figure 7A). As expected, the addition of equimolar TIMP2 to mMMP-2 caused a significant decrease in the rate of fluorescence change. However, addition of equimolar BSP to mMMP-2 + TIMP2 complexes restored the rate of fluorescence change to that of mMMP-2 alone, showing that the TIMP2 became ineffective in the presence of bound BSP (Figure 7A). For complexes of equimolar mMMP-2 + TIMP2, the rate of the reaction was decreased to 67%, and the addition of equimolar BSP restored activity to 97%. Titration of mMMP-2 with TIMP2 using the large molecular weight substrate assay revealed that over a 100-fold excess of TIMP2 was required to inhibit activity to 20% of that seen by mMMP-2 alone (Figure 7B). Increasing the concentration of BSP added to fixed amounts of equimolar TIMP2 and mMMP-2 increased the reaction rate in a dose-dependent fashion (Figure 7C).

The interaction of the hemopexin-free mMMP-2 with TIMP2, BSP, and the fluorescein-gelatin substrate may be reflecting steric effects between these large macromolecules. Potential steric effects of substrate, enzyme, inhibitor, and BSP interactions were studied by using a low molecular weight, freely diffusible peptide substrate to follow enzyme activity. Similar to results with the large molecular weight substrate, the addition of BSP alone did not significantly alter mMMP-2 enzyme product evolution (Figure 7D). Furthermore, TIMP2 inhibited product evolution, as expected, while the addition of BSP to mMMP-2/TIMP2 complexes increased the digestion (Figure 7D). Titration of mMMP-2 with various concentrations of TIMP2 indicated that, at 10-fold excess, TIMP2 inhibited mMMP-2 activity on the small molecular weight substrate to 20%, with equimolar TIMP2 inhibiting the mMMP-2 to 34% (Figure 7E). As before, the addition of equimolar BSP was able to restore mMMP-2 treated with TIMP2 to 85% of normal activity. Increasing the concentration of BSP in reaction mixtures of equimolar TIMP2 and mMMP-2 restored activity further (Figure 7F). These data suggest that BSP reactivation of TIMP2- inhibited MMP-2 does not require the hemopexin domain of MMP-2.

Restoration of TIMP2-Inhibited MMP-2 Activity Requires both Amino-Terminal and Carboxy-Terminal BSP Sequences

The BSP chimeras were tested for their ability to restore activity to TIMP2-inhibited wild-type MMP-2 and mMMP-2 using the small, freely diffusible substrate assay. The hemopexin-free mMMP-2 exhibited a reaction velocity of 0.10 ± 0.02 pmol/s over the first 6 min of the reaction (Figure 8a). The addition of 10 nM TIMP2 reduced activity to 12 ± 5% that of mMMP-2 alone, while the inclusion of 10 nM BSP with the TIMP2 restored activity to 79 ± 12% of mMMP-2 alone (a 6.5-fold increase relative to mMMP-2+inhibitor). For mMMP-2, addition of equimolar chimera proteins exhibited various abilities in restoring TIMP2- inhibited activity. The percentage of the activity of mMMP-2 was 39 ± 11% for BSP/OPN (a 3-fold increase relative to mMMP-2 + inhibitor), 30 ± 16% for BSP/DMP1 (2.5-fold relative to mMMP-2 + inhibitor), 32 ± 12% for DMP1/ BSP (2.7-fold relative to mMMP-2 + inhibitor), and 17 ± 12% for OPN/ BSP chimera. When wild-type active MMP-2 was substituted for the hemopexin-free MMP-2, a reaction velocity of 0.94 ± 0.10 pmol/s was observed over the first 6 min of the reaction (Figure 8b). The addition of 10 nM TIMP2 reduced activity to 19 ± 3% that of MMP-2 alone, while the inclusion of 10 nM BSP with the TIMP2 restored activity to 93 ± 7% of MMP-2 alone (an <5-fold increase relative to MMP-2 + inhibitor). The chimera exhibited a similar pattern in restoring TIMP2 inhibited activity to wild type MMP-2. The percentage of the activity of MMP-2 was 53 ± 20% for BSP/OPN (2.8-fold relative to MMP-2 + inhibitor), 47 ± 13% for BSP/DMP1 (2.5-fold relative to MMP-2 + inhibitor), 58 ± 12% for DMP1/BSP (3-fold relative to MMP-2 + inhibitor), and 19 ± 6% for OPN/ BSP chimera.

DISCUSSION

The MMP gene family consists of at least 25 members of zinc-containing, calcium-dependent extracellular endoproteinases (18). MMPs may be cell surface-associated or secreted into the

extracellular space where they are involved in degrading extracellular matrix components as well as processing of non-matrix components such as cytokines, adhesion molecules, and receptors. MMPs often share functional domains such as the propeptide, the catalytic domain containing the active site, a hinge or linker region, and a hemopexin-like domain. The propeptide domain contains a zinc-ligating free thiol group that contributes to enzyme latency. This has been termed the "cysteine switch" (15,19) or "velcro" (20) mechanism and involves the cysteine residue in the propeptide binding to the catalytic Zn^{2+} of the enzyme. The hemopexin-like domain is thought to be essential for the binding of many natural substrates, contains a secondary TIMP-binding site, and is involved in membrane activation and possibly some proteolytic activities (21–23). MMP-2 and other gelatinases contain cysteine-rich repeats within the catalytic domain that resemble the collagen- binding type II repeats of fibronectin and are required to bind and cleave collagen and elastin (22).

Pro-MMPs can be activated either by proteases that remove the propeptide or by chemical compounds that disrupt or destabilize the zinc-cysteine interaction (24). In the current study, BSP binding to latent proMMP-2 leads to catalytic activity as well as the appearance of free cysteine residues. The presence of exons 2 through 5 of BSP in chimeric constructs with OPN and DMP1 led to proMMP-2 activation, while exons 2 through 5 of DMP1 and OPN linked to the 3′ exons of BSP did not enable proMMP-2 enzymatic activity, indicating that latent MMP-2 activation was specific to exons 2–5 of BSP. Indeed, the 26 amino acid sequence encoded for by exon 4 was required for the highest degree of BSP-mediated activity. Exon 4 alone did not activate the MMP although it could act as a competitive inhibitor and interfere with proMMP-2 activation by intact wild-type BSP. BSP is generally acidic and hydrophilic in nature (p*I* of 3.9 (25)), but exon 4 encodes the protein's only positively charged domain of significant size, being comprised of 1/3 positively charged amino acids (Arg, His, and Lys, p*I* = 10.1). Exon 4 also contains 1/4 of BSP's tyrosine residues, none of which are thought to be sulfated.

Like osteopontin, purified BSP protein subjected to standard one-dimensional proton NMR revealed a lack of ordered structures over the NMR time scale, indicating that the protein was extended and flexible in solution (26). Protein flexibility and lack of ordered structure are shared by a number of proteins that have multiple binding partners (27). Unstructured proteins have multiple contact points across the molecule, and structure is conferred through their binding interactions. In addition to MMP-2, BSP binding partners include hydroxyapatite (25), collagen (28), complement factor H (8), and αvβ3 integrin (29). Thus, in addition to potential structural, mineralization-related, and receptor-mediated signaling roles for the BSP in the extracellular matrix, BSP may regulate matrix turnover based on its modification of TIMP2 inhibition of MMP-2 activation.

We have shown previously that BSP can bind to both proMMP-2 and active MMP-2 (11). The current solution and solid-phase binding studies confirm that the proMMP-2 and active MMP-2 as well as hemopexin-deleted forms of MMP-2 have K_d values in the biologically significant nanomolar range. Binding of BSP to recombinant human MMP-2 that lacked the hemopexin domain yielded K_d values similar to those for proMMP-2 and active MMP-2, suggesting that the hemopexin domain does not contribute significantly to the binding interaction. While the chimera with the amino-terminal portion of BSP (BSP/OPN and BSP/DMP1) exhibited saturable binding to proMMP-2, the K_d values were 20-fold weaker than that of wild-type BSP. In contrast, chimera retaining the carboxy-terminal portion of the BSP protein (78% of the total BSP sequence, with the amino-terminal sequences replaced with either OPN or DMP1 exons 2–5) showed much weaker and non-saturable binding to proMMP-2. BSP protein with exon 4 deleted had a K_d value that was 6-fold weaker than full-length BSP. However, both the chimera lacking the amino-terminal portion of BSP and the BSP construct lacking exon 4 were extremely ineffective at activating proMMP-2. This suggests that while the amino-terminal

regions, especially exon 4, are essential in BSP-mediated proMMP-2 activation, more carboxy-terminal domains of BSP also contribute to the overall binding interaction.

TIMP2 has binding sites in both the hemopexin and catalytic domains (30). The ability of BSP to bind to and restore activity to TIMP2-inhibited mMMP-2 that lacked a hemopexin domain indicates that BSP interactions with the hemopexin domain are not required for BSP-dependent modulation of TIMP2 inhibition. Similar restoration of activity was measurable with both the large natural substrate (gelatin) and small, freely diffusible substrate. Thus, the changes in TIMP2 inhibition of mMMP-2 induced by BSP are not steric effects of exclusion of TIMP2 by the large macromolecular gelatin-MMP-2-BSP complex. The inability of chimera to restore full activity to TIMP2-inhibited wild type and mutant MMP-2 is consistent with distinct amino- and carboxy-terminal domains of BSP contributing to the enzyme reactivation.

In summary, these structure-function studies reveal for the first time that amino-terminal portions of BSP, particularly exon 4, are required for MMP-2 propeptide displacement and enzyme activation. On the other hand, domains spanning the entire BSP sequence contributed to binding affinity and reactivation of TIMP2-inhibited MMP-2. Finally, the hemopexin-like domain of MMP-2 is not required for BSP-mediated enzyme modulation. These observations are consistent with the model of BSP as a flexible, intrinsically unstructured protein that utilizes distinct regions or overlapping interaction surfaces for more than one function.

Acknowledgements

This was supported in part by National Institutes of Health (NIH) grant CA113865 (N.S.F.) and by the Division of Intramural Research, National Institute of Dental and Craniofacial Research Intramural Research Program, National Institutes of Health, Department of Health and Human Services.

References

1. Fisher LW, Torchia DA, Fohr B, Young MF, Fedarko NS. The solution structures of two SIBLING proteins, bone sialoprotein and osteopontin, by NMR. Biochem Bophys Res Commun 2001;280:460–465.
2. Christensen B, Kazanecki CC, Petersen TE, Rittling SR, Denhardt DT, Sorensen ES. Cell type-specific posttranslational modifications of mouse osteopontin are associated with different adhesive properties. J Biol Chem 2007;282:19463–19472. [PubMed: 17500062]
3. Ogbureke KU, Fisher LW. SIBLING expression patterns in duct epithelia reflect the degree of metabolic activity. J Histochem Cytochem 2007;55:403–409. [PubMed: 17210923]
4. Bellahcene A, Castronovo V, Ogbureke KU, Fisher LW, Fedarko NS. Small integrin-binding ligand N-linked glycoproteins (SIBLINGs): multifunctional proteins in cancer. Nat Rev Cancer 2008;8:212–226. [PubMed: 18292776]
5. El-Tanani MK, Campbell FC, Kurisetty V, Jin D, McCann M, Rudland PS. The regulation and role of osteopontin in malignant transformation and cancer. Cytokine Growth Factor Rev 2006;17:463–474. [PubMed: 17113338]
6. Fisher LW, Jain A, Tayback M, Fedarko NS. Small Integrin Binding LIgand N-linked Glycoprotein (SIBLING) gene family expression in different cancers. Clin Can Res 2004;10:8501–8511.
7. Weber GF. The metastasis gene osteopontin: a candidate target for cancer therapy. Biochim Biophys Acta 2001;1552:61–85. [PubMed: 11825687]
8. Fedarko NS, Fohr B, Robey PG, Young MF, Fisher LW. Factor H binding to bone sialoprotein and osteopontin enables tumor cell evasion of complement-mediated attack. J Biol Chem 2000;275:16666–16672. [PubMed: 10747989]
9. Karadag A, Ogbureke KU, Fedarko NS, Fisher LW. Bone sialoprotein, matrix metalloproteinase 2, and alpha(v) beta3 integrin in osteotropic cancer cell invasion. J Natl Cancer Inst 2004;96:956–965. [PubMed: 15199115]

10. Jain A, Karadag A, Fohr B, Fisher LW, Fedarko NS. Three SIBLINGs (small integrin-binding ligand, N-linked glycoproteins) enhance factor H's cofactor activity enabling MCP-like cellular evasion of complement-mediated attack. J Biol Chem 2002;277:13700–13708. [PubMed: 11825898]
11. Fedarko NS, Jain A, Karadag A, Fisher LW. Three small integrin binding ligand N-linked glycoproteins (SIBLINGs) bind and activate specific matrix metalloproteinases. FASEB J 2004;18:734–736. [PubMed: 14766790]
12. Jain A, Fisher LW, Fedarko NS. Bone sialoprotein binding to matrix metalloproteinase-2 alters enzyme inhibition kinetics. Biochemistry 2008;47:5986–5995. [PubMed: 18465841]
13. Fedarko NS, Fohr B, Gehron Robey P, Young MF, Fisher LW. Factor H binding to bone sialoprotein and osteopontin enables molecular cloaking of tumor cells from complement-mediated attack. J Biol Chem 2000;275:16666–16672.
14. Mintz KP, Grzesik WJ, Midura RJ, Robey PG, Termine JD, Fisher LW. Purification and fragmentation of nondenatured bone sialoprotein: evidence for a cryptic, RGD-resistant cell attachment domain. J Bone Miner Res 1993;8:985–995. [PubMed: 8213261]
15. Springman EB, Angleton EL, Birkedal-Hansen H, Van Wart HE. Multiple modes of activation of latent human fibroblast collagenase: evidence for the role of a Cys73 active-site zinc complex in latency and a "cysteine switch" mechanism for activation. Proc Natl Acad Sci USA 1990;87:364–368. [PubMed: 2153297]
16. Midura RJ, McQuillan DJ, Benham KJ, Fisher LW, Hascall VC. A rat osteogenic cell line (UMR 106–01) synthesizes a highly sulfated form of bone sialoprotein. J Biol Chem 1990;265:5285–5291. [PubMed: 2318894]
17. Murphy G, Knauper V. Relating matrix metalloproteinase structure to function: why the "hemopexin" domain? Matrix Biol 1997;15:511–518. [PubMed: 9138283]
18. Verma RP, Hansch C. Matrix metalloproteinases (MMPs): chemical-biological functions and (Q) SARs. Bioorg Med Chem 2007;15:2223–2268. [PubMed: 17275314]
19. Van Wart HE, Birkedal-Hansen H. The cysteine switch: a principle of regulation of metalloproteinase activity with potential applicability to the entire matrix metalloproteinase gene family. Proc Natl Acad Sci USA 1990;87:5578–5582. [PubMed: 2164689]
20. Vallee BL, Auld DS. Zinc coordination, function, and structure of zinc enzymes and other proteins. Biochemistry 1990;29:5647–5659. [PubMed: 2200508]
21. Wallon UM, Overall CM. The hemopexin-like domain (C domain) of human gelatinase A (matrix metalloproteinase- 2) requires Ca2+ for fibronectin and heparin binding. Binding properties of recombinant gelatinase A C domain to extracellular matrix and basement membrane components. J Biol Chem 1997;272:7473–7481. [PubMed: 9054449]
22. Overall CM. Molecular determinants of metalloproteinase substrate specificity: matrix metalloproteinase substrate binding domains, modules, and exosites. Mol Biotechnol 2002;22:51–86. [PubMed: 12353914]
23. Tam EM, Moore TR, Butler GS, Overall CM. Characterization of the distinct collagen binding, helicase and cleavage mechanisms of matrix metalloproteinase 2 and 14 (gelatinase A and MT1-MMP): the differential roles of the MMP hemopexin c domains and the MMP-2 fibronectin type II modules in collagen triple helicase activities. J Biol Chem 2004;279:43336–43344. [PubMed: 15292230]
24. Corcoran ML, Hewitt RE, Kleiner DE Jr, Stetler- Stevenson WG. MMP-2: expression, activation and inhibition. Enzyme Protein 1996;49:7–19. [PubMed: 8796994]
25. Stubbs JT III, Mintz KP, Eanes ED, Torchia DA, Fisher LW. Characterization of native and recombinant bone sialoprotein: delineation of the mineral-binding and cell adhesion domains and structural analysis of the RGD domain. J Bone Miner Res 1997;12:1210–1222. [PubMed: 9258751]
26. Fisher LW, Torchia DA, Fohr B, Young MF, Fedarko NS. Flexible structures of SIBLING proteins, bone sialoprotein, and osteopontin. Biochem Biophys Res Commun 2001;280:460–465. [PubMed: 11162539]
27. Tompa P, Szasz C, Buday L. Structural disorder throws new light on moonlighting. Trends Biochem Sci 2005;30:484–489. [PubMed: 16054818]
28. Fujisawa R, Kuboki Y. Affinity of bone sialoprotein and several other bone and dentin acidic proteins to collagen fibrils. Calcif Tissue Int 1992;51:438–442. [PubMed: 1451011]

29. Fisher LW, McBride OW, Termine JD, Young MF. Human bone sialoprotein. Deduced protein sequence and chromosomal localization. J Biol Chem 1990;265:2347–2351. [PubMed: 2404984]

30. Olson MW, Gervasi DC, Mobashery S, Fridman R. Kinetic analysis of the binding of human matrix metalloproteinase- 2 and -9 to tissue inhibitor of metalloproteinase (TIMP)-1 and TIMP-2. J Biol Chem 1997;272:29975–29983. [PubMed: 9368077]

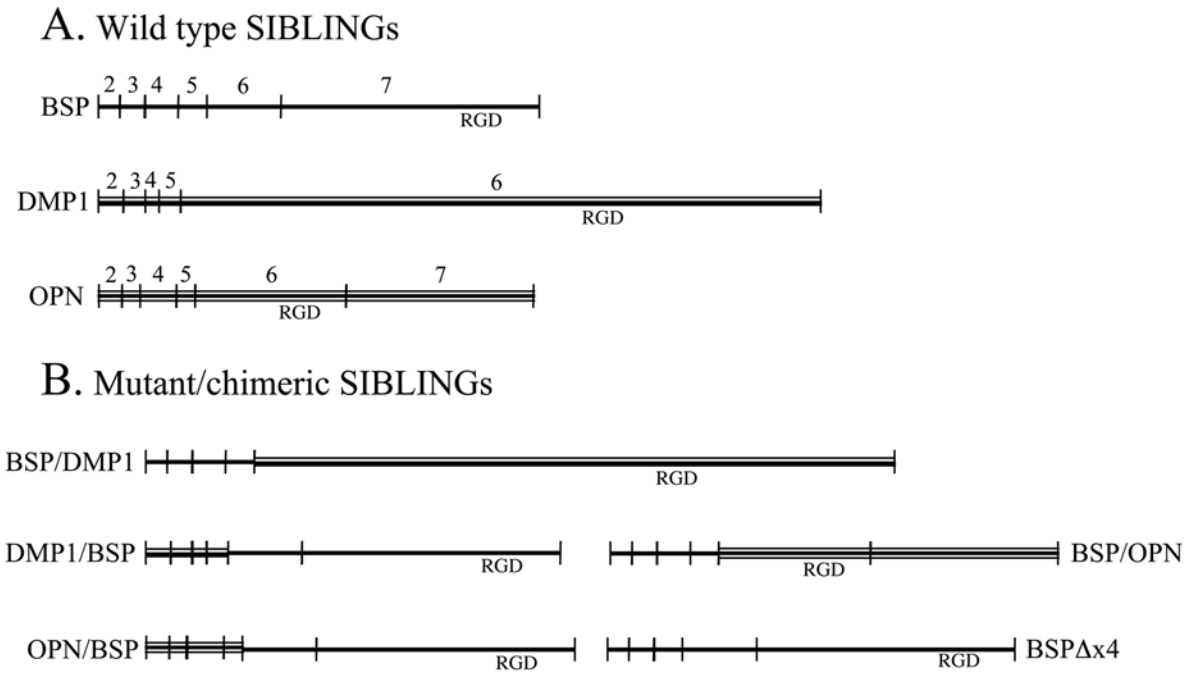

FIGURE 1.

Wild-type, chimeric, and exon 4-deleted BSP recombinant protein constructs. (A) The relative protein domain sizes encoded by the corresponding exons are depicted for BSP, DMP1, and OPN. The first exon is noncoding and not depicted. The second exon contains the start codon, the hydrophobic signal peptide, and the first two amino acids of the mature protein. Exons 3 and 5 contain consensus sequences for serine phosphorylation. (B) SIBLING chimera were constructed whereby amino-terminal portions of one protein were ligated to carboxy-terminal sequences of another. Exons 2 to 5 of BSP were linked to exon 6 of DMP1 (BSP/DMP1) or exons 6 and 7 of OPN (BSP/OPN). Exons 6 to 7 of BSP were also linked to exons 2 to 5 of DMP1 (DMP1/BSP) or OPN (BSP/OPN). An additional BSP species was made by deleting exon 4 (BSPΔx4). The relative location of the integrin-binding tripeptide, Arg-Gly-Asp (RGD), is noted for each protein and mutant/chimera.

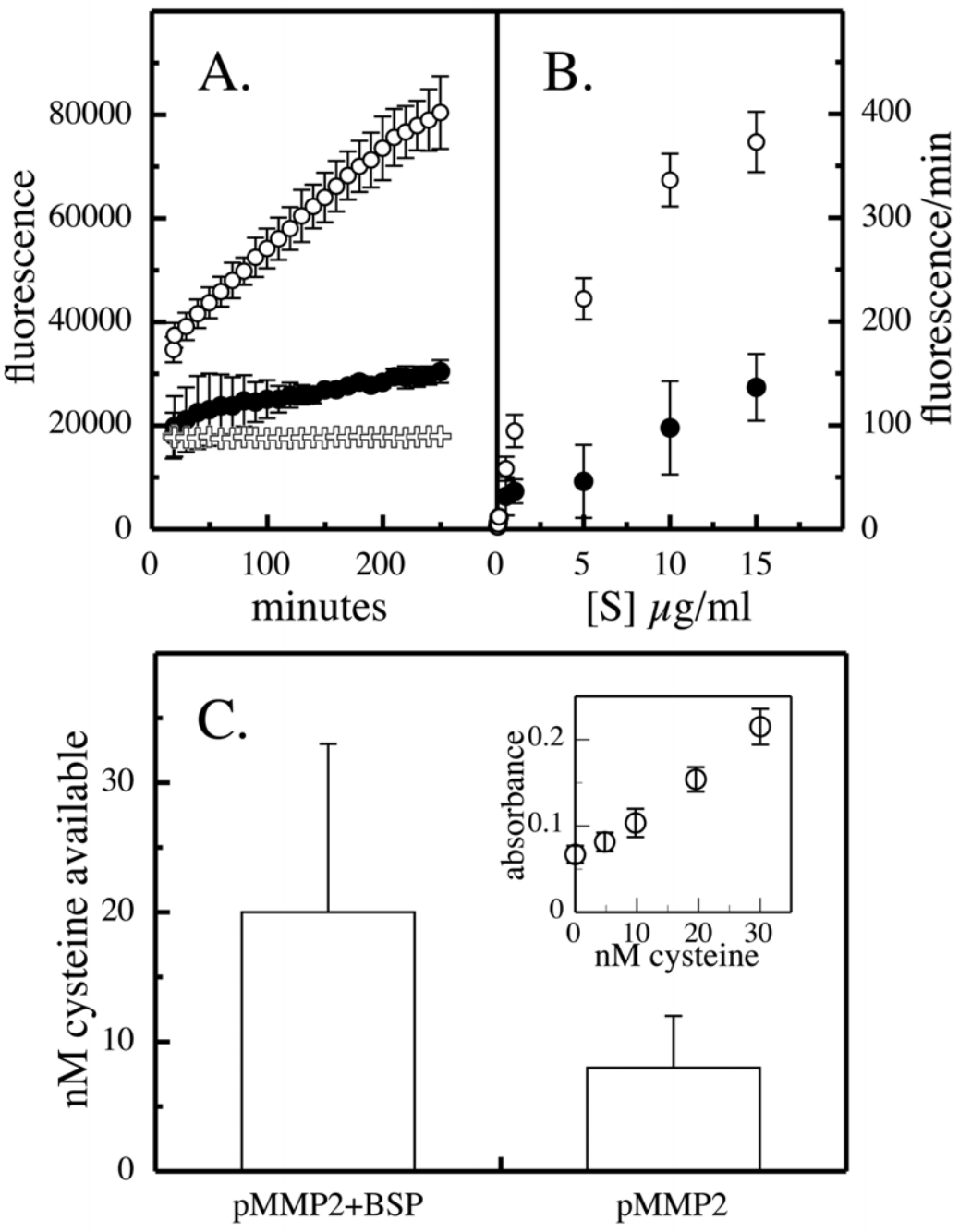

FIGURE 2.

BSP binding to proMMP-2 confers enzymatic activity and exposes the free cysteine residue. (A) The large fluorescein-gelatin substrate was incubated with pro-MMP-2 (closed circle), proMMP-2 + BSP (open circle), or BSP alone (plus). (B) Substrate velocity plots were generated by varying substrate concentration with fixed proMMP-2 levels in the presence (open circle) and absence (closed circle) of BSP. (C) ProMMP-2 at 14 nM final concentration was incubated ± 14 nM BSP in the presence of 180 μM DTNB in reaction buffer (0.1 M sodium phosphate, pH 8.0). The reactions were incubated for 15 min at room temperature, and absorbance was measured at 412 nM. A standard curve (inset) of absorbance versus nM

cysteine was made by incubating noted concentrations of free cysteine under the same reaction conditions. Errors bars represent standard deviation values based on triplicate analyses.

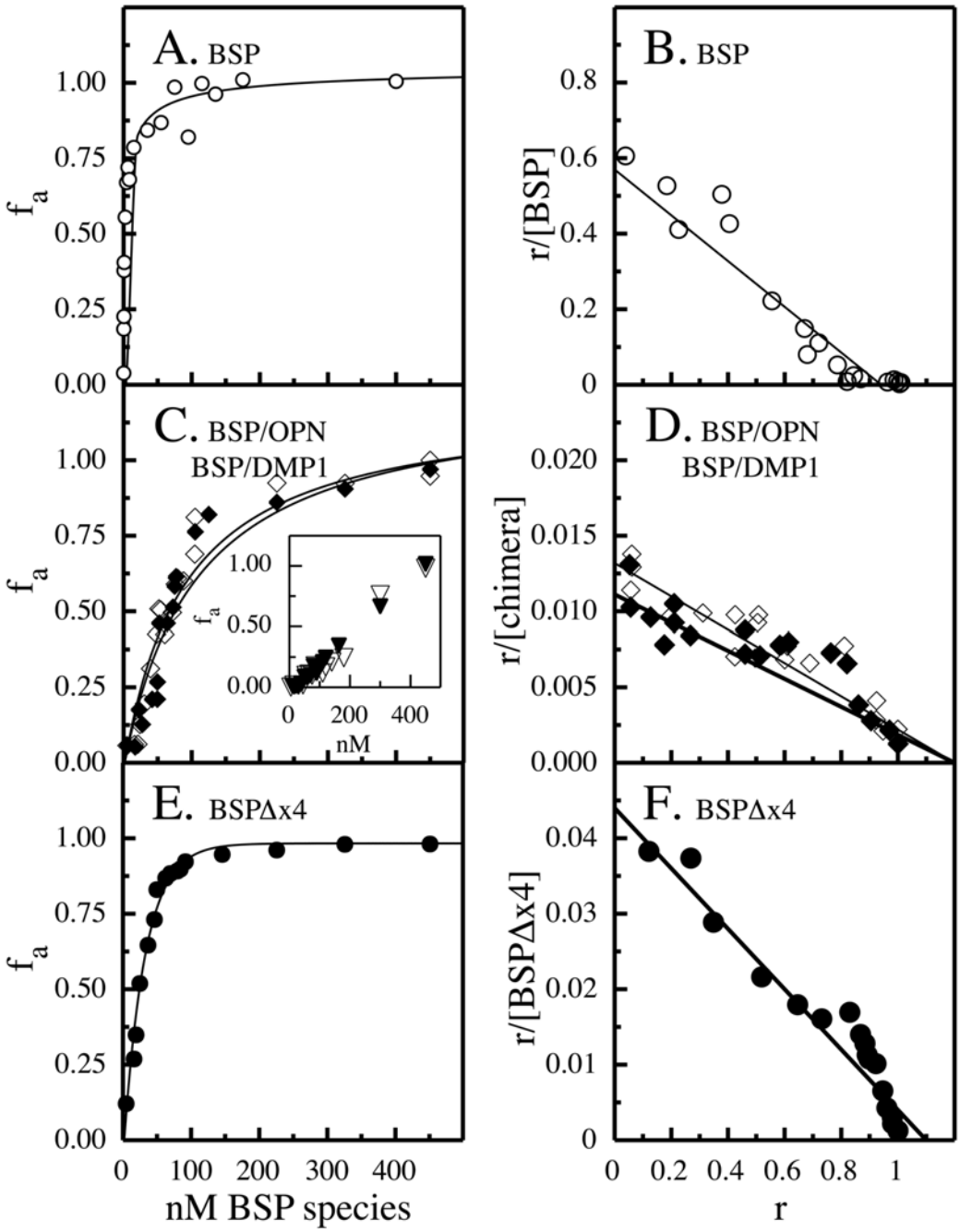

FIGURE 3.

Determination of BSP domains required for binding to proMMP-2. Binding isotherms between proMMP-2 and different forms of BSP (A, C, E) were determined using intrinsic tryptophan fluorescence binding assays as described in Materials and Methods. The corresponding Scatchard plots for proMMP-2 and the different forms of BSP were calculated (B, D, F). The forms of BSP studied included (A, B) wild-type BSP (open circle), (C, D) BSP/OPN (closed diamond) or BSP/ DMP1 chimera (open diamond), OPN/BSP (inverted closed triangle) or DMP1/BSP chimera (inverted open triangle), and (E, F) BSP exon 4 deletion (BSPΔx4, closed circle). The inset figure in panel C depicts the binding isotherm for the OPN/BSP and DMP1/ BSP chimera where no saturation was observed and a corresponding Scatchard analysis could

not be performed. The values plotted represent the average of two separate experiments for each condition run in duplicate.

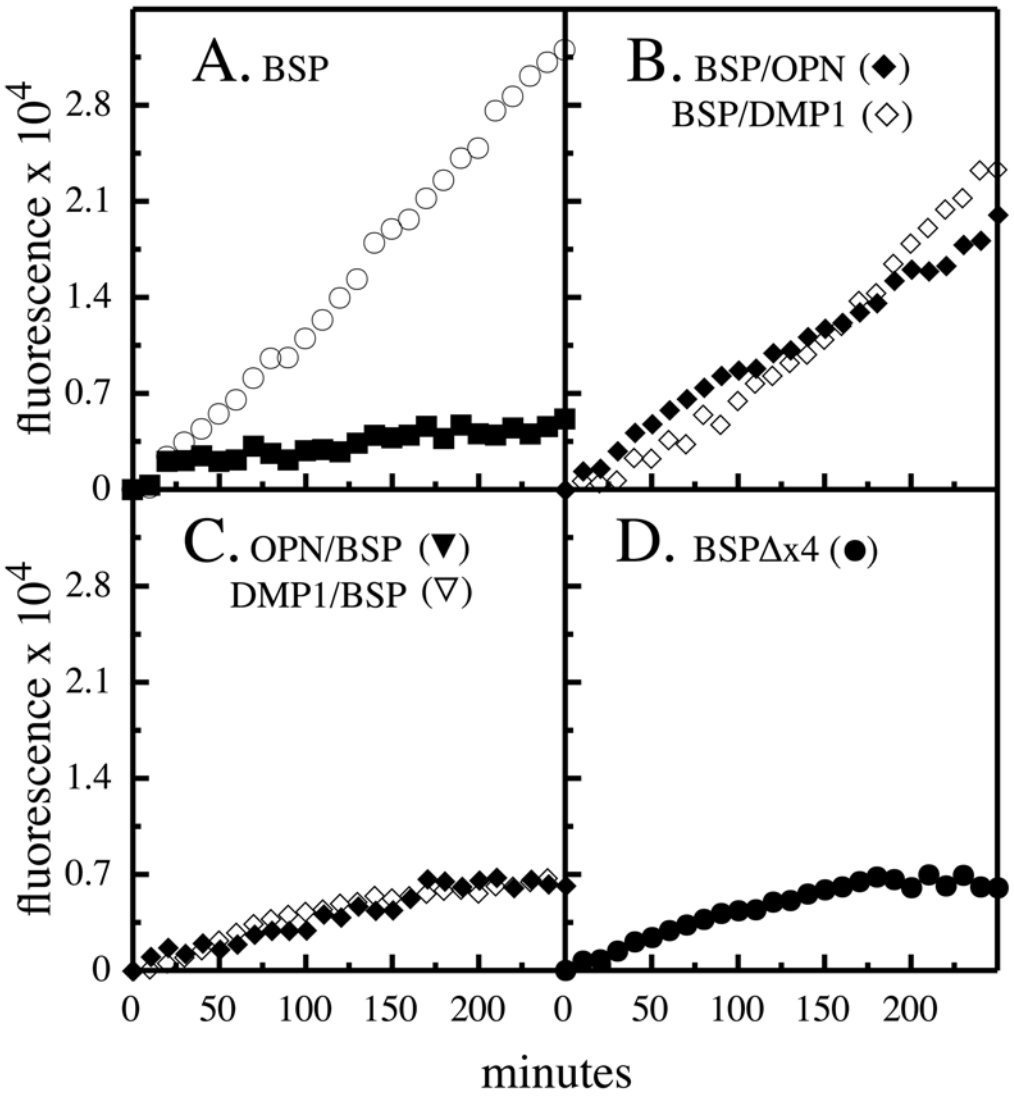

FIGURE 4.

Determination of BSP domains required for activation of proMMP-2. Changes in enzymatic activity for proMMP-2 treated with different forms of BSP were followed using the fluorescein-labeled gelatin substrate and proMMP-2 incubated with vehicle or BSP or noted constructs. The conditions employed were (A) vehicle (closed square) or BSP (open circle), (B) BSP/OPN (closed diamond) or BSP/DMP1 chimera (open diamond), (C) OPN/BSP (inverted closed triangle) or DMP1/BSP chimera (inverted open triangle), and (D) BSPΔx4 (closed circle). Note that the exons 2 to 5 and particularly exon 4 are required for inducing activity in proMMP-2. Enzyme activity assays were performed in triplicate.

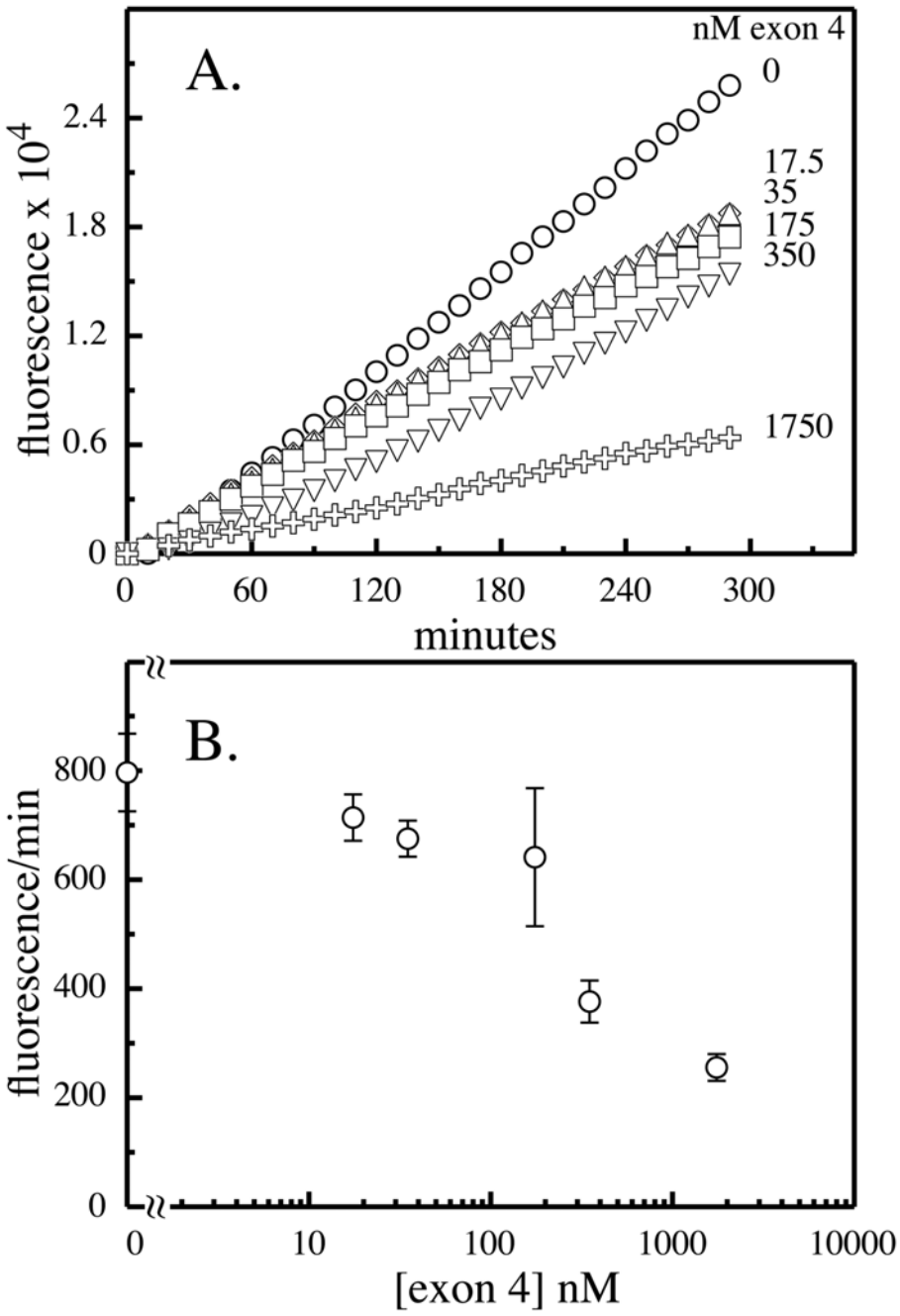

FIGURE 5.

BSP exon 4 peptide reduces intact BSP activation of proMMP-2. (A) Synthetic exon 4 peptide was added at noted concentrations to a mix of 10 nM wild-type intact BSP and 10 nM proMMP-2, and the changes in enzymatic activity were followed using the fluorescein-labeled gelatin substrate. The concentrations of exon 4 peptide were 0 (open circle), or 17.5 nM (open diamond), 35 nM (open triangle), 175 nM (open square), 350 nM (inverted open triangle), and 1750 nM (+). (B) The relative velocity of the reactions was determined as the change in fluorescence over the first 60 min. Enzyme activity assays were performed in triplicate, and error bars represent standard deviations for combined experiments.

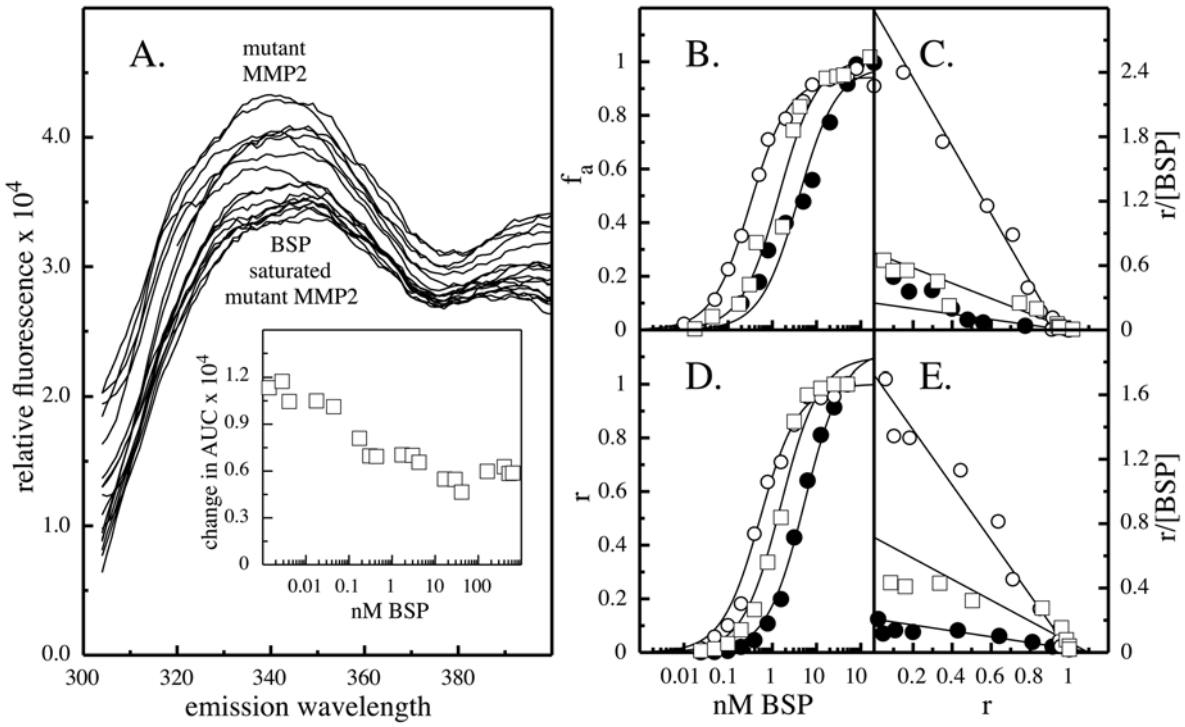

FIGURE 6.

BSP binding to MMP-2 does not require the hemopexin domain. (A) Binding interactions between mutant MMP-2 lacking the hemopexin domain (mMMP-2) and BSP were followed by intrinsic tryptophan fluorescence of the mMMP-2 protein. One nanomolar mMMP-2 was reacted with increasing concentration of BSP. Intrinsic tryptophan fluorescence was monitored by excitation at 295 nm and recording emission from 300 to 500 nm. Binding saturation was followed by monitoring the change in the area under the emission peak curve (inset). (B, C) The area under the emission peak curve was used to determine a binding curve by calculating fractional acceptor saturation versus nM BSP added and the corresponding Scatchard plot. (D) The binding interaction between BSP and proMMP-2 (closed circle), active MMP-2 (open circle), and mMMP-2 (open square) was investigated by solid-phase binding assays. (E) Scatchard plots derived from solid-phase binding assays of BSP and proMMP-2, active MMP-2, and mMMP-2 were determined. For both solution and solid-phase binding assays, the values plotted represent the average of two separate experiments for each condition run in duplicate.

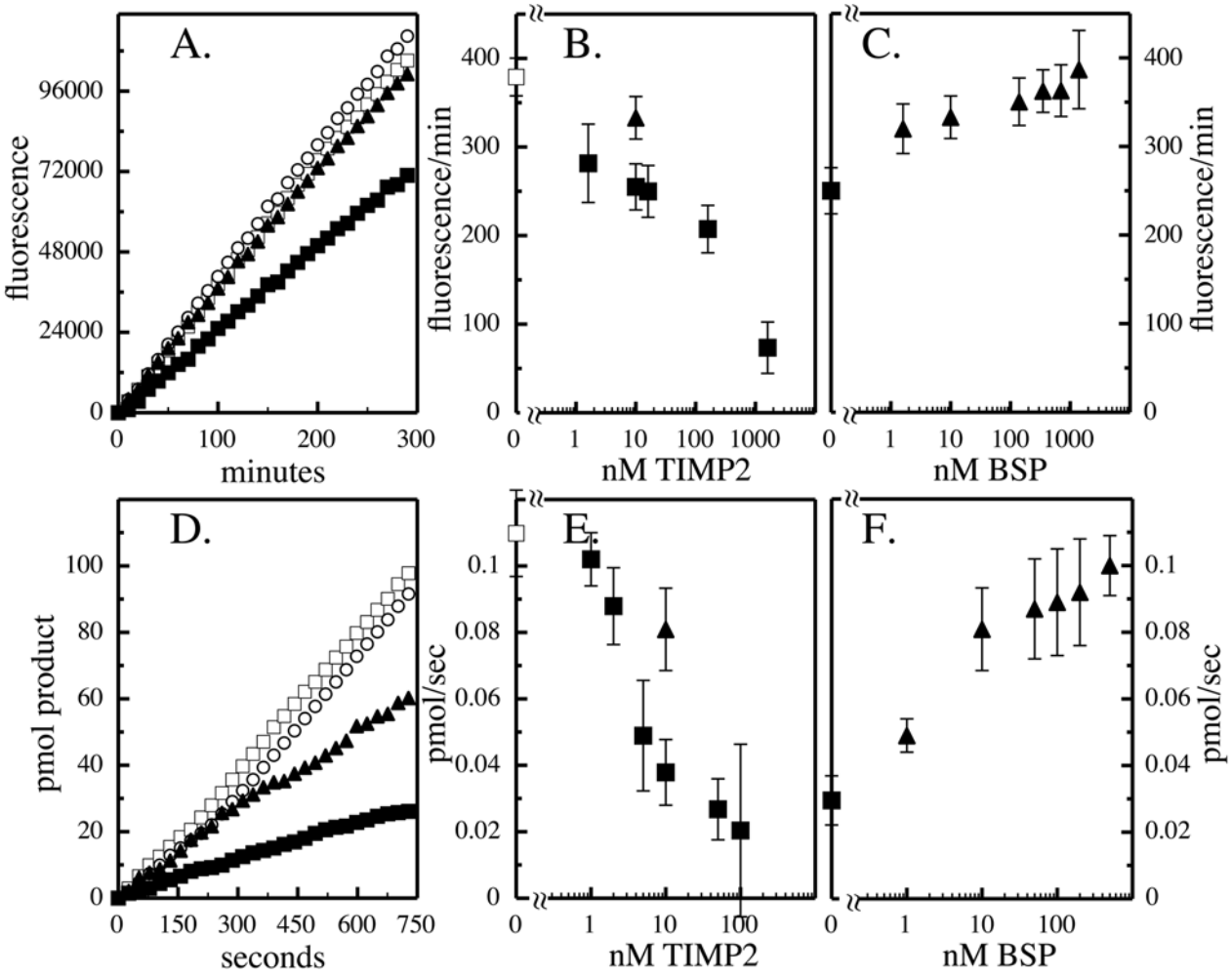

FIGURE 7.

BSP binding to hemopexin-deleted MMP-2 keeps TIMP2 from inhibiting the protease activity. (A) The effect of BSP on the activity of the mMMP-2 was profiled using the fluorescein-labeled large molecular weight (gelatin) substrate assay. Reaction conditions included mutant MMP-2 (open square), mutant MMP-2 + BSP (open circle), mutant MMP-2 + TIMP2 (closed square), and mutant MMP-2 + TIMP2 +BSP (closed triangle). (B) The effect of varying conditions on the relative velocity of the mutant enzyme was analyzed by linear regression analysis over the first hour and the slope determined. (C) The effect of BSP on TIMP2's inhibition of mMMP-2 was further studied by titrating a reaction mixture of equimolar mMMP-2 + TIMP2 with increasing concentrations of BSP. (D) The action of BSP on mMMP-2 activity using the small substrate Ac-PLG-[2-mercapto-4-methylpentanoyl]-LG-OC_2H_5 was determined by following picomoles of product evolution over time. (E) TIMP2 inhibition curves and (F) BSP dose response of mMMP-2 recovery from inhibition by TIMP2 were determined. For substrate titrations and TIMP2 dose response, three separate experiments were combined, and values plotted present the slope of the reaction over the first 6 min with error bars representing the standard deviation.

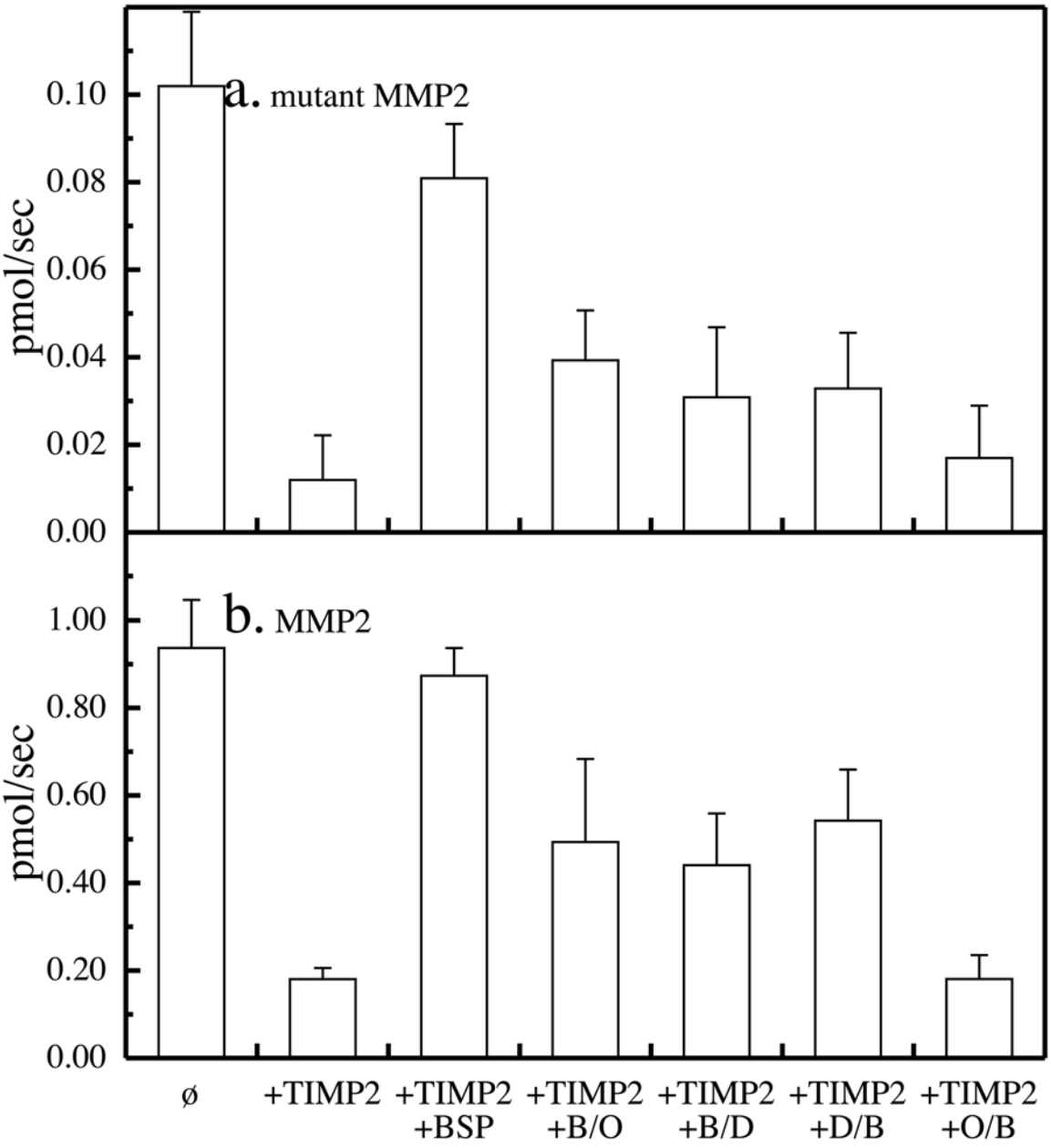

FIGURE 8.

TABLE 1

BSP and MMP-2 binding constants.

Ligand	receptor	K_d (nM)
BSP	mMMP-2[1]	1.40 ± 0.34 (1.54 ± 0.24)[2]
BSP	active MMP-2	0.32 ± 0.02 (0.58 ± 0.06)
BSP	proMMP-2	3.9 ± 0.9 (5.4 ± 0.5)
BSP/OPN	proMMP-2	108 ± 21
BSP/DMP1	proMMP-2	91 ± 13
BSPΔx4	proMMP-2	25 ± 8

[1] Mutant MMP-2 lacking the hemopexin domain.

[2] Values in parenthesis are from solid phase binding assays.

Small integrin-binding ligand N-linked glycoproteins (SIBLINGs): multifunctional proteins in cancer

Akeila Bellahcène, Vincent Castronovo*, Kalu U. E. Ogbureke‡, Larry W. Fisher§ and Neal S. Fedarko||*

Abstract | Numerous components and pathways are involved in the complex interplay between cancer cells and their environment. The family of glycophosphoproteins comprising osteopontin, bone sialoprotein, dentin matrix protein 1, dentin sialophosphoprotein and matrix extracellular phosphoglycoprotein — small integrin-binding ligand N-linked glycoproteins (SIBLINGs) — are emerging as important players in many stages of cancer progression. From their detection in various human cancers to the demonstration of their key functional roles during malignant transformation, invasion and metastasis, the SIBLINGs are proteins with potential as diagnostic and prognostic tools, as well as new therapeutic targets.

Integrin
Integrins are a large family of heterodimeric cell surface adhesion receptors that bind extracellular matrix and cell surface ligands. They promote stable interactions between cells and their environment and mediate intracellular signalling.

**Metastasis Research Laboratory, University of Liege, Tour de Pathologie, -1, Bât. B23, Sart Tilman via 4000 Liège, Belgium.*
‡Department of Oral Biology, School of Dentistry, Medical College of Georgia, Augusta, Georgia 30912, USA.
§National Institute of Dental and Craniofacial Research, National Institutes of Health, Department of Health and Human Services, 9000 Rockville Pike, Bethesda Maryland 20892–4320, USA.
||Department of Medicine, Johns Hopkins University, 5501 Hopkins Bayview Circle, Baltimore, Maryland 21224, USA.
Correspondence to L.W.F.
e-mail: lfisher@dir.nidcr.nih.gov
doi:10.1038/nrc2345

The progression of malignant cells requires complex interactions with the host tissues. Tumour survival and metastasis necessitate overcoming immune surveillance, extracellular matrix barriers and limiting nutrients. Effectively stopping cancer progression appears to require the use of a panel of therapeutic modalities able to interfere with the multiple stages of cancer cell invasion and dissemination. An alternative to targeting specific stages in progression (for example, angiogenesis and metastasis) would be to target select molecules that have key roles in multiple stages of cancer development.

Small integrin-binding ligand N-linked glycoproteins (SIBLINGs[1]), a family of five integrin-binding glycophosphoproteins comprising osteopontin (OPN), bone sialoprotein (BSP), dentin matrix protein 1 (DMP1), dentin sialophosphoprotein (DSPP) and matrix extracellular phosphoglycoprotein (MEPE), are an emerging group of molecular tools that cancer cells use to facilitate their expansion. SIBLINGs are soluble, secreted proteins that can act as modulators of cell adhesion as well as autocrine and paracrine factors by their interaction with cell surface receptors such as integrins. OPN is the only SIBLING for which there is unequivocal evidence of its role in many steps of cancer development and progression, but accumulating data also implicate other family members, notably BSP and DSPP[2–6]. The involvement of SIBLINGs in many of the crucial steps for malignant progression makes them potentially valuable candidates for effective anticancer therapies. In this Review, we describe the major characteristics of SIBLINGs, including their proposed roles in normal tissue and the major activities they display during malignant progression. Finally, we discuss their potential as therapeutic targets and prognostic markers.

Discovery and characteristics of SIBLINGs

SIBLINGs are currently a family of five identically orientated tandem genes within a 375,000 bp region on chromosome 4 (FIG. 1a). The genes (*DMP1*, *DSPP*, integrin-binding sialoprotein (*IBSP*, which encodes BSP), *MEPE* and secreted phosphoprotein 1 (*SPP1*, which encodes OPN)) are probably a result of an early gene duplication and divergence[1]. The term SIBLING refers to the gene family's unifying genetic and biochemical characteristics in general, not to functional activity. SIBLINGs are defined as small, soluble RGD motif containing, integrin-binding ligands to distinguish them from large extracellular matrix proteins such as fibronectin (FN1), collagen and thrombospondin (THBS1). Comparison of any one SIBLING to itself at the amino acid sequence level throughout evolution (predominantly in birds and mammals) shows that they are poorly conserved. Each SIBLING member appears to be able to drift substantially as long as it remains hydrophilic and flexible, and retains a number of motifs and member-related short amino acid sequences. For example, using standard sequence comparison basic local alignment search tool (BLAST) programs[7], human and mouse OPN are identical at only 63% of the amino

At a glance

- Small integrin-binding ligand N-linked glycoproteins (SIBLINGs) are a family of glycophosphoproteins comprising osteopontin (OPN), bone sialoprotein (BSP), dentin matrix protein 1 (DMP1), dentin sialophosphoprotein (DSPP) and matrix extracellular phosphoglycoprotein (MEPE).
- The genes encoding the SIBLINGs are located within a cluster on chromosome 4 and encode soluble, hydrophilic proteins sharing common functional motifs and domains, including an Arg–Gly–Asp (RGD) motif that binds αvβ3 integrin.
- SIBLINGs were initially described as mineralized tissue-associated glycophosphoproteins and were thought to be functionally restricted to these tissues. Recent results show that they are more widely distributed and are expressed in non-mineralized normal tissue, such as metabolically active ductal epithelial cells.
- Some SIBLINGs activate specific metalloproteinases (MMPs; BSP activates MMP2, OPN, MMP3 and DMP1, MMP9). These three SIBLINGs also bind complement factor H and prevent complement attack.
- SIBLINGs are overexpressed in many cancers. OPN and, less so, BSP are by far the more widely studied to date and their levels of expression are correlated with tumour aggressiveness. SIBLINGs can be detected in the blood and their level of expression is associated with prognosis.
- Among SIBLINGs, OPN is involved in almost all steps of tumour progression, including invasion, metastasis and angiogenesis.
- *In vitro* and *in vivo* experimental models demonstrated that interference with SIBLINGs, such as small interfering RNA selective knockdown, has potential anticancer therapeutic value.
- Identifying the specific roles of SIBLINGs in cancer–stroma interactions and signalling cascades involving growth factor–growth factor receptor and cell–matrix interactions could result in the development of additional and refined strategies for the prevention and treatment of metastases.

acid positions and the comparison with chicken drops to 30% identity, although all retain, for example, at least one RGD and N-linked oligosaccharide motif each. Therefore, the SIBLING family was defined structurally by the conserved motifs within their exons, including an abundance of acidic amino acids, the RGD motif, similar post-translational modification motifs (for example, casein kinase phosphorylation and various glycosylation events) and more recently the recognition that at least one site of controlled proteolysis appears to be important in all members (FIG. 1b). The SIBLINGs that have had their three-dimensional structure solved by NMR analysis (BSP and OPN) are extended and flexible in solution, a property shared by a number of proteins that have multiple binding partners and that are involved in bridging macromolecular components (for example, certain ribosomal proteins). Consistent with that observation, SIBLINGs can bind to a number of different protein families, including integrins (through both RGD and non-RGD motifs) and other cell-surface proteins, members of the matrix metalloproteinase (MMP) family and complement factor H (CFH). These interactions enable cell surface localization and sequestration of MMPs and CFH by at least OPN, BSP and DMP1, which in turn enables their biological activities (extracellular matrix degradation and evasion of complement-mediated lysis for example).

Four acidic members (BSP[8], DMP1 (REF. 9), DSPP[10] and OPN[11]) were discovered as abundant proteins trapped within the mineralized matrices of bone and dentin. In the early years of study, each of these proteins was thought to be both skeletal tissue-specific and to have a role in directly nucleating hydroxyapatite crystals within mesenchymal tissues through their phosphate groups and/or polyacidic amino acid domains[9,12]. From the 1990s, various combinations of SIBLING proteins were discovered to be significantly upregulated in a number of epithelial tumours that are known to frequently exhibit pathological microcalcifications and to have strong propensities to metastasize to bone[13]. More recently it has been shown that all five of the SIBLINGs are also expressed in the epithelial cells of metabolically active normal ducts of the salivary gland and kidney[14,15], but not in metabolically passive normal ducts[16]. SIBLINGs are secreted proteins that can be localized through interactions with receptors either on the cell's own surface, enabling autocrine activities, or by diffusing short distances to nearby cells where they may function in paracrine signalling. SIBLINGs propagate biological signals by initiating integrin signalling and by binding and sequestering other proteins to the cell surface.

Roles of SIBLINGs in normal tissues

SIBLINGs bind to cell surface integrins and sometimes CD44 in normal tissues and function as signal transducers to promote cell adhesion, motility and survival (FIG. 2) through activating kinase cascades and transcription factors. The biological activities of SIBLINGs are also modulated by proteolytic processing, which can reveal cryptic binding sites and can remove or separate functional domains, thereby modulating cell adhesion and migration (FIG. 1b).

For example, OPN interacts with a variety of integrins, including αvβ3, αvβ5, αvβ1, α4β1, α8β1 and α9β1, as well as CD44 splice variants. Integrin-mediated cell adhesion and migration are stimulated in assays in which full-length OPN is immobilized on tissue culture dishes. Thrombin cleavage of OPN separates the integrin- and CD44-binding domains, which in some cases promotes adhesion over migration. For example, the thrombin-generated amino-terminal OPN fragment binds to αvβ3 and αvβ5 integrins (through RGD[17]) or to α9β1 and α4β1 integrins (through the cryptic SVVYGLR sequence[18]) and promotes cell adhesion. The carboxy-terminal fragment binds to CD44 variant 6 (CD44v6) — and sometimes to CD44v3 by a heparin bridge — and promotes the formation of foci, invasion and tumorigenesis[19]. Under specific conditions, OPN is also a substrate for MMP3 and MMP7, and the resulting OPN fragments facilitate adhesion and migration *in vitro* through activation of β1-containing integrins[20]. OPN has also been shown to be a substrate for liver transglutaminase and plasma transglutaminase factor IIIa, resulting in protein crosslinking[21] and enhanced cell adhesion, spreading, focal contact formation and migration[22]. Through interactions with cell-surface receptors, OPN and its proteolytic fragments modulate cell adhesion and migration.

Through their action on the transcription factor nuclear factor κB (NFκB), SIBLINGs can also affect cellular proliferation, differentiation and apoptosis in normal tissues. BSP increases survival and decreases apoptosis of bone marrow-derived monocytes and

Dentin
The main, calcareous part of a tooth, beneath the enamel and surrounding the pulp chamber and root canals.

RGD motif
A tripeptide, Arg–Gly–Asp (RGD), found in numerous proteins that support cell adhesion. A subset of the integrins recognize the RGD motif within their ligands, the binding of which mediates both cell–substratum and cell–cell interactions.

Hydroxyapatite crystals
The principal inorganic constituent of bone matrix and teeth, imparting rigidity to these structures, and consisting of hydrated calcium phosphate, $Ca_5(PO_4)_3OH$.

Metabolically active normal duct
Epithelia, such as that of the kidney nephrons, that alter the tonicity of the fluid they process in the course of normal physiology. The kidney nephrons process isotonic urine into the voided hypotonic urine.

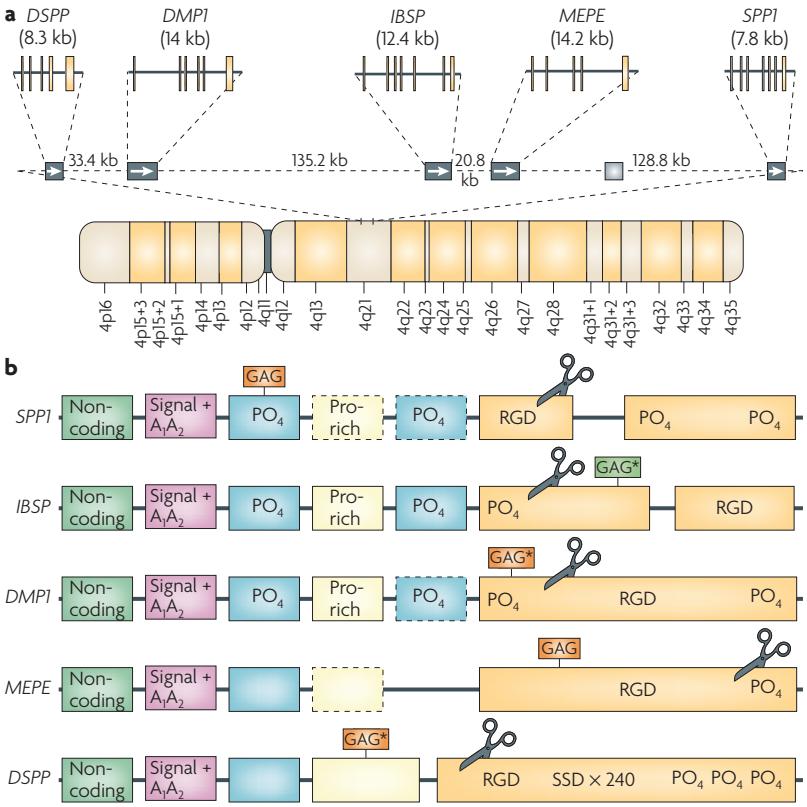

Figure 1 | **Chromosomal localization and exon–intron similarities of human SIBLING genes. a** | The genes are clustered within a 375 kb region of chromosome 4 and are similarly arranged in all completed mammalian genomes to date. Except for an apparent pseudogene (*HSP90AB*[177]) between matrix extracellular phosphoglycoprotein (*MEPE*) and secreted phosphoprotein 1 (*SPP1*) in humans and chimps only (light grey box), there are no other significant open-reading frames within this region. Integrin-binding sialoprotein (*IBSP*) encodes bone sialoprotein (BSP) and *SPP1* encodes osteopontin (OPN). Vertical lines represent exons. **b** | The transcripts of small integrin-binding ligand N-linked glycoprotein (SIBLING) genes. The SIBLINGs, which are composed almost exclusively of hydrophilic amino acids, are likely to be flexible, extended structures in solution. The exons (boxes; not drawn to scale) often have similar motifs and properties and are separated by type 0 introns. The first exon is non-coding. The second exon contains the start codon, the hydrophobic signal peptide and the first two amino acids of the mature protein (A_1A_2). Exons 3 and 5 frequently contain consensus sequences for serine phosphorylation (PO_4). Exon 4 can be relatively proline-rich and, like the other small exons (3 and 5), has been shown in some cases to be spliced out of a subset of mRNA (exons with dashed borders). The integrin-binding tripeptide, Arg–Gly–Asp (RGD), is found within the last one or two large exons (which typically encode >80% of the protein). All SIBLINGs contain variously located N- and/or O-linked oligosaccharides, but only the observed (GAG*) and proposed (GAG) consensus attachment sites of the relatively long chain glycosaminoglycans are shown. (Orange GAG indicates chondroitin or dermatan sulphate chains and green GAG indicates keratan sulphate chains.) Cleavage of SIBLINGs (scissors) by specific proteases (bone morphogenetic protein 1 (BMP1), thrombin, matrix metallopeptidases and so on) is thought to be important, although whether this activates and/or inactivates specific SIBLING functions is currently under investigation. Human DSPP also contains ~240 tandem repeats of the phosphorylated nominal Ser–Ser–Asp (SSD) tripeptide. (For summary of some of the post-translational modifications and protease cleavage sites, see REF. 159.) DMP1, dentin matrix protein 1; DSPP, dentin sialophosphoprotein.

Type 0 introns
Introns that disrupt an open reading frame between codon junctions and therefore permit any splicing combination to other type 0 exons without causing frameshifts.

macrophages through enhanced NFκB signalling[23]. BSP can also induce NFκB-dependent bone resorption by inducing osteoclastogenesis and osteoclast survival[23]. OPN activation of NFκB promotes survival of activated T cells through phosphorylation of the kinase IKKβ (also known as inhibitor of NFκB kinase β (IKBKB)) and inhibition of the transcription factor FOXO3 (REF. 24). A role for OPN-induced activation of NFκB in the survival of dopaminergic neurons[25], endothelial cells[26] and dendritic cells[27] has also been reported.

The above-mentioned pathways (migration, adhesion and apoptosis evasion) are crucial in the development and progression of cancer as nascent neoplasms must successfully navigate these pathways to survive. Therefore it seems possible that the effects of SIBLINGs in cancer biology are due in part to modulation of these pathways.

SIBLINGs and tumour progression

Tumour progression involves a sequential series of events that confer a survival advantage to transformed cells. These events begin with neoplastic transformation and continue through the subversion of proliferation blockades, growth restriction, physical barriers and host defence systems. Cancer cell survival requires proliferation, interaction with the extracellular matrix to create space to grow, pathways for nutrient access and escape of the cells to a new environment. Successful progression also involves cellular responses and evasion of immune surveillance.

Cancer cell adhesion and proliferation. Cancer cells bind to SIBLINGs and their various proteolytic fragments through a variety of integrin receptors by both RGD-dependent and RGD-independent interactions. OPN, and perhaps DMP1, can also interact with specific splice variants of CD44 that are expressed by cancer cells. Interestingly, OPN binding to CD44v6 results in the propagation of cytosolic signals that enhance integrin activation and thus migration (an example of inside-out signalling) in colon HT29 cells[28]. Tumour cells were stimulated to spread following the interaction of CD44 and OPN apparently through β1 integrins, which have well-characterized roles in enabling cell adhesion[29,30]. OPN exhibiting reduced serine/threonine phosphorylation by casein kinase induces the adhesion of human breast cancer cells almost sixfold more than hyperphosphorylated OPN[31], highlighting the possible modifying roles of the many post-translational events on SIBLING functions.

The adhesive properties of the SIBLINGs have also been investigated in the context of bone targeting and recognition by metastasizing cancer cells, and these molecules have been implicated in enhancing the affinity of metastatic cancer cells for bone (discussed in more detail below). Breast cancer cells expressing active αvβ3 integrin adhere to BSP-enriched mineralized bone as well as to recombinant BSP during *in vitro* adhesion and invasion assays[32]. Thus, exogenously added BSP peptides strongly inhibited breast cancer cell adhesion to extracellular bone matrix at micromolar concentrations[33]. Furthermore, multiple myeloma cells adhere to OPN, indicating that the increased stromal expression of OPN that is associated with this disease might be one of the factors enhancing the retention of these cells

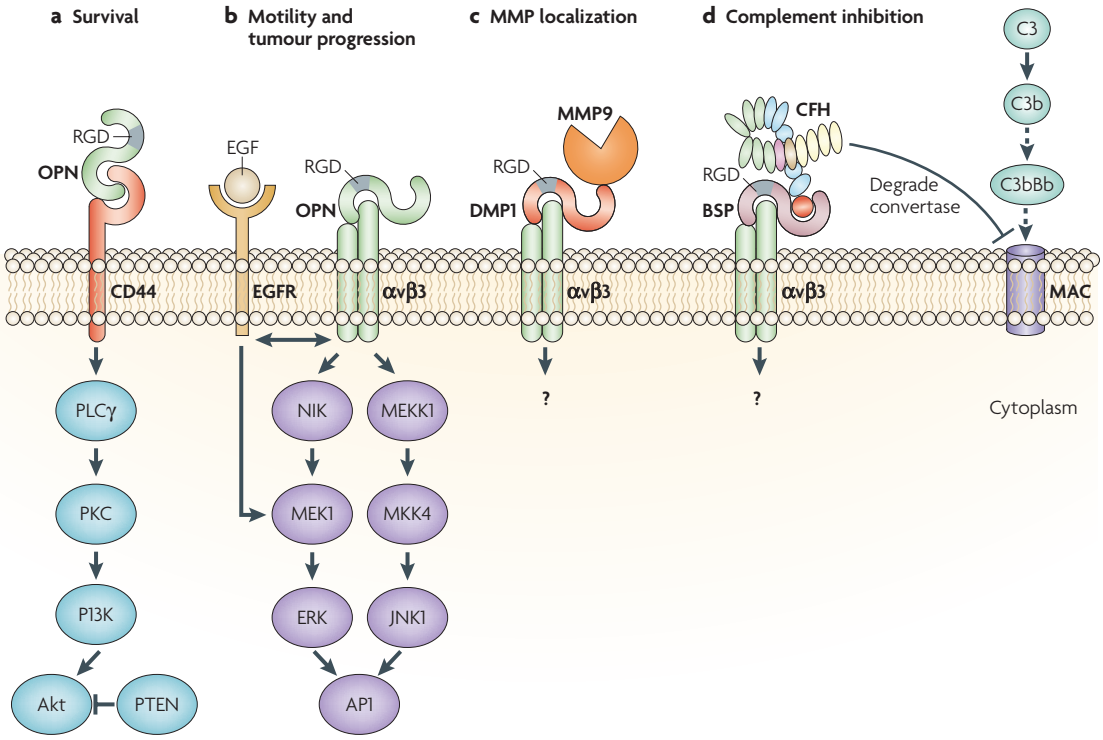

Figure 2 | **SIBLINGs mediate cell–matrix interactions and cellular signalling.** Small integrin-binding ligand N-linked glycoproteins (SIBLINGs; bone sialoprotein (BSP), dentin matrix protein 1 (DMP1) and osteopontin (OPN) are shown) can initiate Arg–Gly–Asp (RGD)-dependent and RGD-independent interactions with several integrins (such as αvβ3 and α9β1, respectively). OPN (and perhaps DMP1) can also interact with the CD44 family of receptors. Some of these complexes are able to mediate the following functions: (**a**) cell survival through phospholipase C-γ (PLCγ)–protein kinase C (PKC)–phosphatidylinositol 3-kinase (PI3K)–Akt pathway activation that leads to anti-apoptotic signals in tumour cells. OPN-induced Akt phosphorylation can be blocked by the tumour suppressor PTEN (phosphatase and tensin homologue). However, *PTEN* is frequently mutated and thus rendered inactive in cancer cells such as melanoma and glioma; (**b**) motility through the activation of the canonical αvβ3 integrin pathway where both nuclear factor-inducing kinase (NIK)–ERK (extracellular signal-related kinase) and MEKK1 (also known as mitogen-activated protein kinase kinase kinase 1 (MAP3K1)–JNK1 (also known as MAPK8) signalling promote cell migration by activating AP1-dependent gene expression (for a review see REF. 178). Upon binding to αvβ3, OPN also stimulates epidermal growth factor receptor (EGFR) transactivation, ERK phosphorylation and AP1 activation; (**c**) bridging of otherwise soluble matrix metalloproteinases (MMPs) to cell membranes and their activation, enabling digestion of local extracellular matrix and thereby aiding tissue remodelling and cell migration through the extracellular matrix, a key step for cancer cell invasion; and (**d**) bridging and activation of complement factor H (CFH) to receptors including αvβ3 integrin. By promoting the degradation of the C3 convertase complex C3bBb, SIBLING-activated CFH disables the formation of the membrane attack complex (MAC) and the subsequent lysis of cancer cells, thus favouring their escape from host immune defence. The ? illustrates that it is not known if all binding of SIBLINGs (with or without ligands) necessarily results in signal transduction. MKK4, MAP kinase kinase 4.

in the bone marrow[34]. Although the RGD domain of DMP1 has been shown to mediate the adhesion and spreading of dental pulp cells *in vitro*[35], no data about DMP1-mediated cancer cell adhesion are available.

SIBLINGs may also affect cancer cell proliferation. BSP accelerates the proliferation of breast cancer cells *in vitro*[6]. Furthermore, *IBSP*-transfected breast cancer cells show increased primary tumour growth following injection into the mammary fat pad of nude mice[36]. OPN stimulates human prostate cancer cell line proliferation when transferred to a mouse xenograft model system[37]. OPN-induced proliferative responses mainly occur through activation of the epidermal growth factor receptor (EGFR)[38] and integrin-mediated intracellular Ca^{2+} signalling[39]. The intracellular signalling pathways operant in OPN modulation of cell proliferation and migration have been well characterized (for a review see REF. 18). The binding of OPN to CD44 promotes cell migration through kinase cascades involving phospholipase Cγ, protein kinase C, phosphatidylinositol 3-kinase (PI3K) and Akt, a serine/threonine kinase that regulates cell cycle progression, growth factor-mediated survival and cell migration (FIG. 2a). The binding of αvβ3 by OPN is associated with SRC kinase-mediated complex formation between αvβ3 and EGFR, which activates the mitogen-activated protein kinase (MAPK) pathway and results in the promotion of tumour growth. The potential effects of SIBLINGs other than BSP and OPN on cell proliferation have not been investigated.

Metabolically passive normal duct
Epithelia, such as that of the lacrimal gland ducts, that do not alter the tonicity of the fluid they process in the course of normal physiology. Tears from the lacrimal acini are isotonic and are secreted unchanged through the duct system.

CD44
A family of cell surface signal-transducing glycoproteins involved in cell–cell interactions, cell adhesion and migration. CD44s bind hyaluronan, a high-molecular-mass polysaccharide found in the extracellular matrix, and a variety of extracellular as well as cell surface ligands. CD44 exists in multiple spliced forms and shows a high variability in glycosylation.

Transglutaminases
A family of enzymes that catalyse the crosslinking of proteins at a glutamine in one chain with lysine in another chain. Although the family members have different structures, they share an active site (Tyr–Gly–Gln–Cys–Trp) and strict Ca^{2+} dependence.

Osteoclast
A cell that breaks down mineralized bone and is responsible for bone resorption.

Dental pulp cells
Cells that comprise the soft tissue forming the inner structure of a tooth and containing nerves and blood vessels as well as possibly dentin stem cells.

Invasion and extracellular matrix degradation. High cancer cell motility combined with increased expression of proteases that degrade the extracellular matrix is generally predictive of invasive capability[40,41]. OPN and BSP are expressed at high levels by numerous cancers and might contribute to their invasive potential. Functional studies using overexpression of OPN in two prostate cancer cell lines reveal that OPN increases invasion and enhances the ability of cancer cells to intravasate into blood vessels in a mouse neoplastic model[37]. OPN also enhances *in vitro* migration of various types of cancer cells including melanoma[42], breast[43], and multiple myeloma[44]. Similarly, transfection of a breast cancer cell line with *IBSP* cDNA stimulated migration and invasion *in vitro*[36].

Invasive cells have the capacity to degrade the extracellular matrix through at least two pathways of controlled proteolysis: the urokinase-type plasminogen activator (uPA, also known as PLAU) pathway and the MMP pathway. Several studies using recombinant OPN show that this SIBLING significantly increases *in vitro* invasiveness. For example, OPN increases the invasiveness of pancreatic cancer cells[45] and non-small cell lung carcinoma cells[46]. Treatment of breast cancer cells with OPN results in higher invasiveness through the basement membrane analogue, Matrigel, and increases both *PLAU* mRNA expression and urokinase activity[47]. In a metastatic murine mammary cancer cell lines model, the binding of OPN to integrin receptors induces MMP2 and uPA expression through integrin-linked kinase (ILK)-dependent AP1 activity[48]. It has recently been shown that OPN induces αvβ3 integrin-mediated AP1 activity and uPA secretion by activating SRC–EGFR–ERK (extracellular signal-regulated kinase) signalling pathways and further demonstrates a functional molecular link between OPN-induced integrin- and SRC-dependent EGFR phosphorylation and ERK- and AP1-mediated uPA secretion, and all of these ultimately control the motility of breast cancer cells[49]. Thus, both increased cell motility and induction of uPA expression are possible mechanisms of increased invasiveness of breast epithelial cells in response to OPN.

Potential mechanisms for SIBLING-enhanced matrix degradation have been described. BSP and OPN induce the activation of MMP2 in GCT23 giant cell tumour cells[50]. OPN binding to αvβ3 is associated with PI3K-mediated NFκB activation and nuclear factor-inducing kinase (NIK, also known as mitogen-activated protein kinase kinase kinase 14 (MAP3K14)) activation of AP1 and NFκB, which stimulate uPA-dependent MMP9 activation[51]. Thus, at least two SIBLINGs can induce MMP expression. Interestingly, NIK-dependent MMP9 activation has been recently implicated in melanoma growth and metastasis to lung[52].

BSP, DMP1 and OPN bind to and modulate the activity of MMP2, MMP9 and MMP3, respectively[53]. SIBLING-mediated MMP activation includes both making the proMMPs enzymatically active to some degree and reactivating MMPs that are inhibited by tissue inhibitors of MMP (TIMPs)[53]. The expression of these three SIBLINGs and their cognate MMPs was correlated in a number of different cancer types[54]. BSP promoted invasion of several osteotropic cancer cell lines *in vitro* by apparently localizing MMP2 to the cell surface through αvβ3 (REF. 55). DMP1 enhanced the invasion potential of a colon cancer cell line by bridging MMP9 to integrins and, perhaps, CD44 (REF. 56). Another mechanism might involve enzymatic processing of SIBLINGs that alters invasion and migration properties. For example, increased hepatocellular carcinoma cell invasion was attributed to OPN peptides cleaved by MMP9 and thrombin[57]. Interestingly, transglutaminase crosslinking of OPN forms proteolysis-resistant inactive OPN polymers that reduced breast cancer cell invasion and migration *in vitro*[58].

Metastasis. Metastasis is a complex process characterized by multiple stages: malignant cells proliferate and spread from the primary tumour mass, invade adjacent capillary or lymphatic vessels, resist immunological attacks and eventually gain access to secondary sites where they proliferate to form a new tumour (for a review see REF. 59). Throughout this multi-step progression, cancer cells interact with extracellular matrix proteins, endothelial cells, platelets, stromal cells and other organ-specific structures. Multifunctional extracellular matrix proteins such as the SIBLINGs are expected to have key roles in metastasis as they affect adhesion, migration and matrix degradation (FIG. 3).

Compelling evidence from cancer cell transfection experiments and mouse xenograft models demonstrate that high-level OPN expression can confer a metastatic phenotype on cells that originally formed benign tumours[60]. Since this initial observation, numerous studies conducted with human biological tissue from various cancer types consistently report that tumours that are likely to progress to more advanced stages present with *de novo* or increased expression of SIBLINGs (TABLE 1). In particular, the correlations observed between high levels of OPN expression in tumour cells and their subsequent metastatic dissemination were supported by gain- and loss-of-function studies demonstrating the pro-metastatic role of OPN (for a review see REF. 61). Thus, the introduction of an OPN expression vector into non-metastatic rat mammary epithelial cells resulted in lung metastasis development in 55% of the inoculated animals that produced primary tumours[60] and the antisense inhibition of OPN inhibited osteolytic metastases of human breast cancer cells[62]. Host-produced OPN also appeared to be of importance for metastasis development, as melanoma cells that do not express OPN showed reduced lung and bone metastases when injected into OPN-deficient mice compared with wild-type mice[63].

High expression of SIBLINGs is associated with osteotropic cancers including breast[64], prostate[65] and lung[66] as well as multiple myeloma[67]. A recent microarray and functional genomic study in an experimental mouse model demonstrated a functional association between OPN, interleukin 11 and either chemokine receptor 4 (CXCR4) or connective tissue growth factor (CTGF)

Osteotropic
Describes tumours that metastasize preferentially to the skeleton.

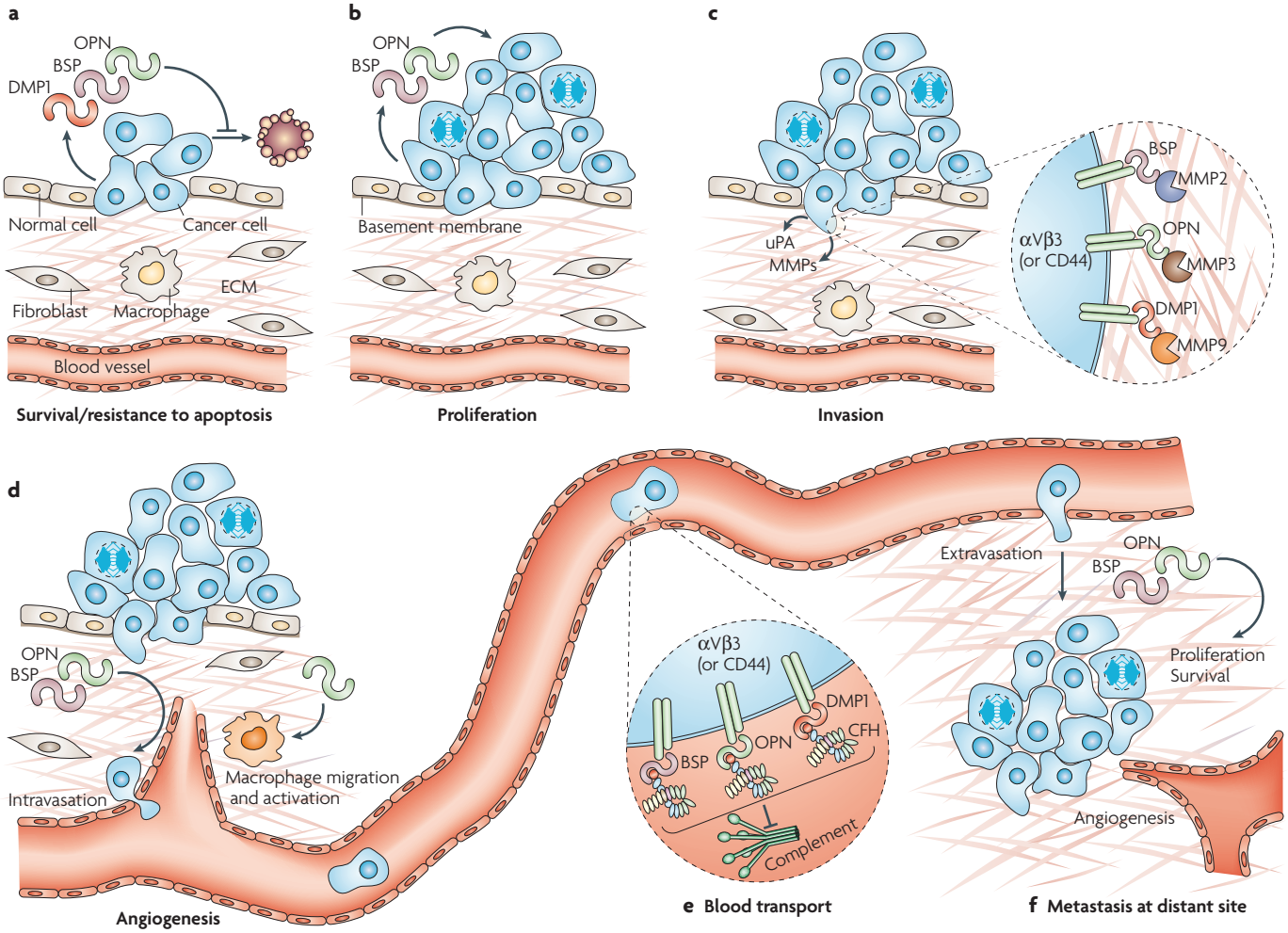

Figure 3 | **The role of SIBLING proteins at different steps of the metastatic cascade. a**, **b** | At the primary site, cancer cells secrete high levels of small integrin-binding ligand, N-linked glycoproteins (SIBLINGs), which favour their proliferation (osteopontin (OPN) and bone sialoprotein (BSP)) and survival (OPN, BSP and dentin matrix protein 1 (DMP1)). **c** | Cancer cells with enhanced adhesive and migratory capabilities can detach from the primary tumour mass and degrade the basement membrane to invade the stroma. The associated proteolysis of the extracellular matrix (ECM) is mediated through matrix metalloproteinases (MMPs) and urokinase plasminogen activator (uPA). OPN enhances uPA activation, cell motility and invasion into the surrounding tissue. The insert shows BSP, DMP1 and OPN bound to their respective receptors (αvβ3 integrins and/or CD44), which may actively promote local proteolysis through binding specific MMPs (MMP2, MMP9 and MMP3, respectively). **d** | As ligands for αvβ3 integrin, OPN and BSP have roles in angiogenesis. The expression of these SIBLINGs by tumour cells promotes the migration and adhesion of activated endothelial cells, which are crucial during angiogenesis. OPN acts as a chemotactic and adhesion molecule for macrophages and promotes their infiltration of the tumour. **e** | The transport of cancer cells in the circulation is one of the limiting steps for metastasis to distant organs because they are confronted by the host immune system. The insert shows that, in this context, the expression and the presentation of BSP, DMP1 and OPN on the cancer cell surface enables them to sequester and activate complement factor H (CFH) and protect themselves from complement-mediated lysis. **f** | At distant site(s), cancer cell extravasation is followed by the formation of a secondary colony. Proliferative, survival and angiogenenic signals by newly formed metastatic colonies occur mainly through mechanisms similar to those that are used during the early steps of tumour progression with tumour-secreted SIBLINGs continuing to act as enhancing factors.

Bone lesions
Lytic lesions are areas of the bone marked by destruction, whereas sclerotic lesions are areas of the bone marked by thickening or hardening. A mixed lytic and sclerotic lesion exhibits facets of both resorption (destruction) and thickening (formation).

in breast cancer cells that favours bone metastasis[68]. Overexpression of BSP also enhanced experimental bone metastasis[69]. The affinity of BSP-expressing cancer cells for bone is emphasized in a study where the transfection of *IBSP* cDNA into a brain-metastasizing breast cancer cell line subclone was sufficient to induce bone metastases, although no bone lesions were observed with the control line[70].

The expression of SIBLINGs by breast and prostate carcinoma prompted the hypothesis that osteotropic cancer cells can become 'bone-like' or express osteomimetic properties that favour 'seeding' in the skeleton by improving their adhesion, proliferation and/or survival in bone. It was shown that during the malignant transformation of prostate epithelium, a switch of gene expression that confers an osteoblastic phenotype (including expression

Table 1 | **SIBLING expression in normal and malignant human tissues as well as correlation with disease progression**

Organ/ tissue	OPN			BSP			DMP1			DSPP		
	Normal*	Tumour‡	Prog'n§	Normal	Tumour	Prog'n	Normal	Tumour	Prog'n	Normal	Tumour	Prog'n
Bladder	Low[164]	High[179]	Yes[180]	ND	High[158]	ND	ND	ND	ND	ND	ND	ND
Bone	High[164]	High[181]	No[181]	High[182]	High[183]	Yes[183]	High[184]	ND	ND	Low[185]	ND	ND
Brain	Low[179]	High[186]	Yes[186]	ND	ND	ND	ND	ND	ND	ND	ND	ND
Breast	Low[164]	High[187]	Yes[188]	Low[64]	High[64]	Yes[135]	Low[121]	High[121]	Yes[121]	ND	ND	ND
Cervix	Low[164]	High[189]	Yes[127]	Low[116]	High[116]	Yes[116]	ND	ND	ND	ND	ND	ND
Colon	Low[164]	High[107]	Yes[190]	Low[54]	High[54]	ND	Low[54]	High[54]	ND	Low[54]	Low[54]	ND
Connective tissue	No[164]	High[191]	ND	ND	ND	ND	ND	ND	ND	ND	ND	ND
Gastric	No[164]	High[192]	Yes[143]	ND	ND	ND	ND	ND	ND	ND	ND	ND
Oral mucosa	No[119]	High[119]	Yes[119]	No[119]	High[119]	No[119]	No[119]	No[119]	No[119]	No[119]	High[119]	Yes[119]
Kidney	High[15,164]	High[193]	Yes[126]	High[15]	ND	ND	High[15]	ND	ND	High[15]	ND	ND
Bone marrow	No[194]	High[195]	ND	ND	ND	ND	ND	ND	ND	ND	ND	ND
Lung	No[164]	High[196]	Yes[133]	Low[54]	High[66]	Yes[136]	Low[54,120]	High[54,120]	ND	Low[54]	High[54]	ND
Lymphocytes	Low[197]	High[106]	Yes[198]	ND	High[67]	ND	ND	ND	ND	ND	ND	ND
Melanocytes	No[199]	High[200]	Yes[200]	ND	High[118]	ND	ND	ND	ND	ND	ND	ND
Oesophagus	ND	High[179]	ND	ND	ND	ND	ND	ND	ND	ND	ND	ND
Ovary	No[164]	High[201]	Yes[125]	Low[54]	Low[66]	ND	ND	ND	ND	ND	ND	ND
Pancreas	No[164]	High[146]	Yes[45]	Low[117]	High[117]	ND	ND	ND	ND	ND	ND	ND
Prostate	No[164]	High[202]	Yes[203]	No[54]	High[65]	Yes[65]	No[54]	ND	ND	Low[2]	High[2]	Yes[2]
Rectum	ND	High[204]	Yes[204]	ND	ND	ND	ND	ND	ND	ND	ND	ND
Thyroid	No[179]	High[132]	ND	No[115]	High[115]	ND	Low[54]	High[54]	ND	ND	ND	ND

*Defines expression of the designated small integrin-binding ligand N-linked glycoprotein (SIBLING) at the protein or mRNA level in normal tissue. ‡Defines expression of the designated SIBLING at the protein or mRNA level in primary malignant lesions. §Defines a positive and significant association between the level of expression of the designated SIBLING in the primary malignant lesions and the subsequent development of distant metastases and/or poor disease survival. Note that the association was negative for dentin matrix acidic phosphoprotein 1 (DMP1) expression in breast cancer and disease progression. BSP, bone sialoprotein; DSPP, dentin sialophosphoprotein; ND, not determined; OPN, osteopontin; Prog'n, progression.

of SIBLINGs) may occur[71]. Indeed, the expression of certain crucial transcription factors that are known to regulate the expression of bone-related genes, such as *RUNX2* and *MSX*, is altered in prostate cancer cells in a way that favours the acquisition of an osteoblast-like profile by these cells (see below for details). The expression of 'bone' proteins by cancer cells does not necessarily target cell metastasis to bone, rather it is more likely that the expression of transcription factors regulating SIBLING genes such as *RUNX2* produces a mesenchymal phenotype that finds in bone a fertile soil for survival. More recently, Notch signalling and ERK activation have been shown to be important for the osteomimetic properties of prostate cancer bone metastatic cell lines[72]. In good agreement with the osteomimicry theory, a parallel between the gene expression profiles of human breast cancer cells with a high propensity to metastasize to bone and differentiating osteoblast cells was revealed[73]. Interestingly, the osteomimicry gene expression profile observed in osteotropic breast cancer cells is comprised not only of SIBLINGs but also of other proteins that are associated with the acquisition of an osteoblastic phenotype, including core-binding factor β (CBFβ, a RUNX co-transcription factor) and the osteoblastic cell–cell adhesion protein cadherin 11 (CDH11)[73].

The known biological activities of OPN and BSP support their role in promoting metastases to the bone, and to other organs. It is likely that future explorations will identify SIBLINGs as essential regulators of the metastatic phenotype. This phenotype is presumably influenced by stromal and inflammatory cells that are closely associated with primary and metastatic tumours. Identifying the specific roles of SIBLINGs in cancer–stroma interactions and signalling cascades involving growth factor–growth factor receptor and cell–matrix interactions could result in the development of additional novel and refined strategies for the prevention and treatment of metastases. Tumour cell survival (at both primary and distant sites) requires successful counter-responses to immune surveillance.

Inflammation and complement evasion. The interplay between inflammation and cancer is currently an area of intense research[74]. Inflammation is part of the innate immune system and can provide an immediate, although non-specific, response. SIBLINGs can have roles in immune cell migration into sites of matrix turnover and

degradation as well as in infection and inflammation. One paradigm for SIBLING function and metabolism within the immune system is that OPN is secreted by activated macrophages, leukocytes and activated T lymphocytes[75–77] and is also a chemotactic cytokine for macrophages[78], dendritic cells[27] and neutrophils[79]. It is possible that OPN expression by tumours actually promotes inflammation-induced cancer growth and progression through, for example, the promotion of macrophage and neutrophil infiltration. Tumour cells that secrete OPN might be propagating chronic inflammation, which can accelerate transformation and tumour progression. OPN might also enhance tumour survival by downregulating macrophage nitric oxide synthase expression and downstream production of nitric oxide[80]. Cytokines can also alter SIBLING levels. Studies have reported that both OPN and DSPP are upregulated by the macrophage inflammatory protein MIP3α (also known as CCL20), a chemokine involved in modulating cell-mediated immunity[81], which is known to promote pancreatic cancer cell migration[82]. The overall action of OPN on the immune system is to regulate the function of macrophage and macrophage-derived cells (that is, osteoclasts). The expression and potential biological activities of the other SIBLINGs in immune cells have not been studied; however, given their adhesive properties and other shared biochemical properties with OPN, it is possible that they have similar as yet undiscovered modulatory roles in inflammation.

Another component of the innate immune response is the complement system, which is composed of about 26 proteins that combine with antibodies and/or cell surface molecules as part of the humoral response. The complement cascade has a role in inflammation, immune adherence, opsonization, viral neutralization, cell lysis and localization of antigen[83]. Nearly all cells are subject to constant low levels of complement attack, but only cells that do not express the correct cell surface proteins, thereby inactivating the early steps of the cascade, are killed. CFH is a major negative regulatory factor that quenches complement-mediated lysis. Cells that become transformed may escape the complement system during their transit through the patient's circulation by upregulating genes that help to control this aspect of immune surveillance. As such, the expression of SIBLINGs (specifically OPN, DMP1 and BSP) by tumour cells might provide such a selective advantage for survival by mediating the binding of CFH to the cell surface through integrins and/or CD44. The activated CFH then inhibits the formation of the membrane attack complex and subsequent cell lysis (FIG. 2d). *In vitro* experiments have demonstrated that these three SIBLINGs can protect murine and human cancer cell lines from attack by complement[84–86].

Angiogenesis. Angiogenesis promotes tumour growth as well as metastatic spread through a complex interplay of positive and negative mediators of extracellular matrix degradation and endothelial cell and vasculature recruitment. There is evidence that αvβ3 is a key angiogenesis-associated receptor that is significantly upregulated on the surface of activated endothelial cells[87]. OPN and BSP have been shown to act as pro-angiogenic factors and, based on their RGD motifs, it is likely that the other SIBLINGs may also interact with αvβ3 integrin and influence the behaviour of endothelial cells. OPN contributes to the genesis of new capillaries infiltrating the cancer lesion in several *in vivo* models[88,89]. BSP also promotes angiogenesis in the chicken chorioallantoic membrane assay through binding αvβ3 (REF. 90).

The integrin αvβ3 mediates the migration of activated endothelial cells during vessel formation. SIBLINGs, as ligands for αvβ3 through the RGD sequence, may stimulate endothelial cell migration. It is also possible that SIBLING modulation of protease activity (uPA or MMP) generates bioactive fragments of extracellular matrix components responsible for angiogenesis. Experimental evidence suggests that antagonizing the ligation of SIBLINGs to integrins is a promising approach for the inhibition of angiogenesis and associated tumour growth. For example, blocking the interaction between OPN and αvβ3 inhibits angiogenesis and stops lung cancer growth in mice[88]. The αvβ3 integrin was shown to be important for OPN-mediated NFκB induction and survival, as adding a neutralizing anti-β3 integrin antibody blocked NFκB activity and induced endothelial cell death when cells were plated on OPN[26]. A recent study demonstrates that OPN triggers vascular endothelial growth factor-dependent breast tumour growth and angiogenesis by autocrine and paracrine mechanisms[91]. Thus, it is possible that, through their interaction with αvβ3, the SIBLINGs may also cooperate with molecules that have important biological functions during angiogenesis and tumoural growth processes, including MMPs, growth factors and their receptors.

Microcalcification. All SIBLINGs are expressed by bones and teeth, and it was originally thought that they acted to directly regulate hydroxyapatite crystal formation[92]. Outside of the skeletal system, pathological dystrophic calcification associated with the upregulation of OPN and/or BSP has been observed. Notable among these are atherosclerotic vascular plaques, renal osteodystrophy and kidney stones[93]. Because of their earlier association with mineralization in bone, the expression of BSP and OPN has been studied in cancers such as breast and thyroid carcinomas, in which ectopic calcification occurs[64,94,95]. Although calcifications are usually associated with benign lesions, certain patterns of calcification — such as tight clusters with irregular shapes — may indicate the presence of a premalignant tumour. Tumours from the primary sites of bone-seeking cancers frequently contain foci of dystrophic calcifications in the form of hydroxyapatite microcalcifications. The cause(s) of these ectopic calcifications are ill-defined and the exact role of the SIBLINGs in the formation of such calcifications is not known. Although it was initially thought that mineral deposition might occur because of the increased local concentration of SIBLINGs (which have well-described characteristics of nucleators of mineralization) it has also been reported that OPN actually blocks ectopic calcification[96]. It is also possible that SIBLING association with ectopic calcification primarily controls and diminishes the immune and inflammatory response that is provoked by inappropriate crystal deposition.

Opsonization
The process whereby opsonins (antibodies or complement proteins) make an invading cell or microorganism more susceptible to phagocytosis by binding to its surface.

Chicken chorioallantoic membrane assay
A biological assay using the well-vascularized chorioallantoic membrane of the chicken egg to evaluate the biological activity of pro- and anti-angiogenic factors.

Renal osteodystrophy
A bone disease characterized by softening and fibrous degeneration of bone and the formation of cysts in bone tissue, caused by chronic renal failure.

Box 1 | **Expression and distribution of SIBLINGs in normal tissues**

With the exception of osteopontin (OPN), which was independently discovered in several tissues, the distribution of the small integrin-binding ligand N-linked glycoprotein (SIBLING) family in normal tissues was originally believed to be limited to bones and teeth[92]. In these calcified tissues, the presumed function of the family was a role in the biomineralization of matrix and a number of published *in vitro* studies do support such a role (for a review see REF. 159). With one exception, the dentin of dentin sialophosphoprotein (*Dspp*)-null mice[160], all of the SIBLING gene knockout mouse models have little if any significant change in basic matrix mineralization. Early reports indicated that OPN is also a component of human breast milk[161], and is expressed in chronic inflammatory cells[162] and kidney[163], as well as some other epithelia[164]. Terasawa *et al.*[165] reported the expression of dentin matrix protein 1 (DMP1) in several mouse soft tissues including liver, muscle, brain, pancreas and kidney. Matrix extracellular phosphoglycoprotein (MEPE) was originally discovered in tumours causing osteomalacia and was shown at that time to be expressed (mRNA only) predominantly in bone and brain with "very low levels of expression" in lung, kidney and placenta[122]. Recent studies have demonstrated that all five members of the SIBLING family are expressed in metabolically active ductal epithelial cells of the salivary gland and kidney[14,15] and all but MEPE were expressed in eccrine sweat ducts[16]. MEPE expression appears to be limited to ductal cells that actively transport phosphate[16]. The role of the SIBLINGs in normal soft tissues is now a subject of intense investigation. SIBLINGs expression can also be transcriptionally regulated (see table). BSP, bone sialoprotein; DLX5, distal-less homeobox 5; FRE, fibroblast growth factor response element; HDAC3, histone deacetylase 3; HOX, homeobox; PPARγ, peroxisome proliferator-activated receptor γ.

	OPN	BSP	DMP1	DSPP
Activators of transcription	RUNX2–Vitamin D receptor[166] AP1 (REF. 167)	RUNX2–DLX5 (REF. 168) RUNX2–HOXA10 (REF. 169) FRE- and HOX-binding proteins[170]	RUNX2 (REF. 171) AP1–SP1–ETS[172]	RUNX2 (REF. 101) CCAAT-binding factor[173]
Repressors of transcription	PPARγ[174]	RUNX2 (REF. 99) RUNX2–HDAC3 (REF. 175)	Unknown	Novel transcription repressor[173] TWIST1 (REF. 176)

Nevertheless, SIBLING-expressing tumours are more readily detectable clinically at early stages, on the basis of associated abnormal mammographic calcifications. Most of the breast calcifications detected at mammography are benign. Radiologists must be able to identify typically benign breast calcifications that do not require biopsy to prevent unnecessary procedures and to reduce patient anxiety. It will be interesting to determine whether the high expression of SIBLINGs that is associated with the detection of suspicious microcalcifications will help to identify lesions that are likely to evolve towards malignancy. The expression of SIBLINGs in premalignant lesions has not yet been investigated and is an interesting field of investigation to fully understand the role of these proteins during cancer progression.

Regulation of SIBLING genes in cancer cells

The promoter regions of *SPP1*, *IBSP*, *DMP1* and *DSPP* have been cloned in different species and they exhibit a number of consensus regulatory sequences, such as potential binding sites for AP1 and NFκB transcription factors. Regulation of SIBLING genes has been best studied in the context of osteoblastic and odontoblastic cell differentiation (BOX 1). RUNX2, a member of the RUNX transcription factor family, is a transcription factor that is crucial for the regulation of genes that support bone formation[97] and as such it is involved in the control of OPN[98], BSP[99], DMP1 (REF. 100) and DSPP[101] expression. All the RUNX proteins are intimately associated with tumour progression, invasion and metastasis[102]. Notably, RUNX2 is aberrantly expressed at high levels in breast and prostate tumours and cells that metastasize to the bone[103]. Interestingly, RUNX2 also transactivates *SPP1* (REF. 104) and *IBSP*[105] in breast cancer cells, suggesting that the expression of SIBLINGs might be subject to the same regulation both in normal osteoblasts and in cancer cells. Human myeloma cells with active RUNX2 protein produce OPN that is involved in the pathophysiology of multiple myeloma-induced angiogenesis[106]. In colorectal cancer, gene-profiling studies identified a positive correlation between metastatic colon tumours and increased OPN expression[107]. More recently, RUNX2 and ETS1 were identified as crucial transcriptional regulators of OPN expression in a murine colorectal cancer cell line and their suppression using antisense oligonucleotides resulted in significant downregulation of OPN[108]. Several additional signalling pathways and transcription factors that are associated with cancer progression regulate OPN expression in models of breast cancer, melanoma and leukaemia (for reviews see REFS 4,61). These include AP1, MYC, OCT1 (also known as POU2F1), upstream stimulating factor (USF), v-Src, transforming growth factor β (TGFβ)–BMP–SMAD–HOX (homeobox), WNT–β catenin–adenomatous polyposis coli (APC)– glycogen synthase kinase 3 (GSK3)–transcription factor 4 (TCF4), Ras–Ras response factor (RRF) and p53. The global picture of OPN gene transcriptional regulation in cancer cells is that of an intricate regulatory network. Studies of the proximal promoter regions of other SIBLING genes are needed to identify regulatory elements that could be responsible for their overexpression in cancer.

Consistent with its role in tumour initiation and progression, *SPP1* expression is also repressed by tumour suppressors such as BRCA1 and phosphatase and tensin homologue (PTEN), and metastasis suppressors such as breast cancer metastasis suppressor 1 (BRMS1). BRCA1 expression inhibits *SPP1* promoter transactivation and

Eccrine sweat ducts
These ducts transport sweat to the surface of the skin and are involved in evaporative cooling.

hence suppresses OPN expression[109]. A *BRCA1* mutation in human primary breast cancer lesions is associated with OPN overexpression, suggesting that it may confer increased tissue-specific cancer risk, in part, by disruption of the suppression of *OPN* transcription by BRCA1 (REF. 109). The tumour suppressor PTEN antagonizes PI3K, which is responsible for promoting cell growth, survival and tumorigenesis, when over-stimulated in cancer cells. OPN was shown to act downstream of the PI3K pathway in melanoma and glioma cancer cells. A link has been found between OPN expression at both the mRNA and protein level that involves PI3K activation of OPN and may help explain how PTEN loss contributes to the development of these malignancies[110,111]. By contrast, BRMS1 inhibits OPN expression through the inactivation of NFκB and subsequent binding to the *SPP1* promoter. Thus, downregulation of OPN might be one of the mechanisms of metastasis suppression by BRMS1 (REF. 112).

SIBLINGs as prognostic indicators in cancer

The first SIBLING found to be overexpressed in cancer was OPN[113,114]. Since then, large numbers of studies have established that increased expression of OPN is a consistent feature for most known human malignancies (TABLE 1). Increased expression of BSP was originally observed in human breast cancer[64] and its putative role in the acquisition of an osteotropic phenotype by metastatic cancer cells soon led to the extension of this observation to other bone-seeking cancers such as prostate[65], lung[66], thyroid[115] and cervical carcinoma[116], as well as multiple myeloma[67] (TABLE 1). Recently, BSP was detected in pancreas[117], skin[118] and oral[119] carcinomas, a group of neoplastic lesions that are not particularly osteotropic when they metastasize. These observations suggest that, as is the case for OPN, BSP expression in cancer cells is not restricted to cancer cells metastasizing to bone but is a common feature of the malignant phenotype. The expression profile in cancer of the three other SIBLINGs — DMP1, DSPP and MEPE — has not been evaluated in detail to date, but data indicate that DMP1 and DSPP are upregulated in several human malignancies[54]. Immunohistochemical studies demonstrated increased expression of DSPP in human prostate[2] and oral[119] cancers, and high levels of DMP1 were observed in human lung[120] and breast[121] cancers. It is expected — based on the detection of *DMP1* and *DSPP* in a variety of human malignancies compared with their normal corresponding tissues on a mRNA–cDNA array[54] — that future studies will verify high expression of these proteins as a consistent feature of most human cancers (TABLE 1). By contrast, MEPE expression seems to be much more restricted than that of the other SIBLINGs, so far being found to be expressed in normal cells associated with phosphate transport[16]. Interestingly, only tumours that result in oncogenic hypophosphataemic osteomalacia appear to express MEPE[122]. Screening of *MEPE* expression at the mRNA level in a collection of human normal and cancer tissues revealed minimal expression in all tissues analysed[54]. This observation suggests that MEPE, unlike other SIBLINGs, does not intervene during cancer progression. The reasons for this are still unclear.

Enhanced expression of SIBLINGs is not only associated with several tumour types, but their levels of expression are also often directly correlated to specific stages of clinical progression. Gene expression analyses have identified *SPP1* to be among the most strongly upregulated genes in human colon cancer[123]. In this study, OPN expression was shown to be an independent prognostic marker for poor overall survival. These observations were supported by a recent study that found that colon cancer patients with tumours expressing high levels of OPN have significantly reduced survival[124]. In another study, OPN was shown to be a predictor of outcome that was independent of clinical characteristics (such as age, lesion size and histological type) in ovarian carcinoma. The prognosis for survival within 36 months was <5% for patients with increased OPN and 75% for those with no OPN increase[125]. Clear cell renal carcinoma patients with OPN-positive tumours also exhibited worse prognosis than patients who had tumours lacking OPN[126]. The prognosis for patients with increased OPN in cervical cancers is also extremely poor, as none survived within 24 months, compared with the 67% survival rate observed within the same time period for patients with no OPN increase[127]. Other cancers with a positive correlation between OPN expression and poor prognosis are breast[128], prostate[129], head and neck[130,131], thyroid[132], non-small cell lung[133] and hepatocellular[134] carcinomas (TABLE 1).

Increased BSP expression in primary breast[135] and prostate[65] carcinoma is also associated with tumour progression. In non-small cell lung carcinoma, BSP expression is associated with bone metastasis development and could be useful in identifying high-risk patients who could benefit from novel modalities of surveillance and preventive treatment[136]. Expression of other SIBLINGs might also correlate with tumour progression. DSPP expression correlates with aggressiveness in human prostate cancers[2] and in oral cancer[119]. Unique among the SIBLINGs, DMP1 expression was inversely associated with progression in human breast cancer[121]. The positive prognostic value of DMP1 for breast cancer patients has only been reported in one study and awaits confirmation. Small interfering RNA (siRNA)-mediated repression of DMP1 enhances migration of human breast cancer cells *in vitro*[121]. Thus, it can be speculated that the expression of DMP1 alters cancer cell motility and hence reduces local invasion and metastatic spreading. This effect could be achieved through a competition of DMP1 with BSP and/or OPN for their binding to the cell membrane integrin receptors and the subsequent activation of their corresponding MMP partner. Such putative mechanisms urge investigations of whether modulation of SIBLING expression might differentially affect cancer cell behaviour.

SIBLINGs can also be detected in the blood, and it is therefore not surprising that several studies have established a correlation between blood levels of OPN and BSP and the presence of a malignant tumour. However, the high affinity interaction of CFH with several SIBLINGs, including OPN and BSP[84], masks all known antibody-binding sites and therefore interferes with accurate direct measurement of these proteins in the serum[137]. Interestingly, this masking implies that the biological

Oncogenic hypophosphataemic osteomalacia
Osteomalacia (softening of the bones) resulting from renal phosphate wasting and low serum 1,25-dihydroxy vitamin D secondary to the presence of a tumour of which complete resection results in rapid resolution of the symptoms and signs.

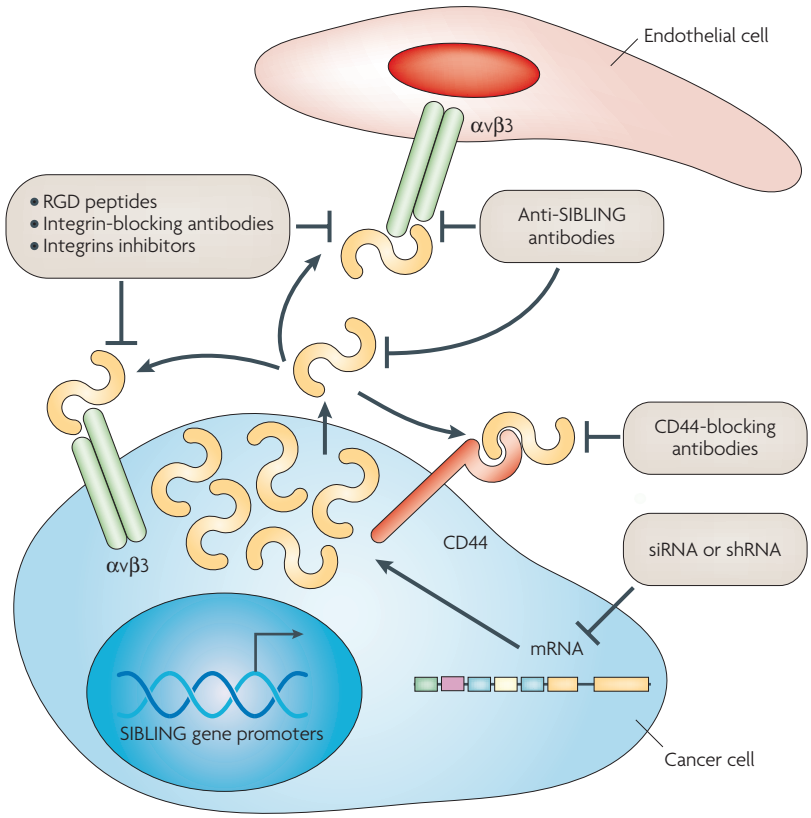

Figure 4 | **SIBLINGs and their cell receptors are potential therapeutic targets for cancer therapy.** Suppression of the expression of small integrin-binding ligand N-linked glycoproteins (SIBLINGs) in cancer cells at the level of mRNA can be accomplished through RNA interference by the use of specific small interfering RNAs (siRNAs) or short hairpin RNAs (shRNAs). Blocking of tumour-derived SIBLINGs at the protein level by specific blocking peptides and antibodies reduces tumour progression and metastatic dissemination because it affects interactions of SIBLINGs with their receptors on the cancer cell surface. This might result in the dysfunction of signalling pathways that affect tumour cell proliferation and survival. Because SIBLINGs exert their effects principally through integrins and CD44, antibody-mediated interference with these receptor–ligand interactions or suppression of associated signal transduction events are other potential means to restrain tumour progression. Inhibition of the binding of SIBLINGs to endothelial cell surface integrin receptors triggers endothelial cell apoptosis and can thereby decrease tumour-associated angiogenesis.

activities of OPN and BSP might be limited to autocrine and/or paracrine effects as the abundant (0.5 mg/ml in blood) complement protein will quickly bind and inactivate them as they diffuse away from their sites of secretion and action. OPN, however, is interesting because 5–10% of the total amount of this SIBLING in the blood escapes the masking by CFH by mechanisms that are currently unknown. Through careful preparation of plasma, this fraction of OPN has been successfully used in many studies, as mentioned below, but when serum is analysed this fraction is masked by CFH. One confounding factor for the use of blood OPN levels is that inflammation also increases OPN levels[138]. In patients with bone metastases, increased plasma (not serum) levels of OPN have been suggested to be the result of both cancer cell secretion and accelerated bone turnover[34]. Similar to increased expression in tumour cells themselves, increased OPN plasma levels appears to be a marker for metastatic progression and poor survival in patients with breast[139], prostate[140], renal cell[141], lung[142], gastric[143], head and neck[144], hepatocellular[145], cervical[127] and pancreatic cancers[146]. Serum BSP (after disruption of the SIBLING–CFH complex) is significantly increased in patients with colon, breast, prostate and lung cancer[137]. BSP blood level also predicts bone metastasis development in patients with breast cancer[147]; predicts tumour burden, neoplastic bone involvement and prognosis in multiple myeloma[148]; and is an independent prognostic factor for human prostate cancer-related death[149]. No data on the blood levels of DMP1, DSPP or MEPE in human malignancies are available. Although detection of increased blood levels of OPN and BSP bear obvious diagnostic and prognostic value, such tests are not yet available to clinicians.

SIBLINGs as therapeutic targets

Because of the plausible roles of SIBLINGs in cancer as pro-oncogenic, pro-metastatic and pro-angiogenic molecules, these proteins also have the potential to be valuable targets for cancer therapy (FIG. 4).

Several studies have already demonstrated the value of OPN and BSP as therapeutic targets in preclinical animal models. Silencing these SIBLINGs using siRNA and short hairpin RNA (shRNA) technology, or interfering with their activities using specific antibodies, inhibits or reduces tumour progression and the development of metastases. Decreasing expression of OPN in human squamous oesophagus carcinoma using shRNA reduces tumour growth and lymph node metastases *in vivo*[150]. Similar experiments performed on murine colon cancer cells led to the inhibition of tumour growth and the formation of liver metastases[151]. Silencing of OPN or BSP using specific antisense oligonucleotides in a human breast cancer cell line resulted in a significant decrease of osteolytic bone metastases in nude rats[62]. Although the use of RNA interference for therapy is attractive, much work remains before such therapeutics become available to patients[152].

Antibody-based anticancer therapies, such as antibodies directed against vascular endothelial growth factor, have recently met with clinical success and are now becoming available to cancer patients[153]. Antibodies directed against OPN were effective in inhibiting development of lung metastases in nude mice inoculated with human hepatocellular carcinoma cells. In this case, OPN, which has been identified as a major gene in the signature for hepatocellular carcinoma, acts as both a diagnostic marker and therapeutic target for metastatic dissemination[154]. Anti-BSP antibodies also have therapeutic potential particularly for the prevention and treatment of breast cancer bone metastases, as suggested by the significant reduction of osteolytic lesion size in a nude rat model of human breast cancer bone metastases[155].

Both integrins and CD44 have well-established roles in tumour progression. Therefore, interfering with these receptor–ligand interactions by controlling receptor cell surface expression, blocking receptor–ligand binding or suppressing associated signal transduction are promising ways to block both tumour development and metastatic dissemination (FIG. 4). CD44 has been targeted by diverse therapeutic strategies, including cytotoxic

and immunotherapeutic approaches[156]. Because of its involvement in many processes that accompany tumour development and metastatic dissemination of cancers, αvβ3 integrin has long been a candidate target for cancer therapy by specific antibodies, peptide inhibitors and non-peptide antagonists that mimic the binding domain of physiological ligands[156,157]. Proof of principle that such strategies block angiogenesis, as well as tumour growth and dissemination, has been obtained in several animal models and small molecule inhibitors of this receptor are under study as drug candidates.

Finally, the ectopic expression of BSP in osteotropic neoplasms recently inspired a gene therapy protocol in bladder cancer using a conditional-replicating adenovirus. A truncated *IBSP* promoter controlling the E1A/B lytic-regulating sequence was used to construct the adenovirus AD-BSP-E1A. This virus had lytic activity on human bladder cancer cell lines and significantly reduced the size of bladder tumours in an orthotopic mouse model, opening a promising new strategy for the treatment of aggressive yet sensitive bladder tumours[158].

From the results so far, one can speculate that SIBLINGs (particularly OPN and BSP) are viable targets that seem likely to form the basis of new anticancer therapies in the future.

Conclusions and future directions

The aim of this Review is to present an overview of some of the data that implicate the SIBLING family at several steps of cancer development and progression. Although OPN is the family member for which there is the most abundant and convincing data of its role as a key player at most of the critical steps in the evolution of malignancies, studies have revealed that BSP holds the same multifunctional role in cancer biology. Such activities are expected to be associated with DSPP and DMP1 also.

Much remains to be learned about the involvement of SIBLINGs in cancer progression, and we hope this Review will inspire cancer researchers to look more closely at this family. Future investigations should validate the use of SIBLINGs as prognostic markers in large population studies, determine their value as surrogate markers for the prediction of metastases in cancer patients and explore their potential as predictive indicators of the patient response to a given therapy (chemotherapy and/or radiotherapy). Studies are also needed to test the potential value of SIBLINGs as markers for the difficult diagnosis of precancerous lesions such as those found in breast, prostate, colon and oral tumours. Refining our knowledge of the mechanisms involved in how SIBLINGs modulate MMPs (in the absence and/or presence of natural or synthetic MMP inhibitors) could lead to the development of potential biomimetics for use in interventions. It is also of interest to determine the biological relevance of the interactions between SIBLINGs and CFH. For therapeutic strategies, the potential synergy of the combined repression of two or more SIBLINGs should also be tested.

SIBLINGs have the biological plausibility to have active roles in tumour cell adhesion, proliferation, invasion, matrix degradation, immune functions (inflammation and complement evasion), angiogenesis and metastasis. Based on the data accumulated so far, it is tempting to speculate that one of the major roles for SIBLINGs and their proteolytic fragments is to orchestrate, in the near proximity of cancer cells, a dynamically changing microenvironment that supports the key local steps that need to be temporally and spatially coordinated for successful invasion. These include adhesion through interactions with specific integrins, matrix degradation through localization and perhaps activation of MMPs, and migration through activation of selective signalling pathways. Such multifunctional activities are possible thanks to the abilities of SIBLINGs to bind multiple proteins. It is also likely that SIBLINGs are crucial for tumour growth and metastasis because they may participate in angiogenesis. The possible collaboration and/or competition between SIBLINGs during these processes remain to be elucidated by future research. Although acquisition of new data is crucial, the results to date make a case for the future of SIBLINGs as prominent molecular tools for diagnostic, prognostic and therapeutic applications in cancer.

1. Fisher, L. W., Torchia, D. A., Fohr, B., Young, M. F. & Fedarko, N. S. Flexible structures of SIBLING proteins, bone sialoprotein, and osteopontin. *Biochem. Biophys. Res. Commun.* **280**, 460–465 (2001).
Like many other proteins that have multiple binding partners, BSP and OPN are shown by NMR to be unstructured and flexible in solution. The SIBLING family is first defined here based on common exon and intron elements.
2. Chaplet, M. *et al.* Expression of dentin sialophosphoprotein in human prostate cancer and its correlation with tumor aggressiveness. *Int. J. Cancer* **118**, 850–856 (2006).
3. Chen, J. *et al.* Bone sialoprotein promotes tumor cell migration in both *in vitro* and *in vivo* models. *Connect. Tissue Res.* **44** (Suppl. 1), 279–284 (2003).
4. El-Tanani, M. K. *et al.* The regulation and role of osteopontin in malignant transformation and cancer. *Cytokine Growth Factor Rev.* **17**, 463–474 (2006).
This is a detailed overview of OPN-mediated cell signalling in relation to cancer progression.
5. Furger, K. A., Menon, R. K., Tuck, A. B., Bramwell, V. H. & Chambers, A. F. The functional and clinical roles of osteopontin in cancer and metastasis. *Curr. Mol. Med.* **1**, 621–632 (2001).
6. Sung, V., Stubbs, J. T. 3rd, Fisher, L., Aaron, A. D. & Thompson, E. W. Bone sialoprotein supports breast cancer cell adhesion proliferation and migration through differential usage of the αvβ3 and αvβ5 integrins. *J. Cell Physiol.* **176**, 482–494 (1998).
7. Tatusova, T. A. & Madden, T. L. BLAST 2 Sequences, a new tool for comparing protein and nucleotide sequences. *FEMS Microbiol Lett.* **174**, 247–250 (1999).
8. Fisher, L. W., Whitson, S. W., Avioli, L. V. & Termine, J. D. Matrix sialoprotein of developing bone. *J. Biol. Chem.* **258**, 12723–12727 (1983).
9. George, A., Sabsay, B., Simonian, P. A. & Veis, A. Characterization of a novel dentin matrix acidic phosphoprotein. Implications for induction of biomineralization. *J. Biol. Chem.* **268**, 12624–12630 (1993).
10. Feng, J. Q. *et al.* Genomic organization, chromosomal mapping, and promoter analysis of the mouse dentin sialophosphoprotein (Dspp) gene, which codes for both dentin sialoprotein and dentin phosphoprotein. *J. Biol. Chem.* **273**, 9457–9464 (1998).
11. Oldberg, A., Franzen, A. & Heinegard, D. Cloning and sequence analysis of rat bone sialoprotein (osteopontin) cDNA reveals an Arg–Gly–Asp cell-binding sequence. *Proc. Natl Acad. Sci. USA* **83**, 8819–8823 (1986).
12. Hunter, G. K., Hauschka, P. V., Poole, A. R., Rosenberg, L. C. & Goldberg, H. A. Nucleation and inhibition of hydroxyapatite formation by mineralized tissue proteins. *Biochem. J.* **317**, 59–64 (1996).
13. Bellahcene, A. & Castronovo, V. Expression of bone matrix proteins in human breast cancer: potential roles in microcalcification formation and in the genesis of bone metastases. *Bull. Cancer* **84**, 17–24 (1997).
14. Ogbureke, K. U. & Fisher, L. W. Expression of SIBLINGs and their partner MMPs in salivary glands. *J. Dent Res.* **83**, 664–670 (2004).
15. Ogbureke, K. U. & Fisher, L. W. Renal expression of SIBLING proteins and their partner matrix metalloproteinases (MMPs). *Kidney Int.* **68**, 155–166 (2005).
16. Ogbureke, K. U. & Fisher, L. W. SIBLING expression patterns in duct epithelia reflect the degree of metabolic activity. *J. Histochem. Cytochem.* **55**, 403–409 (2007).
17. Furger, K. A. *et al.* β3 integrin expression increases breast carcinoma cell responsiveness to the malignancy-enhancing effects of osteopontin. *Mol. Cancer Res.* **1**, 810–819 (2003).
18. Rangaswami, H., Bulbule, A. & Kundu, G. C. Osteopontin: role in cell signaling and cancer progression. *Trends Cell Biol.* **16**, 79–87 (2006).

19. Teramoto, H. *et al.* Autocrine activation of an osteopontin-CD44–Rac pathway enhances invasion and transformation by H-RasV12. *Oncogene* **24**, 489–501 (2005).
20. Agnihotri, R. *et al.* Osteopontin, a novel substrate for matrix metalloproteinase-3 (stromelysin-1) and matrix metalloproteinase-7 (matrilysin). *J. Biol. Chem.* **276**, 28261–28267 (2001).
21. Prince, C. W., Dickie, D. & Krumdieck, C. L. Osteopontin, a substrate for transglutaminase and factor XIII activity. *Biochem. Biophys. Res. Commun.* **177**, 1205–1210 (1991).
22. Higashikawa, F., Eboshida, A. & Yokosaki, Y. Enhanced biological activity of polymeric osteopontin. *FEBS Lett.* **581**, 2697–2701 (2007).
23. Valverde, P., Tu, Q. & Chen, J. BSP and RANKL induce osteoclastogenesis and bone resorption synergistically. *J. Bone Miner. Res.* **20**, 1669–1679 (2005).
24. Hur, E. M. *et al.* Osteopontin-induced relapse and progression of autoimmune brain disease through enhanced survival of activated T cells. *Nat. Immunol.* **8**, 74–83 (2007).
25. Iczkiewicz, J., Jackson, M. J., Smith, L. A., Rose, S. & Jenner, P. Osteopontin expression in substantia nigra in MPTP-treated primates and in Parkinson's disease. *Brain Res.* **1118**, 239–250 (2006).
26. Rice, J., Courter, D. L., Giachelli, C. M. & Scatena, M. Molecular mediators of αvβ3-induced endothelial cell survival. *J. Vasc Res.* **43**, 422–436 (2006).
27. Kawamura, K. *et al.* Differentiation, maturation, and survival of dendritic cells by osteopontin regulation. *Clin. Diagn. Lab. Immunol.* **12**, 206–212 (2005).
28. Lee, J. L. *et al.* Osteopontin promotes integrin activation through outside-in and inside-out mechanisms: OPN–CD44V interaction enhances survival in gastrointestinal cancer cells. *Cancer Res.* **67**, 2089–2097 (2007).
29. Brakebusch, C., Hirsch, E., Potocnik, A. & Fassler, R. Genetic analysis of β1 integrin function: confirmed, new and revised roles for a crucial family of cell adhesion molecules. *J. Cell Sci.* **110**, 2895–2904 (1997).
30. Katagiri, Y. U. *et al.* CD44 variants but not CD44s cooperate with β1-containing integrins to permit cells to bind to osteopontin independently of arginine–glycine–aspartic acid, thereby stimulating cell motility and chemotaxis. *Cancer Res.* **59**, 219–226 (1999).
31. Christensen, B. *et al.* Cell type-specific post-translational modifications of mouse osteopontin are associated with different adhesive properties. *J. Biol. Chem.* **282**, 19463–19472 (2007).
32. Pecheur, I. *et al.* Integrin αvβ3 expression confers on tumor cells a greater propensity to metastasize to bone. *FASEB J.* **16**, 1266–1268 (2002).
33. van der Pluijm, G. *et al.* Bone sialoprotein peptides are potent inhibitors of breast cancer cell adhesion to bone. *Cancer Res.* **56**, 1948–1955 (1996).
34. Standal, T. *et al.* Osteopontin is an adhesive factor for myeloma cells and is found in increased levels in plasma from patients with multiple myeloma. *Haematologica* **89**, 174–182 (2004).
35. Kulkarni, G. V., Chen, B., Malone, J. P., Narayanan, A. S. & George, A. Promotion of selective cell attachment by the RGD sequence in dentine matrix protein 1. *Arch. Oral Biol.* **45**, 475–484 (2000).
36. Sharp, J. A., Waltham, M., Williams, E. D., Henderson, M. A. & Thompson, E. W. Transfection of MDA-MB-231 human breast carcinoma cells with bone sialoprotein (BSP) stimulates migration and invasion *in vitro* and growth of primary and secondary tumors in nude mice. *Clin. Exp. Metastasis* **21**, 19–29 (2004).
37. Khodavirdi, A. C. *et al.* Increased expression of osteopontin contributes to the progression of prostate cancer. *Cancer Res.* **66**, 883–888 (2006).
38. Angelucci, A. *et al.* Osteopontin enhances the cell proliferation induced by the epidermal growth factor in human prostate cancer cells. *Prostate* **59**, 157–166 (2004).
39. Lecrone, V., Li, W., Devoll, R. E., Logothetis, C. & Farach-Carson, M. C. Calcium signals in prostate cancer cells: specific activation by bone-matrix proteins. *Cell Calcium* **27**, 35–42 (2000).
40. Bell, W. R. The fibrinolytic system in neoplasia. *Semin. Thromb. Hemost* **22**, 459–478 (1996).
41. Price, J. T. & Thompson, E. W. Mechanisms of tumour invasion and metastasis: emerging targets for therapy. *Expert Opin. Ther. Targets.* **6**, 217–233 (2002).
42. Hayashi, C. *et al.* Serum osteopontin, an enhancer of tumor metastasis to bone, promotes B16 melanoma cell migration. *J. Cell Biochem.* **101**, 979–986 (2007).
43. Khan, S. A. *et al.* Enhanced cell surface CD44 variant (v6, v9) expression by osteopontin in breast cancer epithelial cells facilitates tumor cell migration: novel post-transcriptional, post-translational regulation. *Clin. Exp. Metastasis* **22**, 663–673 (2005).
44. Caers, J. *et al.* The involvement of osteopontin and its receptors in multiple myeloma cell survival, migration and invasion in the murine 5T33MM model. *Br. J. Haematol.* **132**, 469–477 (2006).
This paper describes possible roles of OPN interactions with integrins and CD44 variants in survival, increasing cell proliferation, inhibiting apoptosis and promoting cell migration, as well as metalloproteinase activity in multiple myeloma cells. It used blocking antibodies (against CD44 and/or αvβ3) to block migration.
45. Kolb, A. *et al.* Osteopontin influences the invasiveness of pancreatic cancer cells and is increased in neoplastic and inflammatory conditions. *Cancer Biol. Ther.* **4**, 740–746 (2005).
46. Hu, Z. *et al.* Overexpression of osteopontin is associated with more aggressive phenotypes in human non-small cell lung cancer. *Clin. Cancer Res.* **11**, 4646–4652 (2005).
47. Tuck, A. B. *et al.* Osteopontin induces increased invasiveness and plasminogen activator expression of human mammary epithelial cells. *Oncogene* **18**, 4237–4246 (1999).
48. Mi, Z., Guo, H., Wai, P. Y., Gao, C. & Kuo, P. C. Integrin-linked kinase regulates osteopontin-dependent MMP-2 and uPA expression to convey metastatic function in murine mammary epithelial cancer cells. *Carcinogenesis* **27**, 1134–1145 (2006).
49. Das, R., Mahabeleshwar, G. H. & Kundu, G. C. Osteopontin induces AP-1-mediated secretion of urokinase-type plasminogen activator through c-Src-dependent epidermal growth factor receptor transactivation in breast cancer cells. *J. Biol. Chem.* **279**, 11051–11064 (2004).
50. Teti, A. *et al.* Activation of MMP-2 by human GCT23 giant cell tumour cells induced by osteopontin, bone sialoprotein and GRGDSP peptides is RGD and cell shape change dependent. *Int. J. Cancer* **77**, 82–93 (1998).
51. Rangaswami, H., Bulbule, A. & Kundu, G. C. Nuclear factor inducing kinase: a key regulator in osteopontin-induced MAPK/IκB kinase dependent NF-κB-mediated promatrix metalloproteinase-9 activation. *Glycoconj. J.* **23**, 221–232 (2006).
52. Rangaswami, H. & Kundu, G. C. Osteopontin stimulates melanoma growth and lung metastasis through NIK/MEKK1-dependent MMP-9 activation pathways. *Oncol. Rep.* **18**, 909–915 (2007).
53. Fedarko, N. S., Jain, A., Karadag, A. & Fisher, L. W. Three small integrin binding ligand N-linked glycoproteins (SIBLINGs) bind and activate specific matrix metalloproteinases. *FASEB J.* **18**, 734–736 (2004).
This paper shows that specific SIBLINGs bind MMPs as well as release them from inhibition by TIMPs and low-molecular-weight inhibitors. CFH blocks formation of the SIBLING–MMP complexes and can inactivate previously formed complexes and therefore potentially acts as a negative regulator of many SIBLING functions.
54. Fisher, L. W., Jain, A., Tayback, M. & Fedarko, N. S. Small integrin binding ligand N-linked glycoprotein gene family expression in different cancers. *Clin. Cancer Res.* **10**, 8501–8511 (2004).
This paper explores SIBLINGs expression in various cancer types on cancer patient microarray. The degree of correlation between a SIBLING and its partner MMP expression within a given cancer type was also addressed.
55. Karadag, A., Ogbureke, K. U., Fedarko, N. S. & Fisher, L. W. Bone sialoprotein, matrix metallo-proteinase 2, and αvβ3 integrin in osteotropic cancer cell invasion. *J. Natl Cancer Inst.* **96**, 956–965 (2004).
56. Karadag, A., Fedarko, N. S. & Fisher, L. W. Dentin matrix protein 1 enhances invasion potential of colon cancer cells by bridging matrix metalloproteinase-9 to integrins and CD44. *Cancer Res.* **65**, 11545–11552 (2005).
57. Takafuji, V., Forgues, M., Unsworth, E., Goldsmith, P. & Wang, X. W. An osteopontin fragment is essential for tumor cell invasion in hepatocellular carcinoma. *Oncogene* **26**, 6361–6371 (2007).
58. Mangala, L. S., Arun, B., Sahin, A. A. & Mehta, K. Tissue transglutaminase-induced alterations in extracellular matrix inhibit tumor invasion. *Mol. Cancer* **4**, 33 (2005).
59. Fidler, I. J. The pathogenesis of cancer metastasis: the 'seed and soil' hypothesis revisited. *Nature Rev. Cancer* **3**, 453–458 (2003).
60. Oates, A. J., Barraclough, R. & Rudland, P. S. The identification of osteopontin as a metastasis-related gene product in a rodent mammary tumour model. *Oncogene* **13**, 97–104 (1996).
61. Wai, P. Y. & Kuo, P. C. The role of Osteopontin in tumor metastasis. *J. Surg. Res.* **121**, 228–241 (2004).
62. Adwan, H., Bauerle, T. J. & Berger, M. R. Downregulation of osteopontin and bone sialoprotein II is related to reduced colony formation and metastasis formation of MDA-MB-231 human breast cancer cells. *Cancer Gene Ther.* **11**, 109–120 (2004).
This was the first paper to demonstrate that downregulating the expression of OPN or BSP in cancer cells inhibits the formation of bone metastases *in vivo*.
63. Nemoto, H. *et al.* Osteopontin deficiency reduces experimental tumor cell metastasis to bone and soft tissues. *J. Bone Miner. Res.* **16**, 652–659 (2001).
64. Bellahcene, A., Merville, M. P. & Castronovo, V. Expression of bone sialoprotein, a bone matrix protein, in human breast cancer. *Cancer Res.* **54**, 2823–2826 (1994).
The first immunohistochemical demonstration of ectopic BSP expression in human breast cancer tumours.
65. Waltregny, D. *et al.* Prognostic value of bone sialoprotein expression in clinically localized human prostate cancer. *J. Natl Cancer Inst.* **90**, 1000–1008 (1998).
66. Bellahcene, A. *et al.* Expression of bone sialoprotein in human lung cancer. *Calcif. Tissue Int.* **61**, 183–188 (1997).
67. Bellahcene, A. *et al.* Bone sialoprotein mRNA and protein expression in human multiple myeloma cell lines and patients. *Br. J. Haematol.* **111**, 1118–1121 (2000).
68. Kang, Y. *et al.* A multigenic program mediating breast cancer metastasis to bone. *Cancer Cell* **3**, 537–549 (2003).
69. Zhang, J. H. *et al.* Over-expression of bone sialoprotein enhances bone metastasis of human breast cancer cells in a mouse model. *Int. J. Oncol.* **23**, 1043–1048 (2003).
70. Zhang, J. H. *et al.* Bone sialoprotein promotes bone metastasis of a non-bone-seeking clone of human breast cancer cells. *Anticancer Res.* **24**, 1361–1368 (2004).
71. Koeneman, K. S., Yeung, F. & Chung, L. W. Osteomimetic properties of prostate cancer cells: a hypothesis supporting the predilection of prostate cancer metastasis and growth in the bone environment. *Prostate* **39**, 246–261 (1999).
A detailed study of the 'osteomimicry hypothesis' to explain the propensity of prostate cancer cells to grow and establish in the bone microenvironment.
72. Zayzafoon, M., Abdulkadir, S. A. & McDonald, J. M. Notch signaling and ERK activation are important for the osteomimetic properties of prostate cancer bone metastatic cell lines. *J. Biol. Chem.* **279**, 3662–3670 (2004).
73. Bellahcene, A. *et al.* Transcriptome analysis reveals an osteoblast-like phenotype for human osteotropic breast cancer cells. *Breast Cancer Res. Treat* **101**, 135–148 (2007).
74. Aggarwal, B. B., Shishodia, S., Sandur, S. K., Pandey, M. K. & Sethi, G. Inflammation and cancer: how hot is the link? *Biochem. Pharmacol.* **72**, 1605–1621 (2006).
75. McKee, M. D. & Nanci, A. Secretion of Osteopontin by macrophages and its accumulation at tissue surfaces during wound healing in mineralized tissues: a potential requirement for macrophage adhesion and phagocytosis. *Anat. Rec.* **245**, 394–409 (1996).
76. O'Regan, A. W. *et al.* Osteopontin is associated with T cells in sarcoid granulomas and has T cell adhesive and cytokine-like properties *in vitro*. *J. Immunol.* **162**, 1024–1031 (1999).
77. Weber, G. F. & Cantor, H. The immunology of η-1/osteopontin. *Cytokine Growth Factor Rev.* **7**, 241–248 (1996).
78. Giachelli, C. M., Lombardi, D., Johnson, R. J., Murry, C. E. & Almeida, M. Evidence for a role of osteopontin in macrophage infiltration in response to pathological stimuli *in vivo*. *Am. J. Pathol.* **152**, 353–358 (1998).
79. Koh, A. *et al.* Role of osteopontin in neutrophil function. *Immunology* **122**, 466–475 (2007).

80. Wai, P. Y. *et al.* Osteopontin inhibits macrophage nitric oxide synthesis to enhance tumor proliferation. *Surgery* **140**, 132–140 (2006).
81. Shiba, H. *et al.* Macrophage inflammatory protein-3α and β-defensin-2 stimulate dentin sialophosphoprotein gene expression in human pulp cells. *Biochem. Biophys. Res. Commun.* **306**, 867–871 (2003).
82. Coussens, L. M. & Werb, Z. Inflammation and cancer. *Nature* **420**, 860–867 (2002).
83. Volanakis, J. E. in *The Human Complement System in Health and Disease* (eds Volankis, J. E. & Frank, M. M.) 9–32 (Marcel Dekker, New York, 1998).
84. Fedarko, N. S., Fohr, B., Robey, P. G., Young, M. F. & Fisher, L. W. Factor H binding to bone sialoprotein and osteopontin enables tumor cell evasion of complement-mediated attack. *J. Biol. Chem.* **275**, 16666–16672 (2000).
85. Jain, A., Karadag, A., Fohr, B., Fisher, L. W. & Fedarko, N. S. Three SIBLINGs (small integrin-binding ligand, N-linked glycoproteins) enhance factor H's cofactor activity enabling MCP-like cellular evasion of complement-mediated attack. *J. Biol. Chem.* **277**, 13700–13708 (2002).
86. Nam, J. S. *et al.* Bone sialoprotein mediates the tumor cell-targeted prometastatic activity of transforming growth factor β in a mouse model of breast cancer. *Cancer Res.* **66**, 6327–6335 (2006).
This paper reports a direct association between TGFβ pro-metastatic activity and BSP expression in breast cancer cells.
87. Brooks, P. C., Clark, R. A. & Cheresh, D. A. Requirement of vascular integrin αvβ3 for angiogenesis. *Science* **264**, 569–571 (1994).
88. Cui, R. *et al.* Abrogation of the interaction between osteopontin and αvβ3 integrin reduces tumor growth of human lung cancer cells in mice. *Lung Cancer* **57**, 302–310 (2007).
A demonstration in a mouse model that disruption of the interaction of osteopontin with the αvβ3 integrin has therapeutic potential to diminish tumour progression.
89. Tang, H. *et al.* Inhibition of osteopontin would suppress angiogenesis in gastric cancer. *Biochem. Cell Biol.* **85**, 103–110 (2007).
90. Bellahcene, A. *et al.* Bone sialoprotein mediates human endothelial cell attachment and migration and promotes angiogenesis. *Circ. Res.* **86**, 885–891 (2000).
The first study to show BSP has angiogenesis-promoting activity using *in vitro* and *in vivo* assays.
91. Chakraborty, G., Jain, S. & Kundu, G. C. Osteopontin promotes vascular endothelial growth factor-dependent breast tumor growth and angiogenesis via autocrine and paracrine mechanisms. *Cancer Res.* **68**, 152–161 (2008).
92. Robey, P. G. Vertebrate mineralized matrix proteins: structure and function. *Connect. Tissue Res.* **35**, 131–136 (1996).
93. Giachelli, C. M. Inducers and inhibitors of biomineralization: lessons from pathological calcification. *Orthod. Craniofac. Res.* **8**, 229–231 (2005).
94. Carlinfante, G. *et al.* Differential expression of osteopontin and bone sialoprotein in bone metastasis of breast and prostate carcinoma. *Clin. Exp. Metastasis* **20**, 437–444 (2003).
95. Tunio, G. M., Hirota, S., Nomura, S. & Kitamura, Y. Possible relation of osteopontin to development of psammoma bodies in human papillary thyroid cancer. *Arch. Pathol. Lab. Med.* **122**, 1087–1090 (1998).
96. Steitz, S. A. *et al.* Osteopontin inhibits mineral deposition and promotes regression of ectopic calcification. *Am. J. Pathol.* **161**, 2035–2046 (2002).
97. Komori, T. Regulation of osteoblast differentiation by transcription factors. *J. Cell Biochem.* **99**, 1233–1239 (2006).
98. Sato, M. *et al.* Transcriptional regulation of osteopontin gene *in vivo* by PEBP2αA/CBFA1 and ETS1 in the skeletal tissues. *Oncogene* **17**, 1517–1525 (1998).
99. Javed, A. *et al.* runt homology domain transcription factors (RUNX, CBFA, and AML) mediate repression of the bone sialoprotein promoter: evidence for promoter context-dependent activity of Cbfa proteins. *Mol. Cell Biol.* **21**, 2891–2905 (2001).
100. Fen, J. Q. *et al.* Dentin matrix protein 1, a target molecule for CBFA1 in bone, is a unique bone marker gene. *J. Bone Miner. Res.* **17**, 1822–1831 (2002).
101. Chen, S. *et al.* Differential regulation of dentin sialophosphoprotein expression by RUNX2 during odontoblast cytodifferentiation. *J. Biol. Chem.* **280**, 29717–29727 (2005).
102. Blyth, K., Cameron, E. R. & Neil, J. C. The RUNX genes: gain or loss of function in cancer. *Nature Rev. Cancer* **5**, 376–387 (2005).
103. Pratap, J. *et al.* Regulatory roles of RUNX2 in metastatic tumor and cancer cell interactions with bone. *Cancer Metastasis Rev.* **25**, 589–600 (2006).
104. Inman, C. K. & Shore, P. The osteoblast transcription factor RUNX2 is expressed in mammary epithelial cells and mediates osteopontin expression. *J. Biol. Chem.* **278**, 48684–48689 (2003).
105. Barnes, G. L. *et al.* Osteoblast-related transcription factors RUNX2 (CBFA1/AML3) and MSX2 mediate the expression of bone sialoprotein in human metastatic breast cancer cells. *Cancer Res.* **63**, 2631–2637 (2003).
106. Colla, S. *et al.* Human myeloma cells express the bone regulating gene RUNX2/CBFA1 and produce osteopontin that is involved in angiogenesis in multiple myeloma patients. *Leukemia* **19**, 2166–2176 (2005).
107. Agrawal, D. *et al.* Osteopontin identified as lead marker of colon cancer progression, using pooled sample expression profiling. *J. Natl Cancer Inst.* **94**, 513–521 (2002).
108. Wai, P. Y. *et al.* ETS-1 and RUNX2 regulate transcription of a metastatic gene, osteopontin, in murine colorectal cancer cells. *J. Biol. Chem.* **281**, 18973–18982 (2006).
109. El-Tanani, M. K. *et al.* BRCA1 suppresses osteopontin-mediated breast cancer. *J. Biol. Chem.* **281**, 26587–26601 (2006).
110. Packer, L. *et al.* Osteopontin is a downstream effector of the PI3-kinase pathway in melanomas that is inversely correlated with functional PTEN. *Carcinogenesis* **27**, 1778–1786 (2006).
111. Kim, M. S. *et al.* Hyaluronic acid induces osteopontin via the phosphatidylinositol 3-kinase/Akt pathway to enhance the motility of human glioma cells. *Cancer Res.* **65**, 686–691 (2005).
112. Samant, R. S. *et al.* Breast cancer metastasis suppressor 1 (BRMS1) inhibits osteopontin transcription by abrogating NFκB activation. *Mol. Cancer* **6**, 6 (2007).
113. Senger, D., Asch, B., Smith, B., Perruzzi, C. & Dvorak, H. A secreted phosphoprotein marker for neoplastic transformation of both epithelial and fibroblastic cells. *Nature* **302**, 714–715 (1983).
114. Senger, D. R., Wirth, D. F. & Hynes, R. O. Transformed mammalian cells secrete specific proteins and phosphoproteins. *Cell* **16**, 885–893 (1979).
115. Bellahcene, A. *et al.* Ectopic expression of bone sialoprotein in human thyroid cancer. *Thyroid* **8**, 637–641 (1998).
116. Detry, C. *et al.* Detection of bone sialoprotein in human (pre)neoplastic lesions of the uterine cervix. *Calcif. Tissue Int.* **73**, 9–14 (2003).
117. Kayed, H. *et al.* Effects of bone sialoprotein on pancreatic cancer cell growth, invasion and metastasis. *Cancer Lett.* **245**, 171–183 (2007).
118. Riminucci, M. *et al.* Coexpression of bone sialoprotein (BSP) and the pivotal transcriptional regulator of osteogenesis, CBFA1/RUNX2, in malignant melanoma. *Calcif. Tissue Int.* **73**, 281–289 (2003).
119. Ogbureke, K. U. *et al.* Up-regulation of SIBLING proteins and correlation with cognate MMP expression in oral cancer. *Oral Oncol.* **43**, 920–932 (2007).
120. Chaplet, M. *et al.* Dentin matrix protein 1 is expressed in human lung cancer. *J. Bone Miner. Res.* **18**, 1506–1512 (2003).
121. Bucciarelli, E. *et al.* Low dentin matrix protein 1 expression correlates with skeletal metastases development in breast cancer patients and enhances cell migratory capacity *in vitro*. *Breast Cancer Res. Treat.* **105**, 95–104 (2007).
122. Rowe, P. S. *et al.* MEPE, a new gene expressed in bone marrow and tumors causing osteomalacia. *Genomics* **67**, 54–68 (2000).
123. Agrawal, D. *et al.* Osteopontin identified as colon cancer tumor progression marker. *C. R. Biol.* **326**, 1041–1043 (2003).
124. Rohde, F. *et al.* Expression of osteopontin, a target gene of de-regulated Wnt signaling, predicts survival in colon cancer. *Int. J. Cancer* (2007).
125. Bao, L. H., Sakaguchi, H., Fujimoto, J. & Tamaya, T. Osteopontin in metastatic lesions as a prognostic marker in ovarian cancers. *J. Biomed. Sci.* **14**, 373–381 (2007).
126. Matusan, K., Dordevic, G., Stipic, D., Mozetic, V. & Lucin, K. Osteopontin expression correlates with prognostic variables and survival in clear cell renal cell carcinoma. *J. Surg. Oncol.* **94**, 325–331 (2006).
127. Sakaguchi, H., Fujimoto, J., Hong, B. L. & Tamaya, T. Clinical implications of osteopontin in metastatic lesions of uterine cervical cancers. *Cancer Lett.* **247**, 98–102 (2007).
128. Rudland, P. S. *et al.* Prognostic significance of the metastasis-associated protein osteopontin in human breast cancer. *Cancer Res.* **62**, 3417–3427 (2002).
This paper demonstrates on a large collection of breast cancer specimens that OPN expression levels are an independent prognostic indicator that correlates with reduced patient survival.
129. Forootan, S. S. *et al.* Prognostic significance of osteopontin expression in human prostate cancer. *Int. J. Cancer* **118**, 2255–2261 (2006).
130. Bache, M. *et al.* Immunohistochemical detection of osteopontin in advanced head-and-neck cancer: prognostic role and correlation with oxygen electrode measurements, hypoxia-inducible-factor-1α-related markers, and hemoglobin levels. *Int. J. Radiat. Oncol. Biol. Phys.* **66**, 1481–1487 (2006).
131. Celetti, A. *et al.* Overexpression of the cytokine osteopontin identifies aggressive laryngeal squamous cell carcinomas and enhances carcinoma cell proliferation and invasiveness. *Clin. Cancer Res.* **11**, 8019–8027 (2005).
132. Guarino, V. *et al.* Osteopontin is overexpressed in human papillary thyroid carcinomas and enhances thyroid carcinoma cell invasiveness. *J. Clin. Endocrinol. Metab.* **90**, 5270–5278 (2005).
133. Donati, V. *et al.* Osteopontin expression and prognostic significance in non-small cell lung cancer. *Clin. Cancer Res.* **11**, 6459–6465 (2005).
134. Pan, H. W. *et al.* Overexpression of osteopontin is associated with intrahepatic metastasis, early recurrence, and poorer prognosis of surgically resected hepatocellular carcinoma. *Cancer* **98**, 119–127 (2003).
135. Bellahcene, A., Menard, S., Bufalino, R., Moreau, L. & Castronovo, V. Expression of bone sialoprotein in primary human breast cancer is associated with poor survival. *Int. J. Cancer* **69**, 350–353 (1996).
136. Papotti, M. *et al.* Bone sialoprotein is predictive of bone metastases in resectable non-small-cell lung cancer: a retrospective case-control study. *J. Clin. Oncol.* **24**, 4818–4824 (2006).
This study identifies BSP expression as a predictive factor of bone metastasis development in patients with resectable NSCLC.
137. Fedarko, N. S., Jain, A., Karadag, A., Van Eman, M. R. & Fisher, L. W. Elevated serum bone sialoprotein and osteopontin in colon, breast, prostate, and lung cancer. *Clin. Cancer Res.* **7**, 4060–4066 (2001).
138. Scatena, M., Liaw, L. & Giachelli, C. M. Osteopontin: a multifunctional molecule regulating chronic inflammation and vascular disease. *Arterioscler Thromb. Vasc Biol.* **27**, 2302–2309 (2007).
139. Bramwell, V. H. *et al.* Serial plasma osteopontin levels have prognostic value in metastatic breast cancer. *Clin. Cancer Res.* **12**, 3337–3343 (2006).
140. Ramankulov, A., Lein, M., Kristiansen, G., Loening, S. A. & Jung, K. Plasma osteopontin in comparison with bone markers as indicator of bone metastasis and survival outcome in patients with prostate cancer. *Prostate* **67**, 330–340 (2007).
141. Ramankulov, A. *et al.* Elevated plasma osteopontin as marker for distant metastases and poor survival in patients with renal cell carcinoma. *J. Cancer Res. Clin. Oncol.* **133**, 643–652 (2007).
142. Chang, Y. S. *et al.* Elevated circulating level of osteopontin is associated with advanced disease state of non-small cell lung cancer. *Lung Cancer* **57**, 373–380 (2007).
143. Wu, C. Y. *et al.* Elevated plasma osteopontin associated with gastric cancer development, invasion and survival. *Gut* **56**, 782–789 (2007).
144. Petrik, D. *et al.* Plasma osteopontin is an independent prognostic marker for head and neck cancers. *J. Clin. Oncol.* **24**, 5291–5297 (2006).
145. Zhang, H. *et al.* The prognostic significance of preoperative plasma levels of osteopontin in patients with hepatocellular carcinoma. *J. Cancer Res. Clin. Oncol.* **132**, 709–717 (2006).
146. Koopmann, J. *et al.* Evaluation of osteopontin as biomarker for pancreatic adenocarcinoma. *Cancer Epidemiol. Biomarkers Prev.* **13**, 487–491 (2004).
147. Diel, I. J. *et al.* Serum bone sialoprotein in patients with primary breast cancer is a prognostic marker for subsequent bone metastasis. *Clin. Cancer Res.* **5**, 3914–3919 (1999).
148. Woitge, H. W. *et al.* Serum bone sialoprotein as a marker of tumour burden and neoplastic bone

involvement and as a prognostic factor in multiple myeloma. *Br. J. Cancer* **84**, 344–351 (2001).
149. Jung, K. *et al.* Comparison of 10 serum bone turnover markers in prostate carcinoma patients with bone metastatic spread: diagnostic and prognostic implications. *Int. J. Cancer* **111**, 783–791 (2004).
150. Ito, T. *et al.* An inducible short-hairpin RNA vector against osteopontin reduces metastatic potential of human esophageal squamous cell carcinoma *in vitro* and *in vivo*. *Clin. Cancer Res.* **12**, 1308–1316 (2006).
151. Wai, P. Y. *et al.* Osteopontin silencing by small interfering RNA suppresses *in vitro* and *in vivo* CT26 murine colon adenocarcinoma metastasis. *Carcinogenesis* **26**, 741–751 (2005).
152. de Fougerolles, A., Vornlocher, H. P., Maraganore, J. & Lieberman, J. Interfering with disease: a progress report on siRNA-based therapeutics. *Nature Rev. Drug Discov.* **6**, 443–453 (2007).
153. Lien, S. & Lowman, H. B. Therapeutic anti-VEGF antibodies. *Handb. Exp. Pharmacol.* **181**, 131–150 (2008).
154. Ye, Q. H. *et al.* Predicting hepatitis B virus-positive metastatic hepatocellular carcinomas using gene expression profiling and supervised machine learning. *Nature Med.* **9**, 416–423 (2003).
This paper combines the demonstration that OPN is a diagnostic and prognostic marker for hepatocellular carcinoma and works as an effective target in antibody-based treatment.
155. Bauerle, T. *et al.* Characterization of a rat model with site-specific bone metastasis induced by MDA-MB-231 breast cancer cells and its application to the effects of an antibody against bone sialoprotein. *Int. J. Cancer* **115**, 177–186 (2005).
156. Weber, G. F. The metastasis gene osteopontin: a candidate target for cancer therapy. *Biochim. Biophys. Acta* **1552**, 61–85 (2001).
157. Brooks, P. C. *et al.* Integrin αvβ3 antagonists promote tumor regression by inducing apoptosis of angiogenic blood vessels. *Cell* **79**, 1157–1164 (1994).
158. Melquist, J. J. *et al.* Conditionally replicating adenovirus-mediated gene therapy in bladder cancer: an orthotopic *in vivo* model. *Urol. Oncol.* **24**, 362–371 (2006).
159. Qin, C., Baba, O. & Butler, W. T. Post-translational modifications of sibling proteins and their roles in osteogenesis and dentinogenesis. *Crit. Rev. Oral Biol. Med.* **15**, 126–136 (2004).
160. Sreenath, T. *et al.* Dentin sialophosphoprotein knockout mouse teeth display widened predentin zone and develop defective dentin mineralization similar to human dentinogenesis imperfecta type III. *J. Biol. Chem.* **278**, 24874–24880 (2003).
161. Senger, D. R., Perruzzi, C. A., Papadopoulos, A. & Tenen, D. G. Purification of a human milk protein closely similar to tumor-secreted phosphoproteins and osteopontin. *Biochim. Biophys. Acta* **996**, 43–48 (1989).
162. Patarca, R., Wei, F. Y., Singh, P., Morasso, M. I. & Cantor, H. Dysregulated expression of the T cell cytokine Eta-1 in $CD4^{-}8^{-}$ lymphocytes during the development of murine autoimmune disease. *J. Exp. Med.* **172**, 1177–1183 (1990).
An early report on the role of OPN Eta-1 in immune dysregulation. Increased OPN expression was associated with a chronic immune response and autoimmune disease.
163. Shiraga, H. *et al.* Inhibition of calcium oxalate crystal growth *in vitro* by uropontin: another member of the aspartic acid-rich protein superfamily. *Proc. Natl Acad. Sci. USA* **89**, 426–430 (1992).
164. Brown, L. F. *et al.* Expression and distribution of osteopontin in human tissues: widespread association with luminal epithelial surfaces. *Mol. Biol. Cell* **3**, 1169–1180 (1992).
165. Terasawa, M. *et al.* Expression of dentin matrix protein 1 (DMP1) in nonmineralized tissues. *J. Bone Miner. Metab.* **22**, 430–438 (2004).
166. Shen, Q. & Christakos, S. The vitamin D receptor, RUNX2, and the Notch signaling pathway cooperate in the transcriptional regulation of osteopontin. *J. Biol. Chem.* **280**, 40589–40598 (2005).
167. Kim, H. J. *et al.* Okadaic acid stimulates osteopontin expression through *de novo* induction of AP-1. *J. Cell Biochem.* **87**, 93–102 (2002).
168. Roca, H., Phimphilai, M., Gopalakrishnan, R., Xiao, G. & Franceschi, R. T. Cooperative interactions between RUNX2 and homeodomain protein-binding sites are critical for the osteoblast-specific expression of the bone sialoprotein gene. *J. Biol. Chem.* **280**, 30845–30855 (2005).
169. Hassan, M. Q. *et al.* HOXA10 controls osteoblastogenesis by directly activating bone regulatory and phenotypic genes. *Mol. Cell Biol.* **27**, 3337–3352 (2007).
170. Nakayama, Y. *et al.* Insulin-like growth factor-I increases bone sialoprotein (BSP) expression through fibroblast growth factor-2 response element and homeodomain protein-binding site in the proximal promoter of the BSP gene. *J. Cell Physiol.* **208**, 326–335 (2006).
171. Pang, J. *et al.* Upregulation of dentin matrix protein 1 promoter activities by core binding factor α1 in human dental pulp stem cells. *Biochem. Biophys. Res. Commun.* **357**, 505–510 (2007).
172. Narayanan, K., Ramachandran, A., Hao, J. & George, A. Transcriptional regulation of dentin matrix protein 1 (DMP1) by AP-1 (c-fos/c-jun) factors. *Connect. Tissue Res.* **43**, 365–371 (2002).
173. Chen, S. *et al.* Regulation of the cell type-specific dentin sialophosphoprotein gene expression in mouse odontoblasts by a novel transcription repressor and an activator CCAAT-binding factor. *J. Biol. Chem.* **279**, 42182–42191 (2004).
174. Oyama, Y., Akuzawa, N., Nagai, R. & Kurabayashi, M. PPARγ ligand inhibits osteopontin gene expression through interference with binding of nuclear factors to A/T-rich sequence in THP-1 cells. *Circ. Res.* **90**, 348–355 (2002).
175. Lamour, V. *et al.* Runx2- and histone deacetylase 3-mediated repression is relieved in differentiating human osteoblast cells to allow high bone sialoprotein expression. *J. Biol. Chem.* **282**, 36240–36249 (2007).
176. Galler, K. M. *et al.* A novel role for Twist-1 in pulp homeostasis. *J. Dent Res.* **86**, 951–955 (2007).
177. Chen, B., Piel, W. H., Gui, L., Bruford, E. & Monteiro, A. The HSP90 family of genes in the human genome: insights into their divergence and evolution. *Genomics* **86**, 627–637 (2005).
178. Guo, W. & Giancotti, F. G. Integrin signalling during tumour progression. *Nature Rev. Mol. Cell Biol.* **5**, 816–826 (2004).
179. Coppola, D. *et al.* Correlation of osteopontin protein expression and pathological stage across a wide variety of tumor histologies. *Clin. Cancer Res.* **10**, 184–190 (2004).
180. Ang, C., Chambers, A. F., Tuck, A. B., Winquist, E. & Izawa, J. I. Plasma osteopontin levels are predictive of disease stage in patients with transitional cell carcinoma of the bladder. *BJU Int.* **96**, 803–805 (2005).
181. Sulzbacher, I., Birner, P., Trieb, K., Lang, S. & Chott, A. Expression of osteopontin and vascular endothelial growth factor in benign and malignant bone tumors. *Virchows Arch.* **441**, 345–349 (2002).
182. Cogan, G. *et al.* Analysis of human bone sialoprotein in normal and pathological tissues using a monoclonal antibody (BSP 1.2 mab). *Connect. Tissue Res.* **45**, 60–71 (2004).
183. Valabrega, G. *et al.* ErbB2 and bone sialoprotein as markers for metastatic osteosarcoma cells. *Br. J. Cancer* **88**, 396–400 (2003).
184. Feng, J. Q. *et al.* Loss of DMP1 causes rickets and osteomalacia and identifies a role for osteocytes in mineral metabolism. *Nature Genet.* **38**, 1310–1315 (2006).
185. MacDougall, M., Dong, J. & Acevedo, A. C. Molecular basis of human dentin diseases. *Am. J. Med. Genet. A* **140**, 2536–2546 (2006).
186. Saitoh, Y., Kuratsu, J., Takeshima, H., Yamamoto, S. & Ushio, Y. Expression of osteopontin in human glioma. Its correlation with the malignancy. *Lab. Invest.* **72**, 55–63 (1995).
187. Bellahcene, A. & Castronovo, V. Increased expression of osteonectin and osteopontin, two bone matrix proteins, in human breast cancer. *Am. J. Pathol.* **146**, 95–100 (1995).
188. Rodrigues, L. R., Teixeira, J. A., Schmitt, F. L., Paulsson, M. & Lindmark-Mansson, H. The role of osteopontin in tumor progression and metastasis in breast cancer. *Cancer Epidemiol. Biomarkers Prev.* **16**, 1087–1097 (2007).
189. Wong, Y. F. *et al.* Genome-wide gene expression profiling of cervical cancer in Hong Kong women by oligonucleotide microarray. *Int. J. Cancer* **118**, 2461–2469 (2006).
190. Eschrich, S. *et al.* Molecular staging for survival prediction of colorectal cancer patients. *J. Clin. Oncol.* **23**, 3526–3535 (2005).
191. Gaumann, A. *et al.* Osteopontin expression in primary sarcomas of the pulmonary artery. *Virchows Arch.* **439**, 668–674 (2001).
192. Ue, T. *et al.* Co-expression of osteopontin and CD44v9 in gastric cancer. *Int. J. Cancer* **79**, 127–132 (1998).
193. Matusan, K., Dordevic, G., Mozetic, V. & Lucin, K. Expression of osteopontin and CD44 molecule in papillary renal cell tumors. *Pathol. Oncol. Res.* **11**, 108–113 (2005).
194. Somerman, M. J., Berry, J. E., Khalkhali-Ellis, Z., Osdoby, P. & Simpson, R. U. Enhanced expression of αv integrin subunit and osteopontin during differentiation of HL-60 cells along the monocytic pathway. *Exp. Cell Res.* **216**, 335–341 (1995).
195. Flamant, S. *et al.* Osteopontin is upregulated by BCR-ABL. *Biochem. Biophys. Res. Commun.* **333**, 1378–1384 (2005).
196. Chambers, A. F. *et al.* Osteopontin expression in lung cancer. *Lung Cancer* **15**, 311–323 (1996).
197. Nagai, S. *et al.* Comprehensive gene expression profile of human activated T_H1- and T_H2-polarized cells. *Int. Immunol.* **13**, 367–376 (2001).
198. Saeki, Y. *et al.* Enhanced production of osteopontin in multiple myeloma: clinical and pathogenic implications. *Br. J. Haematol.* **123**, 263–270 (2003).
199. Geissinger, E., Weisser, C., Fischer, P., Schartl, M. & Wellbrock, C. Autocrine stimulation by osteopontin contributes to antiapoptotic signalling of melanocytes in dermal collagen. *Cancer Res.* **62**, 4820–4828 (2002).
200. Zhou, Y. *et al.* Osteopontin expression correlates with melanoma invasion. *J. Invest. Dermatol.* **124**, 1044–1052 (2005).
201. Tiniakos, D. G., Yu, H. & Liapis, H. Osteopontin expression in ovarian carcinomas and tumors of low malignant potential (LMP). *Hum. Pathol.* **29**, 1250–1254 (1998).
202. Tozawa, K. *et al.* Osteopontin expression in prostate cancer and benign prostatic hyperplasia. *Urol. Int.* **62**, 155–158 (1999).
203. Hotte, S. J., Winquist, E. W., Stitt, L., *Wilson*, S. M. & Chambers, A. F. Plasma osteopontin: associations with survival and metastasis to bone in men with hormone-refractory prostate carcinoma. *Cancer* **95**, 506–512 (2002).
204. Debucquoy, A. *et al.* Molecular responses of rectal cancer to preoperative chemoradiation. *Radiother Oncol.* **80**, 172–177 (2006).

Acknowledgements
The work of A.B. and V.C. is supported by grants from the National Fund for Scientific Research (Belgium), the Centre Anti-Cancéreux of the University of Liège and the European Commission through METABRE Contract CEE LSHC-CT-2004-503049. The work of K.O. is supported by National Institute of Dental and Craniofacial Research/ National Institutes of Health (NIH) Grant K23 017791-01A1, Medical College of Georgia Research Institute Grant STP 00105W005, and the Wendy Will Case Cancer Fund. The research of L.W.F. is supported by the Intramural Research Program of the NIH, Department of Health and Human Services. The work of N.S.F. is supported by grants from the National Cancer Institute (R21CA87311 and R01 CA113865) and from the Department of Defense Congressionally Directed Medical Research Program (W81XWH-04-1-0844 and BC010478).

DATABASES

Entrez Gene: http://www.ncbi.nlm.nih.gov/entrez/query.fcgi?db=gene
β catenin | APC | BMP1 | BRCA1 | BRMS1 | CBFβ | CCL20 | CD44 | CDH11 | CFH | CTGF | CXCR4 | DLX5 | *DMP1* | *DSPP* | EGFR | ETS1 | FN1 | FOXO3 | HDAC3 | *IBSP* | IKBKB | ILK | interleukin 11 | MAP3K1 | MAP3K14 | MAPK8 | *MEPE* | MMP2 | MMP3 | MMP7 | MMP9 | MYC | NFκB | p53 | PLAU | POU2F1 | PPARγ | PTEN | *RUNX2* | SP1 | *SPP1* | SRC | TCF4 | TGFβ | THBS1 | TWIST1

National Cancer Institute: http://www.cancer.gov/
bladder cancer | breast cancer | cervical carcinoma | colorectal cancer | gastric cancer | glioma | head and neck cancer | leukaemia | lung cancer | melanoma | multiple myeloma | non-small cell lung carcinoma | oral cancer | pancreatic cancer | prostate cancer | renal cell cancer | skin cancer | thyroid carcinomas

FURTHER INFORMATION

Larry W. Fisher's homepage:
http://csdb.nidcr.nih.gov/csdb/frame-mbu.html

ALL LINKS ARE ACTIVE IN THE ONLINE PDF

Innovative Minds in Prostate Cancer Today (IMPaCT), Department of Defense Prostate Cancer Research Program. September 8, 2007; Atlanta, GA.

Small Integrin Binding Proteins as Serum Markers for Prostate Cancer Detection.

Alka Jain & Neal S. Fedarko. Johns Hopkins University, Baltimore, MD, 21224

Prostate cancer is the leading cancer diagnosed among men in the United States. Detection is currently based on symptom presentation, physical examination including a digital rectal exam (DRE), measuring serum levels of prostate-specific antigen (PSA) and biopsy. Both the DRE and PSA tests suffer from drawbacks, including an inability to detect early disease and are sometimes uninformative in terms of predicting disease progression. We have been studying a gene family, termed SIBLINGs for Small Integrin Binding LIgand N-linked Glycoproteins) which are normally restricted in expression to skeletal tissue, but are also induced in different cancers. At least three SIBLINGs have the capacity to bind to and modulate the activity of specific matrix metalloproteinases. Because matrix metalloproteinases play a central role in tumor growth and progression, we hypothesize that SIBLINGs may have an active role in prostate cancer development and furthermore that SIBLING levels in serum may be informative marker for prostate cancer detection. We have developed competitive ELISA tests for quantitatively determining the levels of four SIBLINGs: bone sialoprotein (BSP), dentin sialophosphoprotein (DSPP), matrix extracellular phosphoglycoprotein (MEPE), and osteopontin (OPN). We have applied the assays to the analysis of 110 prostate cancer serum samples (mean age 63 ± 5 years) and compared the distribution to that from 110 normal subjects (mean age 65 ± 10 years). The mean values for the normal population were 114 ± 63 ng/ml for BSP, 42 ± 15 ng/ml for DSPP, 93 ± 19 ng/ml for MEPE, and 353 ±130 ng/ml for OPN. The mean values for the prostate cancer group were 348 ± 58 ng/ml for BSP, 167 ± 91 ng/ml for DSPP, 80 ± 11 ng/ml for MEPE, and 537 ± 169 ng/ml for OPN. Receiver operator characteristic (ROC) curves were also determined for each marker. While there was overlap between the high end of normal BSP levels with the low end of the prostate cancer group, the area under the ROC curve (AUC) was a significant 0.92. The SIBLING DSPP exhibit the greatest difference between normal sera and sera derived from prostate cancer subjects with an AUC of 98. Although there was a fair amount of overlap between high-end normal OPN levels and low end prostate cancer sera OPN levels, the determined AUC was 0.81. The markers with discriminatory power (BSP, DSPP and OPN) were compared to PSA values determined on the same subjects. BSP & OPN positively correlated with PSA levels, while DSPP did not.

Small Integrin Binding Proteins as Serum Markers for Prostate Cancer Detection.

Alka Jain, Larry W. Fisher, & Neal S. Fedarko. Johns Hopkins University, Baltimore, MD, 21224

Division of Geriatric Medicine & Gerontology, Johns Hopkins University, Baltimore, MD

2

Corresponding author:
Neal S. Fedarko
Room 5A-64 JHAAC
5501 Hopkins Bayview Circle
Baltimore, MD 21224

Running title: Small integrin binding proteins and prostate cancer.

ABSTRACT

SIBLINGs (Small Integrin Binding LIgand N-linked Glycoproteins) are normally restricted in expression to skeletal tissue, but are also induced in different cancers. SIBLING family members include bone sialoprotein (BSP), dentin matrix protein-1 (DMP1), dentin sialophosphoprotein (DSPP), matrix extracellular phosphoglycoprotein (MEPE), and osteopontin (OPN). When the expression levels of SIBLINGs in normal prostate and in prostate cancer were determined by cDNA array and by immunohistochemical staining of biopsies with monoclonal antibodies against the SIBLINGs, elevated levels was observed for BSP, DMP1, DSPP and OPN. Competitive ELISA tests for quantitatively determining the total levels of SIBLINGs were developed and applied to the analysis of 102 prostate cancer serum samples (mean age 63 ± 5 years) and compared the distribution to that from 110 normal subjects (mean age 65 ± 10 years). The mean values for the normal population were 114 ± 63 ng/ml for BSP, 242 ± 122 ng/ml for DSPP, 93 ± 19 ng/ml for MEPE, and 353 ± 130 ng/ml for OPN. The mean values for the prostate cancer group were 222 ± 98 ng/ml for BSP, 1500 ± 500 ng/ml for DSPP, 80 ± 11 ng/ml for MEPE, and 537 ± 170 ng/ml for OPN. Receiver operator characteristic (ROC) curves yielded area under the curve (AUC) values of AUC of 98 for DSPP, 0.84 for BSP and 0.81 for OPN. When cancer samples were segregated by stage, BSP and OPN levels were significantly elevated only in late stages (when the tumor had spread beyond the prostate gland), while DSPP was significantly elevated in early stages. OPN, but not BSP or DSPP correlated positively with both serum prostate specific

antigen (PSA) and the immune activation marker neopterin. The elevated levels of DSPP in serum was confirmed by another method of detection employing SDS PAGE and western blotting. Of the SIBLING gene family members, DSPP appears to be a strong candidate for use in prostate cancer detection.

INTRODUCTION

Prostate cancer is the leading cancer diagnosed among men in the United States (1). Detection is currently based on symptom presentation, physical examination including a digital rectal exam (DRE), measuring serum levels of prostate-specific antigen (PSA) and biopsy. PSA measures have a significant rate of false positive test results (the PSA is elevated but no cancer is present) that are associated with additional medical procedures, significant financial costs and mental stress (2, 3). In addition both DRE and PSA do not detect early tumors and are sometimes uninformative in terms of predicting disease progression. Biopsies performed for confirmation of abnormal test results or to follow disease progression or response to treatment can have side-effects that impact profoundly upon the quality of life (4).

We have been studying members of a gene family (termed SIBLINGs for Small Integrin Binding LIgand N-linked Glycoproteins) that share conserved motifs including: an abundance of acidic amino acids, the integrin-binding tripeptide, RGD; similar post-translational modification motifs (e.g. casein kinase phosphorylation and various glycosylation events); and at least one site of controlled proteolysis. SIBLINGs are normally expressed in skeletal tissue (5), are also induced in different cancers (6), and have been shown to bind and modulate matrix metalloproteinase (MMP) activity through both the activation of the latent pro-enzyme and reactivation of tissue inhibitor of matrix metalloproteinase (TIMP)-inhibited MMP (7, 8). MMPs have a well defined role in tumor angiogenesis, progression and metastasis (9). The biological activities of SIBLINGs and MMPs are consistent with a role for SIBLINGs in early tumor

progression. This biological plausibility suggests that the levels of these proteins in blood may be used not only as adjuncts to conventional detection of prostate cancer, but also as serological markers for prostate cancer progression (10). A confounding facet of prostate cancer is the variable nature of progression (growth rate, metastasis, etc.) and the absence of non-invasive markers that consistently track with progression. The characterization of novel serum markers whose levels may correlate with disease progression has the potential to benefit individuals with prostate cancer across the spectrum from early detection to disease progression monitoring and modulating therapy.

METHODS

Sample recruitment. Normal subjects (n = 110) were obtained under IRB approved protocols from the Johns Hopkins Bayview Medical Center General Clinical Research Center (JHBMC). The JHBMC normal group was obtained from an existing serum bank using samples from which all patient identifiers were removed. For this study, inclusion criteria as a normal serum donor included measures within the normal range for fasting glucose (< 100 mg/dl), TSH (0.5 - 2.1 mIU/mL), BMI (20 - 25 kg/m^2) as well as a physical assessment by a physician. Exclusionary criteria included a previous history of hypertension, heart disease, diabetes mellitus, renal or hepatic dysfunction, cancer, or any chronic inflammatory condition (e.g., rheumatoid arthritis). Prostate cancer sera (n = 102) and tissue biopsies from subjects recently diagnosed with prostate cancer, prior to initiation of treatment, were obtained through commercial biorepositories (East Coast Biologics, Inc., NorthBerwick, Maine; Promedx, Inc., Norton, MA; LifeSpan BioSciences Inc. Seattle, WA).

SIBLING probes and prostate cancer array analysis. A cancer profiling array (Clontech, Palo Alto, CA) containing normalized cDNA from tumor and corresponding normal tissues from 4 individual patients with prostate cancer was employed to screen for SIBLING as previously described (6). Briefly, several cancer profiling arrays were hybridized in ExpressHyb hybridization solution with ^{32}P-labeled cDNA probes for specific SIBLINGs as per the manufacture's instructions. Washed membranes were quantified by exposure to PhosphorImager screens for up to 24 hours and the exposed screen analyzed on a PhosphorImager (Molecular Dynamics) using the manufacturer's ImageQuant program. The labeled DNA probes for human BSP and OPN were cDNA inserts released from OP-10 and B6-6g plasmids respectively (11, 12); for human DMP1, a ~1.4 kbp coding region of exon 6 was employed (13). For the MEPE probe (1.4 kbp) and DSPP probe (2.64 kbp), the labeled probes were the same cDNA inserts that were used in making the recombinant protein (14, 15).

Antibodies. The production of monoclonal antibodies raised against specific SIBLINGs has been previously described (16). The polyclonal antibodies against BSP, DMP1, MEPE and OPN used in enzyme immunoassays and western blotting have been previously characterized (17-19). A polyclonal antibody for DSPP was developed as follows. Recombinant human DSP fragment (T132-D373) was made by PCR of this portion of exon 4 from human genomic DNA using a high fidelity DNA polymerase and oligonucleotides that introduced an in-frame Nde1 site at the 5' end and an added stop codon plus BamHI site at the 3' end of the PCR product. The purified PCR product was

digested with NdeI and BamHI, ligated into prepared pET-15b (Novagen/EMD Biosciences, LaJolla, CA) bacterial expression vector. The protein made in E. coli was purifed on His-Bind resin (Novagen), dialized against water, freeze-dried, and four injections of ~250 ug protein each was made in rabbit LF-151 using animal care & use committee-approved protocols at an AAALAC-approved facility. Bleeds were taken every two weeks to produce the antiserum used.

Immunohistochemistry methods. Tissue slides were prepared from commercially available human prostrate biopsies. In brief, after being fixed in Formalin and embedded in paraffin wax, 4 μm sections of tissue were prepared and placed on pre-cleaned and charged microscope slides. Slides were dried in a tissue drying oven for 45 minutes at 60ºC. Antigen retrieval was carried out after deparaffinization and rehydration by steaming slides in 0.01M Sodium citrate buffer, pH 6.0 at 99-100º C for 20 minutes. Slides were removed from heat and let stand at room temperature in buffer for 20 minutes. Slides were placed in universal protein block for 20 minutes at room temperature after being rinsed in Tris buffered saline, 0.05 M Tris-HCl, pH 7.5, 0.15 M NaCl containing 0.05% Tween 20 (TBS-T). Slides were then treated with monoclonal antibodies developed against specific SIBLINGs. Antibodies LFMAb25, LFMAb31, LFMAb21 and LFMAb14 were used at 10 μg/ml, 10μg/ml, 0.625μg/ml and 2.5μg/ml to detect the levels of BSP, DMP, DSPP and OPN, respectively. After being exposed to biotinylated anti-mouse secondary antibody, and alkaline phosphatase streptavidin, slides were treated with Vector red alkaline phosphatase substrate. This substrate system produces a pinkish-red reaction product.

ELISA sample preparation. SIBLINGs present in human serum are complexed with complement Factor H (19, 20). Taking advantage of the properties of SIBLINGs that they have a flexible structure (21) and also are highly negatively charged due to their content of acidic amino acids and sialic acid residues, the binding complexes in serum can be disrupted to enable total SIBLING levels to be measured (17). Briefly, serum samples are denatured and reduced to disrupt complexes, subjected to strong anion exchange chromatography to remove reagents that interfere with antibody binding, and then the samples are analyzed by competitive ELISA for total SIBLING levels (17, 18). Uncomplexed OPN (that is presumably not bound to complement factor H) can be measured in plasma/serum by directly assaying the sample with no prior chaotropic treatment (22). Appropriate samples to measure free OPN in a subset of 40 normal and prostate cancer patient samples were also taken for analysis by competitive ELISA.

ELISA procedures. Greiner high binding plates were coated with 20 ng/ml BSP or OPN, 10 ng/ml MEPE, or 25 ng/ml DSPP overnight in 50 mM carbonate buffer, pH 8.0. Recombinant human BDP, and OPN were expressed and purified as previously described (7). Recombinant human MEPE was generated and isolated as previously described (18). Samples and standards were incubated for 2 h with shaking at room temperature with primary antibody. Primary antibodies used were a 1:200,000 dilution of LF-100 antibody (for BSP) or 1:100,000 of LF-124 antibody (for OPN), or a 1:200,000 dilution of LF-155 antibody (for MEPE) or a 1:100,000 dilution of LF-151 (for DSPP) in TBS-T in polypropylene 96 well plates. During the 2 h incubation, antigen coated plates

were blocked with protein-free blocking buffer in TBS (Thermo Fisher Scientific). Antigen coated plates were then rinsed three times with TBS-T and the antibody-sample solution added to the wells. After a second incubation for 1 h at room temperature with shaking the plates were washed three times with TBS-T. A secondary antibody of goat anti-rabbit peroxidase-labeled antibody conjugate, human serum adsorbed (Kierkagaard & Perry, Gaithersburg, MD) at 1:2000 was then added and the plates incubated for 1h. After three washes with TBS-T, substrate (3.3',5,5"-tetramethylbenzidine microwell peroxidase substrate, BioFX Laboratories) was added and after a final 20 min incubation the color reaction was stopped. Absorbance was read at 450 nm and the data analyzed using the program AssayZap (BioSoft, Cambridge, UK). Commercial ELISAs to measure total prostate specific antigen (PSA) and the immune activation marker neopterin were obtained from ALPCO Diagnostics (Salem, NH).

SDS PAGE and Western blot. Serum samples from normal and prostrate cancer subjects were diluted 10X in 50% formamide buffer and reduced with 10mM DTT. Reduced serum samples were resolved by SDS- PAGE 4 -12 % Bis-Tris gels (Invitrogen Inc.) and then transferred to nitrocellulose membrane following standard conditions. Nitrocellulose membrane were rinsed with TBS-T. After a 1-h incubation in protein-free TBS blocking buffer at room temperature on a rotary shaker, primary antibody was added at 1:2000 dilution and incubated overnight at 4 C. The nitrocellulose membrane was subsequently washed in TBS-T three times for 5 min each time and then second antibody in protein-free TBS blocking buffer was added and incubated for 2 h at room temperature. Following removal of the second antibody solution the membrane was

washed three times with TBS-T and incubated for 5 minutes in SuperSignal West DuraSubstrate (Thermo Fisher Scientific) working solution. The chemiluminescent signal was captured using Gel Logic 2200 imaging system.

RESULTS

SIBLING expression

Separate studies have previously reported individual elevated expression of BSP, OPN and, most recently, DSPP by prostate tumors (23-25). The expression levels of all five SIBLINGs by prostate tumors were determined using a commercial cancer array containing normalized cDNA from both the tumor and normal tissue from the same subject. Patient cDNA was reacted with probes for BSP, DMP1, DSPP, MEPE and OPN, the amount of hybridized probe was quantified and the expression levels between normal and tumor tissue were compared (Figure 1). Normal prostate tissue expressed BSP, DMP1, DSPP and MEPE at very low levels. Relative to normal tissue expression, the average levels were elevated at least 9-fold for BSP, DMP1, and DSPP, while MEPE was not significantly elevated. OPN, which yielded the highest relative level of SIBLING mRNA expression, was elevated an average of only 4-fold in tumors, given that normal prostate tissue expression of OPN was significant.

SIBLING immunohistochemistry

The observation of elevated SIBLING expression in samples from subjects with prostate cancer lead to a screening of SIBLING protein levels in tumor tissue by

immunohistochemistry. Serial sections of biopsies from prostate cancer subjects were reacted with monoclonal antibodies against BSP, DMP1, DSPP and OPN (Figure 2). Positive immunoreactivity, as indicated by pinkish-red color development, was observed for these four SIBLINGs, consistent with the expression data. Immunoreactive staining for MEPE was not detectable in the prostate cancer biopsy sections (data not shown).

SIBLINGs in serum

The levels of SIBLINGs in blood samples from a large normal group and a group with prostate cancer were then analyzed. Samples from the prostate cancer group were obtained at diagnosis and prior to treatment. Competitive ELISAs for quantitatively determining the levels of total BSP, DSPP, MEPE and OPN were developed and applied (a ELISA for DMP1 has had recurrent issues with the stability of the recombinant DMP1 protein standard). The levels of BSP, OPN and DSPP protein were elevated, though for BSP and OPN there was overlap between the high end of normal levels with the low end of the prostate cancer group (Figure 3 a - c). Mean values in prostate cancer were elevated 2-fold higher for BSP, 6-fold higher for DSPP, 1.5-fold higher for OPN, while average MEPE values were no different between cancer and normal (Table I). Receiver operator characteristic (ROC) curves yielded area under the curve (AUC) values very significant for DSPP (Figure 3 d - f).

The prostate cancer samples were evenly distributed between stages II, III and IV; where stage II cancer is localized within the prostate but palpable, stage III cancer has broken through the covering of the prostate but is still regional, and stage IV cancer has

spread to other tissues. When the distribution of BSP, OPN and DSPP were profiled by stage using Tukey box plots, discrete patterns were observed (Figure 4 a - c). Both BSP and OPN only significantly increased in late stage disease, while DSPP was elevated from stage II onward. Because PSA is used as a screening tool for prostate cancer, the levels of PSA were determined and compared with SIBLING values for subjects with prostate cancer (Figure 4 d - f). The correlation between SIBLING and PSA was tested by Spearman correlation given the non-parametric distribution of PSA. The serum levels of OPN were significantly positively correlated with total PSA levels, Spearman $r = 0.72$, $p < 0.0001$; while the levels of BSP and DSPP were not significantly correlated with PSA values.

OPN apparently exists in both free and bound forms in serum and plasma as a number of studies have measured OPN directly in plasma/serum without pretreatment of the sample with reducing or chaotropic agents to disrupt binding (26-33). A subset of normal and prostate cancer subjects ($n = 50$) had blood specimens processed appropriately for measuring free OPN. The average level of free OPN accounted for 13 % of total OPN in normal samples and 23% of total OPN in prostate cancer samples (Table I). Free OPN in prostate cancer samples were 3-fold higher then in normal samples (Figure 5a). ROC curve analysis revealed that free OPN had a better discriminatory power then total OPN (Figure 5b). Free OPN also yielded an average increase in levels across all stages, in contrast to total OPN (Figure 5c). Free OPN exhibited a significant correlation with PSA, Spearman $r = 0.71$, $p < 0.0001$, similar to

that observed for total OPN (Figure 5d). Finally, free and total OPN were found to be significantly correlated as assessed by Spearman correlation, $r = 0.47$, $p < 0.005$.

Besides skeletal tissue and tumors, OPN is also expressed by macrophages (34, 35). The contribution of chronic immune activation/inflammation to prostate tumor progression is an area of considerable interest (36). The possibility that elevations in SIBLINGs (and in the very least OPN) were associated with macrophage recruitment and infiltration into tumors was investigated by testing for correlation between a marker of macrophage activation, neopterin, and SIBLINGs. The correlation between SIBLING and neopterin was tested by Spearman correlation given the non-parametric distribution of neopterin (37). Neither BSP or DSPP were significantly associated with neopterin levels (data not shown). The levels of total and free OPN were significantly correlated with neopterin levels, with total OPN yielding a Spearman r value of 0.41, $p < 0.05$ and free OPN yielding a Spearman r value of 0.78, $p < 0.0001$.

Confirmation of serum DSPP levels by another method.

The gene transcript for DSPP yields a precursor protein that is processed into two distinct proteins, dentin sialoprotein (DSP) and dentin phosphoprotein (DPP) (38). In order to verify elevated levels of the SIBLING DSPP in serum from subjects with prostate cancer and to identify the molecular form of DSPP present, western blotting was performed. Serum samples from normal donors and subjects with prostate cancer were resolved by SDS-PAGE using 4 to 20% acrylamide gradient gels following sample reduction, transferred to nitrocellulose membranes and probed with an anti-DSP polyclonal antibody. Sera derived from prostate cancer patients consistently exhibited

robust staining and a three band pattern of (panels a – e) of immunoreactive material. In contrast, normal serum (panel f) stained lighter at an equivalent exposure time and did not exhibit the pattern of fragments (Figure 7).

Discussion

Prostate cancer is the most common type of cancer in men in the United States, other than skin cancer (39). Prostate cancer accounts for over a quarter of all cancers in men, occurs mostly in older men, and the risk increases with age (1). There has been an increase in the incidence of prostate cancer since the early 1980's, most likely due to an increased use of screening using the PSA test (40). However, the role of screening for prostate cancer remains controversial.

The prevention of cancer would be greatly facilitated by the availability of a sensitive and specific screening method that could detect the cancer. One approach to developing markers for the detection of cancer has been to identify specific cellular products that correlate with appearance of a specific neoplasm. Although specificity can be targeted by determining an individual neoplastic profile, there are steps and pathways shared by many different neoplasms that arise from different tissue types. To survive nascent neoplasms must overcome proliferation blockades, growth restriction, physical barrier, and host defense systems. Perturbations in somatic cell division capacity (telomere length and telomerase activity), cell cycle checkpoint regulators (p16), DNA repair versus apoptosis switches (p53), and the induction of proteases (urokinase

plasminogen activator, plasmin and matrix metalloproteinases) may be considered paradigms of generalized markers applicable to prostate cancer (41-45).

SIBLINGs, through their interactions with multiple binding partners such as proteases and cell surface receptors, have biological plausibility to be playing an active role in tumor progression (10). Different cancer types exhibit different patterns of individual SIBLING expression (14) as well as serum SIBLING protein levels (17). A number of separate studies have investigated BSP and OPN levels in prostate cancer. Increased BSP expression in prostate carcinoma has been associated with tumour progression and poor prognosis (23). Induced OPN expression and a positive correlation between OPN expression and poor prognosis has also been observed (46, 47). Both BSP and OPN protein levels in serum were found to be elevated in prostate cancer (17). Relative levels of DSPP as measured by immunohistochemistry were associated with the pathological stage and the Gleason score of the tumors (25). The distribution of DMP1 and MEPE in prostate cancer have not been previously reported.

The expression of SIBLINGs by prostate (and breast) carcinoma prompted the hypothesis that osteotropic cancer cells express osteomimetic properties that favor "seeding" in the skeleton by improving their adhesion, proliferation, and/or survival in bone (48). The expression of these 'bone' proteins by prostate tumor cells do not necessarily target cell metastasis to bone. It is also possible that transcription factors that regulate SIBLINGs (e.g. RUNX2) produce a mesenchymal phenotype that finds bone a fertile soil for survival. In the current study, the total serum levels of BSP and OPN were

found to be significantly elevated only in late stage prostate cancer. While free OPN levels increased significantly from stage II through stage IV, the positive association of both free and total OPN levels with the activated macrophage marker neopterin suggest that OPN levels may be reflecting immune responses in the prostate and not necessarily tumor cell activity. Similarly, the correlation of OPN with serum PSA levels may be indicative of inflammation and not tumor pathology (49, 50).

While there was overlap between the high end of normal BSP and OPN levels with low end of prostrate group, the SIBLING DSPP exhibited the greatest difference between normal sera and sera derived from prostrate cancer subjects. DSPP was initially characterized through the isolation of one of its cleavage products from dentin (51). Subsequent cloning of the gene revealed that the transcript encodes dentin sialoprotein (DSP) and dentin phosphoprotein (DPP) (38). DSP has been hypothesized to be an important factor in dentinogenesis, while DPP may be involved in dentin biomineralization (52). Elevated DSPP expression has been observed in a subset of breast and lung cancers (14) as well as in prostate cancer (25). The antibodies used in immunohiostochemical staining, competitive ELISA and western blotting recognize the DSP portion of DSPP. It is of note that western blotting of sera derived from prostrate cancer patients revealed a three band fragmentation of DSPP that was not detectable in the normal population. Proteolytic processing of DSPP by MMP-2, MMP-20 and kallikrein-related peptidase 4 (KLK4) has been reported (53) and upregulation of both MMP-2 and KLK4 in prostate cancer have been observed (45, 54).

Observations of current study are consistent with SIBLING levels being associated with tumor progression and suggest that SIBLINGs, particularly DSPP, may be developed as informative serum biomarkers. The lack of correlation of DSPP serum levels with PSA values suggests that the two markers might complement each other in increasing sensitivity and specificity. The current study provides evidence in support of future studies screening a large patient population as well as testing baseline value association with disease outcome and response to treatment to determine the utility of this new serum biomarker for prostate cancer detection.

Table I. SIBLING protein levels in prostate cancer.

	NL	PCA
N	110	110
Age (years)	65 ± 10	63 ± 5
BMI (kg/m^2)	23.1 ± 2.6	25.0 ± 4.1
BSP (ng/ml)	114 ± 63	222 ± 98
DSPP (ng/ml)	242 ± 122	1500 ± 495
MEPE (ng/ml)	93 ± 19	80 ± 11
OPN (ng/ml)	353 ± 130	546 ± 170
free OPN (ng/ml)	45 ± 20	127 ± 80
(n = 50 each group)		

FIGURE LEGENDS

Figure 1. SIBLING expression in normal prostate and prostate tumor biopsies. A cancer profiling array was hybridized with cDNA probes for SIBLINGs. The arrays contained samples from paired normal and prostate tumor tissue mRNA from individual subjects. The amount of hybridized probe for BSP, DMP1, DSPP, MEPE and OPN was (a) visualized by PhosphorImager, digitized and quantified by ImageQuant software and the (b) average relative expression levels in normal prostate (NL) and prostate tumor (PCA) determined. Values depicted represent mean ± standard deviation.

Figure 2. Serial sections of biopsies from prostate cancer subjects were immuno-reacted with monoclonal antibodies against the SIBLINGs (a) BSP, (b) DMP1, (c) DSPP and (e) OPN. The pinkish-red color indicates positive immuno-reactivity. All four SIBLINGs exhibit positive staining to varying degrees.

Figure 3. Serum levels of SIBLINGs in prostate cancer sera. Serum levels of total (a) (BSP), (b) OPN, and (c) DSPP in samples from normal subjects (NL) and subjects with diagnosed prostate cancer (PCA) were quantified using competitive ELISAs following sample extraction and clean-up. The solid bar represents mean values. Receiver Operator Characteristic plots and the area under the curve (AUC) were determined for (d) BSP, (e) DSPP and (f) OPN.

Figure 4. Serum SIBLINGs and prostate cancer stage. The distribution of SIBLING values between cancer stages was compared for (a) BSP, (b) OPN and (c) DSPP by box and whiskers plots. In Tukey plots, the box frame defines the lower and upper quartile, the whiskers depict 1.5 x the interquartile range, the line within the box marks the median value and the solid circles represent outliers. Differences between normal and prostate cancer stages were tested by student's t-test. Paired values of SIBLINGs with PSA for each subject were plotted for (d) BSP, (e) OPN and (f) DSPP. *, $p < 0.05$, **, $p < 0.01$, ***, $p < 0.0001$, n.s., not significant.

Figure 5. Free OPN levels in prostate cancer. (a) A subset of normal subjects (NL) and subjects with diagnosed prostate cancer (PCA) had appropriate plasma samples that were analyzed for free OPN and the distribution and mean was determined. (b) Receiver Operator Characteristic plots and the area under the curve (AUC) were determined. The distribution of free OPN values between cancer stages was compared by Tukey box plots, and (d) paired values for free OPN and PSA were plotted.

Figure 6. Osteopontin and macrophage activation. The levels of (a) total OPN and (b) free OPN were plotted as a function of serum levels of the macrophage marker neopterin.

Figure 7. Western blot analysis of serum for immunoreactive DSPP. Serum samples were resolved by SDS-PAGE 4 to 20% acrylamide gradient gels following sample reduction. An anti-DSPP polyclonal antibody was employed as the primary antibody. Sera derived from prostate cancer patients consistently exhibited robust staining and multiple (fragments) (panels a – e) of immunoreactive material. In contrast, normal serum (panel

f) stained lighter at an equivalent exposure time and did not exhibit the pattern of fragments.

1. Ries LAG, Melbert D, Krapcho M, et al. SEER Cancer Statistics Review, 1975-2005. 2008 [cited 2008 12/20/2008]; Available from: http://seer.cancer.gov/statfacts/html/prost.html, based on November 2007 SEER data submission, posted to the SEER web site, 2008

2. Maattanen L, Hakama M, Tammela TL, et al. Specificity of serum prostate-specific antigen determination in the Finnish prostate cancer screening trial. Br J Cancer 2007; 96:56-60.

3. Perrotti M. Understanding PSA and prostate cancer risk assessment. N J Med 2001; 98:35-8.

4. Altwein J, Ekman P, Barry M, et al. How is quality of life in prostate cancer patients influenced by modern treatment? The Wallenberg Symposium. Urology 1997; 49:66-76.

5. Fisher LW, Fedarko NS. Six genes expressed in bones and teeth encode the current members of the SIBLING family of proteins. Connect Tissue Res 2003; 44 Suppl 1:33-40.

6. Fisher LW, Jain A, Tayback M, Fedarko NS. Small Integrin Binding LIgand N-linked Glycoprotein (SIBLING) gene family expression in different cancers. Clin Can Res 2004; 10:8501-11.

7. Fedarko NS, Jain A, Karadag A, Fisher LW. Three small integrin binding ligand N-linked glycoproteins (SIBLINGs) bind and activate specific matrix metalloproteinases. Faseb J 2004; 18:734-6.

8. Jain A, Fisher LW, Fedarko NS. Bone sialoprotein binding to matrix metalloproteinase-2 alters enzyme inhibition kinetics. Biochemistry 2008; 47:5986-95.

9. Coussens LM, Fingleton B, Matrisian LM. Matrix metalloproteinase inhibitors and cancer: trials and tribulations. Science 2002; 295:2387-92.

10. Bellahcene A, Castronovo V, Ogbureke KU, Fisher LW, Fedarko NS. Small integrin-binding ligand N-linked glycoproteins (SIBLINGs): multifunctional proteins in cancer. Nat Rev Cancer 2008; 8:212-26.

11. Fisher LW, McBride OW, Termine JD, Young MF. Human bone sialoprotein. Deduced protein sequence and chromosomal localization. J Biol Chem 1990; 265:2347-51.

12. Oldberg A, Franzen A, Heinegard D. Cloning and sequence analysis of rat bone sialoprotein (osteopontin) cDNA reveals an Arg-Gly-Asp cell-binding sequence. Proc Natl Acad Sci U S A 1986; 83:8819-23.

13. Hirst KL, Ibaraki-O'Connor K, Young MF, Dixon MJ. Cloning and expression analysis of the bovine dentin matrix acidic phosphoprotein gene. J Dent Res 1997; 76:754-60.

14. Fisher LW, Jain A, Tayback M, Fedarko NS. Small integrin binding ligand N-linked glycoprotein gene family expression in different cancers. Clin Cancer Res 2004; 10:8501-11.

15. de Vega S, Iwamoto T, Nakamura T, et al. TM14 is a new member of the fibulin family (fibulin-7) that interacts with extracellular matrix molecules and is active for cell binding. J Biol Chem 2007; 282:30878-88.

16. Ogbureke KU, Fisher LW. Expression of SIBLINGs and their partner MMPs in salivary glands. J Dent Res 2004; 83:664-70.

17. Fedarko NS, Jain A, Karadag A, Van Eman MR, Fisher LW. Elevated serum bone sialoprotein and osteopontin in colon, breast, prostate, and lung cancer. Clin Cancer Res 2001; 7:4060-6.

18. Jain A, Fedarko NS, Collins MT, et al. Serum levels of matrix extracellular phosphoglycoprotein (MEPE) in normal humans correlate with serum phosphorus,

parathyroid hormone and bone mineral density. J Clin Endocrinol Metab 2004; 89:4158-61.

19. Jain A, Karadag A, Fohr B, Fisher LW, Fedarko NS. Three SIBLINGs (small integrin-binding ligand, N-linked glycoproteins) enhance factor H's cofactor activity enabling MCP-like cellular evasion of complement-mediated attack. J Biol Chem 2002; 277:13700-8.

20. Fedarko NS, Fohr B, Robey PG, Young MF, Fisher LW. Factor H binding to bone sialoprotein and osteopontin enables tumor cell evasion of complement-mediated attack. J Biol Chem 2000; 275:16666-72.

21. Fisher LW, Torchia DA, Fohr B, Young MF, Fedarko NS. Flexible structures of SIBLING proteins, bone sialoprotein, and osteopontin. Biochem Biophys Res Commun 2001; 280:460-5.

22. Hotte SJ, Winquist EW, Stitt L, Wilson SM, Chambers AF. Plasma osteopontin: associations with survival and metastasis to bone in men with hormone-refractory prostate carcinoma. Cancer 2002; 95:506-12.

23. Waltregny D, Bellahcene A, Van Riet I, et al. Prognostic value of bone sialoprotein expression in clinically localized human prostate cancer. J Natl Cancer Inst 1998; 90:1000-8.

24. Tozawa K, Yamada Y, Kawai N, Okamura T, Ueda K, Kohri K. Osteopontin expression in prostate cancer and benign prostatic hyperplasia. Urol Int 1999; 62:155-8.

25. Chaplet M, Waltregny D, Detry C, Fisher LW, Castronovo V, Bellahcene A. Expression of dentin sialophosphoprotein in human prostate cancer and its correlation with tumor aggressiveness. Int J Cancer 2006; 118:850-6.

26. Bautista DS, Saad Z, Chambers AF, et al. Quantification of osteopontin in human plasma with an ELISA: basal levels in pre- and postmenopausal women. Clin Biochem 1996; 29:231-9.

27. Bramwell VH, Doig GS, Tuck AB, et al. Serial plasma osteopontin levels have prognostic value in metastatic breast cancer. Clin Cancer Res 2006; 12:3337-43.

28. Petrik D, Lavori PW, Cao H, et al. Plasma osteopontin is an independent prognostic marker for head and neck cancers. J Clin Oncol 2006; 24:5291-7.

29. Ramankulov A, Lein M, Kristiansen G, Loening SA, Jung K. Plasma osteopontin in comparison with bone markers as indicator of bone metastasis and survival outcome in patients with prostate cancer. Prostate 2007; 67:330-40.

30. Ramankulov A, Lein M, Kristiansen G, Meyer HA, Loening SA, Jung K. Elevated plasma osteopontin as marker for distant metastases and poor survival in patients with renal cell carcinoma. J Cancer Res Clin Oncol 2007; 133:643-52.

31. Wu CY, Wu MS, Chiang EP, et al. Elevated plasma osteopontin associated with gastric cancer development, invasion and survival. Gut 2007; 56:782-9.

32. Kadkol SS, Lin AY, Barak V, et al. Osteopontin expression and serum levels in metastatic uveal melanoma: a pilot study. Invest Ophthalmol Vis Sci 2006; 47:802-6.

33. Martinetti A, Bajetta E, Ferrari L, et al. Osteoprotegerin and osteopontin serum values in postmenopausal advanced breast cancer patients treated with anastrozole. Endocr Relat Cancer 2004; 11:771-9.

34. McKee MD, Nanci A. Secretion of Osteopontin by macrophages and its accumulation at tissue surfaces during wound healing in mineralized tissues: a potential requirement for macrophage adhesion and phagocytosis. Anat Rec 1996; 245:394-409.

35. O'Brien ER, Garvin MR, Stewart DK, et al. Osteopontin is synthesized by macrophage, smooth muscle, and endothelial cells in primary and restenotic human coronary atherosclerotic plaques. Arterioscler Thromb 1994; 14:1648-56.

36. Haverkamp J, Charbonneau B, Ratliff TL. Prostate inflammation and its potential impact on prostate cancer: a current review. J Cell Biochem 2008; 103:1344-53.

37. Punjabi NM, Beamer BA, Jain A, Spencer ME, Fedarko N. Elevated levels of neopterin in sleep-disordered breathing. Chest 2007; 132:1124-30.

38. MacDougall M, Simmons D, Luan X, Nydegger J, Feng J, Gu TT. Dentin phosphoprotein and dentin sialoprotein are cleavage products expressed from a single transcript coded by a gene on human chromosome 4. Dentin phosphoprotein DNA sequence determination. J Biol Chem 1997; 272:835-42.

39. Brawley OW, Barnes S. The epidemiology of prostate cancer in the United States. Semin Oncol Nurs 2001; 17:72-7.

40. Pashayan N, Powles J, Brown C, Duffy SW. Incidence trends of prostate cancer in East Anglia, before and during the era of PSA diagnostic testing. Br J Cancer 2006; 95:398-400.

41. Botchkina GI, Kim RH, Botchkina IL, Kirshenbaum A, Frischer Z, Adler HL. Noninvasive detection of prostate cancer by quantitative analysis of telomerase activity. Clin Cancer Res 2005; 11:3243-9.

42. Chakravarti A, DeSilvio M, Zhang M, et al. Prognostic value of p16 in locally advanced prostate cancer: a study based on Radiation Therapy Oncology Group Protocol 9202. J Clin Oncol 2007; 25:3082-9.

43. Cozzi PJ, Wang J, Delprado W, et al. Evaluation of urokinase plasminogen activator and its receptor in different grades of human prostate cancer. Hum Pathol 2006; 37:1442-51.

44. Downing SR, Russell PJ, Jackson P. Alterations of p53 are common in early stage prostate cancer. Can J Urol 2003; 10:1924-33.

45. Zeng H, Xiao Y, Lu G, Chen Y. Immunohistochemical studies of the expression of matrix metalloproteinase-2 and metalloproteinase-9 in human prostate cancer. J Huazhong Univ Sci Technolog Med Sci 2003; 23:373-4, 9.

46. Forootan SS, Foster CS, Aachi VR, et al. Prognostic significance of osteopontin expression in human prostate cancer. Int J Cancer 2006; 118:2255-61.

47. Khodavirdi AC, Song Z, Yang S, et al. Increased expression of osteopontin contributes to the progression of prostate cancer. Cancer Res 2006; 66:883-8.

48. Koeneman KS, Yeung F, Chung LW. Osteomimetic properties of prostate cancer cells: a hypothesis supporting the predilection of prostate cancer metastasis and growth in the bone environment. Prostate 1999; 39:246-61.

49. Banu NA, Azim FA, Kamal M, Rumi MA, Barua AR, Khan KH. Inflammation and glandular proliferation in hyperplastic prostates: association with prostate specific antigen value. Bangladesh Med Res Counc Bull 2001; 27:79-83.

50. Loeb S, Gashti SN, Catalona WJ. Exclusion of inflammation in the differential diagnosis of an elevated prostate-specific antigen (PSA). Urol Oncol 2009; 27:64-6.

51. Veis A, Perry A. The phosphoprotein of the dentin matrix. Biochemistry 1967; 6:2409-16.

52. Qin C, Baba O, Butler WT. Post-translational modifications of sibling proteins and their roles in osteogenesis and dentinogenesis. Crit Rev Oral Biol Med 2004; 15:126-36.

53. Yamakoshi Y, Hu JC, Iwata T, Kobayashi K, Fukae M, Simmer JP. Dentin sialophosphoprotein is processed by MMP-2 and MMP-20 in vitro and in vivo. J Biol Chem 2006; 281:38235-43.

54. Xi Z, Klokk TI, Korkmaz K, et al. Kallikrein 4 is a predominantly nuclear protein and is overexpressed in prostate cancer. Cancer Res 2004; 64:2365-70.

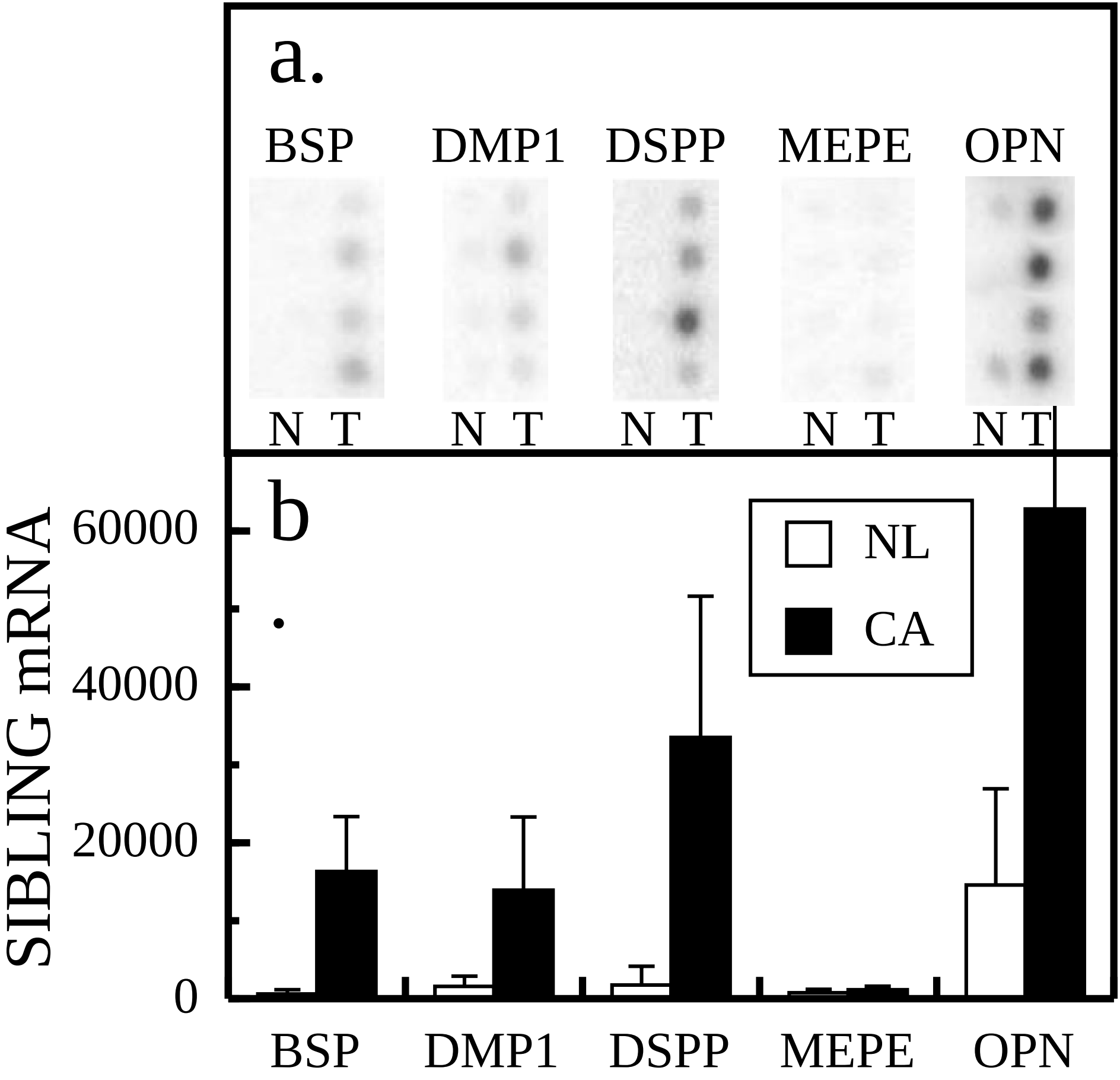
a.
BSP
DMP1
DSPP
MEPE
OPN
N T
N T
N T
N T
N T
b
NL
CA
SIBLING mRNA
60000
40000
20000
0
BSP
DMP1
DSPP
MEPE
OPN

BSP

DMP

DSPP

OPN

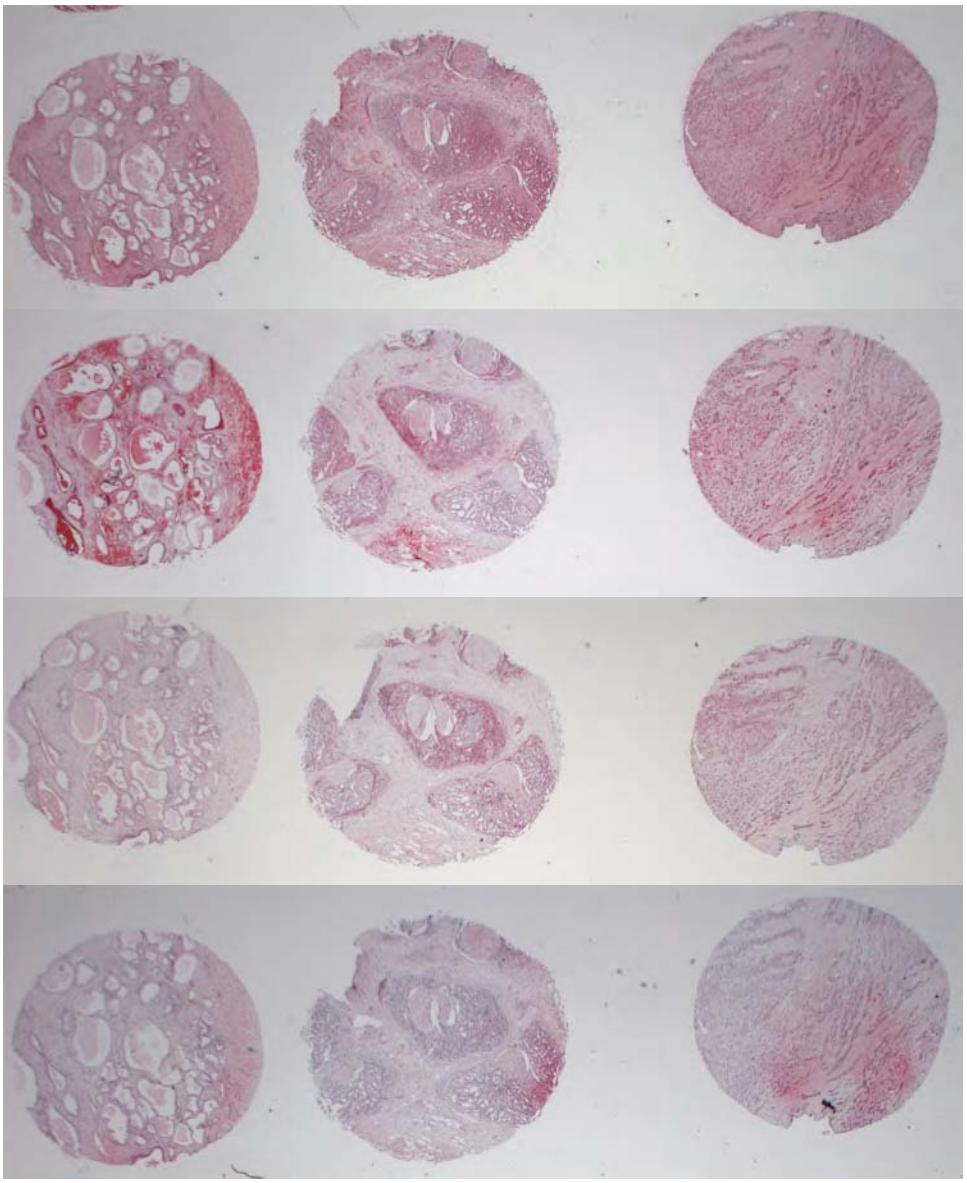

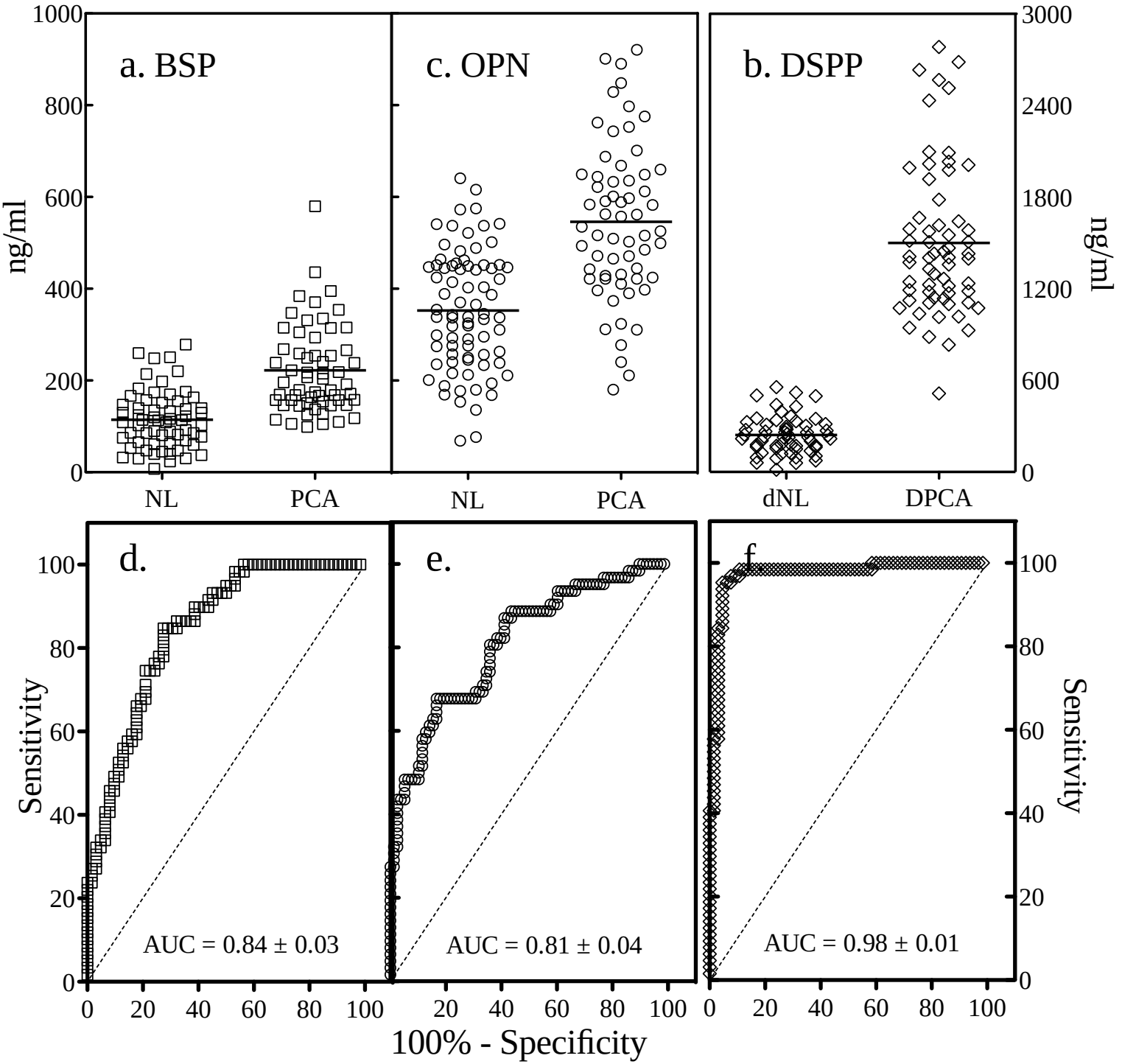
a. BSP
c. OPN
b. DSPP
ng/ml
ng/ml
1000
800
600
400
200
0
3000
2400
1800
1200
600
0
NL
PCA
NL
PCA
dNL
DPCA
d.
e.
f
Sensitivity
Sensitivity
100
80
60
40
20
0
AUC = 0.84 ± 0.03
AUC = 0.81 ± 0.04
AUC = 0.98 ± 0.01
0
20
40
60
80
100
100% - Specificity

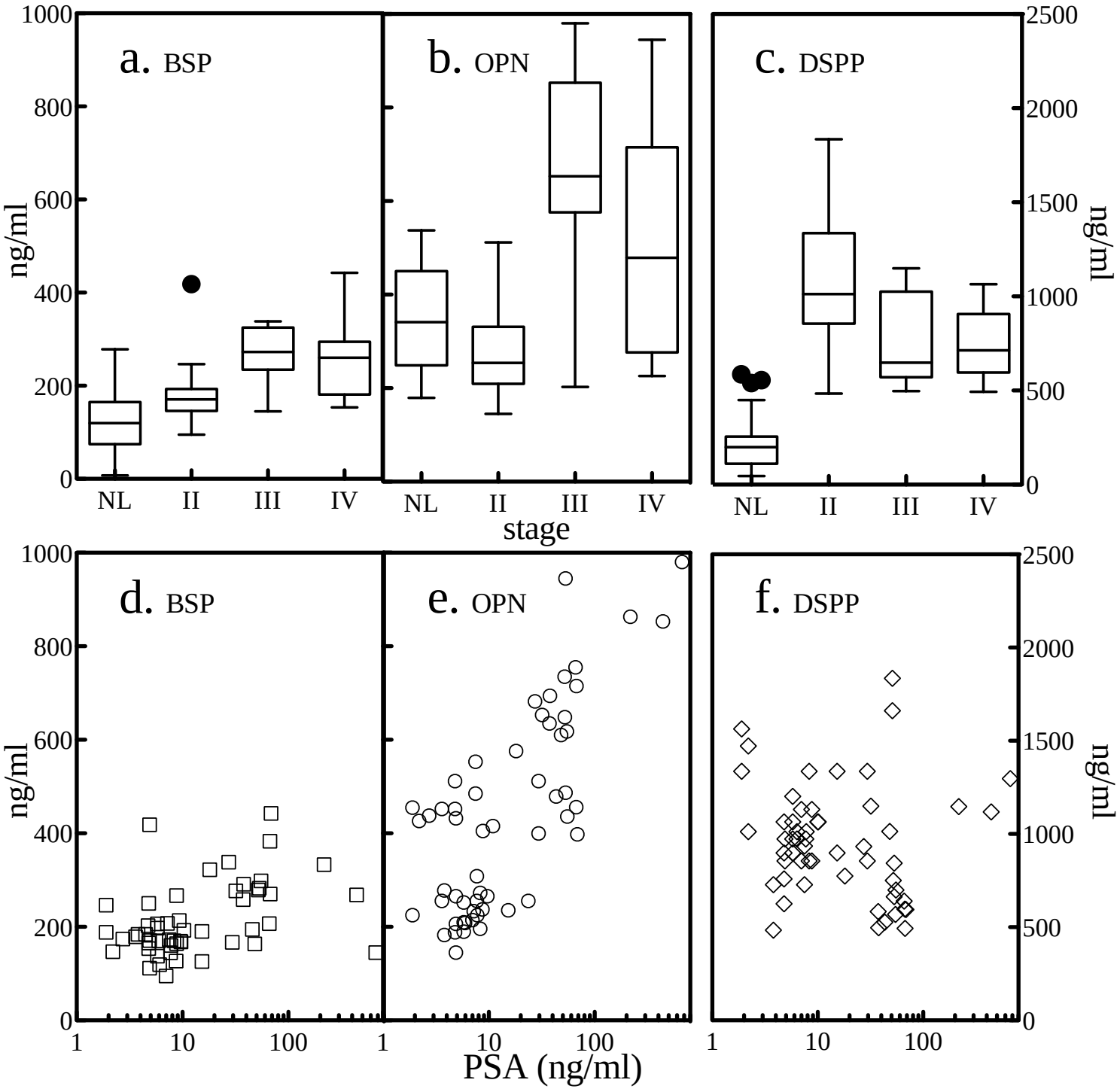
a. BSP
b. OPN
c. DSPP
ng/ml
ng/ml
1000
800
600
400
200
0
2500
2000
1500
1000
500
0
NL
II
III
IV
stage
d. BSP
e. OPN
f. DSPP
1
10
100
PSA (ng/ml)

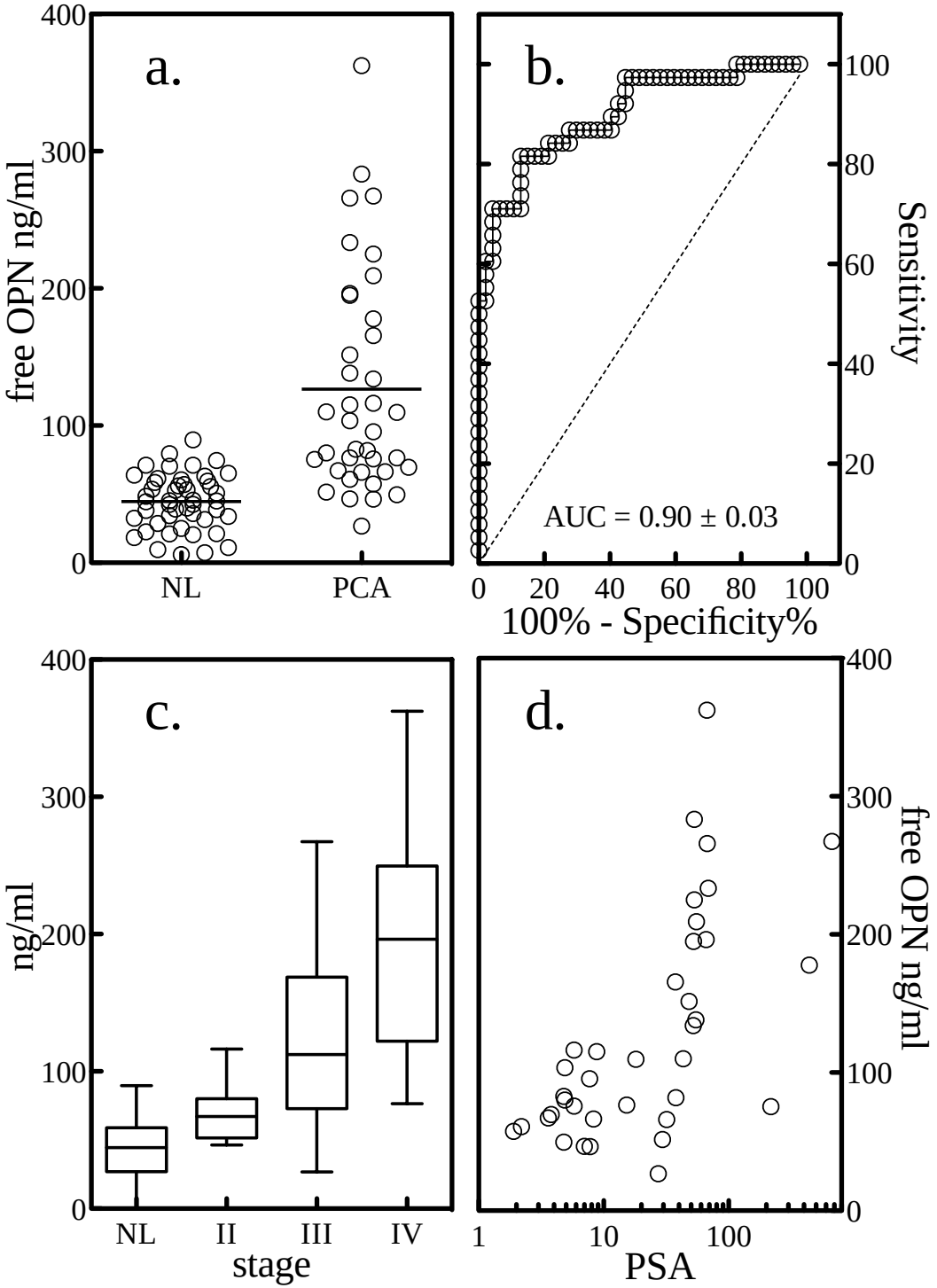
a.
b.
c.
d.
free OPN ng/ml
400
300
200
100
0
NL
PCA
Sensitivity
100
80
60
40
20
0
AUC = 0.90 ± 0.03
0
20
40
60
80
100
100% - Specificity%
ng/ml
NL
II
III
IV
stage
1
10
100
PSA

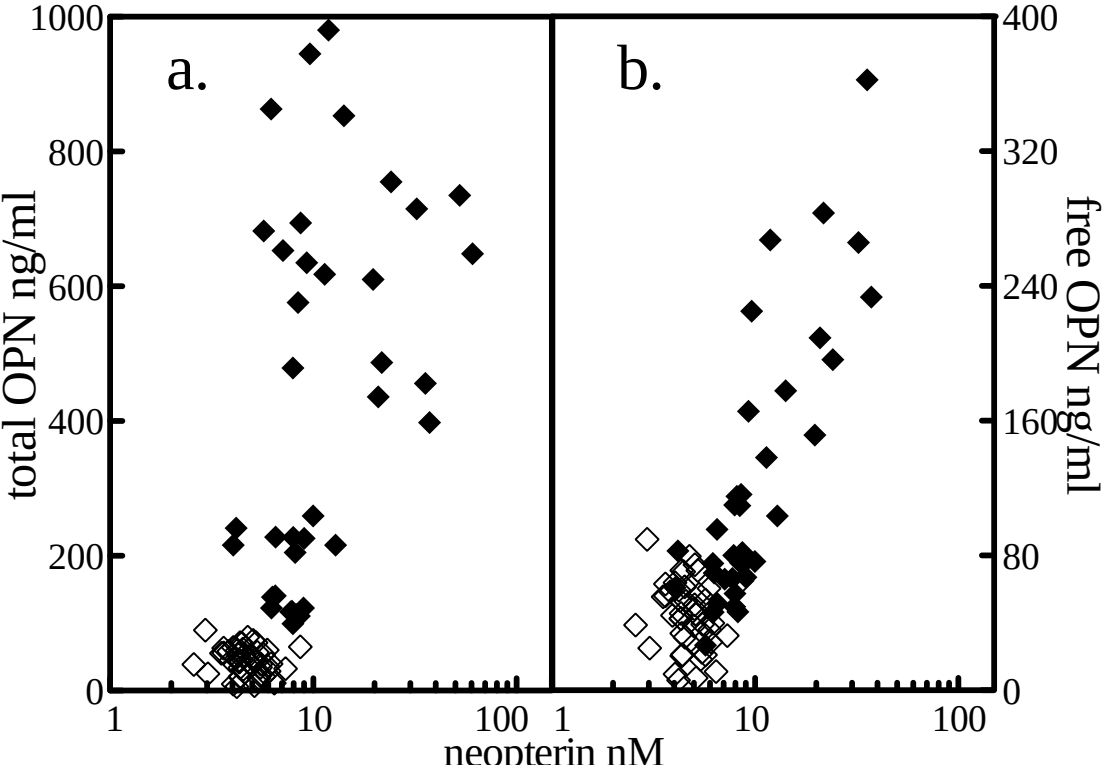
a.
b.
1000
800
600
400
200
0
400
320
240
160
80
0
total OPN ng/ml
free OPN ng/ml
1
10
100
1
10
100
neopterin nM

a DSPP in PCA #01-12

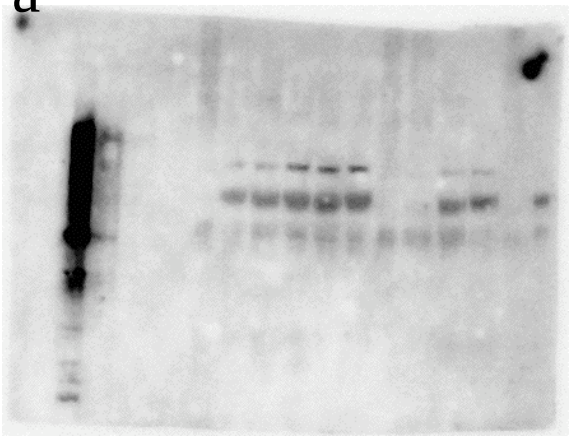

b DSPP in PCA #13-26

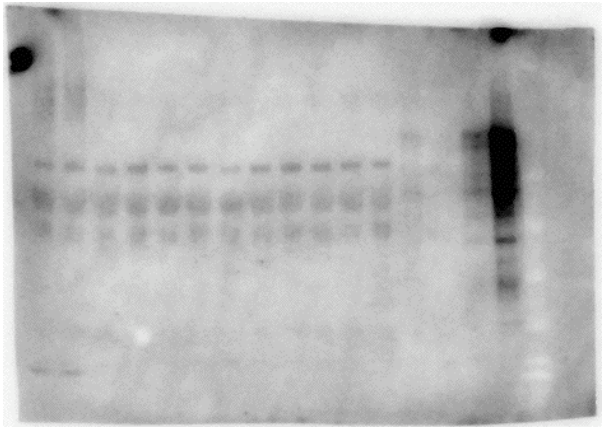

c DSPP in PCA #27-41

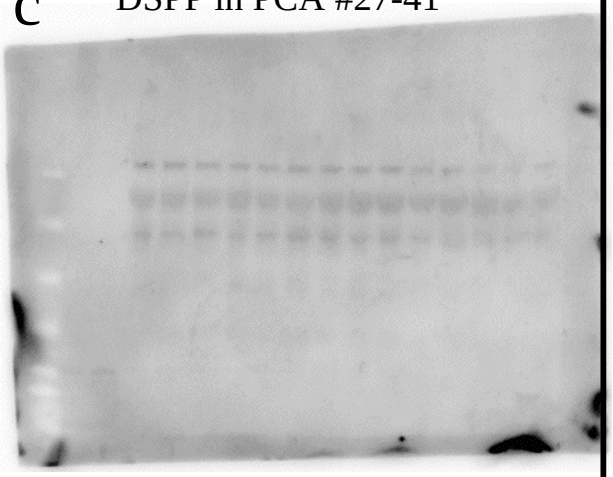

d DSPP in PCA#42-55

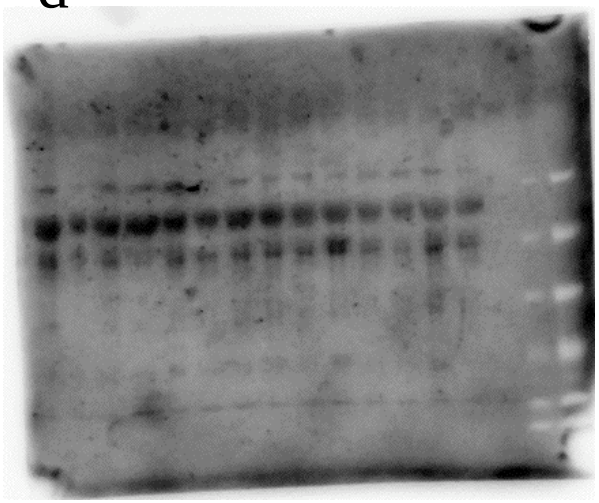

e DSPP in PCA #56-69

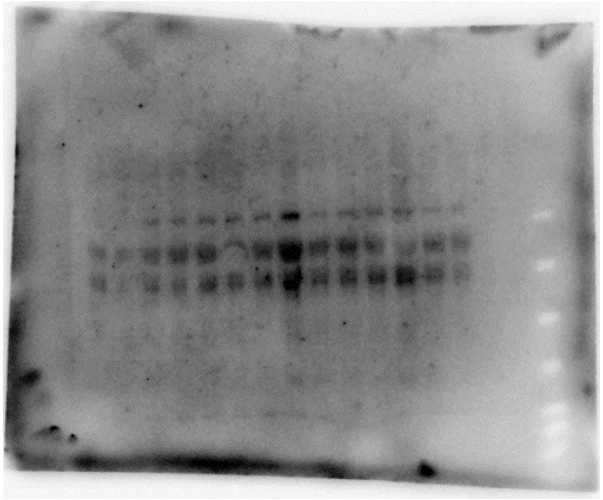

f DSPP in NL #1-10

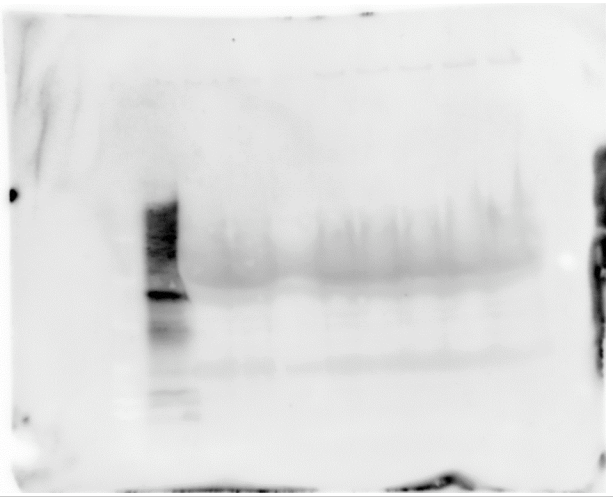

OXFORD UNIVERSITY PRESS
Journal of Gerontology: Medical Sciences

Associations of age, gender, BMI and disease stage with serum levels of the immune activation marker neopterin.

Journal:	*Journal of Gerontology: Medical Sciences*
Manuscript ID:	draft
Manuscript Type:	Research
Date Submitted by the Author:	n/a
Complete List of Authors:	Spencer, Monique; University of Maryland, Medicine Jain, Alka; Medicine/ Geriatric Medicine, The Johns Hopkins Medical Institution Beamer, Brock; Medicine/ Geriatric Medicine, The Johns Hopkins Medical Institution Leng, Sean; Medicine/ Geriatric Medicine, The Johns Hopkins Medical Institution Matteini, Amy; Medicine/ Geriatric Medicine, The Johns Hopkins Medical Institution Punjabi, Naresh; Johns Hopkins Medicial Institution, Medicine/Pulmonary Medicine Walston, Jeremy; Medicine/ Geriatric Medicine, The Johns Hopkins Medical Institution Fedarko, Neal; Medicine, Division of Geriatrics, Johns Hopkins University
Keywords:	aging, immune activation, cancer

Associations of age, gender, BMI and disease stage with serum levels of the immune activation marker neopterin.

Monique E. Spencer, B.S.[1,3,4]

Alka Jain, PhD [1,4]

Brock A. Beamer, M.D.[1]

Sean X. LengM.D., Ph.D.[1]

Amy Matteini, Ph.D.[1]

Naresh M. Punjabi M.D., Ph.D.[2]

Jeremy D. Walston, M.D. [1]

Neal S. Fedarko Ph.D.[1]

[1] Biology of Frailty Program, Division of Geriatric Medicine & Gerontology, Johns Hopkins University, Baltimore, MD

[2] Division of Pulmonary Medicine, Department of Medicine, Johns Hopkins University, Baltimore, MD

[3] Current address: University of Maryland, School of Medicine, Baltimore, MD

[4] Contributed equally to this work.

Corresponding author:

Neal S. Fedarko

Room 5A-64 JHAAC

5501 Hopkins Bayview Circle

Baltimore, MD 21224

ndarko@jhmi.edu

phone: (410) 550-2632

fax: 410 550 1007

Running Title: Aging, immune activation and cancer.

Total word count = 4,338

Text only word count = 2,585

ABSTRACT

Background. Instead of maintaining organ and organismal optimal function, homeostatic mechanisms, in the setting of advanced age or certain disease states, can contribute to pathology and disease progression. Neopterin, a guanosine triphosphate metabolite expressed by macrophages, is a marker of immune activation. The current study was undertaken to measure immune activation, testing for associations with age, gender, BMI, disease state and stage.

Methods. Three distinct groups were studied: healthy lean subjects between the ages of 20 and 87, subjects with BMI values in the obese range, and subjects newly diagnosed with cancer. Neopterin concentrations were measured by competitive ELISA. Values were compared by a Mann Whitney t-test, the paired associations between neopterin and age, or BMI were analyzed by Spearman correlation, while overall associations were modeled by multiple regression of neopterin as a function of age, gender, BMI, and disease status.

*Results***.** In healthy subjects, neopterin levels differed by gender and increased with increasing age for both men and women. Obesity was associated with significantly increased neopterin levels. In the cancer group, neopterin was elevated and correlated with cancer type and stage.

Conclusion. Because neopterin functions in immune modulation, the observed changes in circulating levels of this biomarker are consistent with a role for immune activation in aging, obesity, and cancer. The association of age, gender and BMI with neopterin levels in normal physiological events (aging) and in pathological states (obesity and cancer)

reflects the biology underlying late-age onset diseases and perhaps gender differences in disease incidence.

INTRODUCTION

Immune system activation plays a central role in the aging process in normal, healthy individuals [1,2]. Neopterin, a metabolite of guanosine triphosphate, is produced in macrophages upon stimulation by interferon gamma released by activated T cells [3]. In humans, neopterin is a marker of Th1 cell mediated immune activation and macrophage activity [4]. This marker has been used clinically in the assessment of bacterial and viral infections [5,6], autoimmune diseases [7,8], sleep apnea [9], and in malignant conditions [10].

Chronic immune activation is involved in a number of diverse pathologies including AIDS [11], atherosclerosis [12], autoimmune disease [13], obesity and metabolic syndrome [14,15]. The current study was undertaken to measure neopterin, testing for associations with age, gender, BMI, disease state and stage in three distinct study populations. The three groups included a normal sample of men and women spanning a wide age range (20 to 80), an obese group, and a sample of patients with underlying malignancy. Associations between serum neopterin and age, gender, BMI, and cancer type and stage were determined.

METHODS

Subjects. Three distinct groups were studied. Sera from 161 clinically defined healthy participants between the ages of 20 and 80, with at least 10 subjects per gender per decade, (cohort 1) were obtained under IRB approved protocols from a serum bank (SeraCare Life Sciences Inc., Oceanside, CA) as well as from the Johns Hopkins Bayview Medical Center General Clinical Research Center. For this study, inclusion criteria as a normal healthy serum donor included measures within the normal range for

fasting glucose (< 100 mg/dl), TSH (0.5 - 2.1 mIU/mL), BMI (18.5- 25 kg/m^2) as well as a clinical assessment by a physician. Exclusionary criteria included a previous self-reported history of hypertension, heart disease, diabetes mellitus, dementia, renal or hepatic dysfunction, cancer, or any chronic inflammatory condition (e.g., rheumatoid arthritis).

The second group of subjects, cohort 2, were those who were otherwise healthy but were obese (BMI: 30 – 40 kg/m^2). Patients with a previous history of hypertension, angina, myocardial infarction, percutaneous transluminal coronary angioplasty, coronary artery bypass surgery, congestive heart failure, and stroke were ineligible. Other exclusionary criteria included a history of diabetes mellitus, fasting glucose > 126 mg/dl, pulmonary disease, renal or hepatic dysfunction, dementia, cancer, or any chronic inflammatory condition. The third cohort, which was obtained from a serum repository, consisted of 124 cancer subjects consisting of 66 females with breast cancer, 38 males with prostate cancer and 20 lung cancer subjects (7 female and 13 male). Blood was drawn at time of diagnosis, prior to initiation of treatment. For all three groups, use of anti-inflammatory agents (e.g., steroids) was part of the exclusion criteria. Approval for the study protocol was acquired from the local institutional review board and informed consent was obtained from all patients.

Clinical Measures. Anthropometric measures included height, weight, and waist circumference. A fasting blood sample was obtained in a resting and fasting state in the morning. All venous samples were placed at 4^{o}C prior to serum separation. After centrifugation at 3000 rpm for 20 minutes, serum was stored at -80^{o}C. Serum neopterin

was measured using a commercially available competitive ELISA (ALPCO Diagnostics, Inc.). In the laboratory, this enzyme immunoassay had a sensitivity of 0.8 nM and an inter-assay coefficient of variance of 5.29%.

Statistical Analysis. Univariate statistics of the all three samples collectively and individually were examined. Given the non-normal distribution of serum neopterin levels, group comparisons were subsequently performed using a Mann-Whitney t-test. The association of neopterin with age or BMI was analyzed using the Spearman correlation test. The Kruskal-Wallis test was employed to compare differences in neopterin levels between the three cancer types. The association of neopterin with age, gender, BMI and disease was modeled and analyzed after log transformation of neopterin levels by multiple linear regression. All statistical calculations were carried out using Prism and InStat software (GraphPad, Inc.) and StatView 5 (SAS Institute, Inc.).

RESULTS

The normal healthy cohort consisted of 161 lean subjects (n = 74 for female, n = 87 for male). The mean age was 51 ± 18 for women, 52 ± 17 for men, while the mean BMI values were 22.6 ± 1.4 and 22.1 ± 1.6 kg/m^2 for women and men, respectively. The distribution of neopterin in the serum from this cohort was right-skewed with a median of 5.13 nM (interquartile range: 4.42 – 5.81) and a mean value of 5.25 ± 1.2 nM for women and men combined. Serum neopterin levels were higher in women than men with a medium values of 5.40 versus 5.06 nM, p = 0.0052 (Figure 1b). Spearman correlation

analysis revealed that the association between age and neopterin was significant in both genders (Figure 1c). When neopterin values were stratified by gender and by decade, women exhibited statistically significant higher levels of serum neopterin than males from the fifth through seventh decades of life when compared using a Mann Whitney t-test (Figure 1d).

Multiple linear regression was employed in order to test the relative contribution of age, gender and BMI to neopterin levels in the normal healthy population. The percent of the variance in [*neopterin*] explained by the model was 47% and the variables *age*, *gender* and *BMI* all made significant contributions to the model (Table I). Effect size estimates for age and BMI were standardized to reflect the change in neopterin per a one quartile range unit change in either age or BMI. Neopterin levels increased 0.628 per interquartile range increase in age and decreased 0.167 per interquartile range increase in BMI ($p < 0.0001$). Men were observed on average to have 0.261 lower neopterin levels than women ($p < 0.0001$). The lesser impact of BMI on neopterin levels could be reflecting the relatively narrow range of BMI's in this normal weight population.

The second cohort consisted of 70 obese subjects who were otherwise healthy (n = 22 for female, n = 48 for male). The mean age was 51 ± 12 for women, 48 ± 12 for men, while the mean BMI values were 34.4 ± 2.5 and 34.4 ± 2.8 for women and men, respectively. Serum neopterin was significantly elevated in the obese population, with a mean of 7.32 ± 1.73 nM and a median of 7.38 ($p < 0.0005$ compared to cohort 1). When obese subjects were segregated by gender, the median value of neopterin in the female group (7.32) was higher then for males (6.88), though the difference was not statistically significant (Figure 2 b). When the association of age with neopterin values in the obese

population was investigated it was found to not be statistically significant by Spearman correlation (Figure 2c), suggesting that perhaps obesity saturates the signal or that there was not enough power in the obese group to look at age effects.

Combining normal and obese populations revealed a significant positive correlation of BMI with neopterin across the combined populations (Figure 2 d). The combined normal and obese populations were also modeled by multiple linear regression using log transformed neopterin values (Table I). The variance in log(neopterin) explained by a linear model with variables of *age*, *gender* and *BMI* was 39% ($p < 0.0001$). Standardized beta estimates in the combined population (cohorts 1 and 2) reflected statistically significant increases in neopterin of 0.424 and 0.514 per interquartile range increase in age and BMI, respectively. Men had 0.114 lower neopterin levels compared to women.

Sera from cohort 3, a cancer population consisting of subjects with breast, prostate or lung cancer, were analyzed for neopterin levels. The values of neopterin in the serum from all 124 cancer subjects exhibited a mean value of 15 ± 25 nM and a median value of 8.25 nM. Lung cancer subjects exhibited the highest levels of neopterin, followed by prostate cancer and then breast cancer (Figure 3a). The range of values for age (62 ± 14, 66 ± 14 and 69 ± 8 years) and BMI (24.6 ± 3.3, 25.0 ± 4.1 and 23.2 ± 4.4 kg/m^2) for the cancer subjects was not significantly different between breast, prostate and lung cancer groups, respectively. The effect of gender on neopterin levels was not assessable in the gender specific cancers (breast and prostate). However, the lung cancer group consisted of 7 female and 13 males with median neopterin values of 42.6 and 18.3 nM, respectively, and these medians were significantly different ($p < 0.05$). A Mann-

Whitney test comparing the gender-matched normal and cancer neopterin values yielded significant differences ($p < 0.0001$ for normal female versus breast cancer, normal male versus prostate cancer, and both genders of normals versus lung cancer). Neopterin values segregated by cancer type were significantly different from each other ($p < 0.0001$) when medians were compared by a Kruskal Wallis test with a Dunn's multiple comparison.

We have shown that neopterin levels have a significant positive association with age in the normal population. The influence of age on neopterin values in the cancer population was also investigated. Age was significantly correlated with serum neopterin values in breast cancer subjects as assessed by Spearman correlation (Figure 3b). Neither prostate nor lung cancer neopterin levels were correlated with age (Figure 3c).

The observation of increased neopterin levels in sera from subjects with cancer would suggest that extent of disease (staging) might be correlated with immune activation and its surrogate marker neopterin. The association of cancer stage groupings with serum neopterin values was investigated for breast and prostate cancer where sufficient numbers for comparison were present in each stage. Neopterin increased between normal and stage I breast cancer. The median value for stages I through IV increased with increasing stage (Figure 3d). Stage I and II (representing early stages of breast cancer) neopterin levels were not significantly different from the median of the normal population. The medians of neopterin in the more advanced stages (III and IV) were significantly elevated compared to the normal median value. Metastatic disease (stage IV) was significantly elevated compared with all other stages and had a median value ~2-fold higher then normal (Figure 3d).

Perhaps because of differences in screening and diagnosis, the prostate group in the cancer population consisted of stages II through IV, but no early stage (stage I) subjects. When prostate cancer was segregated by stage, a similar pattern of increasing neopterin levels with increasing stage was observed. The median values of stages II through IV were significantly different from the normal median value (Figure 3e). Among the different stages, stage II and III were significantly different from stage IV. Metastatic disease in prostate cancer was associated with a 4-fold higher median value of serum neopterin when compared to that of the normal male population.

Neopterin levels in the cancer population were also modeled by multiple linear regression. Models describing the association between the log of neopterin levels and breast or prostate cancer were adjusted for age, BMI and stage. For breast cancer, the variables *age* and *stage* contributed significantly to neopterin values (Table II) accounting for 22 % of the variance. For prostate cancer, the variables *BMI* and *stage* contributed significantly to neopterin levels, with the model accounting for 45% of neopterin variance. For both breast and prostate cancer, *stage* contributed the most to neopterin values.

DISCUSSION

Neopterin (6-D-erythro-1′,2′,3′-trihydroxypropyl-pterin) is synthesized from guanosine triphosphate (GTP) by GTP-cyclohydrolase I in response to interferon-γ (IFN-γ) stimulation of human monocytes/macrophages [16,17]. Increased concentrations of neopterin in serum have been found during viral infections, various malignant disorders and autoimmune diseases [7]. The current study demonstrates for the first time that in a well-defined normal population, serum neopterin levels vary with age and gender. The observation of an increase in neopterin production with increasing age is consistent with a number of other studies [18,19]. In general, these previous study populations compared discrete groups of young (< 40 years of age) to old (> 60 years of age). In addition, entry/enrollment criteria in those studies did not necessarily exclude diseases associated with immune activation and increased neopterin concentrations in the elderly, such as atherosclerosis [20] or dementia [21].

The current study models neopterin along a continuous aging trajectory with at least 10 subjects per gender per decade spanning the 20's to the 80's. Our normal as well as the obese group had extensive exclusion criteria to minimize confounding due to age-related conditions. It is possible that in our older normal subjects, pathological processes may have already started that are clinically latent. However, changes were observed in neopterin between relatively young ages (e.g. – third and fifth decades. A novel finding of the current study is that the changes in neopterin with age were associated with gender differences.

Median values of neopterin significantly diverge between male and female subjects beginning at a peri-menopausal age range. Estrogen has well characterized anti-inflammatory effects [22]. The reduction in estrogen with menopause may contribute to increased chronic inflammation and immune activation with an associated increase in serum neopterin levels. The effects of gender on serum neopterin may be linked to gender differences in chronic immune activation. Gender differences in susceptibility to autoimmune diseases have been observed, with women at greater risk than men of rheumatoid arthritis and multiple sclerosis [23].

Serum neopterin levels are elevated in a number of pathologies involving chronic inflammation, including alcoholic hepatitis, hepatitis B and C virus, rheumatoid arthritis, atherosclerosis, diabetes, and inflammatory bowel diseases [4]. The association of neopterin values with BMI observed in the current study including obese subjects is consistent with obesity's chronic inflammatory state and with previous studies on serum neopterin levels [9,24]. Aging also has been associated with low-level inflammation ("inflammaging" [25]), thought to lead to or exacerbate many chronic medical conditions [26,27]. The current study indicates that the effects of age and gender, which contributed significantly to serum neopterin values in the defined normal population, were diminished covariates in subjects with obesity and cancer. Presumably, this is due to greater impact of those diseases on immune and macrophage activation.

At least 15–20% of cancers are attributed to infection-mediated inflammation [28]. In the absence on infection, the tumor microenvironment itself is associated with a localized inflammatory state with altered cytokine and protease levels and activity that are thought to contribute to neoplastic progression [29]. Elevated serum neopterin levels

associated with late stage disease have been previously reported in breast [30], prostate [31] and lung cancer [32]. In our regression modeling, tumor staging as well as donor age contributed significantly to neopterin levels in breast cancer, while BMI and stage contributed significantly to neopterin levels in prostate cancer. It remains to be seen in larger cohorts whether this differential in confounders (breast cancer/age; prostate cancer/BMI) reflects biologic processes (e.g. hormonal) or only that our power did not permit breast cancer/BMI or prostate cancer/age effect to be seen. Assessing the impact of gender on neopterin levels in the setting of cancer was limited in the current study by the small number of lung cancer subjects. Gender effects could not be studied by combining cancer types, given the fundamental differences in the biology of breast and prostate tumor cell progression. The analysis of a large cancer population that includes both genders would enable a better assessment of the relative contribution of gender differences to neopterin. In conclusion, age, gender and BMI are covariates that should be assessed in any use of neopterin as a diagnostic/prognostic marker. The relative contribution of age, gender and BMI to modulating neopterin levels (a surrogate for immune activation) in normal physiological events and in pathological states reflects the biology underlying aging, late-age onset diseases and perhaps gender differences in disease incidence.

REFERENCES

1. Fulop T, Larbi A, Wikby A, Mocchegiani E, Hirokawa K, Pawelec G: Dysregulation of T-cell function in the elderly : scientific basis and clinical implications. Drugs Aging 2005;22:589-603.

2. Stout RD, Suttles J: Immunosenescence and macrophage functional plasticity: dysregulation of macrophage function by age-associated microenvironmental changes. Immunol Rev 2005;205:60-71.

3. Werner ER, Werner-Felmayer G, Fuchs D, et al.: Biochemistry and function of pteridine synthesis in human and murine macrophages. Pathobiology 1991;59:276-279.

4. Murr C, Widner B, Wirleitner B, Fuchs D: Neopterin as a marker for immune system activation. Curr Drug Metab 2002;3:175-187.

5. Denz H, Fuchs D, Hausen A, et al.: Value of urinary neopterin in the differential diagnosis of bacterial and viral infections. Klin Wochenschr 1990;68:218-222.

6. Sheldon J, Riches PG, Soni N, et al.: Plasma neopterin as an adjunct to C-reactive protein in assessment of infection. Clin Chem 1991;37:2038-2042.

7. Berdowska A, Zwirska-Korczala K: Neopterin measurement in clinical diagnosis. J Clin Pharm Ther 2001;26:319-329.

8. Nasonov EL, Samsonov M, Tilz G, Fuchs D: [Neopterin: new immunological marker of autoimmune rheumatic disease]. Klin Med (Mosk) 2000;78:43-46.

9. Punjabi NM, Beamer BA, Jain A, Spencer ME, Fedarko N: Elevated levels of neopterin in sleep-disordered breathing. Chest 2007;132:1124-1130.

10. Reibnegger G, Fuchs D, Fuith LC, et al.: Neopterin as a marker for activated cell-mediated immunity: application in malignant disease. Cancer Detect Prev 1991;15:483-490.

11. Dalgleish AG, O'Byrne KJ: Chronic immune activation and inflammation in the pathogenesis of AIDS and cancer. Adv Cancer Res 2002;84:231-276.

12. Blasi C: The autoimmune origin of atherosclerosis. Atherosclerosis 2008.

13. Vasto S, Candore G, Balistreri CR, et al.: Inflammatory networks in ageing, age-related diseases and longevity. Mech Ageing Dev 2007;128:83-91.

14. Brandacher G, Hoeller E, Fuchs D, Weiss HG: Chronic immune activation underlies morbid obesity: is IDO a key player? Curr Drug Metab 2007;8:289-295.

15. Duncan BB, Schmidt MI: Chronic activation of the innate immune system may underlie the metabolic syndrome. Sao Paulo Med J 2001;119:122-127.

16. Huber C, Batchelor JR, Fuchs D, et al.: Immune response-associated production of neopterin. Release from macrophages primarily under control of interferon-gamma. J Exp Med 1984;160:310-316.

17. Werner ER, Werner-Felmayer G, Fuchs D, et al.: Tetrahydrobiopterin biosynthetic activities in human macrophages, fibroblasts, THP-1, and T 24 cells. GTP-cyclohydrolase I is stimulated by interferon-gamma, and 6-pyruvoyl tetrahydropterin synthase and sepiapterin reductase are constitutively present. J Biol Chem 1990;265:3189-3192.

18. Diamondstone LS, Tollerud DJ, Fuchs D, et al.: Factors influencing serum neopterin and beta 2-microglobulin levels in a healthy diverse population. J Clin Immunol 1994;14:368-374.

19. Ledochowski M, Murr C, Jager M, Fuchs D: Dehydroepiandrosterone, ageing and immune activation. Exp Gerontol 2001;36:1739-1747.

20. Weiss G, Willeit J, Kiechl S, et al.: Increased concentrations of neopterin in carotid atherosclerosis. Atherosclerosis 1994;106:263-271.

21. Leblhuber F, Walli J, Demel U, Tilz GP, Widner B, Fuchs D: Increased serum neopterin concentrations in patients with Alzheimer's disease. Clin Chem Lab Med 1999;37:429-431.

22. Chakrabarti S, Lekontseva O, Davidge ST: Estrogen is a modulator of vascular inflammation. IUBMB Life 2008;60:376-382.

23. McCarthy M: The "gender gap" in autoimmune disease. Lancet 2000;356:1088.

24. Ledochowski M, Murr C, Widner B, Fuchs D: Association between insulin resistance, body mass and neopterin concentrations. Clin Chim Acta 1999;282:115-123.

25. Giunta S: Is inflammaging an auto[innate]immunity subclinical syndrome? Immun Ageing 2006;3:12.

26. Sarkar D, Fisher PB: Molecular mechanisms of aging-associated inflammation. Cancer Lett 2006;236:13-23.

27. Maggio M, Guralnik JM, Longo DL, Ferrucci L: Interleukin-6 in aging and chronic disease: a magnificent pathway. J Gerontol A Biol Sci Med Sci 2006;61:575-584.

28. Kuper H, Adami HO, Trichopoulos D: Infections as a major preventable cause of human cancer. J Intern Med 2000;248:171-183.

29. Aggarwal BB, Shishodia S, Sandur SK, Pandey MK, Sethi G: Inflammation and cancer: how hot is the link? Biochem Pharmacol 2006;72:1605-1621.

30. Yildirim Y, Gunel N, Coskun U, Pasaoglu H, Aslan S, Cetin A: Serum neopterin levels in patients with breast cancer. Med Oncol 2008.

31. Lewenhaupt A, Ekman P, Eneroth P, Nilsson B: Tumour markers as prognostic aids in prostatic carcinoma. Br J Urol 1990;66:182-187.

32. von Ingersleben G, Souchon R, Fitzner R: Serum neopterin levels in lung and breast cancer patients undergoing radiotherapy and/or chemotherapy. Int J Biol Markers 1988;3:135-139.

ACKNOWLEDGEMENTS

This research was supported by NIH grant CA 87311 (N.S.F.), Department of Defense grants W81XWH-04-1-0844 (N.S.F.) and DAMD17-02-0684 (N.S.F.). M.E.S. was supported by grant T35 AG026758 and the Medical Student Training in Aging Research Program run jointly by American Federation on Aging Research and the John A. Hartford Foundation.

Table I. Neopterin Multiple Linear Regression of Normal and Normal + Obese Groups.

	Normal (n = 161) β ± se (p-value)	Normal + Obese (n = 231) β ± se (p-value)
Age	0.0037 ± 0.0003 (< 0.0001)	0.0032 ± 0.0004 (< 0.0001)
Gender	-0.054 ± 0.012 (< 0.0001)	-0.028 ± 0.012 (< 0.05)
BMI	-0.011 ± 0.004 (< 0.01)	0.011 ± 0.001 (< 0.0001)

Coefficients are based on multiple linear regression of log transformed neopterin values. The units for *age* and *BMI* are years and kg/m^2, while for *gender* coding, 0 = female and 1 = male.

Table II. Neopterin Multiple Linear Regression of Breast and Prostate Cancer Groups.

	Breast cancer (n = 66) β ± se (p-value)	Prostate cancer (n = 38) β ± se (p-value)
Age	0.003 ± 0.001 (< 0.01)	-
BMI	-	0.013 ± 0.007 (< 0.05)
Stage	0.057 ± 0.019 (< 0.01)	0.199 ± 0.043 (< 0.001)

Coefficients are based on multiple linear regression of log transformed neopterin values. The units for *age* and *BMI* are years and kg/m^2. The classifications for *stage* were as follows. For breast cancer, stage I tumor size (T) < 2 cm across and cancer cells have not spread to axillary lymph nodes (N). For stage II, T < 2 cm across and the cancer has spread to the lymph nodes under the arm (N positive) or T is 2 to 5 cm and N is negative. In stage III, T > 5 cm or it has spread to other lymph nodes or tissues near the breast. Stage IV is metastatic cancer. For prostate cancer in stage I, cancer is found in the prostate only. In stage II, cancer is more advanced than in stage I, but has not spread outside the prostate. In stage III, cancer has spread beyond the outer layer of the prostate to nearby tissues. Stage IV is characterized by distant metastasis.

FIGURE LEGENDS

Figure 1: Serum neopterin levels among healthy lean subjects. The levels of neopterin in 161 normal subjects were determined by commercial sandwich ELISA. (a) The frequency distribution of the values across all normal subjects was determined. (b) The distribution of neopterin values between genders was compared by box and whiskers Tukey plot where the box frame defines the lower and upper quartile, the whiskers depict 1.5 x the interquartile range and the line within the box marks the median value. (c) The levels of neopterin were plotted as a function of age among women (circle) and men (square) and subjected to Spearman rank correlation analysis. (d) Subjects were grouped by gender and decade of life and the levels of serum neopterin were graphed by box and whiskers plot and compared by Mann Whitney t-test. Shaded boxes represent men.

Figure 2. Serum neopterin levels in obese subjects. The levels of neopterin in 70 obese subjects were determined by commercial sandwich ELISA. (a) The frequency distribution of the values across the obese population subjects was determined. (b) The distribution of neopterin values between genders was compared by box and whiskers plot. (c) The levels of neopterin were plotted as a function of age among women (circle) and men (square). (d) The normal study population (Figure 1) was combined with the obese population and neopterin was plotted as a function of BMI.

Figure 3. Serum neopterin levels among cancer subjects. The levels of neopterin in 124 cancer subjects were determined by commercial sandwich ELISA. The study population

consisted of 66 women with breast cancer, 38 men with prostate cancer and 12 men and 8 women with lung cancer. (a) The distribution of neopterin values among normal weight women (open circle) and women with breast cancer (closed circle), normal weight men (open square) and men with prostate cancer (closed square), all normal subjects (open diamond) and lung cancer subjects (closed diamond) was graphed by scatter plot where the solid horizontal bars depicts the median values. (b) The levels of neopterin in women with breast cancer were plotted as a function of age and subjected to linear regression analysis. (c) Neopterin values in subjects with prostate (closed square) or lung cancer (closed diamond) were plotted as a function of subject age. Subjects with (d) breast cancer stage, or (e) prostate cancer were stratified by stage and the distribution of neopterin values compared by scatter plot where the solid horizontal bars depicts the median values. Comparison between normal and cancer median neopterin values was performed by Mann Whitney t-test, where * = $p < 0.05$, ** = $p < 0.005$, *** = $p < 0.0001$.

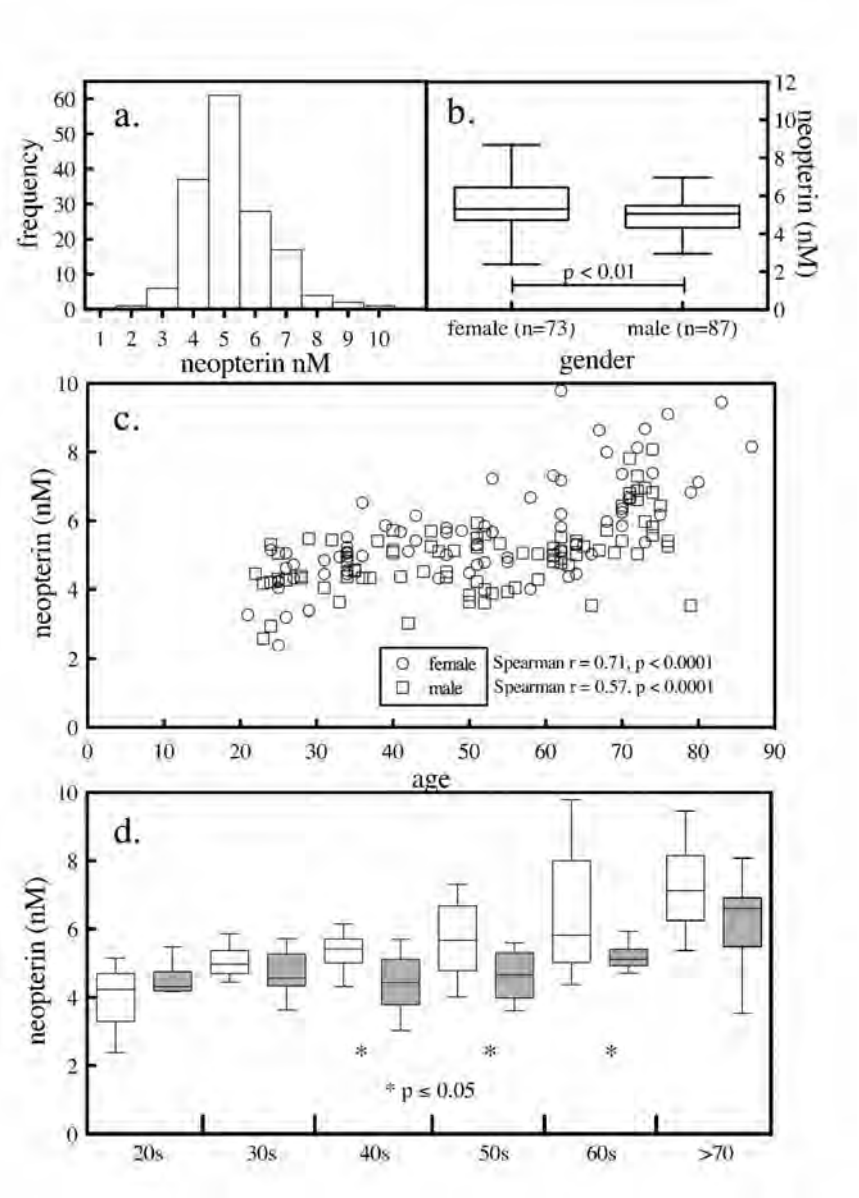

196x268mm (600 x 600 DPI)

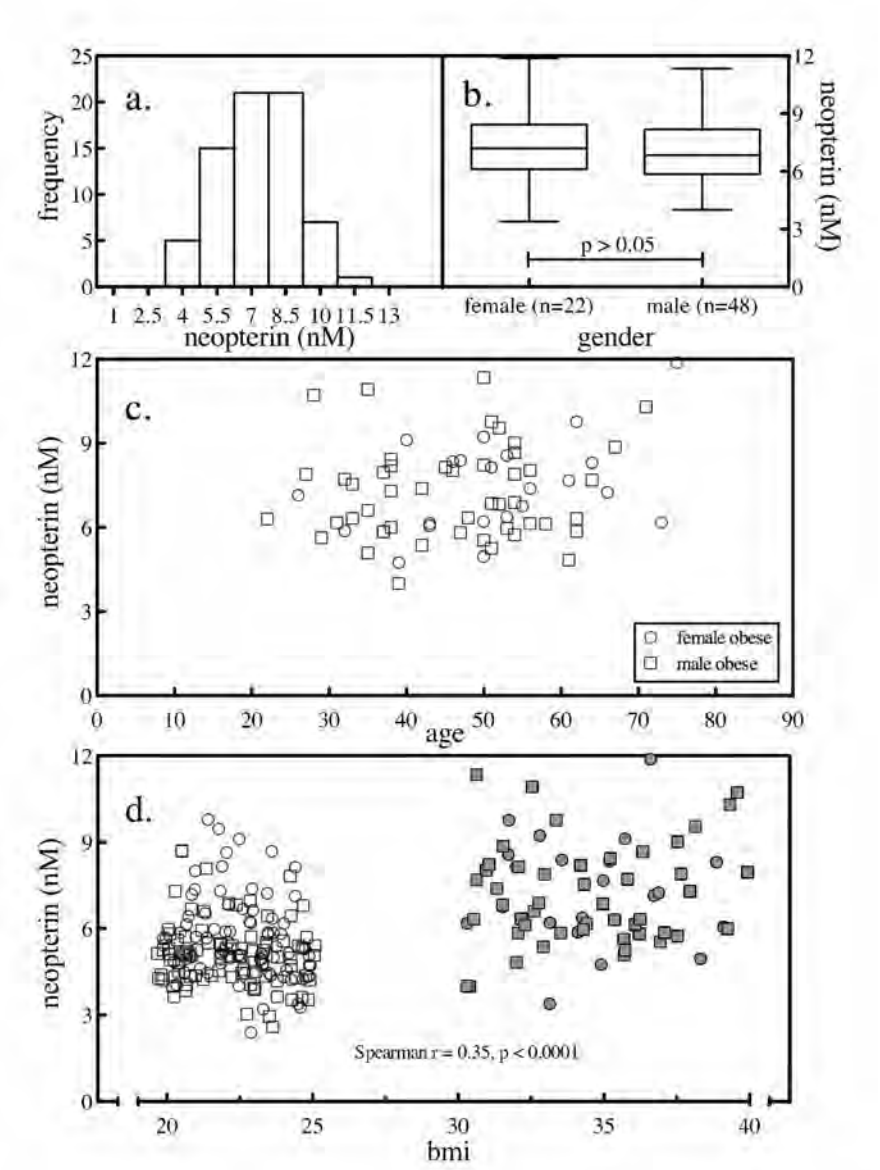

194x264mm (600 x 600 DPI)

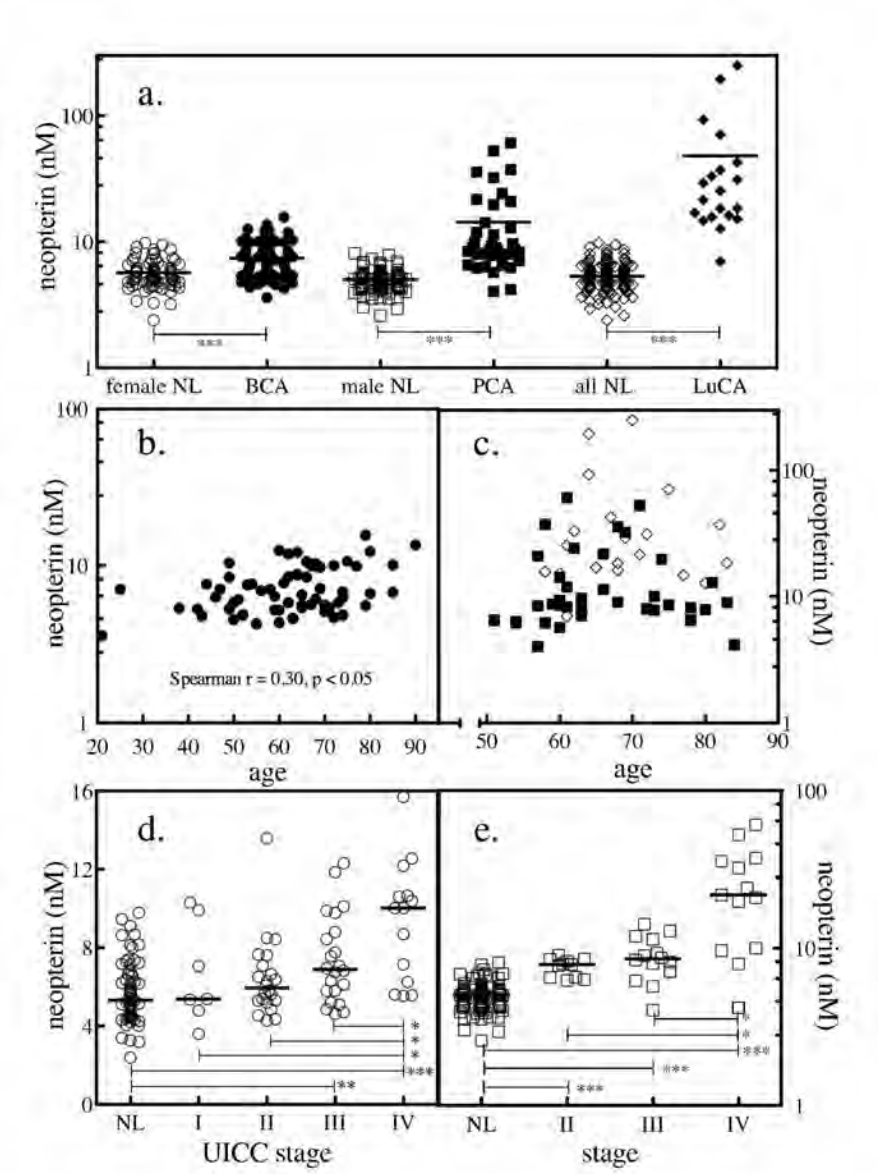

197x268mm (600 x 600 DPI)